

THE INFLUENCE OF GEOGRAPHIC SCALE, CLIMATE AND TROPHIC
DYNAMICS UPON NORTH PACIFIC OCEANIC ECOSYSTEM MODELS.

by

DAVID B. PREIKSHOT

B.A., ROYAL MILITARY COLLEGE, 1989

B.Sc., THE UNIVERSITY OF BRITISH COLUMBIA, 1995

M.Sc., THE UNIVERSITY OF BRITISH COLUMBIA, 2000.

A THESIS SUBMITTED IN PARTIAL FULFILLMENT OF
THE REQUIREMENTS FOR THE DEGREE OF

DOCTOR OF PHILOSOPHY

in

THE FACULTY OF GRADUATE STUDIES

(RESOURCE MANAGEMENT AND ENVIRONMENTAL STUDIES)

THE UNIVERSITY OF BRITISH COLUMBIA

MARCH 2007

©DAVID B. PREIKSHOT, 2007

Abstract

Dynamic simulation models of three nested North Pacific ecosystems (the Strait of Georgia, the British Columbia Shelf and the Northeast Pacific) were constructed to examine how area scale affects modelled historic changes of trophic interactions, fisheries and climate. Species groups were the same for all ecosystem models, with a focus upon commercially important fish species. The models were dynamic and spanned the period from 1950 to the start of the 21st Century. Time series data for biological indicators were compared to predicted model time series, under different scenarios of ecosystem control: top-down, bottom-up, or combinations thereof. Results of these scenarios suggest that while fisheries, and predation / competition effects explain most population changes for commercially important fish species, all species modelled also appear to experience bottom-up effects driven by climate change, and regime shifts. The ecosystem models suggest such bottom-up dynamics through predicted primary production anomalies similar to decadal cycling seen in climate indices like the Pacific Decadal Oscillation (Northeast Pacific), upwelling at 54°N (BC shelf) and Salinity / Fraser River discharge (Strait of Georgia). The results of this work suggest that both the area and scale over which indices of regime shifts and climate change are measured are linked, via bottom-up forcing, to changes in biomasses of all trophic levels in these ecosystems. The ability to link bottom-up and top-down dynamics provides an exciting way for ecosystem models to contribute to the formulation of policy and cross validation of single species stock assessment research.

Table of Contents

Abstract.....	ii
Table of Contents.....	iii
List of Tables.....	vi
List of Figures	ix
List of Abbreviations.....	xvi
Acknowledgements.....	xviii
Dedication.....	xix
1. Introduction.....	1
1.1. Climate change and fish populations.....	2
1.1.1. Background and history.....	2
1.1.2. The Oceanographic link between climate and ecosystems.....	4
1.1.3. North Pacific climate change indices.....	8
1.2. Defining ecosystems for analysis.....	15
1.2.1. Geographic boundaries.....	15
1.2.2. Species modeled.....	16
1.2.3. Delimiting the ecosystems.....	17
1.2.3.1. The Strait of Georgia.....	18
1.2.3.2. The BC Shelf.....	19
1.2.3.3. The Northeast Pacific Ocean.....	20
1.3. Analysis of results.....	21
2. Methods.....	25
2.1. Introduction to the methodology.....	25
2.2. Ecosystem boundaries and biota.....	25
2.2.1. Ecosystem boundaries.....	25
2.2.2. Ecosystem biota.....	26
2.3. Determination of biomass, production, and consumption.....	28
2.3.1. Multi-stanza groups.....	28
2.3.1.1. Arrowtooth flounder.....	30
2.3.1.2. Walleye pollock.....	31
2.3.1.3. Pacific cod.....	32

2.3.1.4. Pacific halibut.....	32
2.3.1.5. Pacific herring.....	33
2.3.1.6. Sablefish.....	34
2.3.2. Marine birds.....	35
2.3.3. Marine mammals.....	37
2.3.4. Pelagic fishes.....	39
2.3.4.1. Salmon.....	39
2.3.4.2. Sharks.....	41
2.3.4.3. Myctophids and other pelagic fishes.....	41
2.3.5. Demersal fishes.....	42
2.3.5.1. Demersal elasmobranchs.....	42
2.3.5.2. Rockfishes.....	43
2.3.5.3. Gadids and greenlings.....	44
2.3.5.4. Flatfishes and small demersal species.....	46
2.3.6. Invertebrates.....	47
2.3.6.1. Zooplankton.....	47
2.3.6.2. Squid.....	49
2.3.6.3. Crustaceans.....	49
2.3.6.4. Benthic invertebrates.....	50
2.3.7. Primary producers.....	51
2.4. Determination of diet compositions.....	52
2.4.1. Diets of multi-stanza groups.....	53
2.4.2. Diets of marine birds.....	53
2.4.3. Diets of marine mammals.....	54
2.4.4. Diets of pelagic fishes.....	54
2.4.5. Diets of demersal fishes.....	56
2.4.6. Diets of invertebrates.....	56
2.5. Fisheries and catch data.....	57
2.6. Comparing dynamic model outputs to reference time series data.....	58
2.6.1. Vulnerabilities and simulating top-down dynamics.....	58
2.7. Climate indices.....	60
3. Results.....	62
3.1. General model responses in dynamic simulations.....	62
3.2. Modelled biomass trajectories.....	64
3.2.1. The Strait of Georgia.....	64
3.2.2. The British Columbia Shelf.....	67
3.2.3. The Northeast Pacific.....	73
3.3. Fitting simulated time series to reference time series data.....	79

3.4. Comparing primary production anomalies to climate indices.....	82
3.4.1. Temporal oscillations in modelled primary production anomalies.....	82
3.4.2. Comparing modelled production anomalies to climate indices.....	83
3.4.2.1. The Strait of Georgia.....	84
3.4.2.2 The British Columbia Shelf.....	86
3.4.2.3. The Northeast Pacific.....	88
4. Discussion.....	91
4.1. General model responses in dynamic simulations.....	91
4.2. Modelled biomass trajectories.....	95
4.2.1. The Strait of Georgia.....	95
4.2.1.1. Strait of Georgia multi-stanza groups.....	95
4.2.1.2. Strait of Georgia salmon.....	97
4.2.1.3. Strait of Georgia demersal fishes.....	100
4.2.1.4. Strait of Georgia marine mammals.....	100
4.2.1.5. Strait of Georgia marine birds.....	101
4.2.2. The British Columbia Shelf.....	102
4.2.2.1. British Columbia Shelf multi-stanza groups.....	103
4.2.2.2. British Columbia Shelf salmon.....	109
4.2.2.3. British Columbia Shelf demersal fishes.....	113
4.2.2.4. British Columbia Shelf marine mammals.....	119
4.2.3. The Northeast Pacific.....	120
4.2.3.1. Northeast Pacific multi-stanza groups.....	121
4.2.3.2. Northeast Pacific salmon.....	128
4.2.3.3. Northeast Pacific demersal fishes.....	132
4.3. Climate variation and modelled ecosystem changes.....	137
4.3.1. Climate variation and the Strait of Georgia model.....	137
4.3.2. Climate variation and the British Columbia Shelf model.....	143
4.3.3. Climate variation and the Northeast Pacific model.....	147
4.3.4. Climate variation and model scale.....	149
References.....	162
Appendix 1.....	185
Appendix 2.....	200
Appendix 3.....	202

List of Tables

Table 1.1: Groups used in the North Pacific Ecopath with Ecosim models.....	17
Table 3.1: Sums of squared differences between predicted and reference biomass time series.....	63
Table 3.2: Sums of squared differences between 'best fit' predicted and reference time series.....	79
Table 3.3: Sums of squared differences between 'best fit' predicted and reference time series.....	80
Table 3.4: Sums of squared differences between predicted and reference biomass time series.....	80
Table 3.5: Improvement of fit, for models by using a PPA and fishing effects.....	81
Table 3.6: Probability that decadal spline fitted PPAs and annual PPAs represented fitting to measurement error.....	81
Table 4.1: Correlations between biomasses of phytoplankton and salmon species in the BCS 'best fit' model.....	110
Table 4.2: Changes in the sums of squared differences (SS) between reference and predicted time series of biomass in the 'best fit' BCS model under different assumptions.....	145
Table A.1.1: Pedigree chart of EwE basic input parameters used for groups in the SoG model.....	185
Table A.1.2: Pedigree chart of EwE basic input parameters used for groups in the BCS model.....	186
Table A.1.3: Pedigree chart of EwE basic input parameters used for groups in the NEPac model.....	187
Table A.1.4: EwE basic input parameters used for multi-stanza groups in the final, mass balanced SoG, BCS, and NEPac models.....	188
Table A.1.5: EwE basic input parameters for bird and mammal groups in the mass balanced SoG, BCS, and NEPac models.....	189
Table A.1.6: EwE basic input parameters for pelagic fishes groups in the mass balanced SoG, BCS, and NEPac models.....	190

Table A.1.7: EwE basic input parameters for demersal fishes groups in the mass balanced SoG, BCS and NEPac models.....	191
Table A.1.8: EwE basic input parameters for invertebrate groups in the mass balanced Sog, BCS and NEPac models.....	192
Table A.1.9: Diet compositions for adult (normal type) and juvenile (bold type) multi-stanza groups.....	193
Table A.1.10: Diet compositions for marine bird groups	194
Table A.1.11: Diet compositions for marine mammal groups.....	195
Table A.1.12: Diet compositions for pelagic fish groups.....	196
Table A.1.13: Diet compositions for some demersal fish groups.....	197
Table A.1.14: Diet compositions for flatfish groups.....	198
Table A.1.15: Diet compositions used for the invertebrate groups.....	198
Table A.1.16: Time series available as reference data for the NEPac BCS, and SoG models.....	199
Table A.2.1. Vulnerability settings, by predator group, for models in this study.....	200
Table A.3.1: Correlation coefficients of the best fit Strait of Georgia PPA and Fraser River flow at Hope, BC.....	202
Table A.3.2: Correlations coefficients of the best fit Strait of Georgia PPA and ocean salinity at Chrome Island, BC.....	203
Table A.3.3: Correlations coefficients of the best fit Strait of Georgia PPA and ocean salinity at Race Rocks, BC.....	204
Table A.3.4.: Correlations coefficients of the best fit Strait of Georgia PPA and upwelling at 48°N.....	205
Table A.3.5.: Correlations coefficients of the best fit BC shelf PPA and upwelling at 48°N.....	205
Table A.3.6.: Correlations coefficients of the best fit BC shelf PPA and upwelling at 51°N.....	206
Table A.3.7.: Correlations coefficients of the best fit BC shelf PPA and upwelling at 54°N.....	206

Table A.3.8: Correlations coefficients of the best fit Northeast Pacific PPA and the Aleutian low pressure index averaged annually.....	207
Table A.3.9: Correlations coefficients of the best fit Northeast Pacific PPA and the Pacific decadal oscillation averaged over seasonal periods.....	207
Table A.3.10: Correlations coefficients of the best fit Northeast Pacific PPA and the northern oscillation index averaged over seasonal periods.....	207
Table A.3.11: Correlations coefficients of the best fit Northeast Pacific PPA and the north Pacific index averaged over seasonal periods.....	208

List of Figures

Figure 1.1: Generalised annual average atmospheric and oceanic circulation of the Northeast Pacific.....	5
Figure 1.2: Annual average (dots) and interdecadal (lines) trends in the winter (November to March) North Pacific Index.....	8
Figure 1.3: Annual average (dots) and interdecadal (lines) trends in the Aleutian Low Pressure Index.....	9
Figure 1.4: Annual average (dots) and interdecadal (lines) trends in the Northern Oscillation Index.....	10
Figure 1.5: Annual average (dots) and interdecadal (lines) trends in the Pacific Decadal Oscillation Index.....	11
Figure 1.6: Summer (June, July and August) upwelling at coastal stations in British Columbia.....	12
Figure 1.7: Winter (December, January and February) upwelling at coastal stations in British Columbia.....	12
Figure 1.8: Average annual (dots) and interdecadal (lines) trends in surface water salinity at Race Rocks (48.31°N, 123.54°W).....	13
Figure 1.9: Average annual (dots) and interdecadal (lines) trends in Fraser River flow measured at Hope, BC.....	14
Figure 1.10: Areas included in the ecosystem models.....	16
Figure 1.11: A comparison of changes in the predicted PPA for a Northeast Pacific EwE model with changes in annual values of the Pacific Decadal Oscillation from Preikshot (2005).....	22
Figure 1.12: A comparison of changes in the predicted PPA for a British Columbia Shelf EwE model with changes in the annual upwelling index (the departure of annual upwelling values from the long term average), measured at 54°N, from Preikshot (2005).....	23
Figure 3.1: Simulated best fit SoG PPAs with trophic links set to $v=1.5$, 2, and 3.....	63
Figure 3.2: Simulated best fit BCS PPAs with trophic links set to $v=1.5$, 2, and 3.....	64
Figure 3.3: Simulated best fit NEPac PPAs with trophic links set to $v=1.5$, 2, and 3.....	64

Figure 3.4: Comparison of changes in the modelled SoG adult herring biomass (EwE) versus the estimated Strait of Georgia spawning stock biomass (SA), 1950 to 2002.....	65
Figure 3.5: Comparison of changes in the modelled SoG coho salmon biomass (EwE) versus the estimated Strait of Georgia coho biomass from Martell et al. (2002), from 1950 to 2002.....	65
Figure 3.6: Comparison of changes in the modelled chinook salmon SoG biomass (EwE) versus the estimated Strait of Georgia chinook biomass from Martell et al. (2002), from 1950 to 2002.....	65
Figure 3.7: Comparison of changes in modelled SoG pelagic piscivorous bird biomass (EwE) versus biomass changes derived from SoG Christmas bird count (CBC) data, 1950 to 2002.....	66
Figure 3.8: Comparison of changes in modelled SoG demersal piscivorous bird biomass (EwE) versus biomass changes derived from SoG Christmas (CBC) bird count data, 1950 to 2002.....	66
Figure 3.9: Comparison of changes in modelled SoG harbour seal biomass (EwE) versus biomass changes from SoG stock assessment data (SA), 1950 to 2002.....	66
Figure 3.10: Comparison of changes in modelled SoG toothed whale biomass (EwE) versus SoG orca count data (orca #), 1950 to 2002.....	67
Figure 3.11: Comparison of changes in modelled SoG lingcod biomass (EwE) versus biomass from SoG stock reduction analysis (SA), 1950 to 2002 (Martell 1999)....	67
Figure 3.12: Comparison of modelled BCS arrowtooth flounder biomass (EwE) versus biomass derived from stock assessment (SA), 1950 to 2002 (Turnock et al. 2003b).....	68
Figure 3.13: Comparison of modelled BCS walleye pollock biomass (EwE) versus biomass derived from a Gulf of Alaska stock assessment (SA), 1950 to 2002 (Dorn et al. 2003).....	68
Figure 3.14: Comparison of modelled BCS Pacific cod biomass (EwE) versus biomass derived from BC stock assessments (SA), 1950 to 2002 (Sinclair et al. 2001).....	68
Figure 3.15: Comparison of modelled BCS halibut biomass (EwE) versus biomass derived from BC stock assessments (SA), 1950 to 2002 (Sullivan et al. 1997 and Clark and Hare 2001a).....	69
Figure 3.16: Comparison of changes in modelled BCS sablefish biomass (EwE) versus biomass derived from BC tagging data (SA), and from catch and mortality ($B=C/F$), 1950 to 2002.....	69

Figure 3.17: Comparison of modelled BCS herring biomass (EwE) to biomass derived from BC stock assessments (SA), 1950 to 2002.....	70
Figure 3.18: Comparison of modelled BCS harbour seal biomass (EwE) to biomass derived from BC stock assessments (SA), 1970 to 2002.....	70
Figure 3.19: Comparison of modelled BCS chinook salmon biomass (EwE) to biomass derived from BC catch statistics (B from catch), 1950 to 2002.....	70
Figure 3.20: Comparison of modelled BCS coho salmon biomass (EwE) to biomass derived from BC catch statistics (B from catch), 1950 to 2002.....	71
Figure 3.21: Comparison of modelled BCS coho salmon biomass (EwE) to biomass derived from BC catch statistics (B from catch), 1950 to 2002.....	71
Figure 3.22: Comparison of modelled BCS coho salmon biomass (EwE) to biomass derived from BC catch statistics (B from catch), 1950 to 2002.....	71
Figure 3.23: Comparison of BCS sockeye salmon biomass (EwE) to biomass derived from BC catch statistics (B from catch), 1950 to 2002.....	71
Figure 3.24: Comparison of changes in modelled BCS hake biomass (EwE) versus biomass derived from stock assessment (SA), 1950 to 2002.....	72
Figure 3.25: Comparison of changes in modelled BCS Pacific Ocean perch biomass (POP EwE) versus biomass derived from stock assessment (POP SA), 1950 to 2002.....	72
Figure 3.26: Comparison of changes in modelled BCS rock sole biomass (EwE) versus biomass derived from stock assessment (SA), 1950 to 2002.....	73
Figure 3.27: Comparison of changes in modelled NEPac arrowtooth flounder biomass (EwE) versus biomass derived from stock assessment (SA), 1950 to 2002.....	73
Figure 3.28: Comparison of modelled NEPac Pacific cod biomass (EwE) to biomass derived from stock assessment (SA), 1950 to 2002.....	74
Figure 3.29: Comparison of changes in modelled NEPac sablefish biomass (EwE) versus biomass derived from stock assessment (SA), 1950 to 2002.....	74
Figure 3.30: Comparison of changes in modelled NEPac halibut biomass (EwE) versus biomass derived from stock assessment (SA), 1950 to 2002.....	75
Figure 3.31: Comparison of changes in modelled NEPac walleye pollock biomass (EwE) versus biomass derived from stock assessment (SA), 1950 to 2002.....	75

Figure 3.32: Comparison of changes in modelled NEPac pink salmon biomass (EwE) versus biomass derived from catch data (B from catch), 1950 to 2002.....	75
Figure 3.33: Comparison of changes in modelled NEPac chum salmon biomass (EwE) versus biomass derived from catch data (B from catch), 1950 to 2002.....	75
Figure 3.34: Comparison of changes in modelled NEPac sockeye salmon biomass (EwE) versus biomass derived from catch data (B from catch), 1950 to 2002.....	76
Figure 3.35: Comparison of changes in modelled NEPac coho salmon biomass (EwE) versus biomass derived from catch data (B from catch), 1950 to 2002.....	76
Figure 3.36: Comparison of changes in modelled NEPac chinook salmon biomass (EwE) versus biomass derived from catch data (B from catch), 1950 to 2002.....	76
Figure 3.37: Comparison of changes in modelled NEPac Pacific Ocean perch biomass (POP EwE) versus biomass derived from stock assessment (POP SA), 1950 to 2002.....	77
Figure 3.38: Comparison of changes in modelled NEPac northern rockfish biomass (EwE) versus biomass derived from stock assessment (SA), 1950 to 2002.....	77
Figure 3.39: Comparison of changes in modelled NEPac Atka mackerel biomass (EwE) versus biomass derived from stock assessment (SA), 1950 to 2002.....	78
Figure 3.40: Comparison of changes in modelled NEPac hake biomass (EwE) versus biomass derived from stock assessment (SA), 1950 to 2002.....	78
Figure 3.41: Comparison of changes in modelled NEPac plaice biomass (EwE) versus biomass derived from stock assessment (SA), 1950 to 2002.....	78
Figure 3.42: Comparison of changes in modelled NEPac yellowfin sole biomass (EwE) versus biomass derived from stock assessment (SA), 1950 to 2002.....	79
Figure 3.43: Comparison of changes in modelled NEPac rock sole biomass (EwE) versus biomass derived from stock assessment (SA), 1950 to 2002.....	79
Figure 3.44: Best fit annual PPA from the SoG model and smoothed PPA values from a LOWESS filter using a second degree polynomial with 10 and 40 year smoothing windows.....	82
Figure 3.45: Best fit annual PPA from the BCS model and smoothed PPA values from a LOWESS filter using a second degree polynomial with 10 and 40 year smoothing windows.....	82

Figure 3.46: Best fit annual PPA from the NEPAC model and smoothed PPA values from a LOWESS filter using a second degree polynomial with 10 and 40 year smoothing windows.....	83
Figure 3.47: Comparisson of SoG PPA to Fraser River flow (averaged from April to July).....	84
Figure 3.48: Comparisson of SoG PPA to Fraser River flow (averaged from June to August).....	84
Figure 3.49: Comparisson of SoG PPA to Chrome Island salinity (averaged from March to May).....	85
Figure 3.50: Comparisson of SoG PPA to Chrome Island salinity (averaged over March and April).....	85
Figure 3.51: Comparisson of SoG PPA to Race Rocks salinity (averaged from February to May).....	85
Figure 3.52: Comparisson of SoG PPA to Race Rocks salinity (averaged over February and March).....	85
Figure 3.53: Comparisson of SoG PPA to upwelling at 48°N (averaged over March and April).....	86
Figure 3.54: Comparisson of SoG PPA to upwelling at 48°N (averaged over March and April).....	86
Figure 3.55: Comparisson of BCS PPA to upwelling at 48°N (averaged from September to March).....	86
Figure 3.56: Comparisson of BCS PPA to upwelling at 54°N (averaged from May to July).....	87
Figure 3.57: Comparisson of BCS PPA to upwelling at 54°N (averaged from March to May).....	87
Figure 3.58: Decadal changes of NEPac PPA and Aleutian Low Pressure Index.....	88
Figure 3.59: Interdecadal changes of NEPac PPA and Aleutian Low Pressure Index.....	88
Figure 3.60: Comparisson of NEPac PPA to PDO Index (averaged from February to July).....	89
Figure 3.61: Comparisson of NEPac PPA to PDO Index (averaged from April to July).....	89

Figure 3.62: Comparisson of NEPac PPA to NOI (averaged from April to October).....	89
Figure 3.63: Comparisson of NEPac PPA to annual NOI.....	89
Figure 3.64: Decadal changes of NEPac PPA and annual NPI.....	90
Figure 3.65: Interdecadal changes of NEPac PPA and annual NPI.....	90
Figure 4.1: Simulated herring predation and fishing mortalities in the 'best fit' EwE SoG simulation.....	95
Figure 4.2: Comparison of simulated adult coho (open circles) and chinook salmon (solid circles) biomasses to simulated juvenile herring biomass in the 'best fit' EwE SoG simulation.....	97
Figure 4.3: Changes in simulated adult chinook salmon predation mortality from marine mammals in the 'best fit' EwE SoG simulation.....	98
Figure 4.4: Changes in simulated adult walleye pollock total and predation mortalities in the 'best fit' EwE BCS simulation.....	104
Figure 4.5: Changes in simulated juvenile sablefish biomass, compared to the average 1950 to 2002 biomass, in the 'best fit' EwE BCS simulation.....	106
Figure 4.6: Changes in the ratio of SoG/BCS biomasses, from stock assessment data reported in DFO (2002a, b, c, d, and e).....	107
Figure 4.7: Comparison of changes in simulated chinook biomass to reference biomass, derived from catch.....	111
Figure 4.8: Comparison of changes in simulated fishing mortality and predation mortality changes for Pacific Ocean perch, in the 'best fit' BCS model.....	114
Figure 4.9: Comparison of lagged changes in Hecate Strait (top graph) and simulated BCS (bottom graph) rock sole biomass to changes in phytoplankton biomass in the 'best fit' BCS model.....	115
Figure 4.10: Comparison of changes in Hecate Strait rock sole biomass to changes in upwelling measured at 54°N during May, June and July.....	116
Figure 4.11: Comparison of changes in upwelling measured at 48°N and 33°N during April, May, and June.....	117
Figure 4.12: Comparison of changes in simulated and stock assessment biomasses for seals when predation by toothed whales was included in the 'best fit BCS model.....	119

Figure 4.13: Changes in the ratio of female arrowtooth flounder spawning stock biomass (SSB) in the Gulf of Alaska (GoA) to the Bering Sea Aleutian Islands (BSAI) from 1976 to 2003.....	121
Figure 4.14: Changes in biomasses of age 3+ walleye pollock in the Gulf of Alaska (GoA) and eastern Bering Sea (EBS) from 1964 to 2003.....	123
Figure 4.15: Changes of adult halibut weight, relative to 1950 in the NEPac and BCS 'best fit' models from 1950 to 2002.....	126
Figure 4.16: Comparison of changes in juvenile sablefish biomass in 'best fit' NEPac model versus estimated numbers of two year olds from stock assessment data, note log scale for age 2 fish.....	127
Figure 4.17: Comparison of changes in catches of sockeye salmon in British Columbia (BC) and Alaska (AK) between 1950 and 2001.....	129
Figure 4.18: Comparison of changes in catches of pink salmon in British Columbia (BC) and Alaska (AK) between 1950 and 2001.....	129
Figure 4.19: Comparison of changes in catches of coho salmon in British Columbia (BC) and Alaska (AK) between 1950 and 2001.....	131
Figure 4.20: Comparison of changes in catches of chum salmon in British Columbia (BC) and Alaska (AK) between 1950 and 2001.....	131
Figure 4.21: Changes in fully selected fishing mortality in Aleutian Islands Atka mackerel from 1975 to 2003.....	134
Figure 4.22: Changes in NEPac modelled PPA estimated at annual intervals versus a PPA estimated with a cubic spline function.....	148
Figure 4.23: Changes in modelled PPAs reproduced by fitting two sine wave functions capturing both decadal and interdecadal variations.....	150
Figure 4.24: Biomass spectra of the Northeast Pacific, (NEPac), BC shelf (BCS), and Strait of Georgia (SoG) models from 1950 (top graph) and 2002 (bottom graph).	157
Figure 4.25: Biomass of catch spectra of the Northeast Pacific, (NEPac), BC shelf (BCS), and Strait of Georgia (SoG) models from 1950 (top graph) and 2002 (bottom graph).....	158
Figure 4.26: Catch-biomass-1 spectra of the Northeast Pacific, (NEPac), BC shelf (BCS), and Strait of Georgia (SoG) models from 1950 (top graph) and 2002 (bottom graph).....	159

List of Abbreviations

ALPI:	Aleutian Low Pressure Index
ATF:	ArrowTooth Flounder
B:	EwE Biomass parameter
BA:	Biomass Accumulation
BCS:	British Columbia Shelf
BGCP:	BioGeoChemical Province
BSAI:	Bering andd Sea Aleutian Islands
CBC:	Christmas Bird Count
DC:	Diet Composition
DWR:	Deep Water Renewal
EN:	El Niño
ENSO:	El Niño Southern Oscillation
EwE:	Ecopath with Ecosim
F:	instantaneous rate of Fishing mortality
GoA:	Gulf of Alaska
INPFC:	International North Pacific Fisheries Commission
INPSFC:	International Pacific Salmon Fisheries Commission
IPHC:	International Pacific Halibut Commission
k:	k parameter of the vonBertalanffy growth equation
kJ/d:	kilo joules per day
kPa:	kilo Pascals
L_{∞} :	theoretical Length at Infinite age
L_{mat}/L_{∞} :	Length at Maturity divided by theoretical Length at Infinite age
LME:	Large Marine Ecosystem
LN:	La Niña
LOWESS:	LOcally WEighted Scatter-plot Smoothing
M:	instantaneous rate of natural Mortality
MLD:	Mixed Layer Depth
NEPI:	Northeast Pacific Pressure Index
NEPac:	Northeast Pacific
NPAFC:	North Pacific Anadromous Fish Commission
NPH:	North Pacific High
NOI:	Northern Oscillation Index
P/B:	EwE Production per unit Biomass parameter (equivalent to Z)
PBS:	Pacific Biological Station
PC:	Principal Component
PCA:	Principal Components Analysis
PDO:	Pacific Decadal Oscillation
PPA:	Primary Production Anomaly
PTV:	Pure Temporal Variation
Q/B:	EwE Consumption per unit Biomass parameter
R:	daily Ration
SJF:	Strait of Juan deFuca
SLP:	Sea Level Pressure

SoG: Strait of Georgia
SOI: Southern Oscillation Index
SRA: Stock Reduction Analysis
SSB: Spawning Stock Biomass
SSD: Sum of Squared Differences
SST: Sea Surface Temperature
SWCVI: Southwest Coast of Vancouver Island
TL: Trophic Level
W: Weight
 W_{mat}/W_{∞} : Weight at Maturity divided by theoretical Weight at Infinite age
WCUI: West Coast Upwelling Index
Z: instantaneous total mortality rate

Acknowledgements

I would first and foremost like to thank Villy Christensen for his guidance through this research. I would also like to express my gratitude to the members of my committee, Dick Beamish, Les Lavkulich and Daniel Pauly for their patience and advice. Thanks are also due to my wife, Tania Tripp, for her unflinching support.

Dedication

This research is dedicated to my daughter, Marina Vida Preikshot, who entered this world with a burden far greater than most of us can ever know. Despite the disability with which she lives, her strength and a ready smile never fail. She taught me more in the first half year of her life than the first 37 of mine all put together.

1. Introduction

Some ocean creatures have short lives in small rock bowls carved out of the foreshore by centuries of wind and waves. Some inhabit vast ocean spaces bound by the continent's shores yet each generation return to a small stream to spawn. Humans have sought to understand all such creatures as they grow, feed, mate and die. Ecosystem modeling has become a popular tool to help structure and investigate our knowledge of such biological interactions. This is especially true for managed ecosystems in which long-term scientific studies have amassed data on both commercially important species and 'charismatic megafauna'. All of these creatures, moving or sessile, herbivorous or predatory, exist across different levels of space and time, *i.e.*, inhabit more than one scale. Of course, no creature spans all levels of space and time, but many overlap in these dimensions. The task of the modeller, therefore, is to determine the interactions that affect the creatures and ecosystem being modelled, and the scales at which these interactions occur. This chapter outlines how ecosystem modeling, specifically of fish-dominated marine ecosystems, can be used to examine the scales of time and space at which different species populations change and the climate mechanisms that appear to be limited to those changes at different spatial scales.

Two phenomena are used to support the research framework. First: the apparent relationship between annual and decadal climate variation and changes in fish populations and, second: the effects of fisheries and predation upon, and competition between, fish species. Ecosystem modeling allows the examination of how these very different time-scaled phenomena might interact when modelled at different area scales. Thus, modelled historic changes in ecosystem, and species, characteristics can be compared to assessment data to examine which mechanisms make the model's predictions similar or divergent from observation. By comparing population changes in ecosystem-based models to single-species-based assessment models, we can examine the ecosystem regulated mechanisms at different area scales. One way to construct such a comparison of scale and population change is to have comparable models, with the same species groups, thus, allowing the direct comparison of changes to different 'fractions' of

the same population. The simplest way to do this is by nesting the models, *i.e.*, each successively larger scale model contains the smaller scale one(s). The results from such a study have value to both research and management. The research benefit would be a rigorous investigation to examine how well hypotheses of ecosystem function, *e.g.*, bottom-up and top-down theories, explain measured temporal and spatial patterns given a synthetic model which contains a database of the best available information on many species. For management such research could help suggest more robust policies that can accommodate likely future ecosystem states as mitigated by both natural and anthropogenic factors. Indeed, ecosystem management drives national and transnational initiatives like the Georgia Basin Action Plan in British Columbia and Washington, The Chesapeake Bay Program, and the Great Barrier Reef Marine Park Authority.

1.1. Climate change and fish populations

1.1.1. Background and history

There is now a huge body of literature regarding the effects of climate change on fish populations, *e.g.*, Beamish (1995), Hare and Mantua (2000), and Hollowed *et al.* (2001). Most of this work presupposes that there is some connexion between climate and recruitment and attempts to correlate climate indices with aspects of the life history of a particular stock of fish. This single stock work has been criticised, however, as being subject to a variety of statistical problems which make the interpretation of the supposed environmental link to fish populations suspect. Particularly troublesome to Walters and Martell (2004) is the willingness of many studies to accept low correlations as indicative of causality despite factors such as: failure to critically analyse alternative hypotheses and time series with fewer degrees of freedom than years of data. One potential solution to such problems would be the analyses of climate and fish recruitment time series over several stocks or for species complexes within ecosystem models (Walters and Martell 2004). It may also be that assumptions of the effects of random impacts are too pessimistic.

Comparisons of climate data to fish recruitment over a range of stocks or species, not surprisingly has been rather more limited than for single-species given the inherently more daunting task of collecting collating and analyzing the data. Much of this multi-stock, multispecies research has been done in the Northeast Pacific (Hare and Francis 1994, Francis *et al.* 1998, Benson and Trites 2002, Aydin *et al.* 2003). The reasons for this may be related to the fact that most of the stocks within the area are under the scrutiny of two affluent countries, Canada and the United States. Many commercially important stocks in the Northeast Pacific have therefore been closely monitored, by the individual countries or transnational management programs, and subject to thorough stock assessments for a relatively (in global fisheries management terms) long time. Examples include:

- 1) halibut, through the International Pacific Halibut Commission (IPHC), 1923 – present;
- 2) salmon, through the International Pacific Salmon Fisheries Commission (IPSFC), 1937 - 1985, the Pacific Salmon Commission (PSC), 1985 – present, the International North Pacific Fisheries Commission (INPFC), from 1952 – 1992, the North Pacific Anadromous Fish Commission (NPAFC), from 1992 to present;
- 3) herring in British Columbia, by the Pacific Biological Station (PBS), since 1929.

Beyond the above species, stock assessment data for all commercially important groundfish species is available back to 1950, in most cases, and even further into the past for some. Having this long and wide historical perspective is important because of an important effect of scale: long-term climate change is more likely to be reflected in long-term, and large-scale, fisheries data (Angel 1994, Denman 1994, O'Neill and King 1998). It is suggested by Denman (1994), that for pelagic ecosystems in particular, there is a close coupling, at all scales, between environmental and biological processes. Several climate indices are available for comparison to biological trends in the North Pacific. Indeed, there has been much research examining the correlations between these climate trends and biological characteristics of North Pacific aquatic species, *e.g.*, Hollowed and Wooster (1992), Beamish (1995), Polovina *et al.* (1995), Mantua *et al.* (1997), Hare and

Mantua (2000), McFarlane *et al* (2000), Clark and Hare (2001), Hollowed *et al.* (2001), and Chavez *et al.* (2003). This family of research has suggested mechanisms that may be responsible for linking climate change to particular species by enhancing or suppressing recruitment conditions (Clark and Hare 2001) or enhancing growth conditions (Polovina *et al.* 1995).

Relatively little work has been done, however, to examine how trophically-linked organisms in the ocean react to environmental cues over time and space. Some preliminary studies toward tracking the trophic effects of climate variation include work in the Bering Sea (Trites *et al.* 1999) and north Pacific gyres (Aydin *et al.* 2003). Much of this work, has been in isolation and the examination of climatic effects has generally been isolated from consideration of top-down effects (Francis *et al.* 1998).

1.1.2. The Oceanographic link between climate and ecosystems

An important mechanism by which climate variation and change affects ocean ecosystems is the interaction of atmospheric winds with water masses (Parrish *et al.* 2000). For example, the surface water circulation of the Northeast Pacific is dominated by the Alaska Gyre. The Alaska Gyre is the counter clockwise flow of surface water in the Northeast Pacific Ocean (see Figure 1.1). This counter clockwise flow is generated by the winds created by the 'Aleutian low' pressure system which tends to persist in the region, usually strengthening in winter (Ware and McFarlane 1989). Low pressure may be thought of as an atmospheric zone in which air is rising, causing apparently lower pressure than a place where air is falling, *i.e.*, a high pressure system. Near the Earth's surface air is drawn to the centre to replace rising air. Due to the Coriolis force the moving air is deflected to the right (in the northern hemisphere). This results in a general tendency to westerly winds in the subtropics and easterlies in the sub polar regions of the Northern Hemisphere (Bearman 1989). When the flow of air towards low pressure centres is balanced by apparent centripetal force as it moves the general result is cyclonic, *i.e.*, counter clockwise air circulation of winds around a low pressure centre (Parrish *et al.* 2000). These cyclones typically manifest themselves over spatial scales of 1 to 10 million

square kilometres for several days, travelling from west to east along the so-called polar front (Bearman 1989).

The inter-annual behaviour of such pressure systems in the Northeast Pacific can be seen in the Aleutian Low Pressure Index (ALPI), a measurement of the area in the Northeast Pacific covered by a pressure of less than 100.5 kPa (Beamish *et al.* 1997). The centre of the Aleutian low pressure system varies in magnitude and position as the seasons change (Parrish *et al.* 2000) and also appears to go through changes in magnitude and position on a decadal scale. Similar atmospheric processes in the Northwest Pacific produce another counter-clockwise wind regime.

Upwelling and downwelling areas are associated with this wind through a phenomenon called 'Ekman transport'. Just as atmospheric wind is deflected by the Coriolis force, so, too are the moving oceanic water masses. The deflection to the right, however, is manifested at the point of contact between air and water. As depth in the water column increases, so does the angle at which the layers of water are deflected to the right. The velocity of deflected water decreases as depth increases, so that the net effect is that

the layer of water moved by the wind (the 'Ekman layer') is deflected as a whole about 90 degrees to the right of the wind direction (Bearman 1989). Thus, even though the surface of the ocean appears to be moving in the same direction as the wind, the whole body of water moving due to the wind moves to the right. This deflection of the water body is called 'Ekman transport'. Based on Figure 1.1 we can infer that the general case in the Northeast Pacific will be movement of water away from the centres of the major

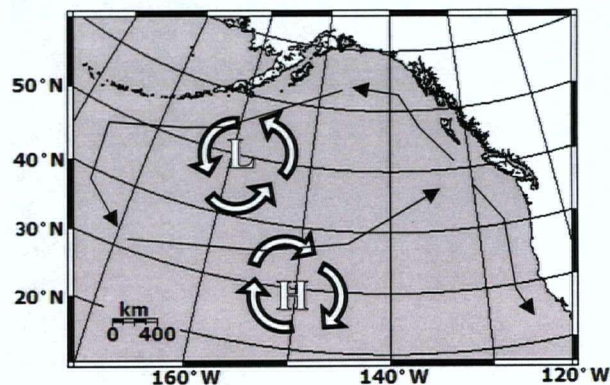


Figure 1.1: Generalised annual average atmospheric and oceanic circulation of the Northeast Pacific. The hollow arrows represent winds generated by air flowing from and towards areas of high (H) and low (L) atmospheric pressure. These winds are deflected to the right by the Coriolis force. The wind acts upon the surface layer of the ocean to generate the current patterns shown as the thin black lines. The counterclockwise flow of surface water is referred to as the Alaska Gyre, and the southern flow, along the coast, is the California current.

gyre, and towards the continental margins of the Pacific Northwest of North America. Such areas are referred to as downwelling zones, as the water transported there must sink or pile up.

The high pressure cells dominant off the coasts of California, Oregon and Washington will tend to cause Ekman transport away from North America causing an upwelling zone, as the coastal surface water which is replaced by deeper water. The oceanography of British Columbia is especially interesting because the boundary of the divergence between upwelling and downwelling occurs off its coast (Thomson 1981).

In the North Pacific downwelling zones tend to be the northern continental margins of B.C., Alaska, Kamchatka and the Kurile Islands. The 'piling up' of water in these places results not only in downwelling but in a compensatory flow away from the hill of water thus created. As was the case with other forces described above, the Coriolis force causes a deflection of such moving water. A current created by such a combination of 'downhill' flowing ocean water is called a geostrophic current. These geostrophic currents form many of the familiar surface currents and are therefore closely associated with the prevailing winds and the resultant upwelling and downwelling zones described above.

In the area of the California current, the implication of these movements is that ocean water is transported away from the continent. Conversely, for the Alaska current, and the Oyashio, ocean water is transported towards Northwest North America and the Kamchatka Peninsula. This has major implications for the production of phytoplankton in the California current which is enhanced by the resulting upwelling of nutrient-rich water from deeper in the ocean (Schwing *et al.* 1996). The waters from the Alaska and Oyashio currents however are forced to the depths as they reach the shore, as there is nowhere else for it to go. Upwelling also occurs at the middle of the Alaska Gyre because the counter clockwise current creates Ekman transport, to the right, which moves upper ocean water away from the middle of the gyre. The deficit of water in the middle of the gyre is made up for by upwelling in the middle of the gyre. Incidentally, this mechanism causes the changes in the mixed layer depth (MLD) noted by Polovina *et al.* (1995) by wind-derived

currents increasing or decreasing in magnitude on seasonal, annual, and decadal scales. Changes in the MLD serve as a valuable indicator for relating atmospheric processes to physical, chemical and biological processes in the open ocean.

The western Pacific subarctic gyre spawns the Oyashio current which runs southward along the Kamchatka Peninsula and the Kurile Islands, joining the eastern flowing currents from the Sea of Okhotsk and the northeastern flowing Kuroshio Current. The combination of these three forms the North Pacific Current, which flows east to join the southern portion of the Alaska Gyre, and northern origin of the California Current.

The place at which these two currents divide is not geographically fixed. Indeed, it moves monthly and interannually in response to seasonal and interannual changes of atmospheric pressure and, therefore, wind. On average the BC coast tends to be in the downwelling zone during the winter but upwelling may, during the summer, extend as far north as North Vancouver Island (Thomson 1981). This movement of water not only has an effect on available nutrients, but also can change the relative temperature of the surface layer of the ocean.

It has been suggested that as the magnitude of the Aleutian Low increases various physical mechanisms are changed to increase or decrease primary productivity. Examples of such changes in the physical nature of the Northeast Pacific are numerous. Polovina *et al.* (1995) devised a model expressing phytoplankton production as a function of nutrient availability and light extinction via changes to the MLD. As the Aleutian low intensifies, the model suggested that the MLD decreases in the Gulf of Alaska region, which may increase phytoplankton production if light extinction is the primary factor limiting production. Such physical changes, expressed through a number of climate indices, could act through primary production to cascade up the food web leading to larger biomasses of several species of commercially exploited fish. Studies that have examined this effect include ones specifically on salmonids (Beamish *et al.* 1997, Mantua *et al.* 1997), groundfish and halibut species in particular (Hollowed and Wooster 1992, Clark and Hare 2001), and also bottom-up cascades on Northeast Pacific ecosystems in general

(Beamish 1995, Hare and Mantua 2000, McFarlane *et al.* 2000, Hollowed *et al.* 2001, Benson and Trites 2002)

1.1.3. North Pacific climate variation indices

Several indices of climate variation have advocates proclaiming their utility in the investigation of climate associated changes in the populations of organisms in the North Pacific Ocean. Indices described in the fisheries literature can be grouped in two categories: physical and biological. Most of these indices, and their relation to the North Pacific, were reviewed by Hare and Mantua (2000) who concluded synchronous changes for these indices in both 1979 and 1989, suggested general climatic, or 'regime', shifts at those times. In this study, seven indicators (three atmospheric, three oceanic, and one terrestrial) were considered for comparison with modelled relationships between climate change and fish populations in the Northeast Pacific; the North Pacific Index (NPI), the Aleutian Low Pressure Index (ALPI), the Northern Oscillation Index (NOI), the Pacific Decadal Oscillation (PDO), Coastal 'Bakun' Upwelling Indexes (CUI), salinity in the Strait of Georgia and Fraser River flow. These climate change indicators span a variety of spatial scales that intersect with the spatial scales of the ecosystems modelled. Other indices exist that describe very large scale climate processes in the Pacific, and beyond, such as the Atmospheric Circulation Index or ACI

The NPI is the area-weighted sea level pressure over the region 30°N-65°N, 160°E-140°W and is used to measure decadal variations linked to El Niño Southern Oscillation (ENSO) and La Niña events. The NPI was first described by Trenberth and Hurrell (1994), see Figure 1.2. The winter

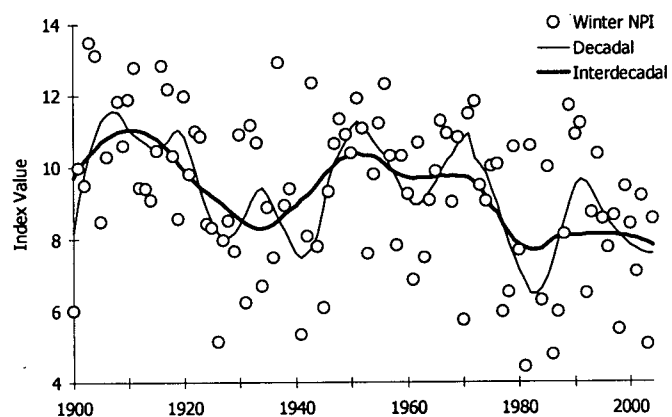


Figure 1.2: Annual average (dots) and interdecadal (lines) trends in the winter (November to March) North Pacific Index. The decadal and interdecadal trends were derived using a LOWESS smoother with 20 and 40 year windows, respectively, and a 2nd degree polynomial.

(November to March) component of this index has been particularly useful in illustrating how change in an atmospheric indicator (*i.e.*, low pressure in the North Pacific) is associated with change in oceanic indicators, *e.g.*, sea surface temperature (SST), nutrients, and primary production. The mechanism that is proposed to cause this is changes in wind-driven transportation of water (Parrish *et al.* 2000). The NPI has been associated with changes in concentration of nitrogen in the Northeast Pacific (Wong *et al.* 1998), suggesting an association with mechanisms driving upwelling and nutrient supply. Analysis of oscillations in the NPI suggests that the climate of the North Pacific varies on two time scales; ≈ 50 and ≈ 20 years (Minobe 2000). The decadal and interdecadal trends shown in Figure 1.2 suggest that the NPI has been at relatively low values since 1980, whereas from 1950 to 1970 it was at relatively high values.

The ALPI, is a measure of the relative intensity of the Aleutian Low pressure system as manifested in December through March, see Figure 1.3. It is calculated as the mean area (km^2) with sea level pressure ≥ 100.5 kPa and expressed as an anomaly from the 1950-1997 mean (King *et al.* 1998). A positive index value reflects a relatively strong, or intense Aleutian Low (Beamish *et al.* 1997). The ALPI

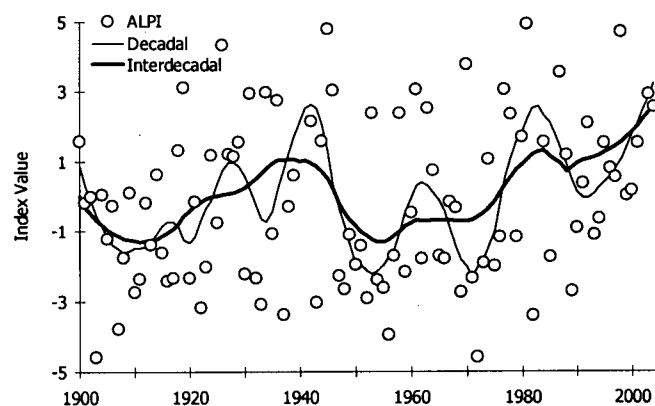


Figure 1.3: Annual average (dots) and interdecadal (lines) trends in the Aleutian Low Pressure Index. The decadal and interdecadal trends were derived using a LOWESS smoother with 20 and 40 year windows, respectively, and a 2nd degree polynomial.

was first described by Beamish and Bouillon (1993) who showed a relation between interannual winter/spring atmospheric pressure and long-term annual catches of pink, chum, and sockeye salmon in the North Pacific. It has been suggested that annual variability in the ALPI may wax and wane and that periods of high annual variability appear to be linked to the mechanisms creating temperature anomalies within the North Pacific (Minobe and Mantua 1999). Since about 1980 the ALPI has tended to be relatively more intense than the 100-year average, which makes sense given the low

values of the NPI over the same time period. Indeed, looking at the two indices there is a mirror image, especially when the smoothed trends in Figures 1.2 and 1.3 are compared.

The NOI (Schwing *et al.* 2002) is based on the difference in sea level pressure (SLP) anomalies at the North Pacific High (NPH) in the Northeast Pacific (35°N, 130°W) and near Darwin, Australia (10°S, 130°E), see Figure 1.4. Because atmospheric connections across the Pacific are

considered by the NOI, it is an indicator not only of climate changes in the Northeast Pacific, but also of tropical climate

changes, *e.g.*, the El Niño Southern Oscillation (ENSO), that influence high latitude climate. The NOI is strongly correlated to SSTs in the world ocean, and subsurface temperatures off the US west coast and is thus assumed to also indicate oceanic teleconnections between the tropics and temperate regions (Schwing *et al.* 2002). The NOI was seen to be strongly associated with changes in the zooplankton community off the coast of British Columbia (Mackas *et al.* 2001). Data for the NOI is measured monthly and can be accessed from the Pacific Fisheries Environmental Laboratory web page (www.pfeg.noaa.gov). Therefore, the NOI can be analysed for interannual variation of seasonal and annual average behaviour. Like the NPI, the NOI appears to have been at an historic low in the 1990s, but unlike the NOI and ALPI it had returned to values more like historic average by 2000.

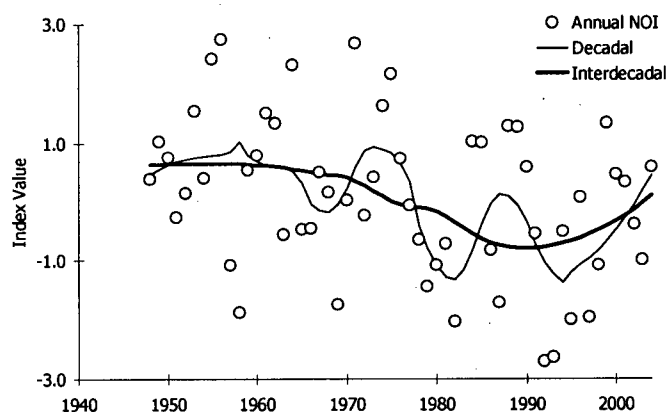


Figure 1.4: Annual average (dots) and interdecadal (lines) trends in the Northern Oscillation Index. The decadal and interdecadal trends were derived using a LOWESS smoother with 20 and 40 year windows, respectively, and a 2nd degree polynomial.

The PDO Index (Mantua *et al.* 1997) is derived from a multivariate analysis of monthly SST anomalies in the North Pacific Ocean, poleward of 20°N. The monthly mean global average SST anomalies are removed to separate this pattern of variability from any global

warming signal that may be present in the data. The PDO has been linked to salmon production in the North Pacific (Mantua *et al.* 1997) and has been shown to coincide with a number of climate change measures; Ocean surface temperatures in the northeastern and tropical Pacific, October-March northwestern North American air temperatures, October-March southeastern US air temperatures, October-March southern US/Northern Mexico precipitation, October-March Northwestern North America and Great Lakes precipitation, Northwestern North American spring time snow pack and water year (October-September) stream flow,

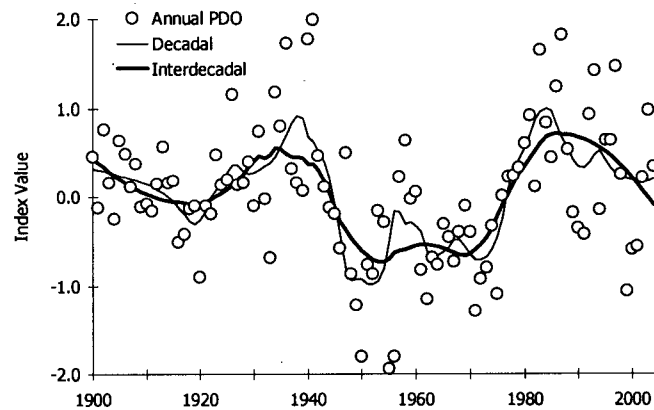


Figure 1.5: Annual average (dots) and interdecadal (lines) trends in the Pacific Decadal Oscillation Index. The decadal and interdecadal trends were derived using a LOWESS smoother with 20 and 40 year windows, respectively, and a 2nd degree polynomial.

and winter and spring time flood risk in the Pacific Northwest (Mantua 1999). The PDO is measured monthly and can be accessed via the internet at:

www.tao.atmos.washington.edu. The PDO appears to have been at relatively high values during the 1930s and most of the 1980s and 1990s, whereas during the 1950s and 1960s it was low, Figure 1.5. This behaviour is generally similar to the behaviour of the ALPI seen in Figure 1.3.

The effect of upwelling upon marine ecosystems is well recognised by oceanographers and fisheries scientists. 'Bakun' upwelling indices have been estimated for several points along the West coast of North America (Bakun 1973) and updated by Schwing *et al.* (1996). These indices are derived as a function of predicted wind due to known sea surface pressure fields. The Pacific Fisheries Environmental Laboratory measures CUIs as $\text{m}^3 \cdot \text{s}^{-1} \cdot 100 \text{ m coastline}^{-1}$, and data is available monthly from 1946 to the present and daily from 1967 to the present at www.pfeg.noaa.gov. As an example of upwelling trends off the BC Coast, Figures 1.6 and 1.7 show the winter and summer values from 48°N, 51°N, and 54°N, off the BC coast. Upwelling and associated currents cause chemical

changes, *e.g.*, nutrients available to phytoplankton or as a mechanism of physical changes, *e.g.*, the transportation of crab larvae to recruiting areas (Botsford and Lawrence 2002). Upwelling off the BC coast is calculated for three stations; Southeast of Vancouver Island at 48°N, off Queen Charlotte Sound at 51°N and off Graham Island, Haida Gwaii, at 54°N. Five aspects of upwelling trends from these stations are germane to the present discussion. The first is that all three stations show strong downwelling conditions prevalent in the winter. Second, the magnitude of winter downwelling is greater than that of summer upwelling, Figures 1.6 and 1.7. This is due to the relatively stronger winds of winter months which generate the water movement. Third, in the summer, the Olympic Peninsula and Queen Charlotte Sound almost always have upwelling, whereas Graham Island varies between upwelling and downwelling decadal trends, Figure 1.6. Fourth, the relative upwelling or downwelling trends appear to wax and wane on cycles varying from 15 to 25 years. Fifth, the winter trends at all three stations appear to be highly correlated, whereas those for summer are less so.

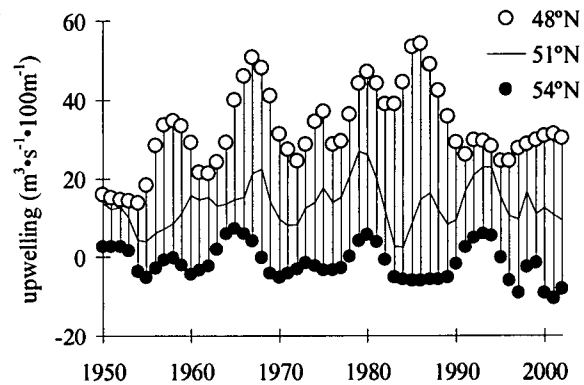


Figure 1.6: Summer (June, July and August) upwelling at coastal stations in British Columbia. The values were filtered by a LOWESS smoother with a 20 year window and a 2nd degree polynomial.

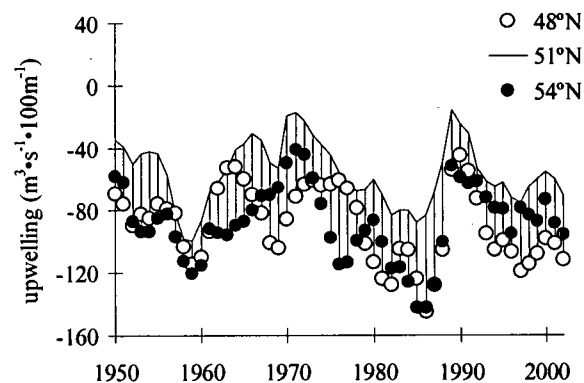


Figure 1.7: Winter (December, January and February) upwelling at coastal stations in British Columbia. The values were filtered by a LOWESS smoother with a 20 year window and a 2nd degree polynomial.

The seasonal trends of upwelling at the BC stations are also an indicator of the latitudinal position for the divergence of the California and Alaska currents. This divergence moves north in the summer, to about 54°N, and south in the winter, usually to about 48°N. The actual position of the divergence northwards or southwards can be detected by the

presence or absence of upwelling in the summer at 51°N and 54°N. The absolute latitudinal position of the seasonal divergence point thus changes from year to year in addition to seasonal and interannual changes of magnitude of upwelling or downwelling. Therefore, the extent of the BC coast that might be characterised at any time by upwelling, downwelling or some mix of the two states is variable for the same time not only in different months but in different years. This implies very different physical and chemical situations for the organisms in the BC shelf can exist at the same calendar date in different years or during subsequent decadal cycles. CUIs have been used in studies examining environmental linkages to such organisms as zooplankton, crabs, groundfish, small pelagics, salmon, and marine birds (Schwing *et al.* 1996).

Variations in ocean salinity are driven by the currents and upwelling trends described above. On the scale of the World Ocean salinity is determined by the movement of upper, intermediate, deep, and bottom water masses which move around the globe on time scales of up to hundreds of years for bottom water (Bearman 1989). Salinity can also vary over relatively small scales, especially in

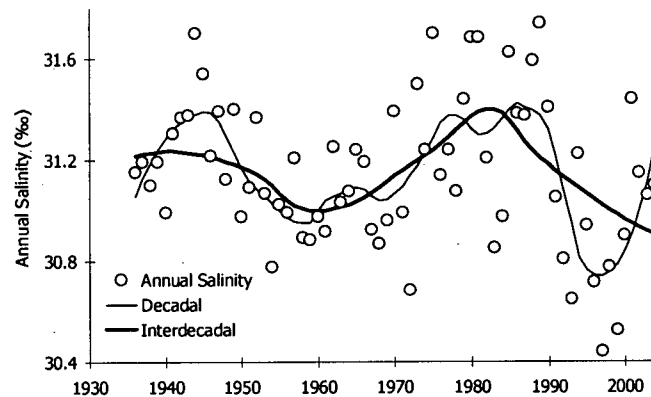


Figure 1.8: Average annual (dots) and interdecadal (lines) trends in surface water salinity at Race Rocks (48.31°N, 123.54°W). The decadal and interdecadal trends were derived using a LOWESS smoother with 20 and 40 year windows, respectively, and a 2nd degree polynomial.

the confines of an inland sea like the SoG, due to the mixing of ocean water, via the Strait of Juan de Fuca, and river water from the Fraser and others. The fjords of the SoG are characterised by decreasing salinity and depth towards the head of the fjord (Thomson 1981). Water movement in the SoG is dependent on seasonal and interannual changes to tides and currents bringing ocean water in from the Pacific Ocean and runoff bringing fresh water from the many rivers. Salinity, therefore, is a useful proxy for general changes in the characteristics of the aquatic environment of the SoG. The Canadian Department of Fisheries and Oceans maintains a data set of various oceanographic

conditions measured at light stations on the BC coast. The longest continuous record for salinity in the area is that for Race Rocks, Figure 1.8. Trends in Race Rocks salinity showed high correlation to salinity trends of other available salinity time series for the Strait of Georgia; Active Pass, Cape Mudge, Chrome Island, Departure Bay, Entrance Island, Race Rocks, and Sisters Islets. The use of salinity measured at Race Rocks as an indicator of characteristic changes in water of the SoG (though it is just outside the SoG) is further supported by the fact that the vast majority of salt water that enters the SoG is carried in on currents moving by the Race Rocks, through the Strait of Juan de Fuca (Davenne and Masson 2001). On a decadal scale salinity in the SoG appears to have gone through two cycles since the 1930s with periods of high salinity in the 1940s and 1980s and low salinity from 1950 to 1970 and during the 1990s. Indeed, the low salinity of the 1990s included the three lowest average annual salinities of the entire period of record.

The Fraser River is the largest source of fresh water for the SoG, and its flow trends and resulting changes in estuarine circulation around the river mouth can effect biological properties at the scale of the whole SoG. The Fraser river has surface mixing dynamics similar to what occurs in a fjord, but spread over a wider area. Estuarine processes in the SoG have been associated with changes in the

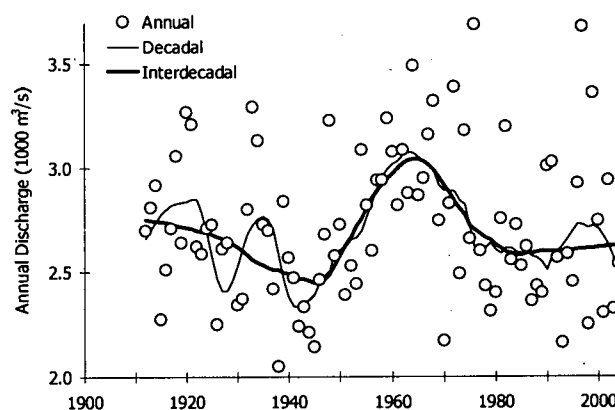


Figure 1.9: Average annual (dots) and interdecadal (lines) trends in Fraser River flow measured at Hope, BC. The decadal and interdecadal trends were derived using a LOWESS smoother with 20 and 40 year windows, respectively, and a 2nd degree polynomial.

dynamics of phytoplankton and zooplankton at time scales ranging from days to years (Li *et al.* 2000, Yin *et al.* 1997). Links between changes in higher trophic level species and salinity in the SoG have not been as conclusive. Fraser River flow was taken from the gauge at Hope, British Columbia, which is available in monthly form from the Water Survey of Canada at <http://www.wsc.ec.gc.ca/>. The interdecadal trend of the Fraser River flow, Figure 1.9, suggested that average annual flow tended to be high in the 1960s and

relatively lower from 1980 to 2004. There does appear to be a moderate influence of the Fraser River upon salinity in the SoG, *i.e.*, high flow results in low salinity, when the trends in Figures 1.9 and 1.8 are compared at the decadal time scale. There appears to have been synchrony between low flow and high salinity in the mid 1940s and 1980s and high flow with low salinity in the 1960s and 1990s. It has also been observed by Moore and McKendry (1996) that a regime-like change in BC snowpack, in the mid 1970s, coincided with a step decrease in annual Fraser River discharge. Any influence of the Fraser River upon the biota of the SoG, though, is likely to be mediated through the effects of Pacific Ocean waters coming via currents from the Strait of Juan de Fuca.

1.2. Defining ecosystems for analysis

1.2.1. Geographic boundaries

Based on the scale differences between these environmental indices, and their wide application to changes in marine populations, an examination of their influence on different sized ecosystems is feasible. Linking the size scale of a climate index to the size scale of an ecosystem is also justified in that the time scale over which change occurs is positively correlated with the spatial scale over which it is measured (Pahl-Wostl 1998). This implies that if an environmental signal is to be detected then it would be more likely to be manifested in ecosystems of similar temporal and spatial scale as suggested by Denman (1994) and O'Neill and King (1998). It is proposed that by modelling three different sized North Pacific ecosystems, a useful hierarchy is created to capture different scale population changes that may more accurately reflect differently scaled climate change indices. The proposed ecosystems to model are: the Strait of Georgia, including DFO statistical areas 13-19, 28, and 29, as defined by Thomson (1981); the BC coast and continental shelf from all fjords, inlets, and embayments to the continental shelf break; the Northeast Pacific and Eastern Bering Sea encompassing all continental shelf waters from the West Coast of Vancouver Island and Strait of Georgia to the Bering Strait.

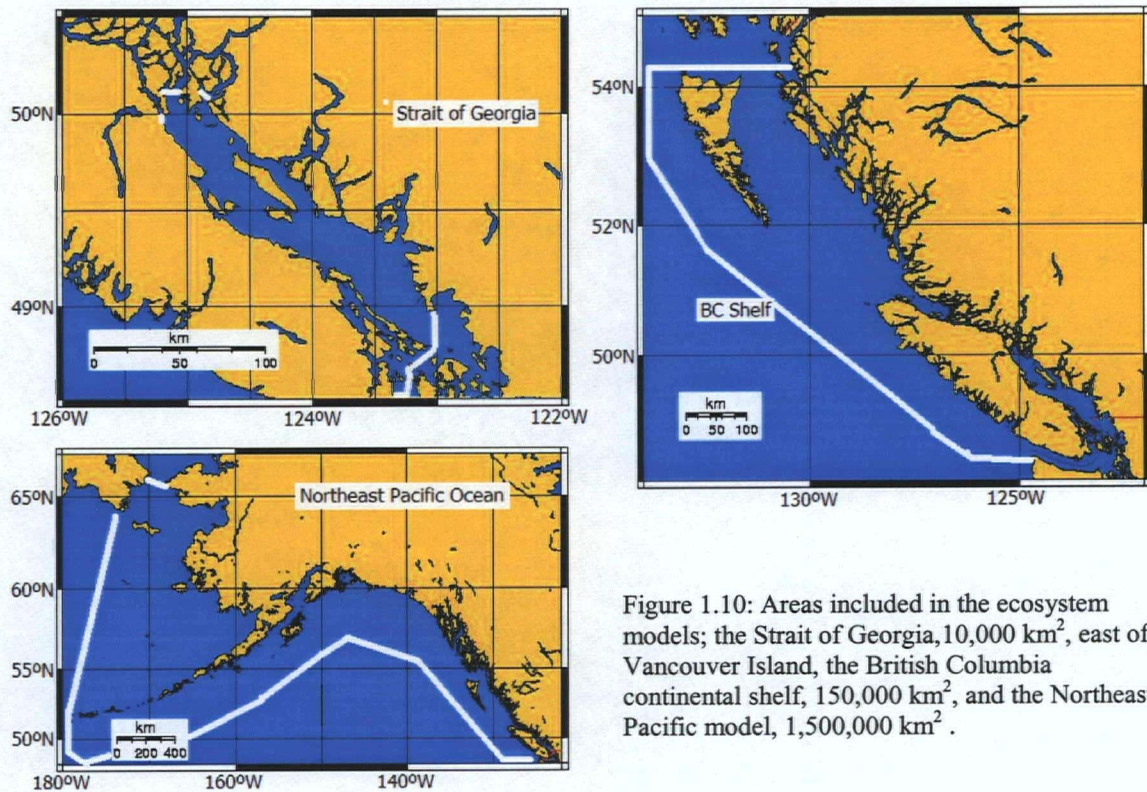


Figure 1.10: Areas included in the ecosystem models; the Strait of Georgia, 10,000 km², east of Vancouver Island, the British Columbia continental shelf, 150,000 km², and the Northeast Pacific model, 1,500,000 km².

These North Pacific ecosystems (Figure 1.10) also approximate the geographic areas over which many climate change phenomena have been manifested and studied (Hare and Francis 1994, Polovina *et al.* 1995, and Francis *et al.* 1998). North Pacific ecosystems are also characterised by high-quality time series data of catch, biomass, and mortality from 1950 to the present from organisations such as Canada's Department of Fisheries and Oceans, The National Marine fisheries Service of the US, and transnational organisations like the International Pacific Halibut Commission and the North Pacific Anadromous Fish Commission. Thus, the ecosystems of the North Pacific present a qualified opportunity to compare ecosystem processes to climate processes. In order to make comparisons between the ecosystems and across scales the ecosystems should also contain the same or very similar species and species groups.

1.2.2. Species modelled

Ecopath with Ecosim (EwE) is a modeling system that emphasises dynamics of large vertebrates, especially fishes and marine mammals. It is in the commercially-exploited

fish and charismatic megafauna that science and management possesses the most detailed knowledge of factors affecting growth, feeding and mortality, *i.e.*, of the main ingredients for an ecosystem model. Further, many of the invertebrates and planktonic organisms are not well characterised in these modelling parameters, although the vast majority of biomass in these marine ecosystems is plankton. It is also known that most of the invertebrate populations, especially the planktonic ones, go through population changes that vary on a much higher frequency and at a much finer resolution than fishes and mammals, *e.g.*, localised blooms, making long-term changes difficult to characterise. Ecopath with Ecosim does have the ability to resolve the effects of organisms that experience changes on very different, *i.e.*, fast or slow, time scales by employing variable speed splitting and by explicitly incorporating the effects of “micro-scale behaviors on macro-scale rates: top-down vs. bottom-up control” (Christensen *et al.* 2004).

Table 1.1 shows that most of the detail in the species groups modelled was in commercially exploited fish. Groups became increasingly aggregated as the trophic ‘distance’ from the commercial fish groups increases. As long as the model captures the gross characteristics of the plankton and invertebrate groups the trophic responses in the groups modelled in higher detail can still be captured.

Table 1.1: Groups used in the North Pacific Ecopath with Ecosim models. Note that not all models included all groups. The BC shelf and Georgia Strait models do not have **Atka mackerel, northern rockfish, and Alaska plaice**.

birds / mammals	pelagic piscivorous birds, demersal piscivorous birds, zooplanktivorous birds, odontocetae, mysticetae, sea lions, seals
pelagic fishes	salmon shark, pelagic sharks, pink salmon, chum salmon, sockeye salmon, coho salmon, chinook salmon, myctophids, predatory pelagic fishes, small pelagic fishes
demersal fishes	dogfish, rajidae / ratfish, Pacific Ocean perch, rockfish other, Pacific hake, lingcod, yellowfin sole, rock sole, flatfish other, small demersals, Atka mackerel, northern rockfish, Alaska plaice
invertebrates	krill, carnivorous zooplankton, herbivorous zooplankton, jellies, large squids, small squids, shrimps, crabs, bivalves, echinoderms, other benthos, phytoplankton, macrophytes, detritus
multi-stanza	arrowtooth flounder, Pacific cod, Pacific halibut, sablefish, walleye pollock, Pacific herring

1.2.3. Delimiting the ecosystems

Notwithstanding the ability of a particular methodology to estimate large-scale population changes to individual species of phytoplankton, the ecosystem characteristics of phytoplankton were used in conjunction with physical and chemical oceanographic characteristics, by Longhurst (1995) to divide the World Ocean into 56 'biogeochemical provinces' (BGCPs). The ecosystems under consideration here correspond, collectively to four originally defined by Longhurst (1995) and subsequently modified in Pauly *et al.* (2000) as the Gulf of Alaska (ALSK), Pacific Subarctic West (PSAW), Pacific Subarctic East (PSAE) and enclosed high latitude seas (BERS, *i.e.*, Bering Sea and Sea of Okhotsk). The modification of Pauly *et al.* (2000) was to merge the BGCP concept, defined by physical criteria, with the Large Marine Ecosystem (LME) concept, defined by ecological criteria, discussed in works by Sherman and others, *e.g.*, Sherman *et al.* (1990). The resulting ecosystems are compatible between the two frameworks and therefore also share a hierarchical scale between biology, chemistry and physical boundaries. Ecosystems thus defined should be well suited for use in comparing physical climatic influences to ecosystem dynamics because the physical oceanographic changes in the ecosystems necessarily reflect climate effects. In this sense, the ecosystems are stable over long time periods

1.2.3.1 The Strait of Georgia

The smallest of the ecosystems to be considered, the Strait of Georgia (SoG), is not big enough to be defined as either a BGCP or a LME, being only about 7,000 km² (Beamish *et al.* 2001) but it has many characteristics that warrant examination as an ecosystem. For example, the SoG is an 'inland sea', and is therefore quite isolated, physically, from surrounding marine waters. With reference to the requirements of an ecosystem model, this implies that the importance of outside factors relative to internal forces is relatively small in the model causing increased predictability (Goodwin and Fahrig 1998).

There have been previous EwE SoG models, *e.g.*, Pauly *et al.* (1996), Beamish *et al.* (2001), and Martell *et al.* (2002). All of these suggested that the majority of the trophic interactions among species modelled occurred within the SoG. Martell *et al.* (2001) showed that many dynamic population changes in higher vertebrates could be explained on the basis of bottom-up and top-down interactions within the SoG. Despite the fact that the SoG is the smallest area scale ecosystem in this study, even the largest scale climate processes necessarily affect it. It has also been suggested that there may be climate effects in the SoG driving bottom-up effects, *e.g.*, wind speed (Martell *et al.* 2001), which act at even smaller scales than the two most obvious SoG climate indices; Fraser River flow and SoG salinity.

1.2.3.2. The BC Shelf

The BC shelf (BCS) ecosystem is approximately 170,000 km² (Hunt *et al.* 2000). The BCS is interesting in that the northern portion of the California current manifests itself in the summer, though the duration and intensity of the upwelling due to the appearance of the current changes on an annual and decadal basis (see Figures 1.6, and 1.7). The place at which the California current and Alaska current divide, however, is not geographically fixed. Indeed, it moves seasonally and interannually in response to seasonal and long-term patterns of atmospheric pressure and therefore wind. On average the whole of the BC coast tends to be in the downwelling zone during the winter, while in the summer the upwelling may extend as far north as North Vancouver Island (Thomson 1981). The movement of water masses not only has an effect on available nutrients, but also impact the relative temperature of upper ocean waters. The organisms within the ocean will respond to the movement of the water masses either through direct movement, *e.g.*, migrating fish, or by modifying their life history to respond to predictable appearances of the water masses, *e.g.*, phytoplankton blooms. The BCS ecosystem is different from the Northeast Pacific as a whole in that there is an almost system-wide seasonal change from upwelling to downwelling. Further, the upwelling and downwelling likely influences the SoG due to the current movement of waters into the SoG via the Juan de Fuca Strait (Davenne and Masson 2001).

Although the southern physical boundaries of the BCS ecosystem are obviously delimited by features such as the Juan de Fuca Strait, land to the east and a continental slope to the west, the northern boundary is the politically imposed Alaska-British Columbia border. There is some movement of fishes, mammals and birds across this border, a concern offset by the availability of high-quality local data sets from the Canadian Department of Fisheries and Oceans, see, *e.g.*, Stocker *et al.* (2001). Another argument to study the BCS as an ecosystem is the presence of local stocks of important and abundant species like salmon and herring (with their own population dynamics) which are part of metapopulations extending along the west coast of North America (with population dynamics resulting from the synthesis of several stocks). Many of the stocks that spend most of their time in Canadian waters are well studied. Detailed assessments for the herring stocks of British Columbia extend to 1950, see, *e.g.*, Schweigert (2000). Contrasting ecosystem interactions of such species considered at both the scale of populations and that of stocks (the Strait of Georgia possesses its own herring stock) will demonstrate how differently scaled climate effects act upon both stocks and the metapopulations to which they belong. Many demersal species like rockfish, sablefish, Pacific cod and lingcod are thought to have a high fidelity to a rather small spatial range (Stocker *et al.* 2001). Such local populations, of larger population complexes, likely respond to climate variations manifested over smaller scales. Thus, temporal changes in the population dynamics of many of the commercially important fish stocks in the BCS ecosystem should be explained by local environmental and fisheries changes.

1.2.3.3. The Northeast Pacific Ocean

The Northeast Pacific ecosystem is comprised of two LME's, the Eastern Bering Sea (EBS, which includes the Aleutian Islands) and Gulf of Alaska (GoA) with a total area of approximately $2.8 \cdot 10^6 \text{ km}^2$ (see www.seaaroundus.org for LME areas and other characteristics). Connecting the two LMEs seems appropriate given the connection between the Gulf of Alaska and Eastern Bering Sea via the Aleutians. There are large movements of fish populations between the two areas, *e.g.*, Bristol Bay sockeye (Burgner

1991), Aleutian walleye pollock (Barbeaux *et al.* 2003), and Gulf of Alaska arrowtooth flounder (Turnock *et al.* 2003). Given this large exchange of biomass between the two LMEs, analysing them as one ecosystem, with migrations considered as movements within that larger continuous area, is a simple alternative to modelling both systems and the processes of their exchanges.

1.3. Analysis of results

For each ecosystem population changes from 1950 to the present will be simulated. The predictions made by these models, to explain changes in populations, are then compared to reference empirical data. By examining how the models explain causes of population change, I seek to determine relationships between different scales of climate indicators and different scales of ecosystems. Detecting relationships between ecosystem scale and climate is possible because the models can be parameterised via a 'vulnerability' setting which indicates how far species are from their carrying capacities. The vulnerability setting is a consequence of dynamics arising from the foraging arena hypothesis of Walters and Juanes (1993), which suggests that prey species attempt to minimize, even at the cost of reducing their own food intake, the risk of being eaten. In EwE the dynamics of this feeding interaction can be varied between a state in which the prey and predators move randomly in their environment, *i.e.*, a Lotka-Volterra type interaction, or one in which consumption by predators is fully dependent upon changes in prey productivity (Walters *et al.* 2000). In Ecosim the vulnerability setting can be adjusted for all trophic (predator-prey) linkages as selected by the modeller. Deciding which vulnerabilities to examine for studying the potential ecosystem dynamics is discussed in Christensen *et al.* (2005) and ways to test their effects on ecosystem dynamics is discussed in Walters *et al.* (2000) and Christensen and Walters (2004). The different predator prey configurations and vulnerability settings of the ecosystems modelled should reflect temporal and spatial differences in predation mortality.

EwE models can also be given input data of fishing and total mortality over time to account for changes in the production of a species over time (Christensen *et al.* 2005).

Reference data of biomass from single-species stock assessment can be used to compare to time series of biomasses predicted by the model. The goodness of fit in such model simulations is measured by Ecosim as a weighted sum of squared differences (SS) between log reference and log predicted biomass (Christensen *et al.* 2005). SS can be influenced by changing vulnerability settings at one of more of the trophic linkages to produce a predicted time series of biomass closer to the reference data. Examples of such biomass exercises include an examination of tuna and billfish ecosystem dynamics in the Central North Pacific Cox *et al.* (2002a, 2002b) and fisheries effects in the Baltic (Harvey *et al.* 2003). It is also possible to have Ecosim minimise the SS by creating a time series of primary production anomalies, *e.g.*, changing phytoplankton production over the time period modelled. One early example of an Ecosim model using a primary production anomaly was of the interactions between lobster and monk seals in the French Frigate Shoals (Polovina 2002). It was determined that when the model incorporated an observed decline in primary production the predicted trajectory of biomasses for both lobster and seals was much closer to reference time series than by accounting for fisheries and trophic interactions alone. Similar primary production forcing was used in the Strait of Georgia by Martell *et al.* (2002) to improve predicted time series of biomass for a range of species including seals, herring, salmon, and hake. This suggests that Ecosim may be a useful tool to investigate large-scale and persistent regime shifts (Christensen and Walters 2004), *i.e.*, the type of research central to this project.

In preliminary work with two of the models for this project, the Northeast Pacific and BCS models, results indicated that the predicted primary production anomalies were correlated with climate indices derived from

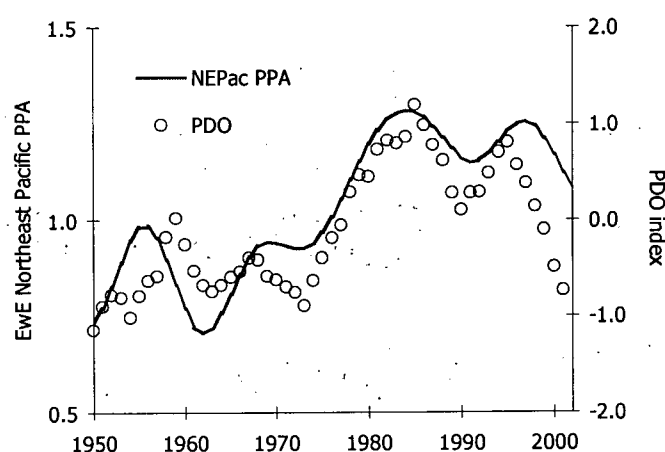


Figure 1.11: A comparison of changes in the predicted PPA for a Northeast Pacific EwE model with changes in annual values of the Pacific Decadal Oscillation from Preikshot (2005). Both time series were smoothed using a five year running average.

changes over similarly scaled areas (Preikshot 2005). In the case of the Northeast Pacific model, the predicted time series were most similar to reference biomass time series from single-species stock assessments in 50-year simulations incorporating PPAs that were highly correlated to the Pacific Decadal Oscillation (Preikshot 2005), see Figure 1.11. The time series for the BCS model differed from the NEPac model in that the assessments of reference time series were from sub-populations or portions of the NEPac stocks. Given this different reference data the predicted primary production anomaly for the BCS model was more highly correlated to the upwelling index measured at 54°N (off the Queen Charlotte Islands), Figure 1.12.

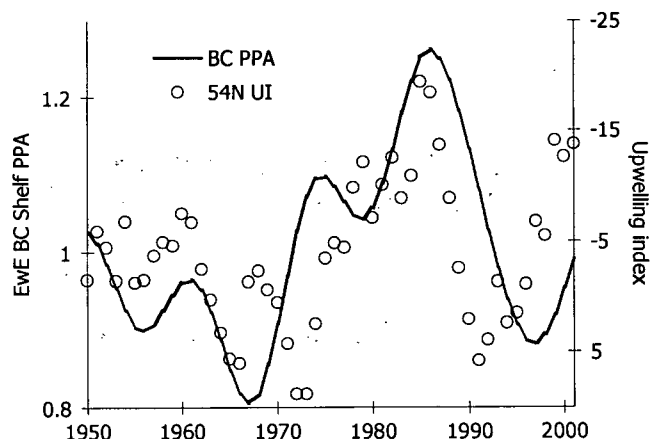


Figure 1.12: A comparison of changes in the predicted PPA for a British Columbia Shelf EwE model with changes in the annual upwelling index (the departure of annual upwelling values from the long-term average), measured at 54°N, from Preikshot (2005). Both time series were smoothed using a five-year running average.

For the correlations shown in Figures 1.11 and 1.12 the PPAs were derived using a five-year running average. Comparisons in this study, however is done using the locally weighted scatter-plot smoothing (LOWESS) technique (Cleveland 1979). LOWESS is preferred to smoothing by use of a moving average because it is less susceptible to outliers in the data set. LOWESS references a moving window of data points, but weights each differently, as opposed to the equal weights of the moving average. Within the data window, a regression line is fitted first by weighting each point in proportion to its distance from the value being estimated with a cubic weighting formula. “These weights are then used to compute a weighted linear regression for points within the window, and this is repeated for all points. Prediction residuals are then computed as the difference between actual values and the weighted regression. The initial weights are then adjusted, giving more weight to observations with low residuals in the first pass and less weight to outliers. This refinement step may be iterated until the weights no longer change appreciably” (Urban

2003). Determining the optimum window size and the degree of the linear regression used in fitting the underlying data can be realised by use of a log likelihood analysis (Hilborn and Mangel 1997).

Biomass time series and primary production anomalies are analysed to examine whether model scale influences periodicity and amplitude of change. The primary production anomalies are also compared to available climate change indices to examine whether model scale is reflected in the presumed underlying environmental changes. Note that because the PPAs are a measure of relative changes in annual production they are not directly comparable between models. However, because parameterisation of phytoplankton B and P/B was quite similar for the initialisation of the simulations, the relative magnitude of change in the PPAs will be quite similar. Though seasonal dynamics can be particularly drastic in small highly productive groups this scale of temporal resolution was not examined here. Past modelling exercises suggest that while highly productive species do respond dramatically to seasonal forcing such results, while visually arresting, do not change the decadal scale temporal behaviour (Christensen and Walters 2004, Christensen *et al.* 2005).

Vulnerability estimates can be used to simulate different ecosystem control hypotheses, *i.e.*, bottom-up or top-down, to examine how PPAs and biomass time series differ under changed assumptions of trophic control. The analysis of these data is conducted to provide insight about the proper scale at which to model ecosystems given the need of management and research to differentiate fishing and climate effects upon species units ranging from stocks, *i.e.*, smaller scale to metapopulations, *i.e.*, larger scales. By understanding how climate change is manifested in aquatic food webs, it may be possible to devise management strategies which are robust to predictable environmental variation. Some excitement has recently been generated with the publication of a study which suggests that El Niño events can be predicted with lead times of as much as two years (Chen *et al.* 2004). Such predictive power, in conjunction with ecosystem modeling, may help determine how to mitigate the effects of both climate change and fishing upon exploited marine species.

2. Methods

2.1. Introduction to the methodology

Three models were constructed of Northeast Pacific ecosystems (see Figure 1.9). The first was for the Strait of Georgia (SoG), as defined by Thomson (1981). The second was the coastal shelf ecosystem lying within the territorial waters of British Columbia, Canada (BCS), which includes the SoG. The third was the Northeast Pacific Ocean (NEPac) comprised of the Eastern Bering Sea, Gulf of Alaska, and BCS. The models were made up of 50 species groups, with greater detail in those species targeted by commercial fisheries. The models were designed to examine how bottom-up and top-down ecosystem control dynamics change with area scale. To validate ecosystem model predictions of historic changes in biomass, predation, and mortalities, comparisons were made to stock assessment data of biomass, total mortality (Z), and catch (Y). Three elements of the models area, species, and dynamics of biomasses and climate, define the three major components of this chapter. These three elements also form a logical progression in describing how an ecosystem model is prepared, *i.e.*, the area the model represents, what the species are, and how changes in those species can be described in that place.

2.2. Ecosystem boundaries and biota

2.2.1. Ecosystem boundaries

Selection of areas for modelling was based on the research goal of examining how populations in ecosystems with similar species composition are affected by climate variation at differencing area scales. It was possible to achieve this goal for the Northeast Pacific because of the long history of stock assessment in the region, coupled with detailed understanding of oceanographic processes. As discussed in the introduction, a strict definition of ecosystem boundaries was not of primary concern in the formulation of the models.

The smallest scale model, the Strait of Georgia, was comprised of the waters bounded by Vancouver Island and the Canadian Gulf Islands, to the west and south, and the British Columbia mainland, to the north and east, including estuaries, fjords, lagoons, river deltas and the like. The area of the Strait of Georgia (SoG), not including estuarine waters was reported as 6 900 km² by Thomson (1981). The British Columbia shelf (BCS) ecosystem was defined as the marine waters of British Columbia, Canada to the 500 m isobath.

The BCS ecosystem also included estuarine waters, the Strait of Juan de Fuca, and the aforementioned SoG. Hunt *et al.* (2000) used a similar area, based on 'oceanographic domains' to study diets of marine birds and mammals, which they called 'California Current North'. The California Current North region was reported to be 166,000 km².

The Northeast Pacific (NEPac) ecosystem included the BCS (and, therefore, also the SoG) and extended north through the Gulf of Alaska (GoA), including the western extension of the Aleutians, and even further north to encompass the eastern continental shelf of the Bering Sea. The northern extent of the NEPac ecosystem was bounded by the geographic constriction of the Bering Strait. As with the BCS ecosystem, the seaward extent of the NEPac ecosystem extended to the 500 m isobath. Hunt *et al.* (2000) provided estimates of the areas of three regions in their diet study which overlap with the NEPac model, California Current North, Gulf of Alaska, and Eastern Bering Sea and shelf, which totalled about 1,600,000 km².

2.2.2. Ecosystem biota

Before describing the derivation of parameters for the basic Ecopath input values and reference time series data used in Ecosim time dynamics models, a couple of matters relating to general practices should be mentioned. Biomass, consumption, mortality, diet and fishery data for the Ecopath basic input were determined by finding the best possible recent estimates. To allow Ecosim runs from 1950 to the present, the biomass, fishing mortality and / or total mortality were then changed for groups when stock assessment data were available. The 1950 models were then rebalanced to accommodate the different

ecosystem demands of that period. All other parameters and species groups were, thus, assumed to be unchanged in the absence of evidence to the contrary.

For most of the fish groups consumption (Q/B), values were determined by the empirical equation available in FishBase (Froese and Pauly 2004), which requires that estimates be provided for W_{∞} , average environmental temperature, the ratio of the square of the height of the caudal fin to its surface area (a measure of the swimming and metabolic activity of a fish with a higher ratio implying more swimming and greater activity), and food type (detritivore, herbivore, omnivore, carnivore) (Palomares and Pauly 1998).

To ease comparisons between the three models, species groups were kept as similar as possible, Table 1.1. The BCS model (53 species) differed from the NEPac model (56 species) by omitting Atka mackerel, northern rockfish, and Alaska plaice. The SoG model included the same groups as the BCS model except, in the SoG model, coho salmon and chinook salmon had both adult and juvenile life history stages. In both the BCS and NEPac models all salmon were modelled as five distinct species, with no consideration of life history stages.

In any EwE model, species may be included as unique groups or aggregated with other species that function similarly in the ecosystem. Such single species, or aggregate species, are called 'functional groups'. Because the focus of this modelling effort was the behaviour of the populations of managed commercial fish species responding to environmental forcing and fishing effects, the greatest detail lies in the functional groups of those species. Indeed, each of the focal species was modelled using what is referred to as multi-stanzas, *i.e.*, more than one life history stage of that species was modelled. Other significant species that interact with these important fishes were modeled as single species functional groups, with no attempt to model life history changes. Most invertebrates, zooplankton and primary producers were put into highly aggregated functional groups, some of which contain hundreds of species.

Because any particular group is defined on a continuum ranging from a part of one species' life history to containing anything from two to hundreds of similarly functioning species the quality of the data used to define that group can vary. Although the reader may gain a thorough knowledge of the precision of the data used in the groups of these models by reading the text below, there are also quick-reference 'pedigree charts', in Appendix 1 (Tables A.1.1 to A.1.3) which visually represent the data quality for each of the Ecopath parameters for each modelled group. The pedigree of the data refers to where a particular value arose and what the uncertainty is associated with that datum. In general terms, higher pedigrees are associated with data more rooted in the ecosystem being modelled and are assumed to be associated with lower uncertainty. Ecopath can take the pedigree values for all the data entered in the model to calculate an overall pedigree index, ranging from 0 to 1, in which lower numbers imply a model constructed from low-precision outside data and higher values a model constructed from locally-derived high-precision values. The pedigree charts are followed by tables that show the specific parameter values used as input for each of the groups, described below, for the three Ecopath models (Tables A.1.4 to A.1.8).

2.3. Determination of biomass, production, and consumption

2.3.1. Multi-stanza groups

There were 12 functional groups within the 'multi-stanza' category. These 12 represented six species as adult and juvenile groups; arrowtooth flounder, Pacific cod, Pacific halibut, sablefish, pollock, and herring (plus coho and chinook in the SoG model). All multi stanza groups have been intensively studied by the research community in the Northeast Pacific. This means that not only were the population dynamics well documented over spans of 20 or more years, but also that energetic, dietary, and ontogenetic research had been conducted on them. All of these groups are culturally significant to the civic, provincial, state, federal and first nations communities of the Pacific Northwest. Further, they all spend the majority of their lives, do the majority of feeding, and experience most of their mortality, within the confines of the ecosystems modelled. Lastly, these groups,

when considered together, occupy most of the three-dimensional physical space available in the modelled ecosystems. Herring moves between shallow coastal areas to deep water pelagic habitats, whereas halibut moves from offshore demersal to coastal demersal habitats seasonally, pollock move daily between deep and shallow water (diel vertical migration), sablefish, and Pacific cod are in shallow coastal waters as juveniles, but move to the deeper waters of the continental shelf and slope as they mature, Coho and Chinook patrol the pelagic environment, and arrowtooth flounder are found in many depths on soft bottoms (Froese and Pauly 2004).

Time series of biomasses were available for the multi-stanza, and heavily exploited, groups because of the mandate of governmental agencies to manage these species. Time series of F, Z, or both, therefore, were also found for some. Assessment time series of biomass were used as reference data for Ecosim time dynamic models, to compare to output biomasses. Note that there may be spatial heterogeneity in any species' distribution within any of the three models, but this consideration can not explicitly be captured in either an Ecopath or Ecosim model. Such matters of distribution could be dealt with using Ecospace (Walters *et al.* 1998), but this approach went beyond the scope of this project. As an example of spatially heterogeneous distribution, the walleye pollock stocks of the Bering Sea / Aleutian Islands (BSAI) have usually been far larger than that of the GoA. From the early 1970s to the early 1980s the two areas, however, had more similar biomasses of walleye pollock. The effects of changes in species distribution are dealt with implicitly, in this project, by diet partitioning and vulnerability settings.

The values of the Ecopath basic input parameters for multi-stanza species can be seen in Table A.1.1., while the parameterisation section on salmon contains the parameter values used for coho and chinook multi-stanza groups in the SoG model. For these multi-stanza groups the basic input parameters are slightly different from standard Ecopath groups. The trophic ontogeny of multi-stanza species are modelled explicitly with each stage containing individuals with similar mortality rates and diet compositions. Biomass and Q/B values for one leading stanza (often one for which assessment data is available) are entered and the biomass and Q/B are calculated for the other stanzas by Ecopath which

assumes that body growth follows a von Bertalanffy growth curve and that the species initially has stable mortality and relative recruitment to have achieved stable age-size distribution (Christensen *et al.* 2005). Thus, in order to allow Ecopath to calculate unknown biomass and Q/B values, the user enters values for the von Bertalanffy curvature parameter (K), a recruitment power value (between 0 and 1), a biomass accumulation rate (BA), a value for weight at maturity divided by asymptotic weight ($W_{\text{mat}}/W_{\infty}$), and a start age for each stanza of that species. In all cases the recruitment power value was set to 1 and the BA value to 0. In most cases K was estimated in FishBase (Froese and Pauly 2004), with estimates of L_{∞} for relevant species if there were more than one species in a group, *e.g.*, other rockfish and myctophids. The $W_{\text{mat}}/W_{\infty}$ estimates were usually obtained from converting L_{mat} and L_{∞} values, as reported in stock assessment documents for the relevant species.

2.3.1.1. Arrowtooth flounder

The geographic range of arrowtooth flounder (*Atheresthes stomias*) extends from California to the Eastern Bering Sea (EBS), although it is more abundant in the northern portion of its range (Hart 1973). Arrowtooth flounder are found in depths from 20 to 1,000 m but are most common from 200 to 400 m and tend to move to deeper water in winter (Love 1996). Information was found on biomass, and mortality for the Gulf of Alaska (GoA) (Turnock *et al.* 2003b), EBS (Wilderbuer and Sample 2003), and BCS (Fargo and Starr 2001). P/B was derived for all populations by using mortality information in (Turnock *et al.* 2003b), which has $M = 0.2 \text{ year}^{-1}$ for age 3+ females and 0.35 year^{-1} for age 3+ males. Therefore we can assume a weighted $M \approx 0.25 \text{ year}^{-1}$ if there will be more females in the resulting cohorts as they age. Fishing mortality was estimated as between 0.01 year^{-1} and 0.03 year^{-1} for the stock over the last few decades, thus $Z \approx 0.25 \text{ year}^{-1}$. Mortality for juveniles was assumed to be higher: 0.5 year^{-1} . $W_{\text{mat}}/W_{\infty}$ was calculated from length at maturity information (Turnock *et al.* 2003b). Length at 50% maturity was estimated at 47 cm, and $L_{\infty} \approx 100 \text{ cm}$, therefore, $L_{\text{mat}}/L_{\infty} \approx 0.5$, *i.e.*, $W_{\text{mat}}/W_{\infty} \approx 0.125$. For arrowtooth flounder only time series for the BSAI and GoA were available. Because there was no BCS-specific biomass time series available, it

was assumed that the BC population would reflect relative changes in the GoA stock. The BCS biomass time series was calculated by assuming that the total biomass in the BCS area was about one tenth of the total biomass in the Gulf of Alaska. Based upon catch per unit effort distribution maps of the arrowtooth flounder fishery in Turnock *et al.* (2003) the portion of the arrowtooth flounder stock in BC is likely to be merely a small fraction of the total biomass. No time series were available for this species in the SoG.

2.3.1.2. Walleye pollock

Walleye pollock (*Theragra chalcogramma*) occurs from central California north to the Bering sea and west to the Sea of Okhotsk and Japan and prefer waters to about 400 m (Hart 1973). Walleye pollock migrate seasonally and move offshore during the winter for spawning (Love 1996). The Alaskan fishery on this species is one of the largest single-species fisheries in the world. There appear to be three distinct stocks in the United States portion of the Bering Sea (Ianelli *et al.* 2003), whereas there is little evidence to suggest the presence of more than one stock in the GoA area (Dorn *et al.* 2003). Stock assessment information was available for BSAI and GoA populations. Dorn *et al.* (2003) estimated M as 0.1 year^{-1} and F as 0.07 year^{-1} and 0.13 year^{-1} in 2003 and 2004, respectively, so $P/B \approx 0.2 \text{ year}^{-1}$. However, Ianelli *et al.* (2003) stated that by age 4 M is 0.3 year^{-1} and was for all subsequent years, while for age 1, 2, 3 it was 0.900 year^{-1} , 0.450 year^{-1} , and 0.300 year^{-1} . FishBase (Froese and Pauly 2004) listed default L_{mat} and L_{∞} values of 39 cm and 73 cm, thus, $W_{\text{mat}}/W_{\infty} \approx 0.15$. As no time series of biomass was found for pollock off the BC coast, it was assumed that the BCS population would reflect relative changes in the GoA stock, as derived above. Maps showing the distribution of catch per unit effort of the pollock fishery in the Gulf of Alaska in Dorn *et al.* (2003) suggested that, like arrowtooth flounder, the proportion of biomass of the stock going into BC waters was a small fraction of the total. The BCS time series of biomass was assumed to be one tenth of the biomass in the Gulf of Alaska, from Dorn *et al.* (2003) divided into the area of the BCS. A time series of catch for walleye pollock in the Canadian EEZ, *i.e.*, the BCS, was obtained from the Sea Around Us (2006) database. For estimating the SoG biomass there were trawl and acoustic surveys available (Beamish *et al.* 1976, Taylor and Barner 1976,

Kieser 1983, and Mason *et al.* 1984), but no stock assessment. Beamish *et al.* (1976) estimated M as 0.84 year^{-1} for pollock in the SoG. Q/B for this group was set for the adult stanza using the FishBase life history tool (Froese and Pauly 2004)

2.3.1.3. Pacific cod

Pacific cod (*Gadus macrocephalus*) occurs throughout the north Pacific from southern California to Korea, preferring to stay in water from 6°C to 9°C with a benthic habit from nearshore shallows to depths of 550 m (Hart 1973). Pacific cod migrate seasonally to shallower water in the spring, after spawning in offshore waters during the late winter (Clemens and Wilby 1961). Stock assessment information was available for three regions: EBS (Thompson and Dorn 2003), GoA (Thompson *et al.* 2003), and the BCS (Sinclair *et al.* 2001). Thompson *et al.* (2003) listed an $M = 0.37 \text{ year}^{-1}$ for the GoA and have recommended an F of 0.29 year^{-1} thus $P/B (Z) \approx 0.66 \text{ year}^{-1}$. Information on $L_{\text{mat}}/L_{\infty}$ was found in Thompson and Dorn (2003) which suggested a ratio of about 0.5, thus a $W_{\text{mat}}/W_{\infty} \approx 0.13$. Assessments of Pacific cod for the BCS extend back to the 1950s (Sinclair *et al.* 2001), while assessments for the BSAI and GoA regions have been done only back to the late 1970s (Thompson and Dorn 2003, Thompson *et al.* 2003). The biomasses appear to have undergone significant changes at both area scales, though the NEPac assessment only dated back to the late 1970s. Pacific cod biomasses are low in the SoG so this species was modelled at a token biomass of $0.001 \text{ t}\cdot\text{km}^{-2}$ in that model.

2.3.1.4. Pacific halibut

Pacific halibut (*Hippoglossus stenolepis*) are found across the north Pacific from Baja California north to the Bering Sea and west to the Hokkaido and the Sea of Okhotsk (Froese and Pauly 2004). It is most commonly found between 55 and 422 m, but may be found in shallower water as juveniles (Hart 1973). The International Pacific Halibut Commission (IPHC) assesses 'stocks' for several geographic regions along the west coast of North America; area 2A (Oregon, Washington), area 2B (British Columbia), area 2C (southeast Alaska), area 3A (central Alaska), area 3B (Alaskan peninsula), Area 4A and

B (Aleutian Islands), and Areas 4C, D, and E (Bering Sea). These 'stocks' have been modelled as separate populations because it was thought that little movement occurred between areas, *i.e.*, high habitat fidelity by adults (Sullivan *et al.* 1997). The P/B of 0.3 year⁻¹ represents the lower range of Zs estimated for several halibut stocks from 1975 to 2000 in Anonymous (2000). Age of 50% maturity is about 11 years (Anonymous 2000), at which point they are ≈ 120 cm long (according to Table A3.5 in Sullivan *et al.* (1997)). FishBase lists L_{∞} as ≈ 270 cm. Thus $L_{\text{mat}}/L_{\infty} \approx 0.44$ and $W_{\text{mat}}/W_{\infty} \approx 0.09$. This figure is an average, females mature at greater lengths and ages than males. Halibut population trends have been closely examined at different time and area scales by the IPHC. Data from Sullivan *et al.* (1997) and Clark and Hare (2001a) provided biomass time series for the BCS from 1974 to the present and for the whole NEPac ecosystem from 1950 to the present. The biomass trajectories for the two areas were similar, though changes in the BCS population appeared to lag the NEPac population by about five years. Pacific halibut is believed to occur with very low biomasses only in the SoG and no time series were available at that scale.

2.3.1.5. Pacific herring

Pacific herring (*Clupea pallasii*) stocks occur from Baja California to the Beaufort Sea, but the area of greatest density occurs from northern California to Central Alaska (Hart 1973). Inshore spawning occurs around the late winter and spring (Clemens and Wilby 1961) with the large spawning aggregations easily visible from boats, the surrounding shores, or even the air. Although significant stocks exist in Alaska most of the detailed information on herring biology was obtained from studies on Canadian stocks. P/B was estimated by adding natural and fishing mortalities reported in Schweigert and Fort (1999). $W_{\text{mat}}/W_{\infty}$ was estimated as 0.22 based on a FishBase (Froese and Pauly 2004) estimate of $L_{\text{mat}}/L_{\infty} = 0.6$. Herring catches have been important to the NEPac area as a whole, but only the populations of the BCS have reliable assessment data readily available (Anonymous 2002a, Anonymous 2002b, Anonymous 2002c, Anonymous 2002d, Anonymous 2002e). Five stocks form the vast majority of herring biomass in the BCS and they are commonly referred to by the geographic area in which they spawn;

Queen Charlotte Islands, Prince Rupert, central coast, west coast Vancouver Island, and Strait of Georgia. The five stocks often increase or decrease at different times, but all underwent dramatic declines during the 1960s as a result of overexploitation by a reduction fishery (Stocker *et al.* 2001). Biomass is therefore well known at the smaller scales of the SoG and the BCS back to 1950, but historic herring biomasses at the larger scale of the NEPac ecosystem are not.

2.3.1.6. Sablefish

Sablefish (*Anoplopoma fimbria*) have two populations in the northeast Pacific, based on growth, mortality and tagging information. A northern population inhabits waters around Alaska and northern British Columbia and a southern one from southern British Columbia to California (Sigler *et al.* 2003). Juvenile sablefish migrate extensively throughout their range and tend to move to deeper water as they mature and in the winter, and are most commonly found in depths of 400 to 900 m (Hart 1973). Thus, the BCS 'stock' includes portions of two separate populations. Sablefish biomass estimates have been conducted upon GoA (Sigler *et al.* 2003) and BCS populations (Haist *et al.* 2001). (Sigler *et al.* 2003) estimate M as 0.1 year^{-1} and suggest an F of between 0.07 year^{-1} and 0.13 year^{-1} in 2003 and 2004, so Z is $\approx 0.2 \text{ year}^{-1}$. Sigler *et al.* (2003) suggest that sablefish males and females, at age 6, achieve 70% and 40% maturity, respectively, with corresponding lengths of 59 and 64 cm. Given that FishBase has sablefish $L_{\max} \approx 120 \text{ cm}$, we can approximate that $L_{\text{mat}}/L_{\infty} \approx 0.5$ and, therefore, $W_{\text{mat}}/W_{\infty} \approx 0.13$. A biomass time series for sablefish was not available for the SoG model as they are present there only as juveniles and in small numbers (R.J. Beamish pers. comm.). The GoA/BSAI sablefish assessment represents the biomass of the northern stock, whereas the BCS assessment will include fish from the southern population as well. Because the biomass of the BCS assessment was seen to be almost an order of magnitude smaller than that for the northern stock alone, the BSAI/GoA assessment was used as the NEPac biomass time series.

2.3.2. Marine birds

Marine bird species were divided into 3 functional groups based on an analysis of their diet compositions; zooplanktivorous birds (parakeet auklet, least auklet, whiskered auklet, crested auklet, and Cassin's auklet), pelagic piscivorous birds (fork-tailed storm-petrel, Leach's storm-petrel, glaucous-winged gull, black-legged kittiwake, and red-legged kittiwake), and demersal piscivorous birds (rhinoceros auklet, common murre, thick-billed murre, tufted puffin, marbled murrelet, pigeon guillemot, horned puffin, double-crested cormorant, pelagic cormorant, and ancient murrelet). Parameters used in the Ecopath models for these groups can be seen in Table A.1.2. Population estimates were found for all species in the three functional groups for British Columbia and Alaska (Vermeer and Sealy 1984, Piatt and Naslund 1995, Hunt *et al.* 2000, Fitzgerald *et al.* 2003, Anonymous 2004b).

It was also possible to estimate a time series of abundance for pelagic piscivorous and demersal piscivorous bird groups in the SoG because of the availability of Christmas bird count (CBC) surveys run under the auspices of the National Audubon Society (2002) since 1900. The time series of abundance for the SoG model was an average of the recorded number per hour of each species observed at 11 CBC sites in the SoG; Campbell River, Comox, Lasqueti Island, Nanaimo, Nanoose Bay, Parksville / Qualicum Beach, Pender Harbour, Squamish, Sunshine coast, Vancouver, and Victoria.

Other bird species found in the North Pacific, such as raptors and shorebirds were omitted from consideration as functional groups in either ecosystem, as they were all found to be either migratory or reliant on the marine environment for only a portion of their food. Population estimates for species in each of the three functional groups were multiplied by values for average adult masses found in Dunning (1993). When both male and female masses were available, the average of the two was used as the multiplier.

The calculation of P/B for bird groups was aided by the fact that bird populations tend to have well-reported survival rates. As instantaneous mortality (Z , *i.e.*, P/B) is equal to the

negative logarithm of the survival rate, this conversion was applied to available survival data. Most survival rates were found in Saether and Bakke (2000), marbled murrelet was from Burger (2001), least auklet from Jones and Hunter (2002), Leach's storm petrel and Cassin's auklet from Vermeer and Sealy (1984). Auklets, murrelets and guillemots for which no data could be found were based on average values for conspecifics. The P/B estimates for each species was multiplied by the fraction of that species' biomass over the whole functional group's biomass to provide biomass weighted P/Bs for all functional groups. A bycatch mortality was also applied to the two piscivorous bird groups based upon known mortality (ranging from 5% to 8% of the local populations) of marbled murrelet in fishing nets (Tasker *et al.* 2000). Other piscivorous birds were also reported as being commonly taken as bycatch in British Columbia net fisheries (Carter *et al.* 1995).

The Q/B values for bird species groups were calculated with a two-step process. The first step was obtaining the average daily energy requirement of an adult of each of the species in $\text{kJ}\cdot\text{d}^{-1}$ provided by Hunt *et al.* (2000) Table 6.3, except for gulls which was derived from gulls and jaegers in Table 6.5, and red legged kittiwake also based upon Table 6.5. Then given the diet compositions and energy density of prey items shown in Hunt *et al.* (2000), average prey energy densities were calculated as $\text{kJ}\cdot\text{g}^{-1}$. Average values for energy in prey items and diet composition of those prey items were taken from Table 7.3, with the following exceptions: albatross from the Table 7.10 entry for Laysan albatross, Leach's storm petrel from Table 7.4, Brandt's cormorant from Table 7.9, red legged kittiwake from Table 7.1, and least auklet from Table 7.1. The daily energy consumption was then divided by the average energy density of that species' prey to yield a daily food consumption in grams. These daily food consumptions were divided by the average adult weights from Dunning (1993) then multiplied by 365 (days in a year) to yield annual Q/B. These Q/B values were then biomass weighted by species for functional groups in the same manner as P/B values.

2.3.3. Marine mammals

Parameters used for marine mammal groups can be seen in Table A.1.2. Biomasses of cetaceans are difficult to quantify due to their highly migratory nature, see, *e.g.*, Hill and DeMaster (1998). While, it is relatively easy to count pinnipeds due to their tendency to 'haul out' at consistent and predictable landfalls for migration, mating, and resting, such counts may be confounded by different portions of a population hauling out at different times or more than once during a census (Olesiuk 1999). Biomasses of mysticetae and odontocetae groups in these models, therefore, are especially speculative. The biomass estimate for mysticetae assumed that the parameter will be similar in the NEPac and BCS models. Only a token biomass was assigned for baleen whales in the SoG which has had only occasional forays of migrating grey whales (Rugh *et al.* 1999), minke whales (with only straying individuals appearing in recent years) and an extirpated stock of humpback whales (Gregar *et al.* 2000). For the estimated biomasses in the NEPac and BCS the work of Trites and Heise (1996) for the west coast of Vancouver Island (WCVI) was used. Trites and Heise (1996) estimated that for grey whales (*Eschrichtius robustus*) there is a summer population ≈ 1167 (range 1,000-1,500) and a winter population of 585 (range 200-1,000) off the WCVI, thus, a yearly average of about 900. They assumed 100 humpbacks (*Megaptera novaeangliae*) in summer although this may be well below the actual number, while there were estimated to be about 100 minke whales (*Balaenoptera acutorostrata*). Though the population estimates in Trites and Heise (1996) were specifically for the WCVI area, the same individuals would likely range over the whole BCS ecosystem. The biomass of the mammal populations was then calculated using the above population estimates and the average weights of male and female marine mammals from Trites and Pauly (1998). The total biomass estimate was then divided by the area of the BCS (a little more than 100,000 km²), yielding a mysticetae biomass of 0.15 t·km⁻². The relative proportion of biomass from each of the three baleen whales to the total biomass was: grey whales 79%, humpback whales 17%, and minke whales 4%. Odontocetae numbers were also based on Trites and Heise (1996) for the WCVI and converted to biomasses using values in Trites and Pauly (1998). Estimated numbers were: Dall's porpoise (*Phocoenoides dalli*) 1,000, harbour porpoise (*Phocoena phocoena*)

1,000, Pacific white sided dolphin (*Lagenorhynchus obliquidens*) 2,000, northern right whale dolphin (*Lissodelphis borealis*) 100, and killer whales (*Orcinus orca*) 200. The resulting estimated biomass for BCS odontocetae was $0.036 \text{ t}\cdot\text{km}^{-2}$. The relative proportion of each species in the total biomass of the group was: Dall's porpoise 8.6%, Pacific white-sided dolphin 21.9%, harbour porpoise 4.3%, northern right whale dolphin 1.5%, and orcas 63.7%. This biomass value was used for the SoG, NEPac and BCS models as there was no compelling evidence to suggest that either the density or functional group composition was different in the larger modeled areas from the estimates suggested for the WCVI. Because orcas formed the majority of biomass for the odontocetae group in the SoG model, a time series of orca numbers from the SoG in Martell *et al.* (2001) was used as a proxy time series of biomass in SoG EwE simulations.

Northern fur seals (*Callorhinus ursinus*) and Steller sea lions (*Eumatopias jubatus*) were modeled as one functional group. Estimated present-day populations for these species in the NEPac region were in Angliss and Lodge (2002). These population estimates were then multiplied by weights in Trites and Pauly (1998) to estimate the NEPac sea lion biomass. A time series for the abundance of Steller sea lions over the whole NEPac area was found in Trites and Larkin (1996). The biomass of northern fur seals in the NEPac was estimated using abundance indices of males in two major NEPac breeding areas; St. Paul and St. George Islands (Anonymous 2004a). Population and biomass estimates for the sea lion group in the BCS and SoG models also included California sea lions (*Zalophius californianus*), as in Trites and Heise (1996). There were 9400 sea lions in BC waters in 1996, with an additional 3500 male California sea lions during summer. Using masses from Trites and Pauly (1998) total biomass in BC was estimated to be $\approx 0.019 \text{ t}\cdot\text{km}^2$, the same value was used for the SoG model.

The P/B for sea lions for all models was based on net production rates for California sea lions off the US West Coast from 1980-1999 (excluding el Niño years) reported in Forney *et al.* (2000). The Q/B for sea lions in both models was taken from Trites *et al.* (1999) for Steller sea lions. Their calculation was done with the same formula used for

odontocetae. Diet composition for sea lions was based on an amalgamation of sea lion diet data in Trites and Heise (1996).

Harbour seal (*Phoca vitulina*) counts for Alaska were obtained from Angliss and Lodge (2002), and multiplied by weights from Trites and Pauly (1998) for the NEPac biomass estimate. The BCS and SoG estimated biomasses were derived from a population assessment by Olesiuk (1999), which was also the source for biomass time series for these models. No time series of harbour seals was found for Alaskan waters, thus there was none for the NEPac model. P/B for harbour seal in all models was based upon Olesiuk (1999), which states that in the Strait of Georgia (SoG) the maximum net productivity was $\approx 11.4\%$ (3 200 seals) when the population was 75% (28 500 seals) of carrying capacity (38,000 seals). Therefore, at maximum carrying capacity, the population should have a total mortality of $\approx 11.4\%$ i.e., a $P/B \approx 0.12 \text{ year}^{-1}$. Q/B for seals in all models was taken from the seal group in Trites *et al.* (1999) that was based on two estimations: mean weight and daily ration. Mean weight data came from Trites and Pauly (1998), which estimated daily ration (R) as a percentage of body weight (W) in kg, assuming $R = 0.1 \cdot W^{0.8}$. The parameters 0.8 and 0.1 were from Innes *et al.* (1987).

2.3.4. Pelagic fishes

2.3.4.1. Salmon

Biomass values for the five salmon species considered in the NEPac model: chinook salmon (*Oncorhynchus tshawytscha*), chum salmon (*O. keta*), coho salmon (*O. kisutch*), pink salmon (*O. gorbuscha*), and sockeye salmon (*O. nerka*), were assumed to be similar to those reported as eastern subarctic salmon biomasses in Aydin *et al.* (2003). NEPac and BCS salmon biomasses and biomass time series were calculated as a function of catch trends, e.g., Hare and Francis (1994, Beamish *et al.* (1997), and Mantua *et al.* (1997). Catch time series of numbers and weight for the five salmon species was summed over two of the regions reported in Eggers *et al.* (2003): Canada for the BCS model and North America for the NEPac model. These catch numbers and weights were then scaled

up to an 'all ages biomass' by year for each species because the catch usually involves only the terminal-year run of return migrating results. This implies that the biomass in the ocean in any year is not just the fish that were caught that year plus escapement, but also includes the biomass of fish caught in subsequent years that were in the ocean as immature salmon. These immature salmon numbers were back calculated using their subsequent year of maturity catch numbers converted to a present year numbers by accounting for their time in the sea and their natural and fishing mortalities. Thus, for pink it would be necessary to account for the catch in year t converted to numbers in the ocean catch in year $t+1$ converted to biomass in the ocean in year t as pink salmon spend two years in the ocean environment (Heard 1991). For chinook, however, it would be necessary to account for the fish caught over year t to $t+3$, as they spend about four years in the ocean (Healey 1991). Estimates for time at sea for the other species were taken from Burgner (1991) for sockeye, Salo (1991) for chum, and Sandercock (1991) for coho. Note that residence times for coho and chinook in the SoG have varied from these values in years near the end of the period of model simulations (R.J. Beamish pers. comm.)

Immature salmon numbers were converted to biomasses by using a von Bertalanffy growth function to estimate mass for each age stanza present in the ocean. Therefore, the majority of the biomass would still be due to the contribution of the mature fish ages for each species, but the longer-lived species would have a greater contribution of the immature salmon to their total biomass. Eggers *et al.* (2003) was used for catch data for all five species. The von Bertalanffy growth function values used to back-calculate immature salmon biomasses were from FishBase (Froese and Pauly 2004). The composition of salmon species in the SoG is complex because it provides only a transitory home for sockeye, chum and pink salmon, whereas many chinook and coho remain there.

P/B and Q/B values for chinook salmon in all models were based on data from the Great Lakes of North America reported in Rand and Stewart (1997). To estimate a Q/B for coho salmon in the North Pacific, the P/Q ratio of the chinook data (0.148) was divided into the P/B for coho from the Great Lakes. Sockeye salmon P/B, from Aydin *et al.*

(2003), was also divided by the chinook P/Q to estimate a North Pacific sockeye Q/B. Pink and chum salmon P/B and Q/B values were estimated as relative to the other salmon species, with pink assigned high P/B and Q/B values, as it is the smallest of the five species, and chum assigned smaller P/B and Q/B values as it is intermediate in size.

2.3.4.2. Sharks

Salmon shark (*Lamna ditropis*) was represented as a unique functional group. The North Pacific population of salmon shark was estimated at 2,000,000 (Nagasawa 1998). Assuming an average mass of 100 kg, based on the average size of individuals sampled by Nagasawa (1998) between 50°N and 56°N, and a total North Pacific area of 10,000,000 km², the estimated biomass amounts to 0.02 t·km². The North Pacific biomass was applied to all models. P/B for salmon shark was assumed to be equal to M, because of the small fishing mortality on the species. Assuming salmon sharks live in waters with average temperature of 12°C FishBase (Froese and Pauly 2004) estimated an M of 0.1 year⁻¹ to 0.2 year⁻¹.

All other pelagic sharks, comprised chiefly of blue shark (*Prionace glauca*) and thresher shark (*Alopias vulpinus*), were modelled as an aggregated group. The biomass for pelagic sharks was the difference between the biomass value for salmon sharks and that reported for all sharks in the eastern subarctic model of Aydin *et al.* (2003). The P/B for pelagic sharks was calculated as an average of M estimated for blue shark (M=0.17 year⁻¹) and thresher sharks (M=0.1 year⁻¹) in FishBase (Froese and Pauly 2004). Pelagic shark Q/B was also calculated as the average FishBase value for blue shark (0.8 year⁻¹) and thresher shark (1.2 year⁻¹).

2.3.4.3. Myctophids and other pelagic fishes

The biomass for myctophids was taken from an estimate for the North Pacific in (Gjosaeter and Kawaguchi 1980). P/B was estimated as equal to M, which was calculated for northern lampfish (*Stenobrachius leucopsarus*) with the life history tool in FishBase

(Froese and Pauly 2004) assuming that the average annual temperature was 10°C.

Northern lampfish was deemed an appropriate example for group parameters as it is the most common myctophid in the North Pacific (Gjosaeter and Kawaguchi 1980). Q/B for myctophids was also derived from FishBase from values for northern lampfish.

A miscellaneous predatory pelagics group was created to account for species like Pacific pomfret (*Brama japonica*), which are common offshore. Biomass for the group, therefore, was based on the value for pomfret in the eastern subarctic model of Aydin *et al.* (2003). P/B was based on M for Pacific pomfret and Pacific bonito (*Cololabis saira*) at 10°C in FishBase (0.66 year⁻¹ and 0.26 year⁻¹). In the absence of any fishery on such species $F \approx 0 \text{ year}^{-1}$ so $Z \approx 0.45 \text{ year}^{-1}$. Q/B was also based on a FishBase average for saury and bonito.

The miscellaneous small pelagics group was made up of species such as smelt and eulachon. P/B was set at 2.3 year⁻¹ to represent a total mortality of 90% per year. No good estimate of biomass for this group was available for the two larger scale models so the ecotrophic efficiency (EE) was set to 0.95, *i.e.*, 95% of mortality is due to explained ecosystem mortality such as predation and fisheries. These high values reflect values used for similar groups in other North Pacific ecosystem models like Beattie (2001) and Martell *et al.* (2002). The P/Q was set at 0.3, which means that production should be 30% of consumption, a reasonable guess, given that the species in this group are small and fast growing (Christensen *et al.* 2005). For the SoG the biomass estimate, 15 t·km⁻² was at the low end of the estimated biomass range (15-40 t·km⁻²) for the small pelagics group in the SoG model of Beamish *et al.* (2001).

2.3.5. Demersal fishes

2.3.5.1. Demersal elasmobranchs

Dogfish (*Squalus acanthias*) are probably the most abundant shark in the North Pacific. Their biomass was estimated in 1994 as 150,000 to 200,000 t for the outer BC coast and

60,000 for the Strait of Georgia stock (Thomson 1994). The outer coast middle value and Strait of Georgia value (175,000 t + 60,000 t) divided by the BCS ecosystem area (176,000) resulted in a biomass $\approx 1.3 \text{ t}\cdot\text{km}^{-2}$. To account for a fishery, F was taken from Beattie (2001), who consulted the DFO Fishery Observer Database, and calculated F as $0.005\cdot\text{year}^{-1}$ and the Z (P/B) = 0.099 year^{-1} . The Q/B for dogfish was estimated as 2.6 year^{-1} by Tanasichuk *et al.* (1991). Jones and Geen (1977) completed a detailed consumption study for dogfish, separating life stages and sexes of adults, resulting in a weighted mean of consumption rates of 2.719 year^{-1} . Note, however, that Brett and Blackburn (1978) estimated dogfish consumption to be somewhat lower and that the Jones and Geen (1977) estimate was based upon animals obtained from commercial herring catches. These biomass, P/B, and Q/B estimates were used for all three models.

The biomass for ratfish (*Hydrolagus collieri*) and skates/rays (rajiformes) was estimated respectively as $0.517 \text{ t}\cdot\text{km}^2$ and $0.335 \text{ t}\cdot\text{km}^2$ by Beattie (2001). These two biomasses were added for the aggregated ratfish/skate/ray group in these models, thus, the biomass $\approx 0.8 \text{ t}\cdot\text{km}^2$. P/B and Q/B values for skates and rays were also from Beattie (2001) and applied to all three models.

2.3.5.2 Rockfishes

Pacific Ocean perch (*Sebastes alutus*) biomass and time series of biomasses were available from stock assessments for; the BCS (Schnute *et al.* 2001), BSAI (Spencer and Ianelli 2003b), and GoA (Hanselman *et al.* 2003). Biomass of Pacific Ocean Perch in the SoG was assumed to be very small. Hanselman *et al.* (2003) estimated M as 0.05 year^{-1} and an F which ranged from 0.01 year^{-1} to 0.32 year^{-1} . The long-term average was about 0.08 year^{-1} , so Z was estimated for the Ecopath basic input for all three models as 0.1 year^{-1} . Q/B for all three models was taken from the default value for Pacific Ocean perch in FishBase (Froese and Pauly 2004).

The 'other rockfish' group contained species commonly referred to as shelf and inshore rockfish (Stocker *et al.* 2001). As such, an estimation of biomass for the group is difficult

because of the diversity of species it contains. For these models the biomass estimate was an extrapolation from Murie *et al.* (1994). Estimates of inshore rockfish density, obtained from observations in a submersible in Saanich Inlet, suggested an average of 5 per 100 m². Assuming an average weight of 2 kg for an inshore rockfish, the biomass density for the study area would have been 0.1 t·km⁻². Shelf rockfish data was taken from Bonfil (1997) for silvergrey rockfish (*Sebastes brevispinis*), yellowtail rockfish (*S. flavidus*), and canary rockfish (*S. pinniger*). Table 2 in Bonfil (1997) lists total B.C. biomass estimates in tonnes as; silvergrey: 6316 t, yellowtail: 4994 t, canary: 2215 t. For widow rockfish (*S. entolomelas*) biomass was estimated from dividing catch reported in Anonymous (1999b) by the average proportion of fish caught over biomass reported for the other three species in Bonfil (1997) to give a biomass estimate for widow rockfish of 4860 t. Thus, for the whole BC coast, the shelf rockfish biomass ≈ 0.163 t·km⁻². By adding these two species the 'other rockfish' biomass is at least 0.263 t·km⁻², but given that there are many unfished species in this group, the true value may be much higher. The P/B and Q/B values were averages for several of these rockfish species calculated with the life history tool of FishBase (Froese and Pauly 2004). These parameters were used in all three models.

Northern rockfish (*Sebastes polyspinis*) stock assessments were available for BSAI (Spencer and Ianelli 2003a) and GoA (Courtney *et al.* 2003) stocks. This assessment was used to estimate biomass and time series of biomasses for that species in the NEPac model. Spencer and Ianelli (2003a) had $F \approx 0.05$ year⁻¹ and an $M \approx 0.07$ year⁻¹. Thus, for the EwE models, $Z \approx 0.12$ year⁻¹.

2.3.5.3. Gadids and greenlings

Pacific hake (*Merluccius productus*) consisted of two populations in the areas modelled. There was a Strait of Georgia (SoG) population and one off the West Coast of Vancouver Island, which is actually the northern extension of one concentrated further south, off the coasts of California, Oregon and Washington. The SoG population, though the dominant fish biomass in the area (Saunders and McFarlane 1998) is so much smaller than that off

the West Coast of Vancouver Island that the latter's stock assessment (Jagiello and Sinclair 2002) was used for the effective BCS biomass and biomass time series data. The population that exists off BC is the northern arm of a large stock distributed along the west coast of North America (Fleischer *et al.* 2005). The biomass of that west coast North America stock was divided by 10 to represent the BC 'stock', *i.e.*, the hake biomass, in the BCS and NEPac models. Because hake do not range north of the Queen Charlotte Islands/Haida Gwaii, the biomass for the NEPac model was presumed to be approximately one tenth (the proportion of area within the NEPac model occupied by the BCS model) that of the BCS. The SoG stock has been surveyed regularly by trawl and sonar (Taylor and Barner 1976, Mason *et al.* 1984, and Shaw *et al.* 1990), but no formal stock assessment was available for that population and, therefore no time series of SoG hake biomass was available for comparison to model outputs. The estimated biomass represents an average of values reported in the most recent survey (Shaw *et al.* 1990). Dorn *et al.* (1999) estimate that the M for hake is about 0.25 year^{-1} and an F_{MSY} of about 0.25 year^{-1} , therefore P/B was determined to be 0.5 year^{-1} for the BCS and NEPac models. For the SoG, Beamish *et al.* (1976) estimated that Z for adult males = 0.74 year^{-1} and females = 0.88 year^{-1} .

Atka mackerel (*Pleurogrammus monopterygius*) exist almost entirely within the Aleutian Islands area. Relatively small numbers are known to be in the GoA (Lowe and Lauth 2003), so the biomass and temporal dynamics of the Aleutian Islands stock (Lowe *et al.* 2003) were used as representative of dynamics for the NEPac ecosystem. Lowe *et al.* (2003) calculated an M of 0.3 year^{-1} and F ranging from 0.06 year^{-1} to 0.7 year^{-1} , with an average of 0.3 year^{-1} , so Z is about 0.6 year^{-1} .

The biomass and biomass time series for lingcod (*Ophiodon elongatus*) in the NEPac and BCS models was assumed to be similar to the Hecate Strait stock reduction analysis (SRA) by Martell (1999). Lingcod biomass and biomass trends in the SoG, from 1950 to the present, were taken from Martell *et al.* (2001) as was time series of fishing mortality. It should be noted that after the completion of SoG simulations and data analysis, a more detailed examination of lingcod biomass trends in the SoG, estimated by SRA, was

provided by Walters *et al.* (2006). P/B in all three models was left as unknown, so the P/Q was set at 0.1, *i.e.*, production being about one tenth of consumption, based on arguments about acceptable P/Q values (Christensen *et al.* 2005).

2.3.5.4. Flatfishes and small demersal species

The majority of yellowfin sole (*Limanda aspera*) biomass in the NEPac ecosystem is within the BSAI area. The biomass and biomass time series were taken from Wilderbuer and Nichol (2003), as were estimates of M (0.12 year^{-1}) and F (0.07 year^{-1}) for a total P/B of 0.19 year^{-1} . The biomass for yellowfin sole in the SoG and BCS was set to the low $0.001 \text{ t} \cdot \text{km}^2$ to indicate its presence.

Alaska plaice (*Pleuronectes quadrituberculatus*) is found chiefly within the BSAI region of the NEPac ecosystem. A stock assessment and time series of biomass for the BSAI population was found in Spencer *et al.* (2003) which also provided estimates of M (0.25 year^{-1}) and F (0.05 year^{-1}) used to determine a $P/B \approx 0.3 \text{ year}^{-1}$.

Three rock sole species (*Lepidopsetta* spp.) are found in the NEPac area. Two are common in the BCS ecosystem, *Lepidopsetta petraborealis* and *L. bilineata* (DFO 1999a). The third species, *L. polyxystra*, dominates in the Bering Sea and overlaps with *L. bilineata* in the GoA (Wilderbuer and Walters 2003). Stock assessments with time series of biomass were available for the BSAI in Wilderbuer and Walters (2003) and the BCS in DFO (1999a). Estimates of M (0.18 year^{-1}) and F (0.04 year^{-1}) were from Wilderbuer and Walters (2003) to give a P/B of 0.22 year^{-1} . No time series of biomass was available for the SoG.

The other flatfish group includes, but is not limited to, butter sole (*Pleuronectes isolepis*), starry flounder (*Platichthys stellatus*), Dover sole (*Microstomus pacificus*), rex sole (*Glyptocephalus zachirus*), sand sole (*Psettichthys melanostictus*), flathead sole (*Hippoglossoides elassodon*), and Greenland turbot (*Reinhardtius hippoglossoides*). Based on biomass estimates for these species in the GoA (Turnock *et al.* 2003a), this

group of species is approximately as abundant as Alaska plaice, rock sole and yellowfin sole combined, *i.e.*, a biomass of about 1.0 to 1.5 t·km⁻². Q/B was estimated as an upper value for all of the species in this group based on values from FishBase (Froese and Pauly 2004). P/Q was estimated as 0.2 as this group represents creature that are in neither particularly short-lived, and fast-growing, nor long-lived and slow-growing (Christensen *et al.* 2005).

An estimate of biomass for miscellaneous small demersals was derived from trawl survey information in Acuna *et al.* (2003) Table 7; Cottidae, Zoarcidae, Agonidae, Cyclopteridae, and 'other fish'. The biomass derived for the EBS from that source is slightly more than 0.5 t·km⁻². Based on the ubiquity of these fishes in the shallower waters that estimate would likely be low because most trawl surveys would be in waters unlikely to contain much of the near-shore small demersal biomass. For example Acuna *et al.* (2003) appendix A Table 1 and 2 list 355 tows, with average depth of 77 m. Less than 14% of those tows were more shallow than 40 m and none were more shallow than 17 m. Thus, it seems likely that the real small demersal biomass would have been much higher than the above estimate. The Q/B estimate (5.256 year⁻¹) was the unweighted mean for three species (poacher, eelpout and a sculpin) given in Wakabayashi (1986). P/Q was estimated as 0.3 following the logic of previous P/Q estimates.

2.3.6. Invertebrates

2.3.6.1. Zooplankton

Krill biomass for these models was based on Mackas (1991) for the WCVI from 1979-1989 using values from his Figure 11, "Average seasonal cycles of euphausiid biomass off the outer coast of Vancouver Island". The average value for the period of record was 4.46 t·km⁻². But Beamish *et al.* (2001) used 80 t·km⁻² as a conservative estimate of euphausiid biomass for the SoG. Thus, an area weighted method was employed to get total BCS biomass with SoG = 18,000km² divided by the the total ecosystem area of 113,000 km². So about 16% of the total are is SoG and the rest was accounted for based

on the Mackas (1991) data, *i.e.*, $(80 \text{ t}\cdot\text{km}^{-2}\cdot 0.16) + (4.5 \text{ t}\cdot\text{km}^{-2}\cdot 0.84) = 16.58 \text{ t}\cdot\text{km}^{-2}$. Interestingly, Aydin *et al.* (2003) had $25 \text{ t}\cdot\text{km}^2$ as an estimate of eastern subarctic Pacific Ocean krill biomass. Fulton *et al.* (1982) estimated a krill P/B = 5.5 year^{-1} from a survey of the Pacific Coast of Canada. Robinson and Ware (1994) estimated that a P/B = 8 year^{-1} would be required for euphausiids in the southwest Vancouver Island upwelling system to support estimated predation. Iguchi and Ikeda (1999) estimated a yearly P/B = 6 year^{-1} for *Euphasia pacifica* in Toyama Bay, Japan. The Q/B was calculated from the average daily consumption of *E. pacifica* required to maintain the population growth, metabolism and reproduction (Iguchi and Ikeda 1999). The average daily consumption was 6.8% of biomass, suggesting a Q/B = 24.82 year^{-1} .

Carnivorous zooplankton biomass was based on values for miscellaneous predatory zooplankton, amphipods, and pteropods in the Eastern Subarctic model of Aydin *et al.* (2003). Herbivorous zooplankton biomass was estimated from copepods and microzooplankton in Aydin *et al.* (2003). Carnivorous zooplankton P/B and Q/B as well as herbivorous zooplankton Q/B was taken from the estimate used by Beamish *et al.* (2001). Herbivorous zooplankton P/B was estimated using results from the model of Robinson and Ware (1994). Q/B for herbivorous zooplankton was based upon estimates used for this parameter for similar species groups in the first systematic study of Ecopath models of the Northeast Pacific EwE models (Pauly *et al.* 1996).

The biomass of jellies in these models, $12 \text{ t}\cdot\text{km}^{-2}$, was taken from Figure 7 in Mackas (1991) for the south Vancouver Island shelf system. Note that this weight is calculated assuming dry weight is 4.2 % of wet weight (Larson 1986). To estimate P/B the growth rates for moon jellies (*Aurelia aurita*) in Hansson (1997) of 0.053 day^{-1} to 0.15 day^{-1} at 5°C to 16.5°C were used. The lower estimate was used in these models, as the assumption had been that ocean temperatures in the modelled area averaged less than 10°C annually. It was further assumed that adult jellies tended to be present for about half the year (Arai 1996), so an annual P/B was estimated as $0.053 \cdot 365/2 \approx 9.6\cdot\text{year}^{-1}$. To estimate Q/B, Matishov and Denisov (1999) had a diurnal consumption rate of 7% of biomass for medusae in the Black Sea. This would translate to an annual consumption per unit

biomass of $365 \cdot 0.07 = 25.55 \text{ year}^{-1}$, which, divided by two to represent disappearance in the winter, is $\approx 13 \text{ year}^{-1}$.

2.3.6.2. Squid

Large squid biomass was the combined estimated biomasses of the three large squid groups, neon flying squid, clubhook squid, and large gonatid squid in the Eastern Subarctic EwE model of Aydin *et al.* (2003), 0.45, 0.012, and 0.03 respectively, for a total biomass of about $0.5 \text{ t} \cdot \text{km}^{-2}$. Small squid biomass was left to be estimated by Ecopath by setting ecotrophic efficiency for the group to 0.9, *i.e.*, 90% of mortality was assumed due to mortality sources modelled. Q/B and P/B for these two groups were also synthesised from the comparable groups in Aydin *et al.* (2003). Humboldt squid began to frequent the continental shelf waters off BC, in 2004 (DFO 2005a). Humboldt squid was not modelled here as its biomass is considered negligible. It was assumed that its appearance was explainable, in part, by the increased sea surface temperatures during the decade preceding 2004 (Cosgrove 2005).

2.3.6.3. Crustaceans

Shrimp biomass was parameterised with consideration given to a combination of previously modelled species groups like the sergestid shrimp in Beattie (2001) and Aydin *et al.* (2003). Thus, the biomass was higher than it would have been for either benthic or pelagic shrimps by themselves. Martell *et al.* (2000) had an F of 0.18 year^{-1} and an M of 0.96 year^{-1} for *Pandalus jordani* off the WCVI, thus, $Z \approx 1.14 \text{ year}^{-1}$. Heymans (2001) had a P/B of 1.45 year^{-1} for *Pandalus borealis* off the east coast of Canada. So for these models Z was 1.2 year^{-1} , the estimation biased toward the locally-derived number. Shrimp Q/B was based on the value used by Bundy *et al.* (2000).

To obtain an estimate of biomass for crabs, an area-weighted system based upon data from Burd and Brinkhurst (1987) and Nyblade (1979) was used; the former for deeper marine waters, the latter for waters of less than 20 m depth. The area assigned to the two

for weighting was 5% shallow water, based on areas reported for SoG depth strata in Guénette (1996). Total instantaneous mortality for male Dungeness crabs (*Cancer magister*) was estimated to be 2.5 year^{-1} ($2.3 \text{ year}^{-1} - 2.8 \text{ year}^{-1}$) from studies in Clayoquot Sound, B.C. (Smith and Jamieson 1989, Smith and Jamieson 1991). Female Z was estimated at 1.3 year^{-1} (Smith and Jamieson 1989, Smith and Jamieson 1991). Boutillier *et al.* (1998) modelled mortality rates of 0.6 year^{-1} to 1.4 year^{-1} , and found resultant exploitation rates of 33-68% for McIntyre Bay, BC and 41 - 54 % for the Hecate Strait. Thus, total Z in the area could be expected to be between 0.97 year^{-1} and 2.01 year^{-1} , leading to an average value of $Z \approx 1.5 \text{ year}^{-1}$. Because there are smaller crabs in this group, the P/B may actually be higher. Wakabayashi (1986) reported the Q/B for the red king crab (*Paralithodes camtschaticus*) and tanner crab (*Chionoecetes bairdi* and *C. oplilio*) in Alaskan waters, and the mean value of those estimates was used in these models: $Q/B = 3.541 \text{ year}^{-1}$.

2.3.6.4. Benthic invertebrates

To estimate biomass for bivalves, echinoderms, and 'other benthos' in the three models an area weighted system using data from Burd and Brinkhurst (1987) and Nyblade (1979) was used as with crabs. For bivalve P/B, Jørgensen *et al.* (2000) had a P/B for *Macoma baltica* of 1.5 year^{-1} , and had listed a value of 0.3 year^{-1} for *Mytilus* sp. For the models here, the average of the two P/B values was used, 0.9 year^{-1} . P/B for echinoderms was from Jørgensen *et al.* (2000) for "echinodermate". P/B for 'other benthos' was derived from Jørgensen *et al.* (2000) as a weighted average of, *Spirorbis* sp., a polychaete, $P/B=4$ (45% of other benthos biomass), amphipoda : $P/B= 0.024 \text{ day}^{-1}$, i.e., 8.76 year^{-1} (10% of other benthos biomass), and *Litorina saxatilis*, a gastropod: $P/B = 4.1 \text{ year}^{-1}$ (45% of other benthos biomass). Thus, the weighted average $P/B \approx 4.5 \text{ year}^{-1}$. Q/B was left unknown and P/Q was estimated for all three groups. P/Q values were assigned to bivalves, echinoderms and other benthos on the basis of general knowledge of their biology. Because other benthos includes many fast-growing herbivores, their P/Q was high, whereas the lower value of 0.20 for bivalves reflects their longer-lived, slower-

growing nature. Echinoderms were assigned a middle value, they grow slowly, but many are heavily predated upon, e.g., holothuroideans and echinoideans.

2.3.7. Primary producers

For the estimation of phytoplankton biomass in the SoG, consideration was given to Beamish *et al.* (2001) which had values of $36 \text{ t}\cdot\text{km}^{-2}$ and $72 \text{ t}\cdot\text{km}^{-2}$ for the SoG modelled for the years 1998 and 2001. For the BCS model the average of the Beamish *et al.* (2001) biomasses: $50 \text{ t}\cdot\text{km}^{-2}$ was used towards the calculation of an area-weighted value which also considered the results of work by Robinson and Ware (1994). Robinson and Ware (1994) found that the average biomass off the WCVI $\approx 2.7 \text{ gC}\cdot\text{m}^{-2}$. A conversion factor of 6 was applied to their carbon weight to get wet weight for use in the BCS model. The conversion ratio was averaged from references for different diatoms in Jørgensen *et al.* (2000). From this reasoning an estimate of $16.2 \text{ t}\cdot\text{km}^{-2}$ was calculated for the WCVI area. To calculate a biomass for all of the BCS, the SoG biomass was weighted as 10% of the total area, and the WCVI estimate used for the other 90% of the total ecosystem area, yielding an area weighted biomass for the BCS $\approx 20 \text{ t}\cdot\text{km}^{-2}$. A similar relationship between near shore and deeper water habitat was assumed for the NEPac model so the same biomass was used as for the BCS model. Phytoplankton P/B for all three models was also taken from Beamish *et al.* (2001).

Data from exposed rocky shores collected by Nyblade (1979) suggested a macrophyte biomass of $2300 \text{ g}\cdot\text{m}^{-2}$, *i.e.* astonishingly high but limited to the most favourable habitat for macrophyte growth. Although only a small portion of any of these three ecosystems modelled here, this estimate suggests very high biomasses even when averaged over the whole of the ecosystems. For example, even if it was estimated that if the available macrophyte habitat accounted for only 0.1% of the total ecosystem area, a potential BCS or NEPac estimate of $2.3 \text{ t}\cdot\text{km}^{-2}$ would apply. In the shallower SoG it might be expected that the number would have been perhaps fifty times greater given the assumed habitat available using the depth strata information in Guénette (1996). Until the advent of a more precise methodology to estimate macrophyte distribution and biomass throughout

these ecosystems, estimation of the biomass with an assumed EE of 0.9 was deemed appropriate.

2.4. Determination of diet compositions

For most of the species groups the diet compositions were kept as similar as possible for all three models. Diet allotments differed only when specific diet studies had been done for one of the species groups modelled in a particular place and time. If such studies indicated a diet difference more appropriate to the area and scale of one of the models such information was used. These instances are noted in the text. In the absence of such detailed information, the only alteration to a diet composition occurred in the model balancing procedure. In no case was it necessary to entirely remove a diet item from a predator's diet to balance any of the models. Generalised diet compositions for all three NEPac models can be found in Appendix 1 (Tables A.1.9 to A.1.15). The reader is reminded that the Q/B ratio reflects the total amount of food consumed by a group in a model and tends to be smaller for slower growing species and higher for those with high metabolisms.

The hypothetical diet compositions in Appendix 1 may be different from the applied diet compositions after the Ecopath mass-balanced portion of the three models had been obtained. These balanced model diet compositions were not reported because the protocols for balancing a model involve judgement calls on the part of the modeller as to which input parameters should be changed. Each modeller must decide this individually. As a general rule diet composition tends to be the least conservative of the parameters in any Ecopath model. Thus, other parameters like biomass and mortalities are more likely to be known for a given species group in an ecosystem. The reader is directed to discussions on how to balance an Ecopath model in Christensen *et al.* (2005) for more insights on the tradeoffs of changing various parameters. Therefore, these diets represent a generalised starting point which future modellers may use as a guide and for comparison, and which hopefully will be improved as more data become available.

2.4.1. Diets of multi-stanza groups

The diet compositions (DC) of adult arrowtooth flounder, Pacific cod, Pacific halibut, walleye pollock, and sablefish were taken from Yang and Nelson (1999). Arrowtooth flounder juvenile diet composition was based on information on diet of juvenile arrowtooth flounder in FishBase (Froese and Pauly 2004). Juvenile herring, Pacific cod, and walleye pollock diet compositions were from Sturdevant (1999). The herring juvenile diet composition was modified to show some trophic ontogeny. Juvenile Pacific halibut diet composition was from St.-Pierre and Trumble (2000). Juvenile sablefish diet composition was inferred from information in FishBase (Froese and Pauly 2004) to represent feeding chiefly on zooplankton as age 0-1 with small fish and benthos included as the juveniles neared adulthood. As a general rule if a species with multi stanza groups was in the diet composition of a predator species 1/3 of this was apportioned to the juvenile stanza, and 2/3 to the adult stanza, unless the study noted any age differentiation in that predator's diet items. The generalised diet compositions for these groups can be seen in Table A.1.6.

2.4.2. Diets of marine birds

Bird diets were synthesised from Dragoo *et al.* (2001), Bertram *et al.* (2001), Sydeman *et al.* (2001), Burkett (1995), Wehle (1983), and Ainley *et al.* (1981). These diet compositions provided the original logical basis for splitting birds into 3 functional groups: pelagic piscivorous; demersal piscivorous; and zooplanktivorous. Diets of all 21 species of birds in section 2.3.2 were determined as closely as possible for all species and then aggregated by model. As with the mammal diet compositions, each bird group's diet composition was weighted by the biomass compositions of the species in each group for each of the three models. Because detailed population estimates were available for all species for all three models diet compositions for species groups were slightly different in the models reflecting the different abundances of species within each group over the different area scales modelled. The generalised diet compositions for these groups can be seen in Table A.1.7.

2.4.3. Diets of marine mammals

Mysticetae diet was taken from Pauly *et al.* (1998) and was weighted by the share of biomass of the three whale species that made up this group, see section 2.3.2.

Odontocetae diet composition was also based on Pauly *et al.* (1998) which was weighted by the species biomass share of each species group, see section 2.3.2. The species in the group ate primarily fish, followed by zooplankton, squid, benthic animals and higher vertebrates, such as seals. The fish component of the diet in Pauly *et al.* (1998) was not reported by species or family. For the purpose of this study the diet composition contributed by fish and squid was also informed by the diet composition attributed to fish for toothed whale groups in Aydin *et al.* (2003). The diet component arising from 'higher vertebrates' was assumed to be seals and sea lions eaten by the 'transient' group of the orca population, which is a mammal eater, versus the 'resident' type of killer whale, which is a fish eater (Ford *et al.* 2000). The two types are considered to have sufficient genetic distinction that they are considered separate stocks (Forney *et al.* 2000). The rockfish component of odontocetae diet was distributed to reflect the relative abundances of the rockfish groups in each of the models. Also, pollock was included as a small part, approximately 1%, of the odontocetae diet composition, as it seemed likely dolphins and porpoises would take advantage of a prey item so abundant in all three models. Sea lion diet composition was based on an amalgamation of Steller sea lion diet data in Trites and Heise (1996) and pollock was added based on the UBC Marine Mammal Research Unit web page which suggests pollock constitute anywhere from 25 to 50 % of SSL diet. Seal diet composition was derived from harbour seal diets in Everett, Washington used in Preikshot and Beattie (2001). The generalised diet compositions for these groups can be seen in Table A.1.8.

2.4.4. Diets of pelagic fishes

Chinook salmon diet was based on a synthesis of information in Aydin *et al.* (2003) and feeding of chinook off Northern California as reported in Hunt *et al.* (1999). Aydin *et al.*

(2003) have their eastern subarctic chinook diet almost evenly divided between pelagic forage fish, small squid, and mesopelagic fish. Coho salmon diet composition was adapted from LeBrasseur (1966), which reports 'fish' as one of the groups in coho diet. In order to assign the most likely prey groups, some representative part of this predation, most was split between miscellaneous pelagics and herring with miscellaneous small demersals assigned a trace of coho predation. Myctophids, *i.e.*, the mesopelagics of Aydin *et al.* (2003), were also included as a small fraction of coho diet. Aydin *et al.* (2003) have coho diet almost evenly divided between pelagic forage fish, small squid, and mesopelagic fish. Chum and pink salmon diet composition was adapted from eastern subarctic chum and pink salmon groups in Aydin *et al.* (2003). Sockeye diet composition was adapted from Kaeriyama (2000) and eastern subarctic sockeye in Aydin *et al.* (2003), although Aydin *et al.* (2003) have sockeye eating less squid than the former document suggests. Therefore, a greater portion of the diet composition of sockeye in these models was carnivorous zooplankton compared to the sockeye group of Aydin *et al.* (2003).

Miscellaneous predatory pelagic diet composition was based on eastern subarctic pomfret in Aydin *et al.* (2003) and the entry for bonito in FishBase (Froese and Pauly 2004) which listed their diet as squid, fish, and shrimp. Miscellaneous small pelagic diet data was inferred from Sturdevant (1999), and represented a mixture of diets for eulachon and capelin. Myctophid diet composition was derived from Moku *et al.* (2000). Pelagic sharks diet composition was taken from Cortes (1999) for blue shark and thresher shark, and qualitatively informed by Aydin *et al.* (2003). Salmon shark diet composition information was obtained from Nagasawa (1998), in which Figure 6 shows that of stomachs containing food 2/3 of prey was salmonids and 1/3 was 'other species'. The salmonid portion was divided up among the five salmon species roughly according to their biomass proportion for all salmon species in the models. The other species portion of salmon shark diet was divided up among pollock, dogfish, myctophids, miscellaneous predatory pelagics, miscellaneous small pelagics, large squids and small squids. The generalised diet compositions for these groups can be seen in Table A.1.9.

2.4.5. Diets of demersal fishes

Dogfish diet was adapted from Jones and Geen (1977), though this may underestimate the amount of krill which form a large portion of the diet of dogfish under 15 years old (R.J. Beamish pers. comm.). The diet of the 'other flatfish' group was based on feeding of flathead sole diet described in Yang and Nelson (1999). Lingcod diet was taken from Beattie (2001), which was, in turn, derived from Cass *et al.* (1986). Miscellaneous small demersal diet composition was adapted from sculpin diets reported in Appendix Table 3 of Wakabayashi (1986). Pacific hake diet composition was adapted from Table 2 in Rexstad and Pikitch (1986). Pacific Ocean perch diet was synthesized from the findings of Brodeur and Livingstone (1988) and Yang (1993). Rajidae / ratfish diets were based on qualitative and quantitative information in Casillas *et al.* (1998), who noted that ratfish have a remarkably varied diet which included molluscs, squid, nudibranchs, opisthobranchs, annelids, small crustaceans, and even seaweed. Rock sole diet composition was taken from Wakabayashi (1986). Other rockfish diet composition was made up of an aggregation of roughey rockfish, dusky rockfish, and shortspine thornyhead in found in Yang (1993). Yellowfin sole diet was taken from Wakabayashi (1986). The generalised diet compositions for these groups can be seen in Table A.1.10. and Table A.1.11.

2.4.6. Diets of invertebrates

The diet composition of the highly aggregated 'other benthos' group was based on the diet composition of macrobenthos in Okey and Pauly (1999). Bivalves, carnivorous zooplankton, crabs, shrimps, echinoderms diet compositions were adapted from previous EwE models of northeastern Pacific ecosystems, *e.g.*, Okey and Pauly (1999), Beattie (2001), Preikshot and Beattie (2001) and Aydin *et al.* (2003). It must be borne in mind that because many of the invertebrate groups are highly aggregated, their dynamics in Ecosim analyses are likely to reflect general flows of energy derived from primary production which is passed on to higher trophic levels, the true focus of these models. Herbivorous zooplankton diet composition was from Robinson and Ware (1994). The

diet composition of jellies was based upon a mixture of the eastern subarctic diet compositions for the large jelly and ctenophore group in Aydin *et al.* (2003). Krill diet composition was from Robinson and Ware (1994). Large squid's diet composition was based on a mixture of eastern subarctic diet compositions for clubhook squid, neon flying squid and large gonatid squid in Aydin *et al.* (2003). Small squid's diet composition was based on eastern subarctic micronectonic squid diet composition in Aydin *et al.* (2003). The generalised diet compositions for these groups can be seen in Table A.1.12.

2.5. Fisheries and catch data

For almost all functional groups catches and times series of catches for the two models were obtained from the same assessment documents used for generating biomass and time series of biomass. The exception to this was a time series of fishing mortality assigned to seals in the BCS model. In this case, an F of 0.1 year^{-1} for each year from 1950 to 1971 was included for seals to represent the hunt which existed at that time. This is the same mortality that was used by Martell *et al.* (2002) for their model of the Strait of Georgia. Representation of bycatch and discards in the models was derived from discard rates reported for target and non-target species in Gulf of Alaska fisheries in Gaichas and Boldt (2003) and Hiatt and Terry (2003). For non-target species this would suggest a total of 30,000 t, *i.e.*, $0.07 \text{ t} \cdot \text{km}^{-2}$, in only the Gulf of Alaska, made up of a mixture of species including dogfish, skates, miscellaneous small demersals, crabs, echinoderms, and other benthic invertebrates. For the so-called target species in the GoA, then, discard rates were reported as usually 20% of the total catch and this was used as the standard for species in the model. A more pessimistic analysis by Alverson *et al.* (1994) estimated that about 1,000,000 t of bycatch occurred in the whole Northeast Pacific basin. The area of the entire Northeast Pacific is approximately $5,000,000 \text{ km}^2$, based upon summing the areas of the BCS, the Alaska Gyre, the Gulf of Alaska, and the Eastern Bering Sea reported in Hunt *et al.* (2000), which suggested that discards were on the order of $0.2 \text{ t} \cdot \text{km}^{-2}$. Alverson *et al.* (1994) also point out that various trawl fisheries in the NEPac area have discard rates from 2-3 times that retained. Thus, for the trawl fisheries the functional groups miscellaneous small demersals, other rockfish, dogfish and rajidae / ratfish were

added to the bycatch such that bycatch was twice the catch. The sum of discards thus calculated on non-target and target species was $0.17 \text{ t} \cdot \text{km}^{-2}$ comparable to the general value suggested by Alverson *et al.* (1994).

2.6. Comparing dynamic model outputs to reference time series data

After having ‘balanced’ all three ecosystem models, dynamic simulations were run in Ecosim from 1950 to the present, to examine the effects of different ecosystem control scenarios, *i.e.*, top-down and bottom-up factors related to how close the consumers are to their carrying capacity, on output time series of biomass. For more on balancing EwE models, see Christensen *et al.* (2005). Table 11 shows time series that were used as reference data for both models in their Ecosim simulations. The model output time series of biomass were compared to reference time series of biomass listed in Table A.1.16. for all model simulations. The goodness of fit in these runs is measured by Ecosim as a weighted sum of squared differences (SS) between log reference and log predicted biomass (Christensen *et al.* 2005). This comparison provides the basis upon which the modeller can determine how the model represented potential biomass dynamics that may have occurred to match the biomass dynamics suggested by the reference stock assessment data. Biomass dynamics in Ecosim runs of these models were altered by changing either the vulnerabilities of various prey to predator species or by introducing primary production anomalies that would change the time series of phytoplankton production. The vulnerability parameter changes the rate at which prey species move in and out of states vulnerable to predation, *i.e.*, changes the ability of predators to assert top-down control upon their prey. The primary production anomalies (PPAs) change the total amount of energy going into the ecosystem allowing for the simulation of bottom-up forcing increasing or decreasing food availability throughout the ecosystem.

2.6.1. Vulnerabilities and simulating top-down dynamics

Ecosim allows the modeller to change the so-called ‘vulnerability’ of prey to predators in any ecosystem modelled. Therefore, the rate at which prey species move in and out of

states of being vulnerable to predation can be increased or decreased. This allows the emulation of 'top-down' dynamics (Christensen and Walters 2004). A low vulnerability setting implies two conditions, limited prey availability to a predator and that at the start of a simulation the predator is near its carrying capacity. Therefore, all other things remaining equal, the predator can not greatly increase the predation mortality it exerts upon a prey species thereby emulating bottom-up control. Conversely, a high vulnerability setting implies that a large portion of the prey species can become available for the predator to exploit and that the predator's biomass was well below carrying capacity at the start of the simulation. Therefore, high vulnerability emulates top-down control (Christensen *et al.* 2005).

To determine which vulnerabilities result in the largest changes in fitting the predicted biomass to the reference biomass time series, EwE can examine the model's sensitivity to vulnerability changes in each predator-prey link (Christensen *et al.* 2005). This procedure changes each vulnerability setting by 1% and reruns the Ecosim model to see how much the sum of squared differences between the predicted and reference time series was changed. This process, thus, determines which predator prey linkages result in greater changes to the predicted biomass time series relative to reference time series, easing the selection of vulnerabilities which, if changed, will more likely allow the modeller to fit predicted to reference data. The linkages deemed most likely to result in improvement of the fit can be selected by predator column, prey row, or individual trophic link. These selected vulnerabilities are examined via a Marquardt nonlinear search algorithm to find values which minimise the sum of squared differences between predicted and reference data (Christensen *et al.* 2005). A similar technique was used to calculate potential primary production anomalies for the models, instead by altering annual primary production over the run of the models to minimise the sum of squared differences of predicted to reference data. In this study, vulnerabilities were assigned by columns, *i.e.*, for all prey a predator species consumes.

As a way of exploring the effects of the vulnerability setting upon the models dynamics, the three models were run in Ecosim using three vulnerability settings to all trophic

linkages; bottom up ($v=1.5$), top down ($v=3$), and mixed bottom up / top down control ($v=2$) to see how SS values were affected by fishing effects, primary production anomalies, and combined fishing effects and primary production anomalies. Each of the vulnerability setting runs of the Ecosim model was done while comparing the reference time series of biomass (1950 - present). As implied above, the performance of each model run was judged by the SS value of predicted to reference biomass time series, lower SS implying a greater probability of explaining actual ecosystem dynamics. The final alteration to vulnerabilities was an attempt to find the lowest possible SS for each model by optimising the vulnerability by changing the values for sensitive predator columns. Note that for the determination of lowest SS for estimating vulnerabilities only biomass time series were considered, not catch.

2.7. Climate indices

In the comparison of the PPAs predicted by the models to climate time series, seven climate indicators were used; the Northern Oscillation Index (NOI), the Pacific Decadal Oscillation (PDO), the North Pacific Index (NPI), the Aleutian Low Pressure Index (ALPI), 'Bakun' West Coast Upwelling Indices (WCUI) at 48°N 125°W, 51°N 131°W, 54°N 134°W, 57°N 137°W, 60°N 146°W, 60°N 149°W, salinity in the Strait of Georgia, and Fraser River flow. In the case of most indices, especially those measured on daily or monthly increments, seasonal extremes can dominate annual average behaviour, hiding seasonal trends. Thus, when daily or monthly data was available, the climate indices were also broken up into seasons exhibiting similar values. As might be expected this resulted in divisions equivalent to the classic seasons; winter (December to February), spring (March to May), summer (June to August) and autumn (September to November). Note that such divisions were not always the case and that when different monthly grouping were used they are noted in the text of the Results section (chapter 3). To facilitate the determination of interannual cycles, a locally weighted scatter-plot smoothing (LOWESS) algorithm was applied to all data sets.

Monthly salinity data for two stations; Race Rocks and Chrome Island were taken from records maintained by the Department of Fisheries and Oceans at http://www-sci.pac.dfo-mpo.gc.ca/osap/data/SearchTools/Searchlighthouse_e.htm. Salinity data was available for Race Rocks from 1921 to the present, but the Chrome island time series only went back to 1961. In order to re-create the missing 1950 to 1961 data for Chrome Island data for that period was generated using data from nearby Entrance Island assuming a linear relationship between salinity at the two stations based upon an observed high correlation in the overlapping 1961-2004 data.

3. Results

The goal of this project was to determine how climate change and fisheries might be manifested in ecosystem models at different area scales, and this is illustrated through four groups of results. First, in section 3.1., a description of how general changes to assumptions about carrying capacities (vulnerabilities) and primary production anomalies (PPAs) affected the dynamics of each of the three models. Second, in section 3.2., biomass trajectories predicted by the 'best fit' EwE simulations are compared to biomass trends of managed species that have either assessment data or some type of abundance index. This section will, therefore, not show all outputs of all simulations that were conducted with the models considered. The 'best fit' biomass trends presented were those which ultimately produced the lowest sums of squared differences between simulated biomasses and reference biomasses after optimising vulnerability dynamics and PPAs in each of the three models. Third, in section 3.3, derived PPAs, from 1950 to 2002, from the 'best fit' simulations are compared to various climate indicators. This chapter will only provide a description of output data and how it compared to reference data and climate change indices. Discussion as to why these results emerged from the research can be found in Chapter 4.

3.1. General model responses in dynamic simulations

For information about parameter settings used in the simulations described below please refer to the appendices. The biomass trajectories were derived from simulations which have a primary production anomaly estimated with 10 spline points (see methods). Trajectories thus derived exhibit smoother interannual changes that better illustrate interannual trends rather than highlighting particular yearly anomalies.

As described in the methodology, EwE can estimate vulnerabilities and PPAs, to predict time series of biomasses that more closely match reference biomass time series from stock assessments. For each of the models, simulations were done from 1950 to the most recent data (2002 or 2003 depending on the model) to show the effect upon predicted

biomass dynamics when vulnerabilities for all trophic links were set to; 1.5, 2, and 3. At each of these vulnerability settings a PPA (using 10 spline points to approximate decadal climate forcing) was calculated to minimise the SS between predicted and reference biomass time series.

Table 3.1 shows that, even when accounting for trophic effects only, the models tended to better fit the reference data than the 'no model' straight line scenario would have over the period modelled. Note that for all models, at all vulnerabilities, the fit was always better when bottom-up climate forcing in the form of a PPA was added (all effects). For each ecosystem the predicted PPAs exhibited the same inflection points for changes from different primary production regimes regardless of the global vulnerability setting in that ecosystem model. The difference in the estimated PPAs appeared in the magnitudes of the peaks and troughs of production regimes from varying global carrying capacity. Note, too, that these runs usually predicted periods of relatively high or low primary production similar to the 'best fit' PPAs in which vulnerabilities were optimized for each predator group in the model, Figures 3.1 to 3.3.

Table 3.1: Sums of squared differences between predicted and reference biomass time series in the three ecosystem models under three global vulnerability assumptions, both without (trophic) and with simulated best fit primary production anomalies (all effects). These scenario SS are contrasted with total SS, i.e, fitting a straight line to the data (no model). The relative SS for models run under different assumptions of trophic control and total 'no model' SS are shown in **BOLD**.

v	Effect	SoG	BCS	NEPac
1.5	Total (no model)	257.85	840.99	445.89
	trophic only	202.41	681.61	349.82
		0.78	0.81	0.78
	all effects	168.42	576.85	280.66
2		0.65	0.69	0.63
	trophic only	202.77	676.53	384.54
		0.79	0.80	0.86
	all effects	169.44	589.07	284.7
3		0.66	0.70	0.64
	trophic only	238.55	699.45	464.7
		0.93	0.83	1.04
	all effects	206.1	634.4	322.07
		0.80	0.75	0.72

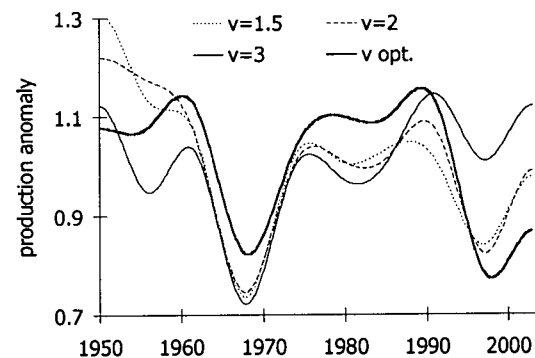


Figure 3.1: Simulated best fit SoG PPAs with trophic links set to $v=1.5$, 2, and 3 across all trophic linkages compared to the overall best fit PPA, in which optimal v 's were estimated for each predator group.

SoG simulations shown in Figure 3.1. had minimum primary production in the late 1960s and another relatively low period in the late 1990s. BCS simulations, Figure 3.2., had production peaks in the early 1950s and late 1980s. All BCS simulations suggested that the period of lowest primary production occurred in the late 1990s. SoG and BCS simulations all had several periods of alternating low and high primary production in each ecosystem, varying decadal, though both suggested that primary production was very low in the late 1990s. The NEPac simulations, on the other hand, suggested that there were just two levels of primary production (Figure 3.3). The first, from 1950 to 1977, is characterised by values below the long-term average. The second period, from 1977 to the end of the simulation, was characterised by primary production higher than the long-term average. The abrupt shift in phytoplankton biomass, during the 1970s, shows when the transition from low to relatively higher primary production happened.

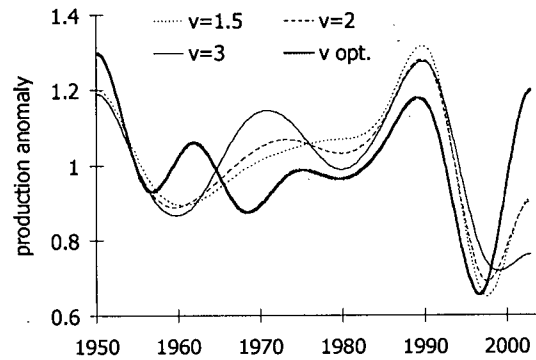


Figure 3.2: Simulated best fit BCS PPAs with trophic links set to $v=1.5$, 2, and 3 across all trophic linkages compared to the overall best fit PPA, in which optimal v 's were estimated for each predator group.

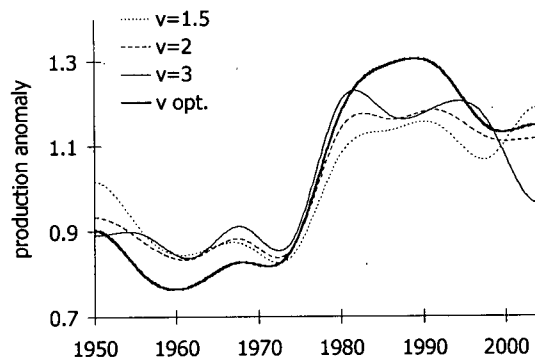


Figure 3.3: Simulated best fit NEPac PPAs with trophic links set to $v=1.5$, 2, and 3 across all trophic linkages compared to the overall best fit PPA, in which optimal v 's were estimated for each predator group.

3.2. Modelled biomass trajectories

3.2.1. The Strait of Georgia

Figure 3.4. shows changes in the adult herring group in the model, defined as those fish capable of spawning, *i.e.*, spawning stock biomass (SSB). The SoG stock assessment for

herring (DFO 2002d) provided the time series of biomass to which the model adult herring time series was compared. The model estimations of biomass changes from 1950 to 2002, although not matching the magnitude of absolute changes over the period, was able to reconstruct both the periodicity and direction of changes in biomass. Both the model and DFO (2002d) suggest the herring SSB was at its lowest in the late 1960 and that, by 2002, the biomass was at a similar size to that of 1950. Modeled SSB failed to capture the increase in SSB from 1990 to 2002 from recent stock assessment data (DFO 2002d). No time series was available to compare to the modelled juvenile herring biomass.

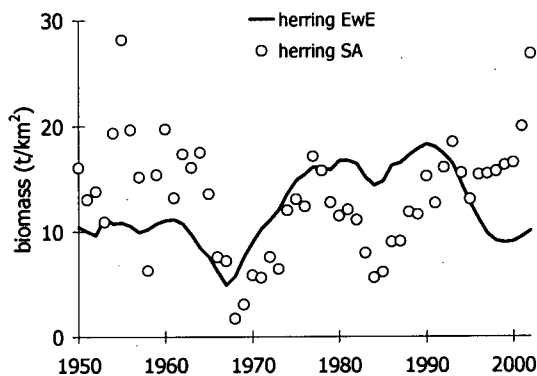


Figure 3.4: Comparison of changes in the modelled SoG adult herring biomass (EwE) versus the estimated Strait of Georgia spawning stock biomass (SA), 1950 to 2002.

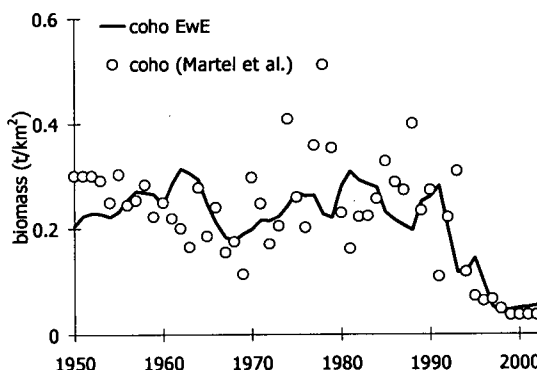


Figure 3.5: Comparison of changes in the modelled SoG coho salmon biomass (EwE) versus the estimated Strait of Georgia coho biomass from Martell *et al.* (2002), from 1950 to 2002.

In Figures 3.5 and 3.6 known declines in the abundance of both coho and chinook throughout the 1990s, were reflected in the declining biomasses for these two groups. However the model did not match the estimated mid 1970s peak in biomass suggested for both species in assessments done for chinook and coho in an earlier EwE Strait of Georgia model (Martell *et al.* 2002).

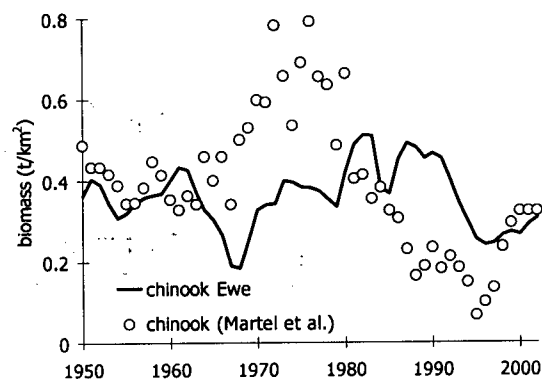


Figure 3.6: Comparison of changes in the modelled chinook salmon SoG biomass (EwE) versus the estimated Strait of Georgia chinook biomass from Martell *et al.* (2002), from 1950 to 2002.

Figures 3.7 and 3.8 show modelled biomasses for the pelagic piscivorous bird and demersal piscivorous bird groups compared to abundance indices derived from Audubon Society Christmas bird counts (CBCs) conducted in the Strait of Georgia region (www.audubon.org/). For both bird groups the downward trend suggested by count data was emulated by the simulation from 1950 to 2002.

Biomass trends from both the Georgia Basin CBC and model outputs suggested particularly marked declines in biomass of both species groups in the 1960s and 1990s.

The similarity of modelled changes in SoG harbour seal biomass to that suggested by the stock assessment of Olesiuk (1999) is shown in Figure 3.9. Olesiuk's (1999) assessment started at the end of an active cull on harbour seals in British Columbia and his assessment suggested that harbour seal populations increased after the end of the cull. The model reflected this increase and also suggests the population levelled off by the late 1990s.

The EwE model also suggested biomass dynamics of toothed whales similar to that of the number of resident orcas accounted for in the Strait of Georgia from 1960 to 1999

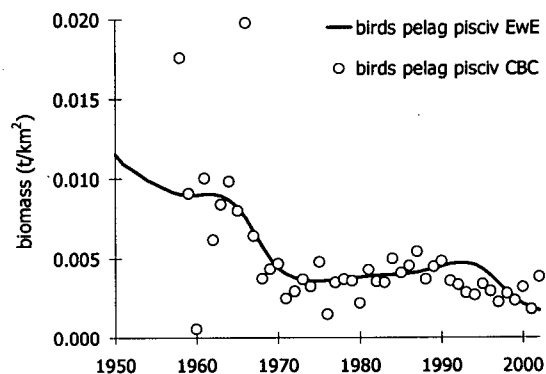


Figure 3.7: Comparison of changes in modelled SoG pelagic piscivorous bird biomass (EwE) versus biomass changes derived from SoG Christmas bird count (CBC) data, 1950 to 2002.

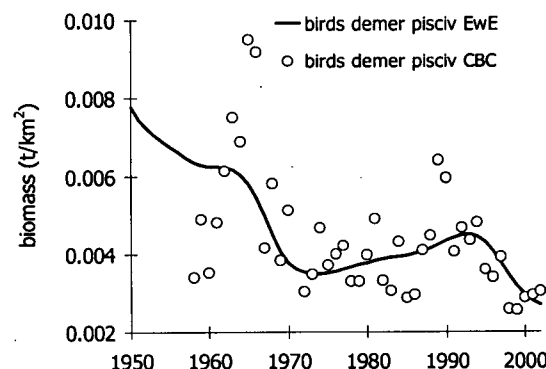


Figure 3.8: Comparison of changes in modelled SoG demersal piscivorous bird biomass (EwE) versus biomass changes derived from SoG Christmas (CBC) bird count data, 1950 to 2002.

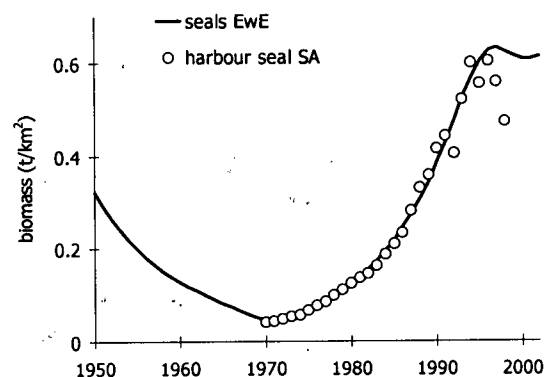


Figure 3.9: Comparison of changes in modelled SoG harbour seal biomass (EwE) versus biomass changes from SoG stock assessment data (SA), 1950 to 2002.

(Martell *et al.* 2002), see Figure 3.10.

While the populations of the two groups tended to changes in the same direction at the same time the magnitude of change was far greater in the case of harbour seals, especially the biomass increase from the early 1970s to the late 1990s. However, the decline in orca biomass at the end of the period modelled is far more profound in the EwE simulation than suggested by count data.

Martell (1999) estimated historic changes in lingcod biomass in the Strait of Georgia. Both the EwE model and the historic biomass assessment suggested a steady decline from 1950 to 1990 followed by a period of stability, see Figure 3.11.

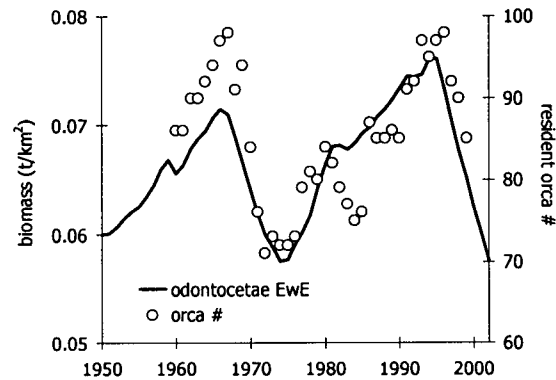


Figure 3.10: Comparison of changes in modelled SoG toothed whale biomass (EwE) versus SoG orca count data (orca #), 1950 to 2002.

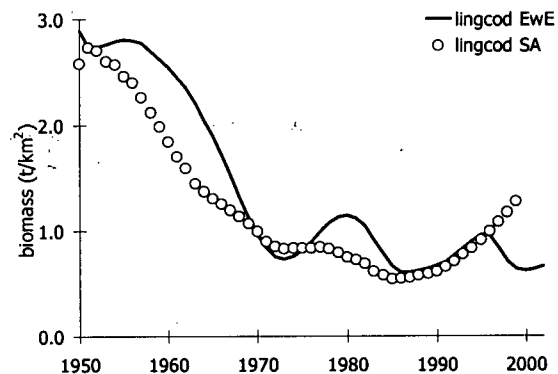


Figure 3.11: Comparison of changes in modelled SoG lingcod biomass (EwE) versus biomass from SoG stock reduction analysis (SA), 1950 to 2002 (Martell 1999).

3.2.2. The British Columbia Shelf

Due to the manner in which marine fish stocks are managed for the Pacific Coast of Canada, assessment data was available for a larger number of species than for the Strait of Georgia alone. Reference biomass time series for two of the species modelled for the BCS; pollock and arrowtooth flounder were based on assessment data from the Gulf of Alaska (see methods section). Almost all BCS biomass trajectories showed a decline over the last decade of the simulation, a change supported by stock assessments for commercially exploited species. The exceptions to the trend of recent decline were arrowtooth flounder, halibut, herring, and Pacific Ocean perch.

In the case of arrowtooth flounder, the assessment of Turnock *et al.* (2003), suggested that the biomass in the Gulf of Alaska began to increase dramatically in the mid-1970s. The BCS simulation mirrored this increase, Figure 3.12, although the model suggested a stabilisation of biomass in the 1990s, whereas the assessment had a relentless increase to the start of the 21st Century.

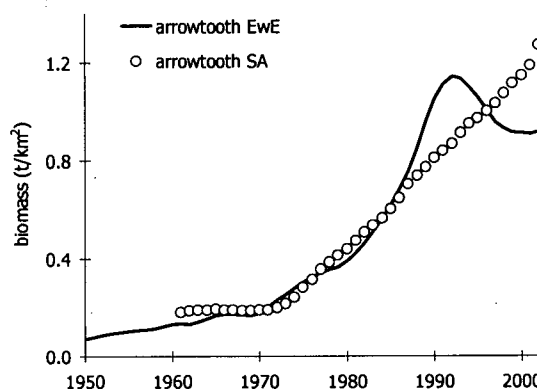


Figure 3.12: Modelled BCS arrowtooth flounder biomass (EwE) versus stock assessment (SA) biomass, 1950 to 2002 (Turnock *et al.* 2003b).

The biomass of pollock in the BCS ecosystem was also based on an assessment of a Gulf of Alaska stock, that of Dorn *et al.* (2003). Both the EwE model and the stock assessment (Figure 3.13) showed pollock biomass increasing from the early 1970s to early 1980s, then declining until the end of the 1990s and slightly recovering at the beginning of the 21st Century.

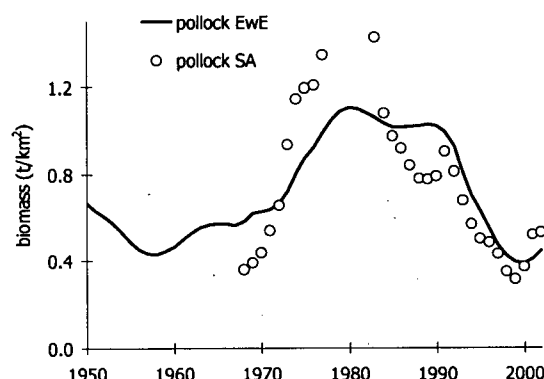


Figure 3.13: Modelled BCS walleye pollock biomass (EwE) versus biomass derived from a Gulf of Alaska stock assessment (SA), 1950 to 2002 (Dorn *et al.* 2003).

The assessment of Pacific cod by Sinclair *et al.* (2001) suggested that the biomass of that species off the BC coast has gone through several cycles over the period from 1950 to 2000. The EwE model also suggested such waxing and waning, Figure 3.14, although the peak assessment biomass of the mid-1970s was missed completely by the model. Both the model

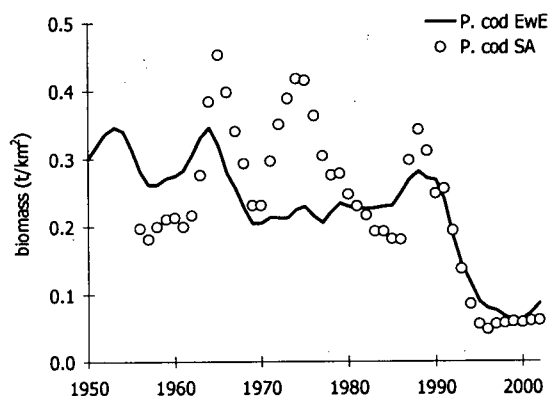


Figure 3.14: Modelled BCS Pacific cod biomass (EwE) versus BC stock assessment (SA) biomass, 1950 to 2002 (Sinclair *et al.* 2001).

and assessment have a dramatic decrease in biomass from the late 1980s to mid-1990s, followed by a relative stabilisation at the lowest levels of either time series.

Assessments such as Sullivan *et al.* (1997) and Clark and Hare (2001) found that biomass of halibut on the BC coast decreased from the 1950s to early 1970s, stayed low throughout the 1970s, then increased to the most recent year of assessment. The EwE model halibut biomass did not show as profound a decline at the beginning of the simulation, but did share the characteristic increase through the 1980s and 1990s, Figure 3.15.

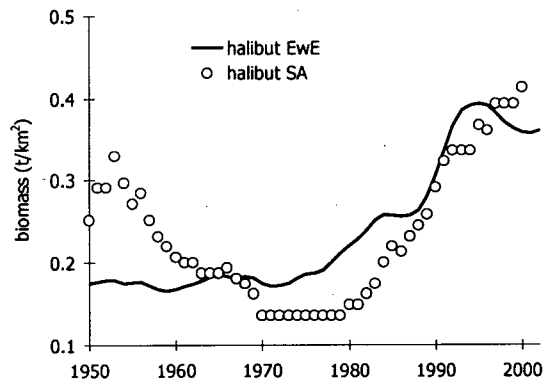


Figure 3.15: Comparison of modelled BCS halibut biomass (EwE) versus biomass derived from BC stock assessments (SA), 1950 to 2002 (Sullivan *et al.* 1997 and Clark and Hare 2001a).

A recent assessment of sablefish (Kronlund *et al.* 2002) provided a time series that merely covered the period from the early 1990s to the start of the 21st Century. A longer time series of biomass for comparison to the model was derived from catch (Haist *et al.* 2001) and an estimate of fishing mortality data (see methods for details). Figure 3.16 shows that, for the overlapping time period of these two

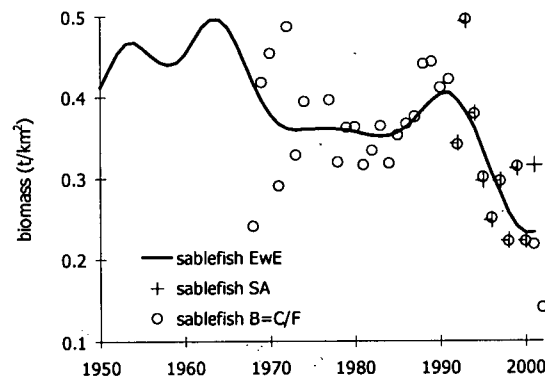


Figure 3.16: Comparison of changes in modelled BCS sablefish biomass (EwE) versus biomass derived from BC tagging data (SA), and from catch and mortality ($B=C/F$), 1950 to 2002.

reference biomass time series (the 1990s), values were quite similar. The EwE-predicted time series for sablefish biomass, in fact, followed the catch-derived trend of biomass stability through the 1970s: some increase in the late 1980s and early 1990s, followed by a steady decline from the mid 1990s to the end of the simulation.

The herring biomass of the BCS was represented by the SSB of five major stocks (DFO 2002a, 2002b, 2002c, 2002d, and 2002e). When summed, these assessments suggest that a major collapse in SSB during the late 1960s followed by a period of recovery and cycling around historic averages from the 1970s to the end of the assessment period, Figure 3.17. The biomass of herring adults in the EwE model also has a collapse in the late 1960s and similar cycling trends for the period after. Neither the EwE-modelled biomass crash of the late 1960s nor the biomass recovery of the 1970 is as large as the changes suggested by assessment data.

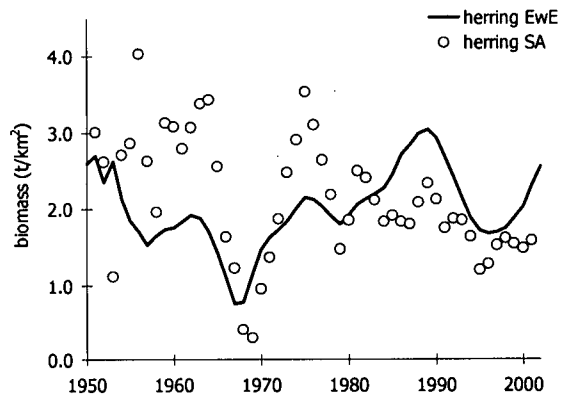


Figure 3.17: Comparison of modelled BCS herring biomass (EwE) to biomass from BC stock assessments (SA), 1950 to 2002.

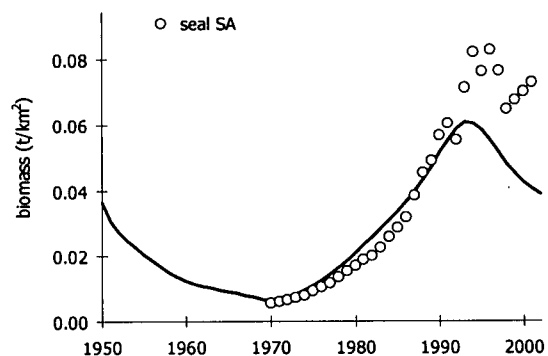


Figure 3.18: Comparison of modelled BCS harbour seal biomass (EwE) to biomass from BC stock assessments (SA), 1970 to 2002.

One species of marine mammal was explicitly modelled for the BCS: harbour seals. A trend in biomass very similar to that seen in the Strait of Georgia emerged from assessment and model biomass trajectories, Figure 3.18. Both the EwE model and the assessment of Olesiuk (1999) suggested that harbour seal population in BC increased dramatically after the early 1970s.

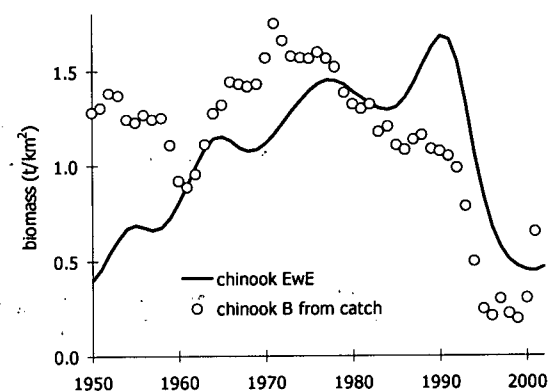


Figure 3.19: Comparison of modelled BCS chinook salmon biomass (EwE) to catch statistics biomass (B from catch), 1950 to 2002.

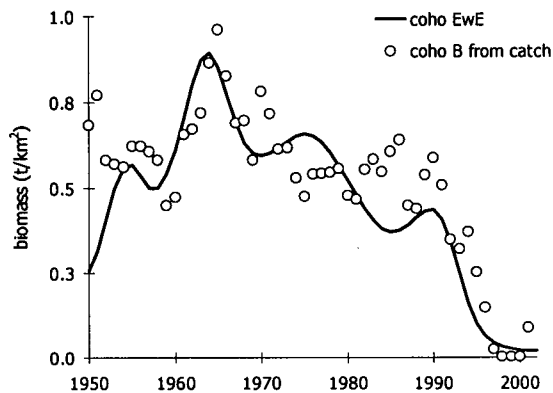


Figure 3.20: Comparison of modelled BCS coho salmon biomass (EwE) to biomass derived from BC catch statistics (B from catch), 1950 to 2002.

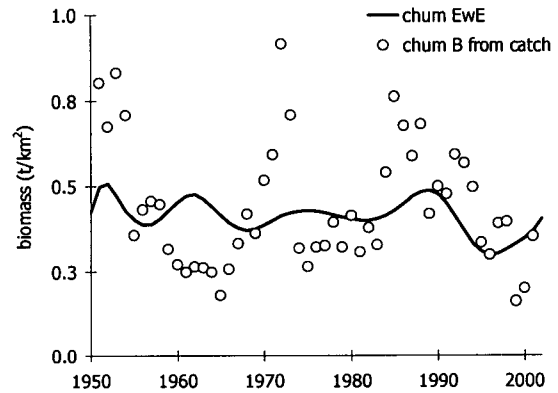


Figure 3.21: Comparison of modelled BCS chum salmon biomass (EwE) to biomass derived from BC catch statistics (B from catch), 1950 to 2002.

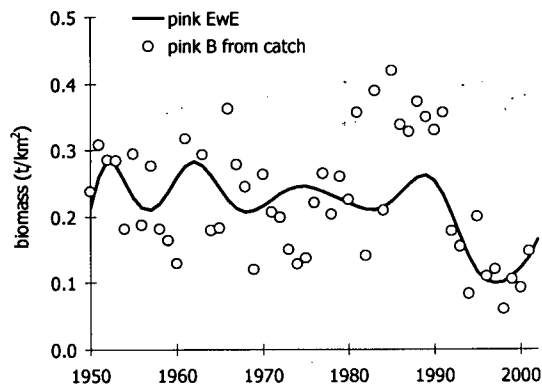


Figure 3.22: Comparison of modelled BCS pink salmon biomass (EwE) to biomass derived from BC catch statistics (B from catch), 1950 to 2002.

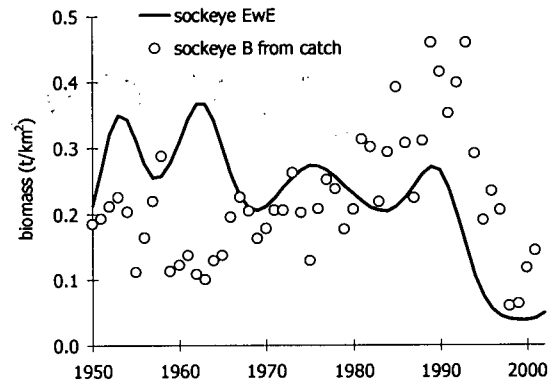


Figure 3.23: Comparison of BCS sockeye salmon biomass (EwE) to biomass derived from BC catch statistics (B from catch), 1950 to 2002.

The biomass time series to which the five salmon species in the EwE model were compared were derived from catches of salmon in BC reported by Eggers *et al.* (2003), see methods. The highs and low of the EwE biomass trend for chinook and coho match closely the biomass dynamics suggested by changes in biomass derived from Eggers *et al.* (2003), Figures 3.19 and 3.20. Modelled and reference biomass time series for chum, pink, and sockeye salmon were very similar only in the last decade of the simulation when there was a general decline in all three species, Figures 3.21, 3.22, and 3.23. The decline of sockeye salmon was the most profound in both the reference and modelled biomass time series. The model further suggested that average sockeye biomasses were higher from 1950 to 1965 than from 1970 to 1990, though the catch rate-derived biomass suggests that the opposite was true. In the case of pink and chum salmon there was no

obvious trend arising from the catch biomass time series other than relatively low biomasses in the 1970s, which the model does not emulate. Model and reference time series for pink and chum are similar in their long-term averages and suggest that declines in both have been less profound than in the three other commercially important salmon species.

The biomass of hake off the west coast of North America was used to derive a reference biomass time series for BCS hake (Jagiello and Sinclair 2002). The EwE simulation suggests very similar biomass dynamics to the reference time series, although the absolute peak that the assessment suggested to have occurred in the late 1980s was not reproduced in the model biomass trajectory, Figure 3.24.

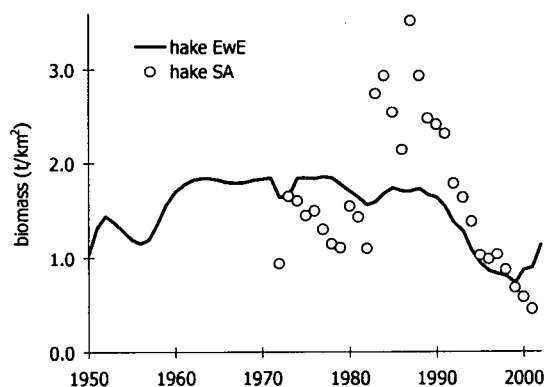


Figure 3.24: Comparison of changes in modelled BCS hake biomass (EwE) versus biomass derived from stock assessment (SA), 1950 to 2002.

The assessment of Pacific Ocean perch by Schnute *et al.* (2001) suggests that the biomass declined greatly between 1960 and the early 1980s, recovered slightly until the early 1990s and then declined again, though less profoundly. The BCS EwE model suggests a similar biomass time series although not the decline from the late 1990s to early 21st Century, Figure 3.25.

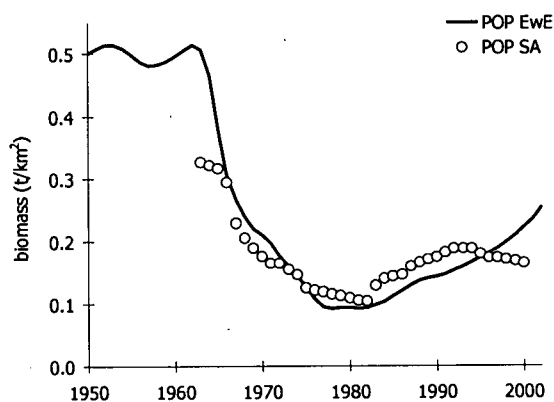


Figure 3.25: Comparison of changes in modelled BCS Pacific Ocean perch biomass (POP EwE) versus biomass derived from stock assessment (POP SA), 1950 to 2002.

The biomass of rock sole suggested by assessment data for the Queen Charlotte Islands and Hecate Strait (DFO 1999a) was used as a reference for the biomass produced by the BCS EwE simulation. Like salmon, the rock sole biomass trend produced by the model

was similar to the primary production anomaly seen in Figure 3.53. The pattern of increase and decrease suggested by the assessment and that resulting from the model simulation for rock sole were very similar, although the model did not match the absolute peak and valleys of the assessment biomasses, Figure 3.26.

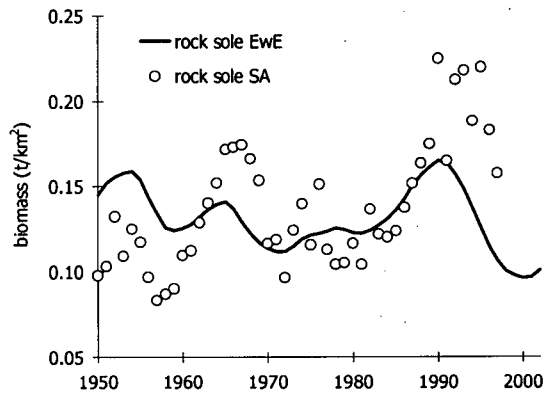


Figure 3.26: Changes in modelled BCS rock sole biomass (EwE) versus biomass derived from stock assessment (SA), 1950 to 2002.

3.2.3. The Northeast Pacific

It is fascinating that all of the biomass trajectories for species modelled in the Northeast Pacific (NEPac) EwE simulations from 1950 to 2003 show increases in the mid 1970s. Further, 13 out of the 17 species with comparative biomass data from stock assessments or abundance indices had higher average biomasses in the second half of the period modelled. The exceptions to this trend were chinook salmon, hake, Atka mackerel, and Pacific Ocean perch. This general increase in biomass appears to be very similar to the changes in primary production suggested by the 'best fit' NEPac simulation, Figure 3.60.

Arrowtooth flounder in the whole of the NEPac, like in the smaller scale BCS model increased dramatically from the mid 1970s to the beginning of the 21st Century. The stock assessments of Turnock *et al.* (2003) and Wilderbuer and Sample (2003) reflect this sudden increase, beginning in the mid 1970s, as does the EwE NEPac simulation, Figure 3.27. However the model did suggest that arrowtooth biomass levelled off near the end of the 1990s, whereas the assessments suggested a continued increase.

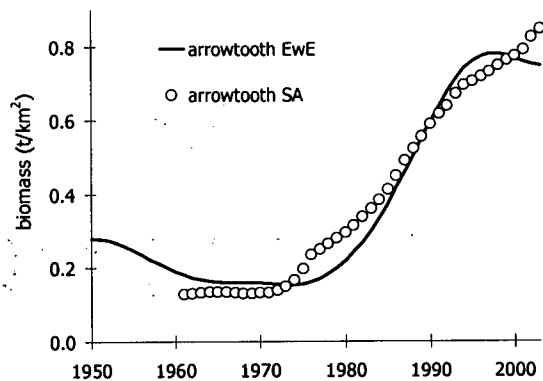


Figure 3.27: Comparison of changes in modelled NEPac arrowtooth flounder biomass (EwE) versus biomass derived from stock assessment (SA), 1950 to 2002.

The Pacific cod assessments of Thompson *et al.* (2003) and Thompson and Dorn (2003) when combined with Sinclair (2001) indicate that biomass began to increase in the mid 1970s, peaked in the late 1980s and declined somewhat after that, but not to historic lows. The NEPac simulation suggested a similar dynamic, although the absolute lowest biomass level in the model was not as small as that from the assessment data, Figure 3.28.

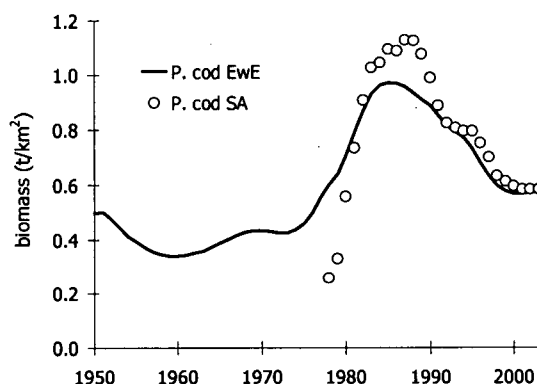


Figure 3.28: Comparison of modelled NEPac Pacific cod biomass (EwE) to biomass derived from stock assessment (SA), 1950 to 2002.

Sablefish in the NEPac area, like the BCS, appear to have undergone at least two cycles of waxing and waning biomass over the last fifty years (Sigler *et al.* 2003), with peaks occurring in the late 1960s and mid 1980s. Although the NEPac EwE model mirrors the assessment's rising in the late 1970s and peaking mid 1980s biomass, it does not match the earlier cycle of increase and decrease, Figure 3.29. The EwE model also did not match the magnitude of biomass decline after 1990 suggested by the assessment.

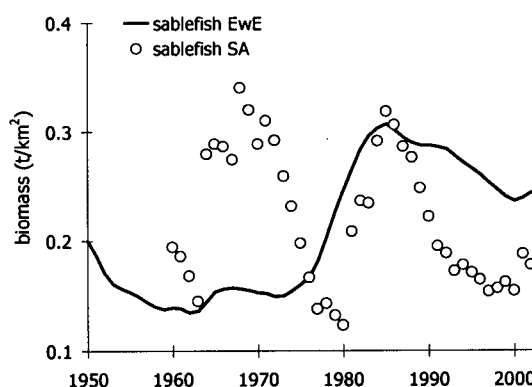


Figure 3.29: Comparison of changes in modelled NEPac sablefish biomass (EwE) versus biomass derived from stock assessment (SA), 1950 to 2002.

The modelled biomass changes suggested for halibut are very similar to those suggested by assessment data (Sullivan *et al.* 1997 and Clark and Hare 2001), Figure 3.30. These changes are quite similar to those seen in the assessment data and simulated halibut biomass time series from the BCS model, Figure 3.15.

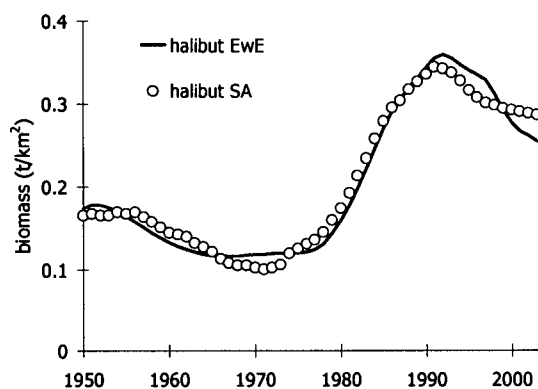


Figure 3.30: Comparison of changes in modelled NEPac halibut biomass (EwE) versus biomass derived from stock assessment (SA), 1950 to 2002.

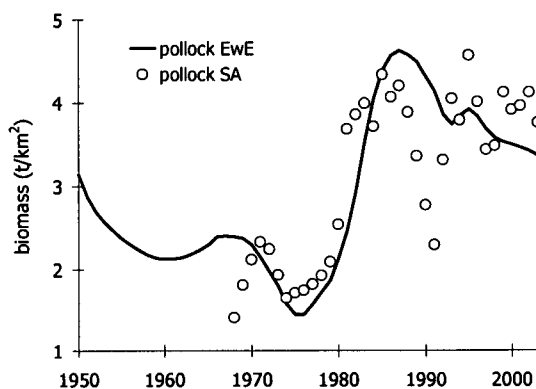


Figure 3.31: Comparison of changes in modelled NEPac walleye pollock biomass (EwE) versus biomass derived from stock assessment (SA), 1950 to 2002.

Assessment data (Dorn *et al.* 2003) and Ianelli *et al.* (2003) and the NEPac model all suggested that pollock biomass increased dramatically after the mid 1970s, Figure 3.31. A biomass dip in the early 1990s shown in the assessment data is not reflected in the NEPac simulation, but both indicate that biomass remained relatively high after 1980.

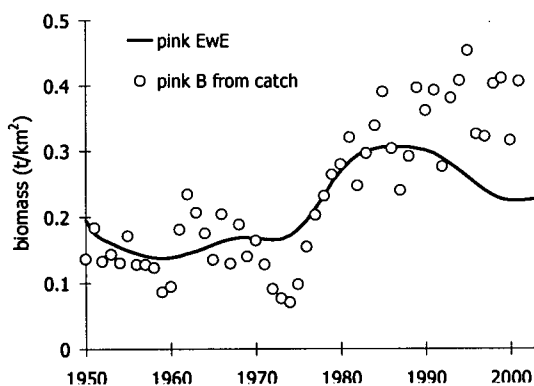


Figure 3.32: Comparison of changes in modelled NEPac pink salmon biomass (EwE) versus biomass derived from catch data (B from catch), 1950 to 2002.

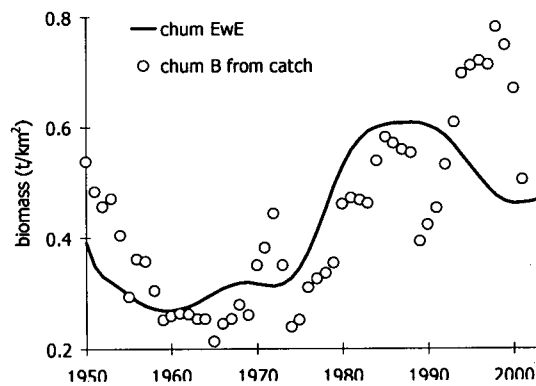


Figure 3.33: Comparison of changes in modelled NEPac chum salmon biomass (EwE) versus biomass derived from catch data (B from catch), 1950 to 2002.

As was the case for BCS salmon, biomass time series used for NEPac salmon, as a comparison to the model output biomass, was derived from catches reported in Eggers *et al.* (2003). Of the five major salmon species, pink, chum, and sockeye showed the largest agreement between biomass changes derived from the catch data and that predicted by the NEPac model, Figure 3.32, 3.33, and 3.34. The model and catch-derived time series for sockeye differed only in that the latter time series suggested a higher absolute peak

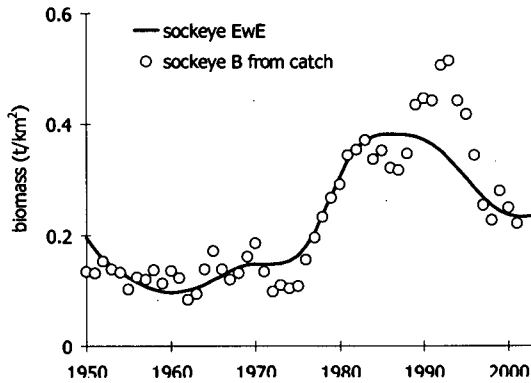


Figure 3.34: Comparison of changes in modelled NEPac sockeye salmon biomass (EwE) versus biomass derived from catch data (B from catch), 1950 to 2002.

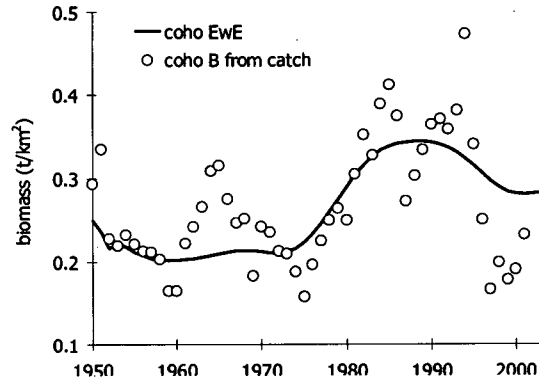


Figure 3.35: Comparison of changes in modelled NEPac coho salmon biomass (EwE) versus biomass derived from catch data (B from catch), 1950 to 2002.

biomass in the early 1980s. The modelled biomass trajectories for pink and chum were slightly lower than the catch-derived reference biomass time series in the late 1990s. Both reference and modelled biomass time series for coho salmon suggested a general increase in the late 1970s and higher average biomass after that time, Figure 3.35. However the model does not emulate a small peak in coho

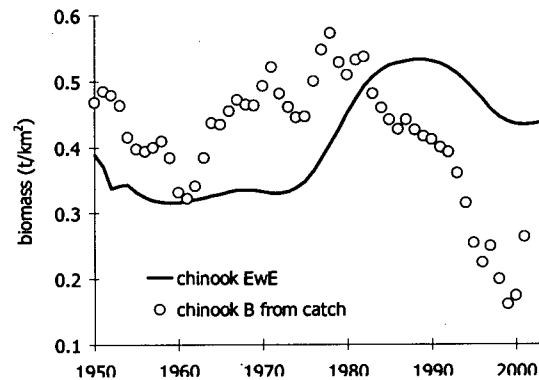


Figure 3.36: Comparison of changes in modelled NEPac chinook salmon biomass (EwE) versus biomass derived from catch data (B from catch), 1950 to 2002.

biomass that the catch-derived data indicates for the mid 1960s. Chinook salmon biomass dynamics suggested by the NEPac model resembled that derived from catch data only in the decline in the last decades of the simulation (Figure 3.36). The decline at the end of the simulation, however, is not as profound as that suggested by the catch data. The average biomass levels suggested by the chinook catch data after 1980 is lower than before that time, which is in opposition to the dynamics suggested by the NEPac model. That most salmon in the NEPac model thus had higher biomasses towards the end of the simulation that exceeded their historic averages, is quite in contrast to the case of salmon in the BCS region, see Figures 3.19 to 3.23.

Biomass trajectories for Pacific Ocean perch indicated by both the NEPac model and assessment data, derived by combining Schnute *et al.* (2001), Hanselman *et al.* (2003),

and Spencer and Ianelli (2003) suggest that there was a major decline from the early 1960s to late 1970s, Figure 3.37. After 1980 both the model and assessment data suggest a moderate recovery, although not nearly to the historic biomass average. This trend of massive biomass decline followed by a moderate recovery is very similar to the trend shown for this species in the BCS model and assessment data, Figure 3.25.

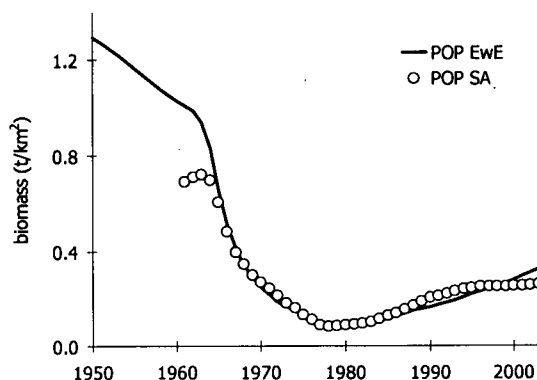


Figure 3.37: Comparison of changes in modelled NEPac Pacific Ocean perch biomass (POP EwE) versus biomass derived from stock assessment (POP SA), 1950 to 2002.

Although assessment data for Northern rockfish was only available from 1977 onwards, (Courtney *et al.* 2003) and Spencer and Ianelli 2003), there does appear to be a trend similar to most of the other species in the NEPac area, *i.e.*, relatively higher biomass after the mid 1970s, Figure 3.38. The NEPac simulation biomass trend does have a lower average before than after the mid 1970s and the period for which it does overlap with assessment data (1977-2003) it matches the qualitative and quantitative changes suggested by the stock assessment.

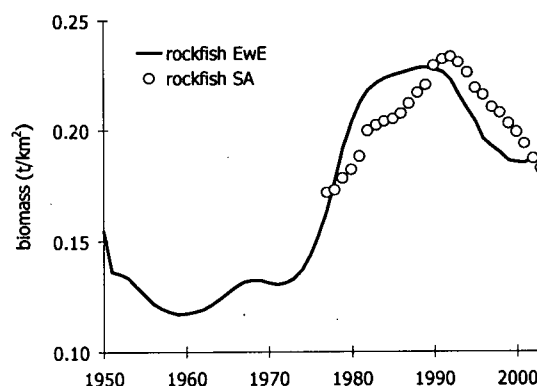


Figure 3.38: Comparison of changes in modelled NEPac northern rockfish biomass (EwE) versus biomass derived from stock assessment (SA), 1950 to 2002.

Atka mackerel, (Lowe and Lauth 2003 and Lowe *et al.* 2003) and hake (Jagiello and Sinclair 2002) assessments suggested that while these two species experienced increased biomasses, starting in the mid 1970s, they then behaved quite differently from most of the other species over the NEPac region. Both Atka mackerel and hake biomasses appear to have peaked in the late 1980s and then declined to levels lower than, or near to, historic

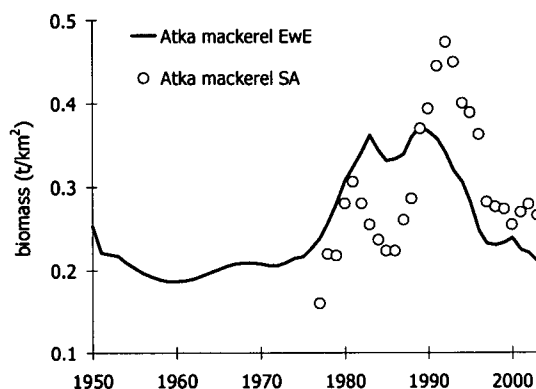


Figure 3.39: Comparison of changes in modelled NEPac Atka mackerel biomass (EwE) versus biomass derived from stock assessment (SA), 1950 to 2002.

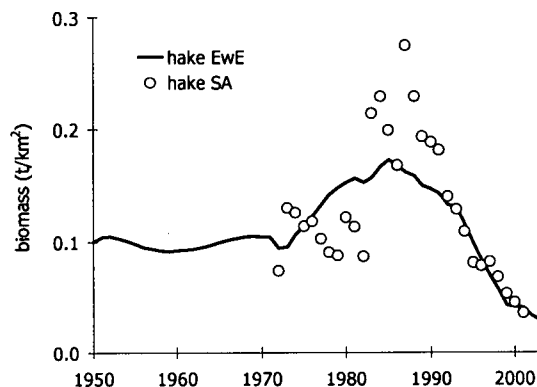


Figure 3.40: Comparison of changes in modelled NEPac hake biomass (EwE) versus biomass derived from stock assessment (SA), 1950 to 2002.

lows, Figures 3.39 and 3.40. Although the NEPac simulation does not attain the absolute peak biomass suggested by assessment data, the model does match historic low and average biomasses as well as timing and direction of biomass change.

Three of the flatfish species in the NEPac region (plaice, yellowfin sole, and rock sole) showed surprisingly similar trends in population trajectories based on assessments (Spencer *et al.* 2003, Wilderbuer and Nichol 2003, Wilderbuer and Walters 2003, and DFO 1999a), Figures 3.41, 3.42, and 3.43. All three species appear to have declined from the mid 1960s to early 1970s. All three exhibited the same increasing biomass

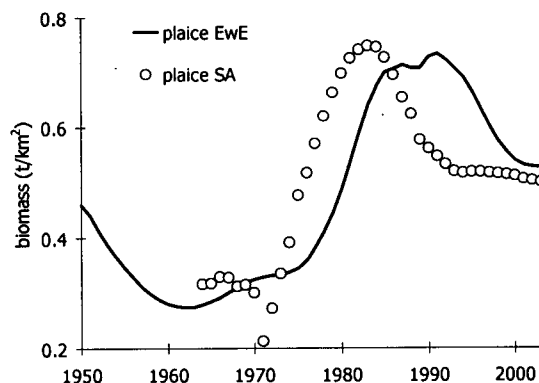


Figure 3.41: Comparison of changes in modelled NEPac plaice biomass (EwE) versus biomass derived from stock assessment (SA), 1950 to 2002.

trend of many of the other species in the NEPac area, but with that increase beginning somewhat earlier in the 1970s, see, *e.g.*, salmon (Figures 3.32 to 3.36), pollock (Figure 3.31), and sablefish (Figure 3.29). The earlier timing of biomass increase, however, coincides with the biomass increase suggested for larger flatfish species in the NEPac area, halibut (3.30) and arrowtooth flounder (Figure 3.27). The NEPac model produced biomass dynamics for plaice very similar to the stock assessment, although somewhat

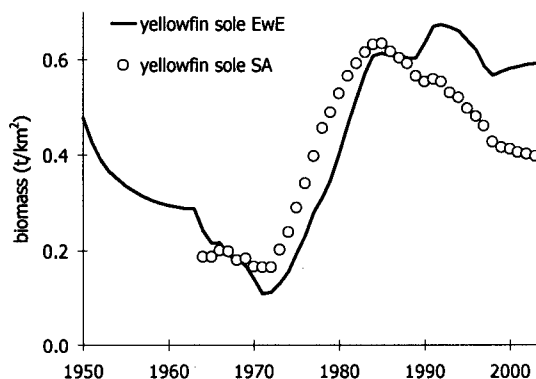


Figure 3.42: Comparison of changes in modelled NEPac yellowfin sole biomass (EwE) versus biomass derived from stock assessment (SA), 1950 to 2002.

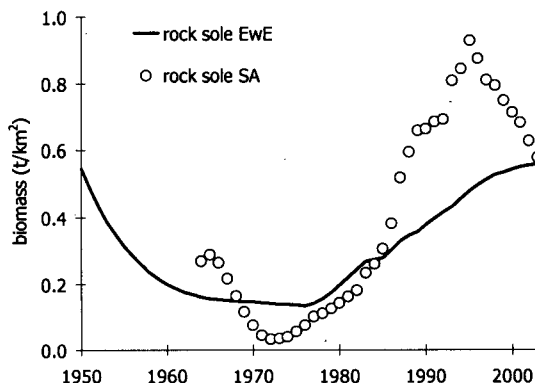


Figure 3.43: Comparison of changes in modelled NEPac rock sole biomass (EwE) versus biomass derived from stock assessment (SA), 1950 to 2002.

lagging in the timing of increases and decreases. The timing of changes in the biomass of yellowfin sole in the NEPac model was more similar to that of the assessment data, although the decline suggested for the last ten years of the assessment did not appear in the simulation. The NEPac model captured the long term qualitative change in rock sole biomass indicated by the stock assessment but did not match the timing or magnitude of the late 1970s increase.

3.3. Fitting simulated time series to reference time series data

Table 3.2 shows the weighted sum of squared deviations (SS) for the three ecosystem models in which trophic effects *alone*, or trophic effects, *i.e.*, carrying capacity, *and* a PPA (derived using a cubic spline function with 10 spline points over the 52 year simulations to approximate decadal cycling) were used by EwE to explain

biomass dynamics for the time period of the simulation. These scenario SS are contrasted with the baseline SS, *i.e.*, fitting a straight line to the data (no model) by the bold numbers which indicate the relative size of the scenario SS to the baseline SS. All three models

Table 3.2: Sums of squared differences between 'best fit' predicted and reference time series in ecosystem model runs with and without primary production anomalies. Relative magnitudes of model run SS to 'no model' case in **bold**.

	SS environ	SS trophic	SS both
SoG	307.82	182.85	156.48
	1.19	0.71	0.61
BCS	716.37	508.9	438.72
	0.85	0.61	0.52
NEPac	396.83	279	170.91
	0.89	0.63	0.38

suggested that the SS was lowest when a PPA was applied in conjunction with trophic effects and fishing mortality. The SS improvement was greater in the SoG and BCS models when the fitting routine was run using only the reference time series for biomass, Table 3.3. Note from tables 3.2 and 3.3. that in many cases, when environmental effects *alone* were accounted for, the models, when fitted to reference data, actually produced SS values greater than the no model case, *e.g.*, SoG in Table 3.3. and both SoG and NEPac in Table 3.4. Models also proved to have slightly lower SS when the PPA was fitted as annual estimates rather than the 10 variables of the PPA arising from a fitted cubic spline function. Table 3.4 shows model fits to reference data when differing assumptions of global vulnerabilities across all trophic linkages were used. Therefore, all vulnerabilities set to 1.5 implies that all predators are near carrying capacity while 2 and 3 suggests they are further away, allowing for more top-down type dynamics.

Table 3.3: Sums of squared differences between 'best fit' predicted and reference time series in ecosystem model runs with and without primary production anomalies when biomass time series alone were used in the SS calculation. Relative magnitudes of model run SS to no model case indicated in **bold**.

	SS environ	SS trophic	SS both
SoG	197.6	73.31	50.73
	1.84	0.68	0.47
BCS	227.29	154.6	121.07
	0.87	0.59	0.46
NEPac	190.96	133.05	63.07
	1.17	0.81	0.39

Table 3.4: Sums of squared differences between predicted and reference biomass time series in the three ecosystem models under three global vulnerability assumptions, both without (trophic) and with simulated best fit primary production anomalies (all effects). These scenario SS are contrasted with total SS, *i.e.*, fitting a straight line to the data (no model). The differences between model runs under different assumptions of trophic control and total SS are shown in **bold**.

v	SS	SoG	BC Shelf	NEPac
	Total (no model)	257.85	840.99	445.89
1.5	trophic only	202.41	681.61	349.82
		0.78	0.81	0.78
	all effects	168.42	576.85	280.66
		0.65	0.69	0.63
2	trophic only	202.77	676.53	384.54
		0.79	0.8	0.86
	all effects	169.44	589.07	284.7
		0.66	0.7	0.64
3	trophic only	238.55	699.45	464.7
		0.93	0.83	1.04
	all effects	206.1	634.4	322.07
		0.8	0.75	0.72

As stated all the aforementioned fits were to cubic spline functions designed to approximate decadal cycling. There was slight improvement of the fit to an annual, rather than the spline curve for the Strait of Georgia model, the SS having been lowered by

approximately 7.5% for the biomass fitted inter-annual anomaly *vis a vis* the spline anomaly, whereas in the Northeast Pacific model the reduction in SS for the inter-annual versus the spline PPA was only about 1.7%, Table 3.5.

One concern of generating PPAs to explain ecosystem-wide changes in biomass is “obtaining a spurious anomaly sequence that just represents measurement errors in the fitting data” Christensen *et al.* (2005). In order to examine the likelihood of a PPA thus occurring, EwE can test whether an anomaly is due to chance (see methods). In all models it was demonstrated that here was either a small, or close to zero, chance that the PPA represented no real shared effect (see Table 3.6).

Each of the three ecosystem models contains an environmental forcing function used to drive time series of phytoplankton biomass. The resultant changes in phytoplankton biomass cause bottom-up changes to flow through the model. The methods section describes how EwE can generate a forcing function which causes bottom-up forcing that fits generated biomass time series to reference time series. The resultant PPAs for each of the three models are shown below. In each model the PPA used to derive the best fit across all species biomass time series was derived *after* vulnerabilities were adjusted. The vulnerabilities for each predator prey linkage can also be altered to produce optimal fits of generated to reference time series of biomass (see methods). The vulnerability settings that were in use while the models were generating the ‘best fit’ PPAs can be seen in Appendix 2, Table A.2.1. The best fit PPA for each model was a yearly production anomaly and not a fitted spline function. The comparisons of PPAs to climate indices were made using annual PPA data smoothed using a LOWESS filter. Note, therefore, that the spline functions produced PPAs very similar to the smoothed annual data. Because

Table 3.5: Improvement of fit, for models by using a PPA *and* fishing effects, indicated by percentage decrease of SS value over simulations using trophic effects *alone* to explain historic variation in biomass.

	decadal PPA	annual PPA
SoG	0.252	0.308
BCS	0.233	0.282
NEPac	0.558	0.566

Table 3.6: Probability that decadal spline fitted PPAs and annual PPAs represented fitting to measurement error, i.e., no real shared effect for each model.

	decadal PPA	annual PPA
SoG	0.376	0.183
BCS	0	0
NEPac	0	0

the resolution of the annual fitting procedure was estimated at a finer temporal grain, the absolute amplitude tended to be greater than for PPAs thus generated.

3.4. Comparing primary production anomalies to climate indices

3.4.1. Temporal oscillations in modelled primary production anomalies

The annual PPA derived for the Strait of Georgia is shown in Figure 3.44. The two other times series in Figure 3.44. represent the annual PPA smoothed using a LOWESS filter (Cleveland 1979) with a second degree polynomial and smoothing windows of 20 and 40 years. For the analysis of temporal trends in this and other PPAs four smoothing windows were used; 10, 20, 30, and 40 years. The smoothed data suggests that changes in modelled productivity occurred on both decadal and bi-decadal scale. The longer-scale fluctuation appears to have been at its lowest in the late 1960s and at the end of the simulation, with peaks at the beginning of the simulation and the mid 1980s. The overlying decadal changes had the net effect of causing the two production troughs being even lower, while shifting peaks in production to the late 1950s, mid 1970s and early 1990s.

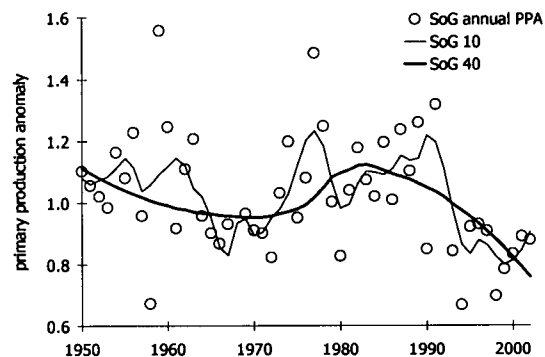


Figure 3.44: Best fit annual PPA from the SoG model and smoothed PPA values from a LOWESS filter using a second degree polynomial with 10 and 40 year smoothing windows.

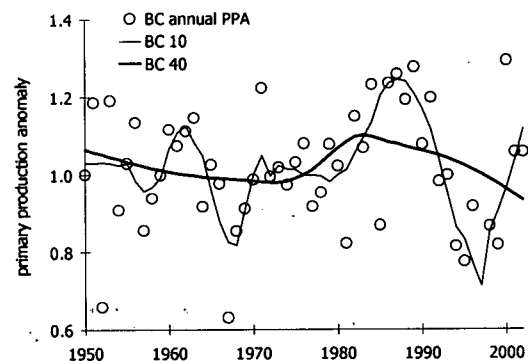


Figure 3.45: Best fit annual PPA from the BCS model and smoothed PPA values from a LOWESS filter using a second degree polynomial with 10 and 40 year smoothing windows.

For the BCS model the PPA derived to best fit the biomass data to reference time series is seen in Figure 3.45. When the PPA data was smoothed on a 40-year scale, the trend in production appeared to be similar to the longer bidecadal changes seen in the Strait of Georgia PPA. However at the shorter decadal scale, while the decadal oscillations appear also to occur synchronously with those of the Strait of Georgia model, the peak of the early 1990s was greater and that of the 1950s smaller. Another difference at the decadal scale was the apparent recovery in production at the end of the BCS simulation, compared to the Strait of Georgia model ending at the bottom of a production cycle.

The Northeast Pacific model exhibited very different dynamics in its fitted PPA, Figure 3.46. Regardless of the smoothing window used, the PPA appeared to be changing on a bidecadal cycle with a trough in production during the early 1960s and a peak in the late 1980s. The smoothed PPAs for the Strait of Georgia and BCS had similar oscillations, but the trough was later, and the peak earlier than for the smoothed Northeast Pacific PPA.

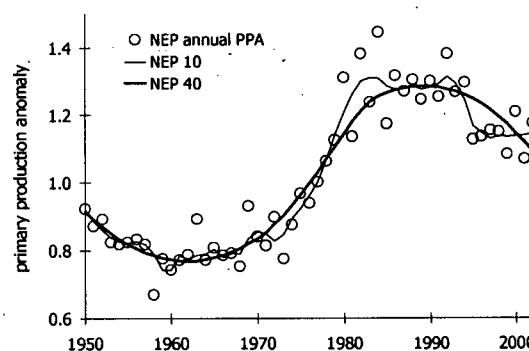


Figure 3.46: Best fit annual PPA from the NEPAC model and smoothed PPA values from a LOWESS filter using a second degree polynomial with 10 and 40 year smoothing windows.

At the longer period of oscillation the Strait of Georgia model suggests production was at a historic low by the end of the simulation, *i.e.*, in 2002. The BCS model suggested that while production was low by the end of the simulation, this nadir was comparable to the previous trough in production in the late 1960s. The Northeast Pacific model suggested that production may have been declining by the end of the simulation, but was still at the long-term average in 2003.

3.4.2. Comparing modelled production anomalies to climate indices

For the purposes of describing these results no causality is intended or implied by the correlations shown below. The correlations are guides to useful paths of investigation

and, as such, will be described in the text as weak: $0.0 < R^2 < 0.33$, moderate: $0.34 < R^2 < 0.66$, or strong: $0.67 < R^2 < 0.99$. Although arbitrary and only meant to be a qualitative guide to describing these results, this characterisation scheme seems apt given the results of the statistical analysis of the correlations in which it was shown that correlations below $R^2 = 0.27$ were not significant at an $\alpha = 0.05$. The actual values of the described correlations as well as correlations not discussed in the text can be seen in the Appendix 3 tables relevant to this, Tables A.3.1. to A.3.11. In order to illustrate the comparative amplitudes and frequencies of decadal and inter-decadal oscillations of the derived PPAs versus the climate indices, PPAs and climate indices with the highest correlation at smoothing windows of 10 and 30 years are shown in Figures 3.47 to 3.68.

3.4.2.1. The Strait of Georgia

The best fit PPA for the Strait of Georgia, Figure 3.44, was compared to four climate time series; Fraser River flow measured at Hope, BC (Environment Canada 2005), salinity at Race Rocks (DFO 2003), salinity at Chrome Island (DFO 2003), and coastal upwelling at 48°N (Bakun 1973 and Schwing *et al.* 1996). Table A.3.1. shows that when the Strait of Georgia PPA was compared to historical changes in Fraser River, there was a weak, and insignificant, positive correlation to winter flow, *i.e.*, January, February, and March.

Moderate and significant negative correlations were seen when spring and summer flows were compared to the Strait of Georgia PPA. At a decadal scale of change the largest

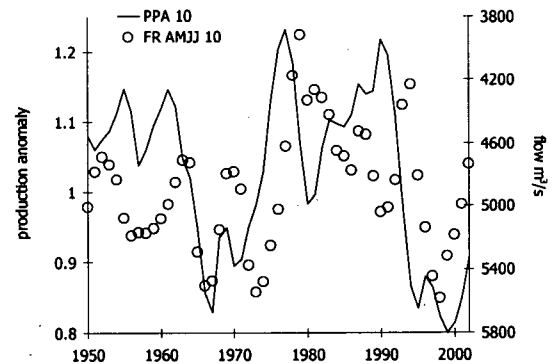


Figure 3.47: Comparisson of SoG PPA to Fraser River flow (averaged from April to July). Data smoothed with a LOWESS filter using a second degree polynomial and 10-year smoothing window.

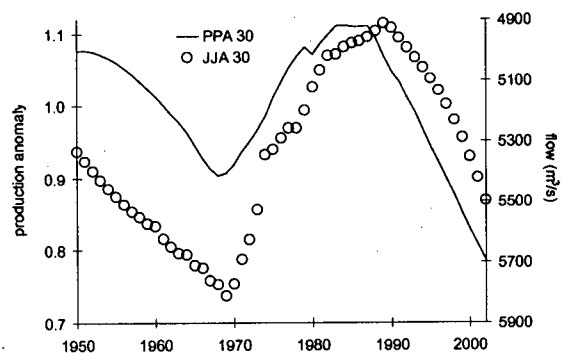


Figure 3.48: Comparisson of SoG PPA to Fraser River flow (averaged from June to August). Data smoothed with a LOWESS filter using a second degree polynomial and 30-year smoothing window.

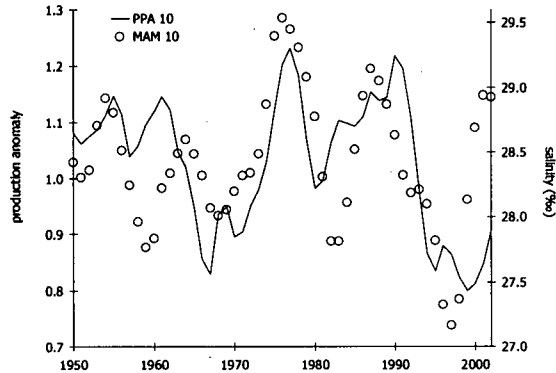


Figure 3.49: Comparisson of SoG PPA to Chrome Island salinity (averaged from March to May). Data smoothed with a LOWESS filter using a second degree polynomial and 10-year smoothing window.

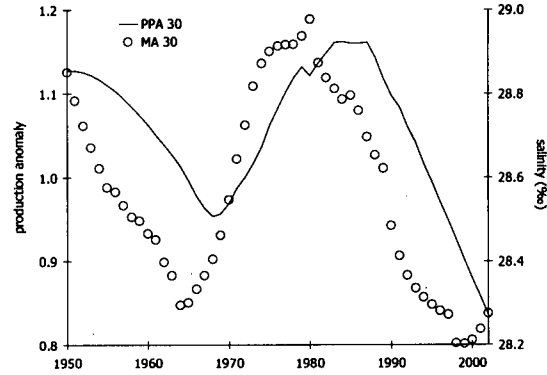


Figure 3.50: Comparisson of SoG PPA to Chrome Island salinity (averaged over March and April). Data smoothed with a LOWESS filter using a second degree polynomial and 30-year smoothing window.

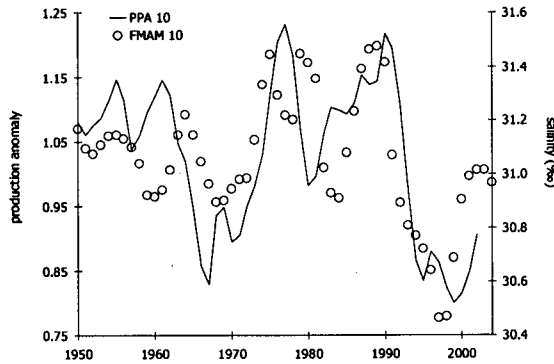


Figure 3.51: Comparisson of SoG PPA to Race Rocks salinity (averaged from February to May). Data smoothed with a LOWESS filter using a second degree polynomial and 10-year smoothing window.

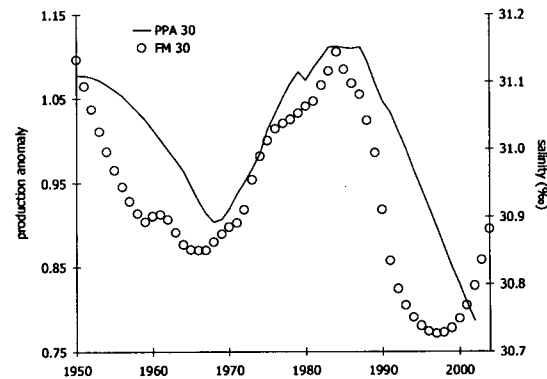


Figure 3.52: Comparisson of SoG PPA to Race Rocks salinity (averaged over February and March). Data smoothed with a LOWESS filter using a second degree polynomial and 30-year smoothing window.

negative correlation was observed for periods spanning spring and summer Figure 3.47, whereas at longer, bidecadal scales the correlation was highest with summer Fraser River flow values from June, July and August, Figure 3.48.

When the Strait of Georgia PPA was compared to salinity values the correlations were moderately to strongly positive at all times of year and at all time scales, Tables A.3.2. and A.3.3. The correlations with salinity measured at Race Rocks tended to be higher than those for Chrome Island. The largest correlations tended to be in months earlier in the year (February to May) than the highest Fraser River correlations (April to August). For Chrome Island the correlations was highest in the spring; March, April, May: Figures

3.49 and 3.50. The Race Rocks salinity showed the highest correlations for values from the end of winter into the middle of Spring; February to May, Figure 3.51 and 3.52.

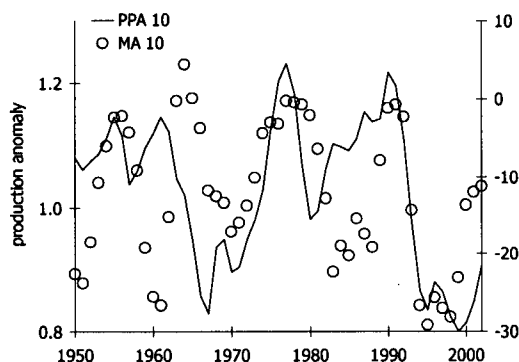


Figure 3.53: Comparisson of SoG PPA to upwelling at 48°N (averaged over March and April). Data smoothed with a LOWESS filter using a second degree polynomial and 10-year smoothing window.

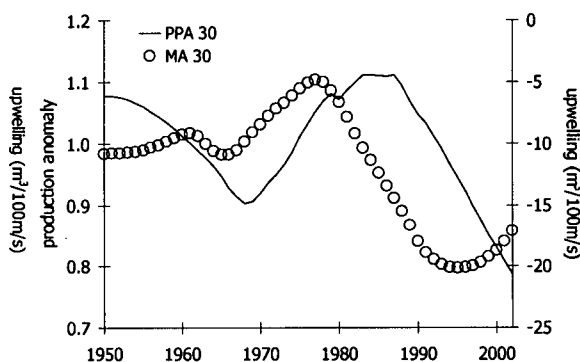


Figure 3.54: Comparisson of SoG PPA to upwelling at 48°N (averaged over March and April). Data smoothed with a LOWESS filter using a second degree polynomial and 30-year smoothing window.

The Strait of Georgia PPA showed mostly weak, but some moderate and significant, positive correlations to upwelling data from 48°N, Table A.3.4. The highest correlation was for upwelling in the spring months of March and April, Figures 3.53 and 3.54.

3.4.2.2 The British Columbia Shelf

The BCS best fit PPA, Figure 3.45, was compared to coastal upwelling at three locations along the coast of BC; 48°N, 51°N, and 54°N (Bakun 1973 and Schwing *et al.* 1996). The positive correlations with upwelling values for 48°N were generally weak to moderate, while negative correlations tended to be smaller or even insignificant. The highest positive correlations were for the summer and fall, Table A.3.5. Figure 3.55 shows the moderate positive correlation between the BCS PPA and upwelling occurring at 48°N, in

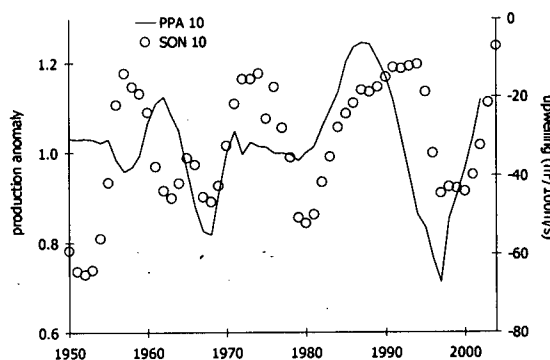


Figure 3.55: Comparisson of BCS PPA to upwelling at 48°N (averaged from September to March). Data smoothed with a LOWESS filter using a second degree polynomial and 10-year smoothing window.

the fall, at a decadal scale. At longer time scales there was actually a negative correlation for the first 15 years then a strongly positive one for the rest of the time of comparison.

Comparisons between the BCS PPA and coastal upwelling at 51°N and 54°N were different from those at 48°N in that there were a few weak positive correlations and many moderate negative correlations. The highest negative correlations were usually associated with upwelling that occurred either in the spring or summer, Tables A.3.6 and A.3.7. The BCS PPA tended to move into, and out of, different production regimes at the same time and rates as upwelling at both 51°N and 54°N. This effect was most pronounced when the PPA was compared to upwelling during the months of May, June, and July at the decadal scale. Also, the upwelling rates and occurrence of changes from one regime to another were very similar at these two stations, even producing the highest correlations to the PPA when averaged over the same months of the year. Figures 3.56 shows the similarity of decadal oscillation of upwelling at 54°N and the BCS PPA. Figure 3.57 illustrates how regime changes were also similar at longer time scales. The corresponding graphs for 51°N are not shown as they convey essentially the same information

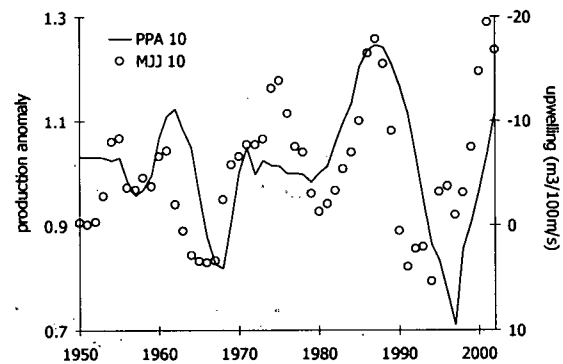


Figure 3.56: Comparisson of BCS PPA to upwelling at 54°N (averaged from May to July). Data smoothed with a LOWESS filter using a second degree polynomial and 10-year smoothing window.

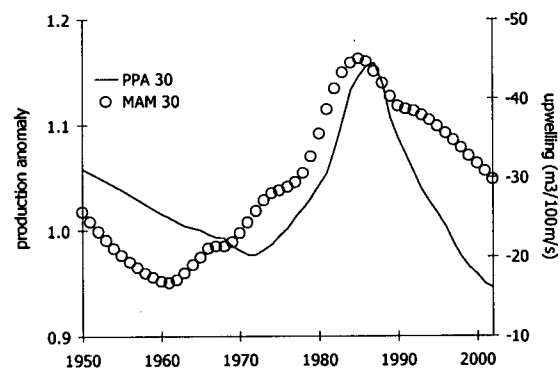


Figure 3.57: Comparisson of BCS PPA to upwelling at 54°N (averaged from March to May). Data smoothed with a LOWESS filter using a second degree polynomial and 30-year smoothing window.

3.4.2.3. The Northeast Pacific

The Northeast Pacific PPA, Figure 3.46, was compared to four climate Indices; the Aleutian low pressure index (Beamish *et al.* 1997), the northern oscillation index (Schwing *et al.* 2002), The North Pacific index (Trenberth and Hurrell 1994), and the Pacific decadal oscillation (Mantua *et al.* 1997). Almost all of the correlations between the best fit PPA and these indices were strong and significant at all time scales of comparison, with changes on the longer interdecadal scale appearing to be more important to both the amplitude and frequency of changes. The Aleutian low pressure index (ALPI) is only calculated for the winter periods of successive years so the correlations between it and the northeast Pacific PPA were not conducted for monthly and seasonal portions of the year, Table A.3.8. At all time scales of smoothing, the ALPI appeared to vary on a decadal and bidecadal timescale, with the longer-scale oscillation being relatively higher after the mid 1970s. When the northeast Pacific best fit PPA was compared to the ALPI the longer time scale oscillations appear similar, Figures 3.58 and 3.59, but the shorter time scale oscillation does not appear to be as pronounced in the PPA, especially in the first two decades of the simulation.

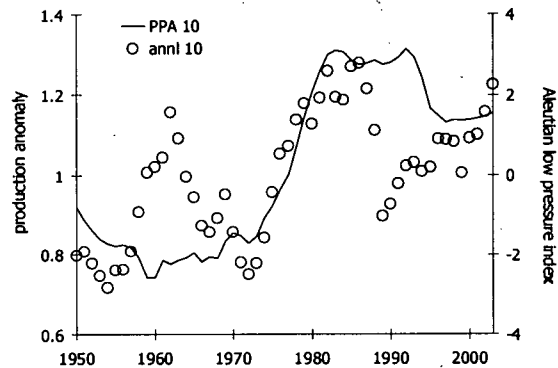


Figure 3.58: Decadal changes of NEPac PPA and Aleutian Low Pressure Index. Data smoothed with a LOWESS filter using a second degree polynomial and 10-year smoothing window.

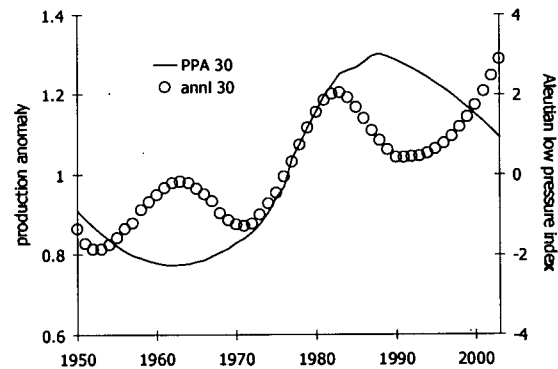


Figure 3.59: Interdecadal changes of NEPac PPA and Aleutian Low Pressure Index. Data smoothed with a LOWESS filter using a second degree polynomial and 30-year smoothing window.

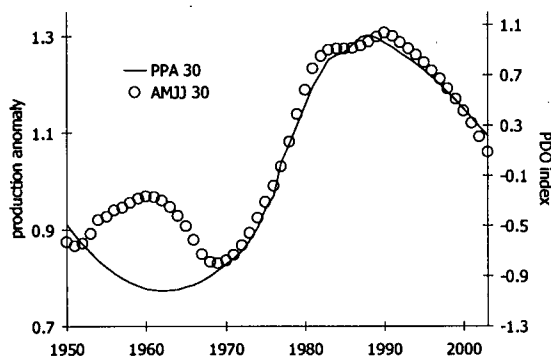


Figure 3.60: Comparison of NEPac PPA to PDO Index (averaged from February to July). Data smoothed with a LOWESS filter using a second degree polynomial and 10-year smoothing window.

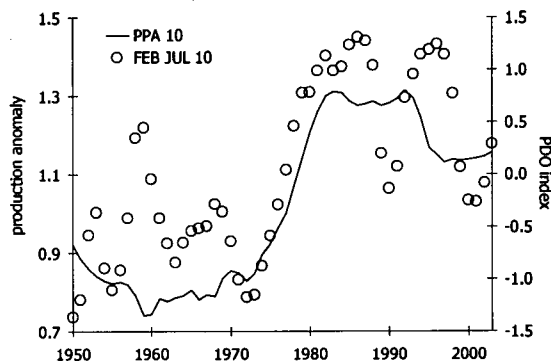


Figure 3.61: Comparison of NEPac PPA to PDO Index (averaged from April to July). Data smoothed with a LOWESS filter using a second degree polynomial and 30-year smoothing window.

The Pacific decadal oscillation (PDO) exhibited similar characteristics in that there appeared to be oscillations on both decadal and bidecadal scales with the period after the mid 1970s represented by generally higher than average values. The correlations between the PDO and the PPA were highest for values from the late winter to summer, February to July, or from the late spring to early summer, April to July, Table A.3.9. As with the

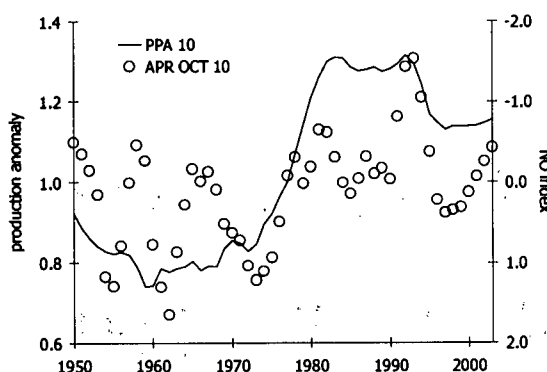


Figure 3.62: Comparison of NEPac PPA to NOI (averaged from April to October). Data smoothed with a LOWESS filter using a second degree polynomial and 10-year smoothing window.

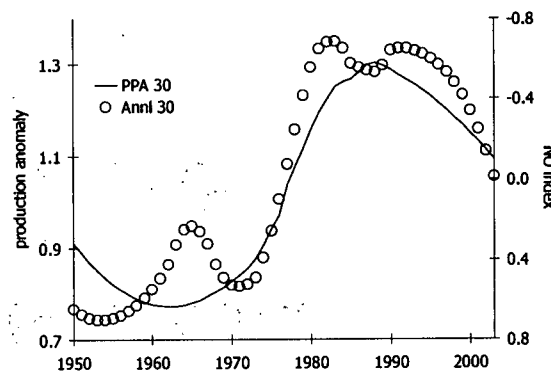


Figure 3.63: Comparison of NEPac PPA to annual NOI. Data smoothed with a LOWESS filter using a second degree polynomial and 30-year smoothing window.

ALPI the variation of the PDO was mirrored by the PPA in change at the bidecadal scale but not as well at shorter time scales, Figures 3.60 and 3.61.

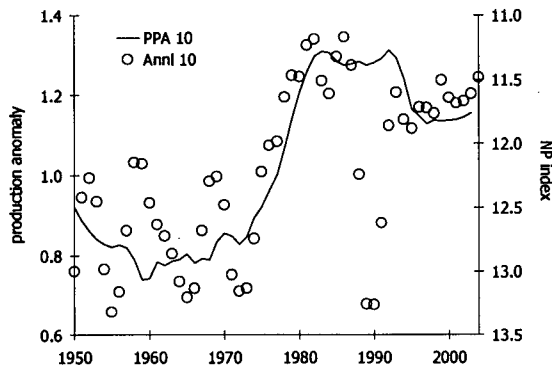


Figure 3.64: Decadal changes of NEPac PPA and annual NPI. Data smoothed with a LOWESS filter using a second degree polynomial and 10-year smoothing window.

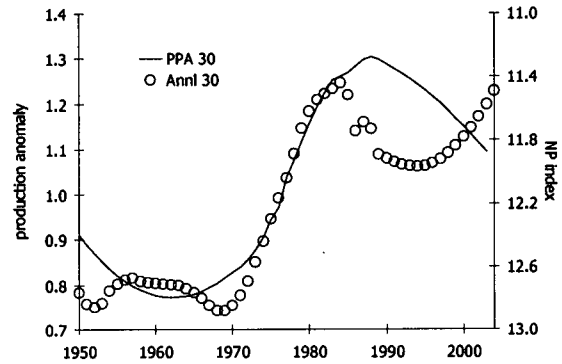


Figure 3.65: Interdecadal changes of NEPac PPA and annual NPI. Data smoothed with a LOWESS filter using a second degree polynomial and 30-year smoothing window.

The northern oscillation index (NOI) had a strong negative correlation with the PPA at all time scales, Table A.3.10. There did appear to be a strong correlation for the summer for data smoothed over shorted time spans, Figure 3.62. For data smoothed over longer windows the strongest correlations occurred for annual data, Figure 3.63. The North Pacific Index (NPI) also had a strong negative correlation to the PPA at all time scales. Annually derived values of the NPI were more strongly correlated to the PPA than any of the seasonal values at all time scales of smoothing, Table A.3.11. As with the other North Pacific climate indices there appears to be decadal-scale changes in the NPI, but the predicted PPA suggested only weakly decadal-scale oscillatory behaviour, Figures 3.64 and 3.65.

4. Discussion

Topics in this discussion follow the sequence of the results. Therefore, general implications of modelled primary production anomalies are discussed first. The second major portion of the discussion is concerned with the dynamics of species populations over time in each of the models. The third portion of the discussion is an analysis of the behaviour of modelled primary production anomalies (PPAs) compared to relevant climate indices. The last major section of this discussion is an analysis of how climate and model behaviour change in the differently-scaled models. These sections are then summarised and conclusions drawn from the chapter.

4.1. General model responses in dynamic simulations

All simulations of the Strait of Georgia (SoG) made using different parameterisations of vulnerability, Figure 3.1, showed remarkable similarity in that they suggest that periods of low primary production occurred in both the late 1960s and the late 1990s. The run with vulnerabilities optimised for each predator column, however differed from the others in that it predicted that the low production anomaly of the late 1990s was more profound than that of the late 1960s. All simulations agreed that there were two periods of relatively high production; the 1950s and 1975 to 1990. All models suggest that primary production was returning to long-term average values by the end of the 20th Century.

The modelled return of the PPA to more normal conditions parallels the return of cooler sea surface temperatures (SSTs) in the SoG in 1999 after warm years in most of the 1980s and 1990s (DFO 2000). These results are similar to the type of 'regime changes' that have been demonstrated by comparing climate indices to fish populations, mentioned in the introduction, *e.g.*, Beamish (1995), Mantua *et al.* (1997) and Clark and Hare (2001b). The implication of the SoG model simulations in this study is that primary production in the SoG may change from high to low production regimes on a roughly 10 to 15 year interval. Control over such regimes in the SoG could very well be exerted by the type of zooplankton / phytoplankton dynamics described in Li *et al.* (2000) influenced

by climate forcing. In terms of primary production, they suggested that the Strait of Georgia / Strait of Juan de Fuca (SJF) system varies interannually between three regimes; regime 1: a larger spring bloom in the SoG than in SJF, regime 2: a larger spring bloom in the SJF, regime 3: larger spring bloom in the SJF *and* low zooplankton biomass in the SoG. These regimes are mediated by zooplankton grazing and the movement of surface and deep water between the SoG and SJF (Li *et al.* 2000) transporting nutrients, zooplankton and phytoplankton through the two bodies of water. A similar model of the SoG by Martell *et al.* (2001) also suggested that primary production changes had occurred during the period from 1950 to 2000 and that changes in primary production were similar to changes in wind regimes in the SoG during that time. Like the model here, simulations of PPAs in Martell *et al.* (2001) also suggested that there was relatively high primary production in the 1950s and late 1970s, with relatively lower primary production characterising the late 1960s and 1990s. Unlike this model, that of Martell *et al.* (2001) had primary production returning to levels near the long-term average in the 1980s. The process of water turnover in the SoG at depth and on the surface is driven by the tides, currents and winds. The characteristics of the water moving into the SoG is determined partly by the water characteristics off the west coast of Vancouver Island and the runoff from rivers feeding into the SoG. Thus, there is agreement between this model and others that changes in production in the SoG have occurred and that they are linked to changes in how water is moved in to and out of the SoG.

As with the SoG model, simulation results of estimated BC shelf (BCS) PPAs, from 1950 to 2003, were similar despite different settings of the vulnerability parameters, Figure 3.2. Again, the simulations produced time series of PPAs that resemble regimes, though the predicted regimes shifts from periods of low to high primary production are divergent in the 1960s and 1970s. All simulations did suggest that the periods from about 1950 to 1955 and 1983 to 1992 were times of relatively high primary production, while the period from about 1993 to 2002 was one of very low primary production. The PPA from the simulation with vulnerabilities optimised by predator column in the diet matrix diverged from the other simulations in that it suggested that short-term high-production periods occurred in the early 1960s and mid 1970s. The other three simulations suggested that

primary production in the early 1960s was relatively low and that the period of relatively high primary production in the 1970s began sooner than suggested by the optimised vulnerability simulation. The profound decline in primary production which all the simulations suggested to have occurred in the 1990s is mirrored by warming off the BC coast through much of the 1990s associated with el Niño (DFO 2000). Robinson and Ware (1999) constructed a pelagic ecosystem model of the La Perouse Bank off the Southwest coast of Vancouver Island which accounted for changes in hake, chinook salmon, dogfish, euphausiids, copepods, diatoms and adult and juvenile herring. This La Perouse model suggested that primary production exhibited anomalies like those of the BC shelf model presented here. Similar to the BC shelf simulations in this study, the La Perouse model suggested that primary production was relatively low in the 1990s compared to the 1980s. However, the La Perouse model shows primary production as likely being low during the mid 1970s, whereas the BC shelf models suggest that primary production was near the historic average during the mid 1970s. Robinson and Ware (1999) attributed the modelled decline of primary production in the 1990s to both anomalously low upwelling and the impact of an extreme el Niño event in 1997. The La Perouse model accounts for a more limited species mix than the BC shelf model and represents only a small fraction of the BC shelf model ecosystem so this divergence in PPAs is not surprising. Unfortunately, few other dynamic ecosystem models have been constructed to provide contrast for what may be causing changes off the BC coast.

The effect of different vulnerability settings on the simulated PPAs of the Northeast Pacific (NEPac) model was negligible. All simulations suggested that from 1950 to about 1975 primary production tended to be low. All NEPac simulations predicted that in the late 1970s there was a sudden shift to a regime in which primary production was relatively high, a state that persisted to the end of the modelled period. The simulations were divergent in the predictions of the timing and magnitude of the PPA maximum in the 1980s and 1990s. Simulations also differed slightly in the magnitude of declining primary production near the end of the simulation. In terms of the regimes mentioned for the SoG and the BC shelf, the NEPac system appears to have experienced at least two (1950 to 1977 and 1978 to end) with suggestions of a third perhaps at the end of the

second regime starting in the early 1990s, *i.e.*, the declining arm of the PPA in the scenarios with optimised vulnerabilities and high vulnerability settings. The suggestion that there were three distinct primary production regimes over the Northeast Pacific from 1950 to 2003 is strikingly similar to results from work by Hare and Mantua (2000). Hare and Mantua updated their analysis in Boldt (2003) and found from a principle components analysis of 100 biotic and abiotic time series from the North Pacific environment that there were three climate regimes and, hence, two regime shifts in the North Pacific from 1950 to 2003. The first regime shift occurred in 1977 and the second in 1989, though the evidence for the second regime shift was more recognisable from the biological time series (Hare and Mantua 2000).

It was argued by Parrish *et al.* (2000) that the mechanism responsible for the changes in biotic and abiotic variables in the North Pacific was changes in mid latitude ($\approx 30^{\circ}\text{N}$ to 40°N) winds which change the patterns of Ekman transport, described in section 1.1.2., in the North Pacific region. Polovina *et al.* (1995) showed that intensification of the Aleutian Low Pressure index (ALPI) after 1977 was responsible for a shallowing of the mixed layer depth (MLD) in the Alaskan gyre. This shoaling of the Alaska Gyre was coupled with a plankton dynamics model and suggested a strong increase in primary production (Polovina *et al.* 1995). While the models in this research used different assumptions and mechanisms to predict primary production, the NEPac model generated approximately the same decadal changes in primary production as the Polovina *et al.* (1995) model. The prediction of similar timing and direction of changes to phytoplankton biomass, using different models to derive that outcome, is compelling evidence that climate regimes have forced changes in phytoplankton at the scale of the NEPac. This finding is quite interesting because much of the dynamics of phytoplankton tend to be thought of in terms of small time scales and small areas, *e.g.*, blooms over small coastal patches of $\approx 10 \text{ km}^2$, and doubling times of hours to days implying hundreds of generations per year. When contemplated over the scale of the North Pacific it would appear that the phytoplankton community also responds at scales of decades and millions of km^2 .

4.2. Modelled biomass trajectories

4.2.1. The Strait of Georgia

There were eight species groups in the SoG for which reference time series of biomass or abundance were available for comparison. In the results there is an obvious effect, on predicted biomasses, by PPA declines in the late 1960s and 1990s. What is surprising is that this effect is quite obvious even in the highest-trophic level species in the analysis. Six of the eight species groups modelled had biomass trends that mirrored the timing and direction of changes seen in the reference time series of biomass or abundance, though with varying time delays. Two of the species groups, adult chinook salmon and adult herring, had some aspects of their predicted biomass trends in common with reference assessment data but there were also periods during which the SoG model failed to capture the timing and direction of biomass change.

4.2.1.1. Strait of Georgia multi-stanza groups

The biomass of herring in the SoG is quite well documented due to the historic and continued economic value of the fishery upon that species. The SoG 'best fit model' suggested that there were sharp declines in herring biomass in the late 1960s and late 1990s. Although different stock assessment model scenarios have

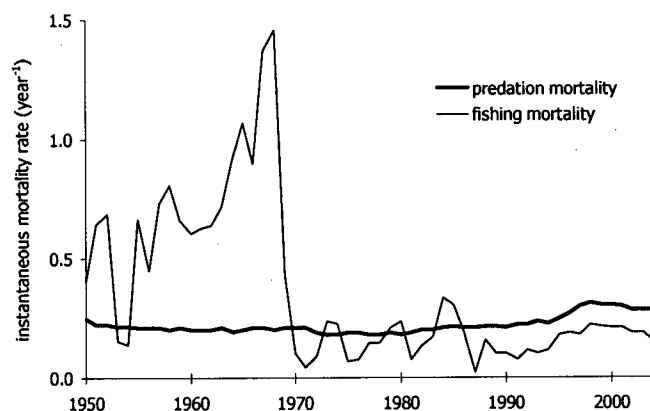


Figure 4.1: Simulated herring predation and fishing mortalities in the 'best fit' EwE SoG simulation.

been used to estimate historic abundance of the SoG herring stock, all predict that the stock biomass was at its lowest point in the late 1960s and at, or near, the historic high by 2003 (Schweigert 2003). While the 1960s biomass decline from the EwE SoG model is similar to that suggested by stock assessment, the biomass decline in the 1990s is not

supported by stock assessment data. Figure 4.1 shows changes in factors affecting mortality of adult herring in the EwE SoG model. In Figure 4.1 it would appear that the largest mechanism contributing to biomass decline in the late 1960s was the high fishing mortality from the herring reduction fishery. The SoG herring reduction fishery has been held by the Department of Fisheries and Oceans to be the chief cause of the decline in herring biomass in the late 1960s (Anonymous 2002d). Note, that that when the SoG model was run without the 'best fit' primary production anomaly (PPA) the biomass decline of the 1960s was not as profound. Therefore, some portion of the modelled late 1960s biomass decline was likely due to bottom-up forcing and decreased food availability. Figure 4.1 also suggests that the modelled herring biomass decline in the late 1990s was associated with mortality due to predation, since the mid-1980s predation mortality was higher than fishing mortality in the model and further increased through the 1990s. This predation mortality arose from the expanded biomass of seals, Figure 3.9, not coho and chinook which had declined at that time, Figure 3.5 and 3.6. Bottom-up forcing also appears to be a part of the herring biomass decline in the late 1990s as the decline did not occur when the model was run without a PPA.

The difficulty in obtaining a more satisfactory model emulation of the biomass trajectory suggested by the stock assessment likely arises from two issues; the fact that the SoG herring stock spends part of its life history outside the SoG and changing patterns of herring distribution within the SoG since 1950. Ware and Schweigert (2002) suggest that as much as 10,000 t per year of herring produced in the SoG may be exported to other BC herring stocks. It is also known that the SoG herring actually spend half the year at most, from late fall to early spring, in the Strait (Stocker *et al.* 2001). Because a significant, but varying, portion of the biomass leaves *and* the spawning stock spends much of the year outside the ecosystem much of the mortality and diet occurs beyond the SoG ecosystem. It is, therefore, not surprising that the SoG model was incapable of capturing the magnitude and direction of herring biomass changes, especially in the late 1990s. The other major change the SoG model could not account for is the apparent northern movement of herring spawning during warm years like the late 1990s (Hay *et al.* 2005). How such movement of spawning may influence juvenile or adult survival was not

accounted for in the model and could profoundly change the way biomass changed in the late 1990s.

4.2.1.2. Strait of Georgia salmon

A surprising result from the SoG model was that whereas the simulated trajectory of coho biomass behaved similarly to its abundance index (Figure 3.5) the simulated trajectory of chinook was quite dissimilar from its abundance index (Figure 3.6).

Especially problematic was that the SoG model suggested that chinook biomass should have collapsed in

the late 1960s and late 1990s. Figure 4.2 shows that juvenile herring biomass may have been a large factor in the behaviour of simulated adult chinook and coho salmon biomass. For both, the modelled feeding times increased during the late 1960s and 1990s in response to the relative paucity of juvenile herring. Adult chinook salmon had a 'double whammy' in the late 1960s, with a lot of adult herring in its diet, whereas adult coho had little adult herring in their diet. It has been suggested that in the 1990s juvenile chinook salmon ate progressively less herring and more zooplankton (R.J. Beamish pers. comm.) due to growth related issues in these salmon rather than changes in herring abundance.

In the late 1990s, although both fish species appeared to again be responding to decreased modelled herring biomasses, a larger portion of their biomass decline was attributable to a huge increase in predation mortality from seals. Figure 4.3 shows that in the SoG model the increased seal biomass, hence predation, was estimated to exert high mortality rates upon adult chinook salmon. Further, the modelled mid-1960s had sea lions exerting higher mortality rates upon adult chinook salmon, which would exacerbate the decline in

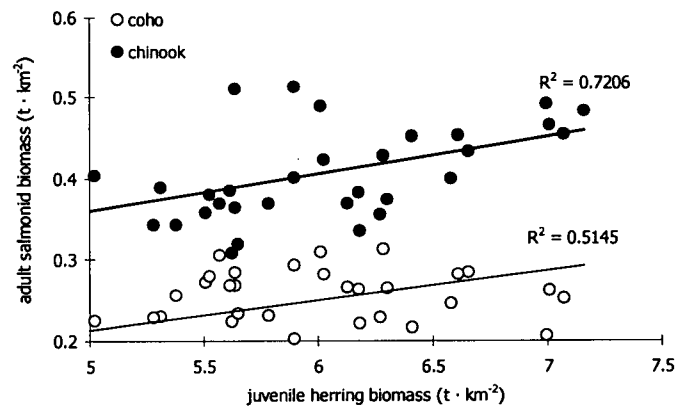


Figure 4.2: Comparison of simulated adult coho (open circles) and chinook salmon (solid circles) biomasses to simulated juvenile herring biomass in the 'best fit' EwE SoG simulation.

adult chinook salmon biomass at that time. Other species, such as sharks, had adult chinook and coho in their diets, but the marine mammals were, by far, the largest non-fishery source of mortality for these salmonids. Similar mortality changes were

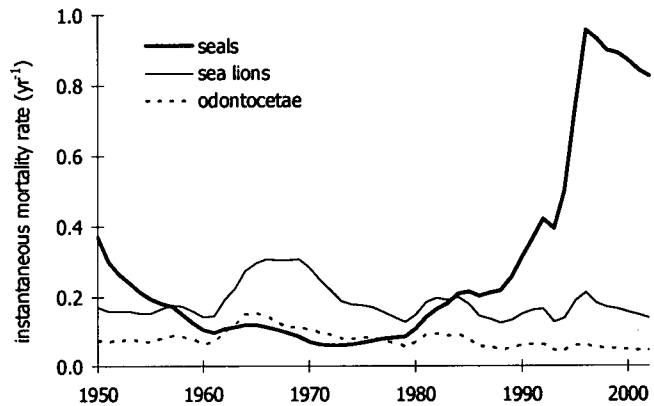


Figure 4.3: Changes in simulated adult chinook salmon predation mortality from marine mammals in the 'best fit' EwE SoG simulation.

experienced by adult coho salmon in the SoG model. The SoG model also suggested that both coho and

chinook adults spent more time feeding when herring biomasses were low, thus exposing them to a higher likelihood of predation. The modelled higher likelihood of predation in times of scarcer food was, therefore, exacerbated by the increased seal biomass and was manifested as the collapse in both chinook and coho biomasses in the late 1990s.

The hypothesis that seals may have been partly responsible for declining biomasses of chinook and coho salmon in the SoG could be described as controversial. Even if demonstrable, decreasing a marine mammal population to foster salmonid populations would not likely be a socially acceptable management policy. It has been noted in some SoG rivers that seals do, indeed, prey heavily upon return migrating chinook salmon. For example, Trites *et al.* (1996) suggest that in the mid 1990s seals were responsible for consuming about 33% of out-migrating chinook smolts and 35% of return-migrating chinook adults in the Puntledge River. This mortality estimate is within the range of 22-47% reported for seal-related adult chinook mortality in the Puntledge River by DFO (1999b). It would not at all be surprising if other chinook stocks in the SoG experienced similar seal-induced mortality upon both juveniles and adults. It was further noted by Trites *et al.* (1996) that seals also consumed 16% and 15%, respectively of out-migrating chum fry and coho smolts in the Puntledge.

The chief factors that have been cited for the decline in coho salmon biomass in the 1990s are damaged freshwater spawning and rearing habitat and poor ocean survival, which is usually ascribed to a combination of decreased ocean productivity and increased fishing mortality. In the case of habitat it has been noted that industrial, urban, and agricultural land uses have decreased the amount of habitat available for chinook (DFO 1999b) and coho (DFO 2002f). The response to this has been the construction of spawning channels and hatcheries, but declining biomasses of adult chinook and coho in the late 1990s suggests these artificial propagation programmes have had limited effect on these salmonids in the SoG. Beamish *et al.* (1995) suggest that the reason for such biomass declines was decreased ocean carrying capacity for chinook in the SoG as evidenced through declining catches in the 1980s and 1990s. They noted that despite increased chinook smolt numbers in the SoG through the 1980s and 1990s, there was "an increase in the mean temperature of the Strait of Georgia, a decline in annual Fraser River flows, and an abrupt decrease in the marine survival of hatchery-reared chinook released into the Strait of Georgia" Beamish *et al.* (1995). Similarly, for Washington State coho, Ryding and Skalski (1999) found smolt survival was closely tied to sea surface temperature and the seasonal movement of the northern arm of the California current. Hobday and Boehlert (2001) examined survival and growth of coho and also found that ocean conditions, specifically shallow mixed layer depths being associated with increased survival and decreased adult body size.

Based on the suggestion from the SoG model, and fisheries oceanographic literature, that the SoG has become less productive for coho and chinook and the fact that seal predation is likely to remain significant, biomasses of these two salmonids are unlikely to increase even if fishing mortality remains low. Coho and chinook biomasses may quickly recover if the SoG switched back to a more productive regime, but in the absence of knowledge to the contrary it is impossible to predict when such a change will occur. It may also be that the SoG has simply become more favourable for the production of pink and chum salmon via earlier plankton blooms (R.J. Beamish pers. comm.). There have been attempts to use devices to scare seals away from estuarine areas where seals congregate to eat salmon (Jurk and Trites 2000 and DFO 1999b). However the number of seals in the

SoG remains at historic high levels and scaring them off of one site would likely only move them to other areas where they will forage with equal success (and greater hunger).

4.2.1.3. Strait of Georgia demersal fishes

The long-term decline of lingcod biomass in the SoG has been well documented in several assessments, *e.g.*, Martell (1999), DFO (2001), DFO (2005b) and Walters *et al.* (2006), see Figure 3.11. In response to this decline, commercial fisheries upon lingcod were curtailed in the early 1990s, but no substantial increase in biomass occurred after these restrictions due to unfavourable oceanographic conditions (DFO 2001). Therefore, in 2002 recreational fisheries upon lingcod in the SoG were also curtailed. It has been reported that 1990 represented the low point for lingcod spawning biomass in the SoG, approximately 2% of historic levels, but that by 2005 the spawning biomass had increased to 15% of historic levels (DFO 2005). The SoG model appears to mirror these results with overfishing being the most likely source of high mortality from 1950 to 1990 causing biomass declines over that period. The SoG model did suggest that by 1990 lingcod biomass may have begun a slow increase, which was ultimately negatively affected by the primary production collapse predicted for the 1990s. This dampening effect of poor bottom-up forcing agrees with the suggestion in DFO (2001) that significant and quicker recovery of lingcod biomass would be facilitated by a return to pre-1990 oceanographic conditions in the SoG.

4.2.1.4. Strait of Georgia marine mammals

The most striking result of the SoG model was the unabated growth of harbour seal biomass, from the late 1960s to the late 1990s, Figure 3.9. This modelled growth is in accord with the assessment of Olesiuk (1999) who noted that the SoG harbour seal population had increased from about 3,000 in the early 1970s to stabilise at about 40,000 by the end of the 20th Century. The immediate effect of this population increase in the SoG model was greatly increased predation mortality upon coho and chinook salmon. Seal biomass may have continued to increase because of the continued availability of

hake to eat, which formed a larger portion of their diet. Thus, the stabilisation of the harbour seal population, suggested by the SoG model, was due to increasing predation mortality from toothed whales towards the end of the simulated time. Note, however, that the toothed whale biomass in the SoG model was chiefly comprised of orcas which have two behaviour patterns common to BC near-shore waters; those that eat fish, so-called residents, and those which eat marine mammals, so-called transients (Ford *et al.* 1994). Transients, spend very limited time in the SoG, thus they are effectively a small portion of the toothed whale group. Therefore, their implied increased predation upon the seals should be treated with caution. The modelled declines in toothed whale biomass in the 1960s and 1990s appears to have been driven by decreased availability of prey species at those times, which was manifested as increased feeding times and total mortality. It is also interesting to note that there were several anecdotal reports of transient orcas in the SoG from 2004 to 2006 (Anna Hall, Marine Mammal Research Unit, University of British Columbia, personal communication to Villy Christensen). Thus, although the SoG model could not explicitly have predicted that more transient orcas may feed upon seals by the end of the simulated period, the modelled increase of orca predation upon seals is an implicit way to express this trophic change.

4.2.1.5. Strait of Georgia marine birds

The two groups of marine birds which were compared to abundance data in the SoG model, demersal piscivorous and pelagic piscivorous birds, both showed long-term declines over the simulated time period (Figures 3.7. and 3.8). The modelled biomass trends for both bird groups shared another trait in that there appeared to be two step declines in biomass; the first in the 1960s and the second in the 1990s. Both of these steps were contemporaneous with declines in primary production predicted by the SoG model. The overall prediction of a decline in marbled murrelet populations (the largest component of the demersal piscivorous bird group) was supported by population modelling in Beisinger (1995) who examined data from Alaska and British Columbia to suggest rates of decline from 4 to 6% per year. Burger (1995) suggested that onshore logging and el Niño events have caused declines in marbled murrelet densities in Barclay

and Clayoquot Sounds of 20-60% from 1979 to 1993, and that similar processes have occurred in the SoG since 1900. The coincidence of sudden steep declines in marine birds, in both the SoG model and Christmas Bird Count (CBC) data imply that there may have been an environmental cause for the largest portion of biomass decline since 1950. A parallel situation may have occurred off the coast of California in 2005 when large die-offs of marine birds were reported to have been caused by poor ocean production from weaker than normal upwelling in the California Current system (Martin 2005). Preliminary research based upon autopsies of birds washed up on-shore at the time showed that the leading cause of death was starvation, caused by the decline in offshore winter prey resources (Nevins *et al.* 2005). One reasonable hypothesis explaining the steep declines in SoG marine bird biomasses in the 1960s and 1990s would be the effect of several years of poor primary production upon not only the survival of adult birds, but their ability to find enough resources for reproduction. A mechanism much like this was found to be responsible for decreased growth in marine bird chicks. Bertram *et al.* (2001) showed that nesting Cassin's and rhinoceros auklets on Triangle Island (off the north coast of Vancouver Island) had chicks with slower growth rates when faced with seasonal anomalies of high sea surface temperatures and early arrival of spring, which combined to reduce zooplankton availability.

4.2.2. The British Columbia Shelf

As was the case with results from the SoG model, the BCS model biomass trajectories were almost uniformly characterised by declines in the late 1990s that were linked to a predicted contemporaneous decline in the PPA. Other aspects of the biomass dynamics were less coherent. For example, the biomasses of some species, like Pacific Ocean perch and arrowtooth flounder, had long-term decreases or increases over the span of the simulation, 1950 to 2002. Other species, like herring and Pacific cod showed much greater frequency of biomass changes during the simulation.

4.2.2.1. British Columbia Shelf multi-stanza groups

Two of the multi-stanza groups in the BCS model; walleye pollock and arrowtooth flounder had temporal biomass dynamics which were compared to assessment data not based specifically on the BCS area. There has been some work towards the assessment of arrowtooth flounder biomass changes in BCS waters but only between 1980 and 2000 and then only for half the years during that time (Fargo and Starr 2001). For walleye pollock there has been some attention to the biomass in the SoG, *e.g.*, Beamish *et al.* (1976), Keiser (1983), and Mason *et al.* (1984) area but, like arrowtooth flounder, there is no continuous record of how BCS biomass may have changed since 1950. Nevertheless from 1996 to 2005 catches for both species have not been insignificant in BC with landings ranging from 1,000 to 5,000 t per year for pollock and 3,000 to 15,000 t per year for arrowtooth flounder (DFO 2006).

The biomass of adult arrowtooth flounder (ATF) in the BCS model was characterised by a steady increase until the early 1990s which was similar to the increase of the GoA ATF SSB in Turnock *et al.* (2003), Figure 3.12. This increasing biomass began to reverse by the early 1990s in response to bottom-up forcing from extremely depressed phytoplankton production in the 1990s. A high vulnerability for ATF interactions with its prey was the most significant contributor to the large increase in modelled adult ATF biomass. High vulnerability settings producing better fits of predicted adult ATF biomass to reference GoA SSB data, suggested that ATF was far below carrying capacity at the start of the simulated period (Christensen and Walters 2004). The only large difference between the modelled adult ATF biomass and the ATF SSB from the GoA was the continued increase of the latter through the 1990s. Interestingly, the incomplete time series of total ATF biomass in the Hecate Strait area (the northern third of the BCS), reported in Fargo and Starr (2001), suggested that the mid 1990s were characterised by a decline relative to the late 1980s. Unfortunately, the Hecate Strait ATF biomass data only covers a portion of the period simulated in the BCS model but there is a suggestion that at the scale of the BCS ATF populations responded to different climate forcing than was the case at the scale of the GoA.

Because there has been equivocal evidence to substantiate stock structure of pollock off the west coast of North America (Dorn *et al.* 2003 and Fargo and Starr 2001) the pollock SSB trend of the Gulf of Alaska (GoA) was used as a proxy for biomass trends off the BC coast. The BCS model suggested that the biomass of adult pollock behaved similarly

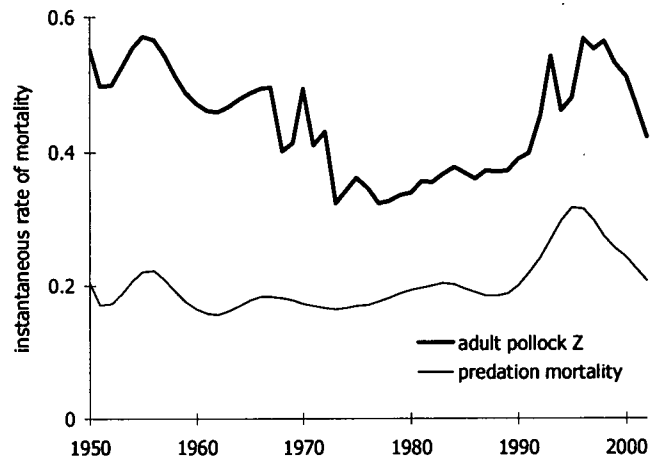


Figure 4.4: Changes in simulated adult walleye pollock total and predation mortalities in the 'best fit' EwE BCS simulation.

to pollock SSB trends from the GoA (see Figure 3.13) with the biomass peaking in the early 1980s, declining through the 1980s and 1990s, with a small recovery starting near the beginning of the 21st Century. The increasing adult biomass of the 1970s and the accelerating decline from the 1980s through the 1990s in the BCS model resulted from changes in fishing and predation mortality. During the early 1970s, total mortality declined and stayed low until the 1990s. The increase in total mortality in the 1990s was associated with an increase in predation mortality upon adult pollock, notably from toothed whales, sea lions and Pacific halibut, Figure 4.4. The decline in the 1990s was likely exacerbated by poor recruitment of juveniles as the BCS model indicated that there was a high positive correlation of phytoplankton production to juvenile pollock biomass. Thus, in the 1990s when phytoplankton production in the BCS model was very low, so too was the biomass of juvenile pollock for several years. In Anonymous (2003) it was suggested that pollock, in common with several groundfish species in the GoA, entered a period of low recruits per spawner in the late 1980s which persisted until the close of the 20th Century. Such a regime shift was also noted by Hare and Mantua (2000), who suggested that several fish species in the North Pacific, including GoA pollock, entered a period of lower productivity in the 1990s.

In the BCS model the biomass of Pacific cod went through several phases of expansion and decline. This result was similar to the waxing and waning of the summed Pacific cod stock biomasses for the west coast of Vancouver Island and the Hecate Strait in Sinclair *et al.* (2001). The major difference between the two biomass time series was that the BCS model did not show the peak biomass in the mid 1970s that was predicted by the reference stock assessment data (Figure 3.14). One factor contributing to this may have been the inability of the BCS model to emulate recruitment anomalies that were predicted for the two stocks of Pacific cod assessed in Sinclair *et al.* (2001). In the assessment, large positive recruitment anomalies for both Hecate Strait and west coast Vancouver Island Pacific cod were suggested to have occurred in the early 1960s, 1970s and 1980s, which contributed to larger adult populations in the middle of those decades. The articles of Sinclair *et al.* (2001) and Stocker *et al.* (2001) both note that the 1990s were witness to a succession of the worst recruitment anomalies for Pacific cod and major contributors to depressed populations off the BC coast. The BCS model mirrored this with the simulation suggesting that the lowest biomasses for both adult and juvenile Pacific cod occurred at the end of the 20th Century. Increased predation mortality, especially imposed by the larger number of arrowtooth flounder, almost doubled the modelled total mortality rate upon juvenile Pacific cod. There was also predicted increases of predation upon adult Pacific cod from sea lions in the BCS model. Both of these mortality mechanisms are interesting hypotheses that could be tested by diet composition studies of the respective predators and would be valuable in implementing an ecosystem management approach for Pacific cod.

The BCS model suggested that adult halibut biomass increased from 1970 to the end of the 20th century, after relative stability over the first twenty years of the simulation. Stock assessment data for halibut SSB were synthesized from Sullivan *et al.* (1997) and Clark and Hare (2001a) and suggested similar dynamics, though with slight declines from 1950 to 1970 (Figure 3.15). As with arrowtooth flounder, fitting predicted biomass to the reference stock assessment data suggested that adult Pacific halibut be given high vulnerability settings for its interactions with its prey, implying a 1950 biomass below carrying capacity. Clark *et al.* (1999) note that throughout the North Pacific most

groundfish entered a regime of increased productivity in the late 1970s, which persisted for most until the early 1990s. For many flatfish, like ATF and Pacific halibut, however, this regime persisted until the end of the 20th Century. In particular it was noted that recruitment for Pacific halibut had increased in all regions of the Northeast Pacific after the late 1970s regime shift (Clark *et al.* 1999). All halibut in the Gulf of Alaska are believed to behave as one reproductive unit (Sullivan *et al.* 1999), so the pervasive changes in recruitment have also occurred on a scale larger than the BCS model. A final contributor to the robustness of halibut biomasses to the large decline in bottom up forcing near the end of the simulation may be its benthic feeding habits, as suggested in Clark *et al.* (1999). The BCS model showed that Pacific halibut adults had no appreciable increases in feeding time and some of its significant prey items, *e.g.*, arrowtooth flounder, actually became much more abundant near the end of the simulation.

Survey catch rates of adult sablefish in British Columbia declined continuously from 1990 to 2001 (Kronlund *et al.* 2002). Reliable stock assessment of sablefish in BC only reaches back to the early 1990s, when comprehensive tag recovery was initiated as part of a fall survey program (Haist *et al.* 2001). King *et al.* (2000) were able to construct an

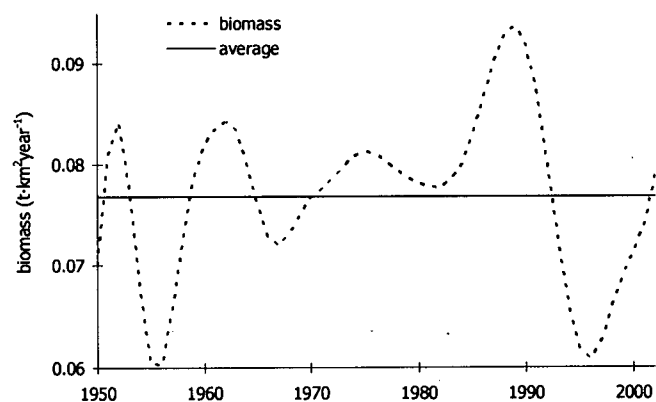


Figure 4.5: Changes in simulated juvenile sablefish biomass, compared to the average 1950 to 2002 biomass, in the 'best fit' EwE BCS simulation.

index of year class 'success' which was below average from 1960 to 1976, very high for the 1977-year class, year classes from 1978 to 1990 being generally above average, and years after 1990 generally below average. A parallel index of adult sablefish biomass was constructed by simply taking the ratio of catch to estimated fishing mortality. Figure 3.16 suggests that the parallel index produced biomass estimates very similar to the tagging based index and that these were similar to the biomass for adult sablefish predicted by the BCS model for the period in which all three overlap. While the estimated biomass of

adult sablefish was highest from 1950 to 1970 in the BCS simulation, that of juvenile sablefish was often not (Figure 4.5). The pattern of juvenile sablefish biomass change from 1950 to the 21st Century was therefore similar to the dynamics suggested by King *et al.* (2000). Changes in the modelled juvenile sablefish biomass were driven by predation mortality, especially from dogfish and arrowtooth flounder, resulting from changes in foraging time. Juvenile sablefish biomass was also strongly correlated to modelled phytoplankton biomass suggesting that changes in the adult population also responded to primary production but in later years. Schirripa and Colbert (2006) found that for sablefish in the California Current ecosystem (which intersects the southern half of the BCS model) growth and survival of larval and juvenile sablefish was strongly associated with upwelling and Ekman transport bringing them to optimal feeding areas and providing better forage. Thus, the association between juvenile sablefish and phytoplankton in the BCS model may be implicitly accounting for the physical oceanographic effects like those described in Schirripa and Colbert (2006) as well as the direct energetic effect of bottom-up forcing. Examining the potential effects of transportation and primary production could be done via a spatial model and may help resolve how the two mechanisms compliment or interfere.

Herring biomass changes in the BCS model were similar to the biomass trends of the SoG model, with the exception of the period from 1974 to 1984, Figure 3.17. The BCS biomass changes were quite similar to the biomass trend from stock assessments for the five large British Columbia stocks (DFO 2002a, b, c, d, and e). An interesting phenomenon that was observed in comparing the BCS and SoG data was the tendency, in the years after 1990, for the SoG stock to comprise an

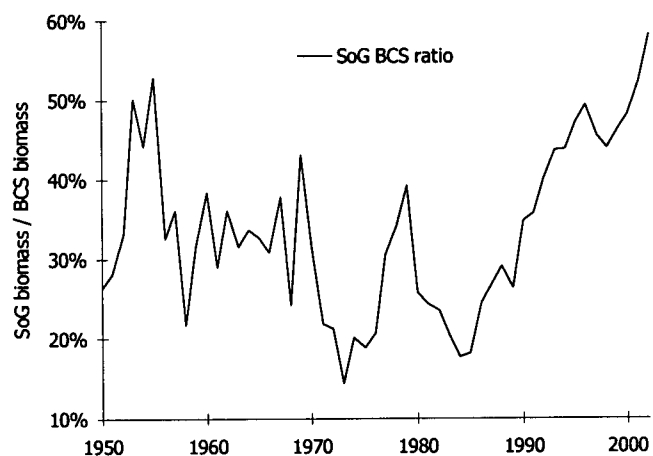


Figure 4.6: Changes in the ratio of SoG/BCS biomasses, from stock assessment data reported in DFO (2002a, b, c, d, and e).

increasingly large fraction of all the herring biomass in the BCS ecosystem, see Figure 4.6. As reported in section 4.2.1.1., SoG herring likely export a significant, though varying, proportion of their biomass to other BCS stocks (Ware and Schweigert 2002). Given this biomass export, the effective ratio of biomass *derived* from the SoG to the total BCS biomass may be even higher than calculated from the stock assessments. This implies that from 1985 to 2002, an increasing proportion of the control over the biomass dynamics for the BCS were determined by factors affecting the SoG stock. These two dynamics appear to be very different, as suggested by Figure 4.6. Indeed, when the biomass trend from all other BCS stocks (west coast Vancouver Island, Central Coast, Queen Charlotte Islands, and Prince Rupert) were compared to the SoG biomass trend, it was observed that there was almost no correlation between the yearly values of the two ($R^2 = 0.044$). Thus, the BCS model may not be capable in an explicit way of accounting for bottom-up dynamics influencing herring population trends because of the disproportionate effect of the SoG stock, which exists on a smaller scale than the whole BCS model. Therefore, it was not surprising to see that neither the BCS nor SoG model captured the absolute magnitude of biomass changes in the modelled adult herring populations because the herring moved across the modelled boundaries (and across spatial scales) quite readily.

Another complication could arise in the dynamics of juvenile herring biomasses. In a study of recruitment dynamics of various Northeast Pacific herring stocks, it was shown that the Prince Rupert stock behaved more like Southeast Alaskan herring stocks than the four Southern BC stocks, which had recruitment more similar to each other (Williams and Quinn 2000a).

While all recruitment changes in all Northeast Pacific stocks examined were shown to be related to large scale climate indices like the North Pacific Index, local small scale manifestations were changing the direction of response between BC and southeast Alaskan recruits. It is known that variation in near-shore currents is generated by seasonal changes in fresh water input from streams. However, even though a climate index may move in one direction across the whole Northeast Pacific, the effect on the seasonal flow

pattern of rivers in the Alaska and BC regions differ (and also, therefore, the near shore currents they create) resulting in divergent patterns of recruitment success (Williams and Quinn 2000b).

4.2.2.2. British Columbia Shelf salmon

In this section it is important to bear in mind four life history characteristics of the salmon species modelled which may distort each group's simulated behaviour:

- salmon groups were not split into age stanzas;
- time spent by juvenile salmon in fresh water varies both between species and among stocks of any one species (see *e.g.*, Stocker et al 2001 and Groot and Margolis 1991);
- distribution of adult salmon in the ocean, especially pink, sockeye, and chum, can be outside the BCS ecosystem (Burgner 1991, Heard 1991, and Salo 1991),
- the population reconstructions used for comparison were not based on a peer reviewed stock assessment, but rather upon a 'back of the envelope' estimation (see section 2.3.4.1.).

The net effect of these four factors was that the salmon groups modelled were representations of averages of dozens of stocks for each species rather than any of the stocks, or similar stock complexes, which are most often the focus of management and research. Of the five salmon species simulated in the BCS model, chinook and coho experienced the greatest changes in biomass (Figures 3.19 and 3.20). Sockeye, pink, and chum salmon biomasses all varied much less over the simulation, but had a tendency to increase or decrease in step (though not magnitude) with chinook and coho (Figures 3.21., 3.22., and 3.23). All salmon species appear to have experienced a decline in biomass through the mid 1990s, though pink and chum increased in the late 1990s and recovered substantially by the end of the simulation. The major source of this variation was the vulnerability settings for each salmon species as a predator. Prey vulnerability

settings for chinook and coho were very high, $\gg 10$, sockeye was high ≈ 5 , pink was 1.82, and chum was very low ≈ 1 . Because of the relatively low vulnerability setting of prey to pink and chum, their 1990s biomass declines were smaller in magnitude because of a compensatory response of decreased feeding time and hence, decreased natural mortality (Christensen and Walters 2004). Conversely, the higher vulnerability settings for prey to sockeye, coho and chinook resulted in smaller, or no, declines in feeding times as biomass declined and proportionally higher natural mortality rates. As in the SoG model, predation mortality from seals grew in proportion to their biomass. The magnitude of seal predation mortality, however, was never as high in the BCS model as in the SoG model.

The apparent resilience of pink and chum biomasses in the BCS model mirrors trends across British Columbia stocks from the estimation of biomass based on catch data. However, Walters and Korman (1999) suggest that one reason for the resilience of pink and chum is

Table 4.1: Correlations between biomasses of phytoplankton and salmon species in the BCS 'best fit' model. Results are the R^2 values for direct year to year comparison (no lag) and for comparisons between phytoplankton biomass in year X with salmon biomasses in year X+1 (1 year), X+2 (2 year), X+3 (3 year), and X+4 (4 year).

		no lag	1 year	2 year	3 year	4 year
	pink	0.514	0.664	0.575	0.350	0.122
	chum	0.798	0.914	0.715	0.367	0.085
	sockeye	0.300	0.479	0.497	0.384	0.200
	coho	0.046	0.117	0.150	0.133	0.073
	chinook	0.055	0.154	0.220	0.224	0.155

their ability to take advantage of colonisation opportunities, a factor for which the BCS model did not explicitly account. In terms of responding to bottom-up climate forcing, the pink and chum groups in the BCS model had biomass variation which were most highly correlated to changes in phytoplankton biomass, while correlations to sockeye biomass were moderate and chinook and coho were weak, see table 4.1. Note also that the correlation between phytoplankton biomass and salmon biomass were highest when lagged. More specifically, the best correlated lags by species appear to have some relation to the the length of time they spend in the ocean. Thus, chinook has the highest correlation at the greatest lag. At the other end of the spectrum, pink salmon have the highest correlation when lagged by one year. This suggests that ocean conditions encountered by juvenile salmon echo in later years as favourable, or poor, adult returns.

Meuter *et al.* (2002a) observed that the highest correlation of oceanic survival of sockeye, pink, and chum occurred at a 'regional' scale (similar to the size of the BCS), delineated by oceanic upwelling regimes. Further, Meuter *et al.* (2002b) suggest that the same change in sea surface temperatures across the whole Northeast Pacific resulted in opposite changes in survival rates between Alaskan and BC stocks of sockeye, pink, and chum salmon, which will be explored further in the Northeast Pacific section of the discussion.

Coho and chinook salmon biomass changes were much more dramatic over the simulation and mirrored the dramatic biomass changes suggested by the data derived from catches. Chinook salmon biomass varied differently from the catch biomass data during the first 10 years of the simulation and by suggesting that peak biomasses occurred in the late 1990s, whereas the catch biomass data showed that

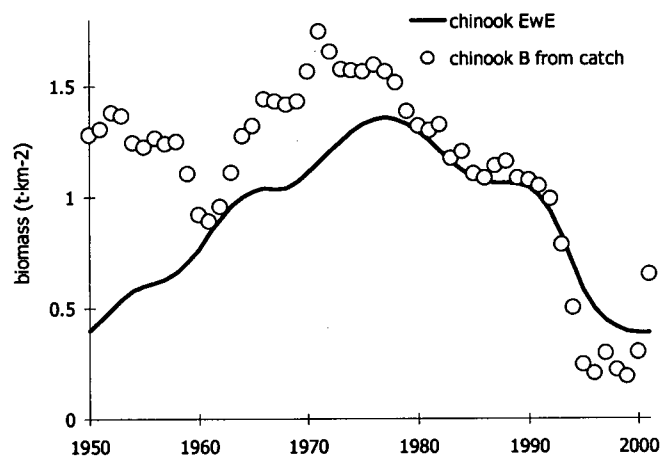


Figure 4.7: Changes in simulated chinook biomass to reference biomass, derived from catch, assuming: a) low krill vulnerability as prey and b) no compensatory changes in natural mortality for chinook from changes in feeding time, in the 'best fit' BCS model.

the peak was in the early 1970s. Besides the aforementioned high prey vulnerability, one reason for the behaviour of chinook salmon biomass was that the BCS model showed a prey switch to krill and small squids, whereas most diet data would suggest that chinook would have been preying mostly on small forage fish groups, *e.g.*, adult and juvenile herring and miscellaneous small pelagics. However, the BCS model suggested that krill composed as much as 60% of chinook diet. Diet composition studies such as those summarised by Healey (1991) suggest that herring and other forage fish like sand lance form the bulk of oceanic chinook diet in terms of volume ingested. Thus the model likely failed to correctly account for the chinook salmon diet composition for most of the

simulation. The fit of the BCS chinook biomass time series could be improved given two assumptions. First, the sensitivity of the fraction of 'other mortality' to changes in chinook feeding time being set to zero, implying that there was no compensatory changes in mortality for chinook (Christensen and Walters 2004). Second, the vulnerability of krill to chinook as predator being set to extremely low values, such as one, implying donor control for that prey item alone. When the above two conditions were applied a more satisfactory fit for chinook biomass resulted and chinook diet composition was maintained as primarily herring and forage fish, Figure 4.7. Like the 'best fit BCS model', the modified version failed to fit the predicted decline in chinook biomass during the first decade simulated.

Coho was the only salmon species for which the BCS model predicted the timing, direction and magnitude of biomass changes, Figure 3.2. Scale likely plays a very important role in explaining this result. Two of the caveats mentioned at the outset of this section will be used to explain why. First, salmon populations have traditionally been studied as stocks implying that most of the significant factors causing salmon populations to change occur at scales far smaller than the 150,000 km² encompassed by the BCS model. Secondly, many of the modelled salmon populations spend significant portions of their lives outside the BCS ecosystem.

With respect to the first issue of spatial scale it has almost become a corollary in studies of salmon populations that the mid 1970s regime shift was responsible for net gains in salmon biomass in GoA stocks and losses in California Current stocks (Hare and Mantua 2000). However, as noted above in Meuter *et al.* (2002a), when salmon stocks experienced similar changes in marine survival it tended to be more highly correlated when the streams to which they migrated were separated by less than 1,000 km. Also, Botsford and Lawrence (2002) observed that while there were north Pacific basin-scale processes changing chinook stocks in the mid 1970s, those changes were manifested differently between northern and southern populations of chinook salmon within the California Current ecosystem. It is important to note that for coho salmon, Botsford and Lawrence (2002) found that population changes were more coherent at the scale of the

GoA and California current. This would be consistent with the relative simplicity with which the BCS model was able to reproduce changes in the reference time series of coho biomass.

Several mechanisms are likely to be responsible for local variability to common, larger scale, environmental signals. When salmon emerge as fry, the freshwater environment in which they find themselves may be altered by watershed effects of climate such as water temperature and flow, and the timing of seasonal changes in these variables. Also, when young salmon first enter the marine environment, predation and competition processes at the scale of the near-shore can affect survival and change migration patterns. For example, Beamish *et al.* (2002) suggested that declining ocean survival rates of coho salmon, after 1990, may be linked to climate-driven declines of food availability during their first year of life. They concluded that changes in in Coho marine survival were manifested over spatial scales on the order of the BCS model presented here.

Chum, pink and sockeye actually spend a significant portion of their ocean life history phase outside of the BCS ecosystem as modelled, going to the open ocean pelagic environment of the GoA. It may, therefore, be surmised that any environmental signal to which they might respond would be on a correspondingly larger scale. Beamish *et al.* (1997) found that increases in Fraser River sockeye salmon production occurred at the same time as increases across the Pacific subarctic for sockeye production. Thus, it would appear that sockeye respond to climate signals on a far larger scale than the SoG or BCS models. It is not surprising that the larger scale NEPac model was better able to reproduce biomass dynamics for sockeye, pink and chum which tend to exist in an ecosystem quite larger than the SoG or BCS, as we shall see in section 4.2.3.2.

4.2.2.3. British Columbia Shelf demersal fishes

The three demersal fish species, not modelled as multi-stanza groups (Pacific Ocean perch, hake and rock sole), displayed very different biomass trajectories due to the varied nature of their life histories, and the fisheries that have targeted them (Figures 3.24, 3.25,

and 3.26). Pacific Ocean perch were unique in the BCS simulation in that their biomass was relatively immune to changes in primary production, and mostly appear to be a function of changes in fishing mortality. Rock sole biomass changes, however, were very sensitive to changes in phytoplankton production, with fishing mortality playing a more muted role. The changes in hake biomass were reflective of both changes in bottom-up and top-down dynamics.

Pacific Ocean perch (POP) is a very long-lived (to perhaps 100 years) fish, although males and females reach sexual maturity by their eighth year (Stocker *et al.* 2001). There was a significant foreign trawl fishery off the west coast of Canada, which reported exceptionally high catches between 1960 and 1975 (Schnute *et al.* 2001). In the BCS model these high trawl-yield years were

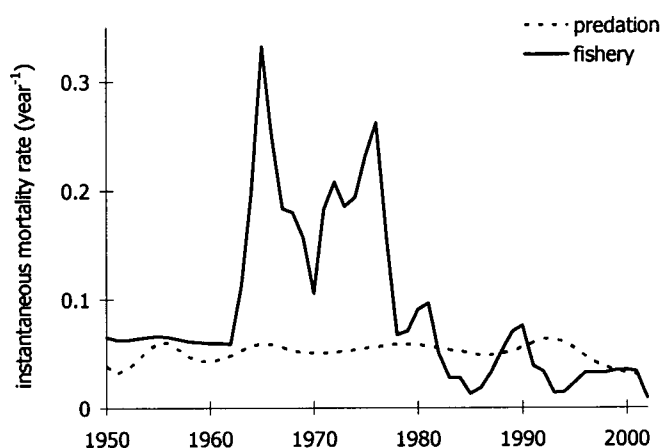


Figure 4.8: Comparison of changes in simulated fishing mortality and predation mortality changes for Pacific Ocean perch, in the 'best fit' BCS model.

manifested in POP as an instantaneous fishing mortality often near 0.2 year^{-1} and greater than 0.3 year^{-1} in 1965 (Figure 4.8). The result of this high mortality rate was the reduction, by 1980, of POP biomass to one fifth of its 1950 value in the BCS model or one third from the Hecate Strait assessment in Schnute *et al.* (2001). It has long been recognised that long-lived slow-maturing species may be particularly susceptible to collapse in the face of high fishing mortality, *e.g.*, Reynolds *et al.* (2002). Hilborn *et al.* (2002) suggest that for groundfish, from the California to Washington area, a long term robust fishing mortality rate is one that reduces the per recruit spawning potential to 55% of that in an unfished state, *i.e.*, F_{55} . The GoA assessment for POP was done assuming that the population could sustainably be subjected to an F_{40} policy. The fishing mortality rate that was suggested to achieve this target was $F=0.06 \text{ year}^{-1}$ (Hanselman *et al.* 2003). A glance at Figure 4.8 shows that for most of the 1960s and 1970s POP in the BCS were

likely being overfished. After the fishing mortality was reduced in the 1980s the biomass appears to have begun a slow recovery associated with the longer time over which POP mature. In the BCS model the POP biomass continued to increase in the last ten years simulated, whereas the stock assessment data suggested POP biomass tailed off during the 1990s due to poor recruitment that was likely associated with a regime shift in the late 1980s (Schnute *et al.* 2002). The BCS model certainly does suggest a regime shift occurred in the late 1980s as evidenced by the change during that time from very high to very low phytoplankton production in the 1990s. This late 1980s regime shift has been noted at the scale of the BC ecosystem by pervasive changes in its fish populations at that time (McFarlane *et al.* 2000). If POP recruitment was particularly sensitive to oceanographic regime changes the model might be able to more accurately track the biomass decline of the last ten years by splitting POP into adult and juvenile groups.

Rock sole biomass appeared to vary in response to changes in phytoplankton production. When the biomass change from the stock assessment for the Hecate Strait (DFO 1999a) was plotted directly in comparison to the BCS phytoplankton production the two time series did not appear to be changing at the same time. However, when the phytoplankton production in the BCS model (reflected by estimated biomass) for any year X was plotted against changes in rock sole biomass from DFO (1999a) for year X+5 the correspondence between the two was very high, indeed (Figure 4.9).

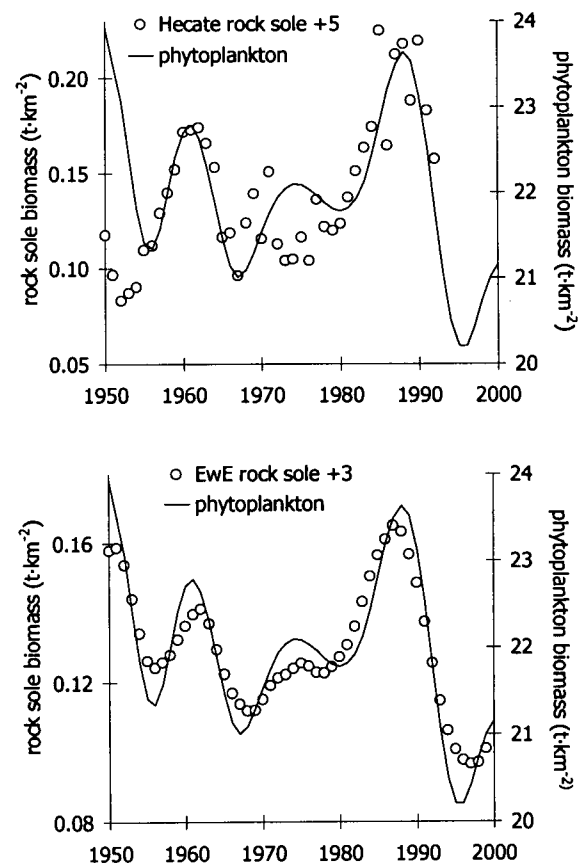


Figure 4.9: Comparison of lagged changes in Hecate Strait (top graph) and simulated BCS (bottom graph) rock sole biomass to changes in phytoplankton biomass in the 'best fit' BCS model. The lag periods for Hecate rock sole time series was five years into the future and that for BCS rock sole was three years.

When the BCS phytoplankton production from year X was plotted against BCS rock sole biomass from year X+3 the same improvement in the relationship of changes in the two trajectories occurred. Therefore, the bottom-up forcing conditions in any year appear to affect the biomass a few years into the future. One simple explanation for this would be the creation or inhibition of favourable recruitment conditions from bottom-up mechanisms which were in later years manifested as large or small recruitment cohorts to adult populations. Such a mechanism would imply that for rock sole the physical process causing increased or decreased phytoplankton biomass may be also responsible for conditions fostering or hindering rockfish larval and/or juvenile survival.

As shown in Figures 3.55 to 3.57 primary production was strongly associated with upwelling. Because rock sole are benthic it would be unlikely that changes in phytoplankton production would be directly linked to the survival and biomass of either adults or juveniles. Larval, age 0, rock sole, however, does inhabit the pelagic environment and feeds upon the zooplankton therein such as copepods, mysids, and amphipods (Holladay and

Norcross 1995). However, Paul *et al.* (1995) noted that the peak of rock sole appearance in the pelagic was before spring bloom suggesting that, like adults, they are directly effected by the same physical processes the suppress or promote phytoplankton biomass. Fargo and Wilderbuer (2000) proposed that the mechanism for this may be sea surface temperature though they hesitate to say whether this might act through predators, prey, or competitors, which are all named as likely mediators. Because rock sole spawn in a few select and restricted near-shore areas (Wilderbuer *et al.* 2002 and Fargo and Wilderbuer 2000) it is suspected that, for BC stocks in particular, space for larvae is at a premium and density dependence plays a large role in recruitment dynamics (Fargo and

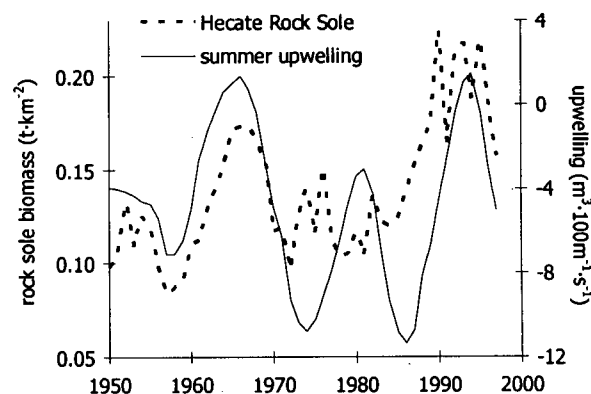


Figure 4.10: Comparison of changes in Hecate Strait rock sole biomass to changes in upwelling measured at 54°N during May, June and July. Note that the upwelling data was smoothed with a LOWESS filter using a second degree polynomial and 20 year smoothing window.

Wilderbuer 2000). In such a situation it is easy to hypothesize that oceanographic conditions may affect the strength of that density dependence in any given spawning year. Indeed, upwelling at the scale of the Hecate strait, particularly in the summer, corresponded very well with the biomass trend from DFO (1999a). Figure 4.10 shows that years with positive upwelling at 54°N were coincidental with peaks in the biomass time series of Hecate Rock sole, with both having their highest peaks during the mid 1960s and early 1990s.

Hake have been primarily thought of as a California Current species (Helser *et al.* 2004). Because the seasonal movement of the bifurcation of the California and Alaska currents off the coast of BC causes the California Current to migrate northwards in the summer, however, hake can become the most important predator off the west coast of Vancouver Island during summer (DFO 2005a).

However, hake spawn off south central California during the late winter (Helser *et al.* 2004) so any physical oceanographic processes aiding or hindering the survival of larvae and juveniles can not be accounted for by the BCS model. There is also an important ontogeny that occurs in hake which witnesses increasing piscivory as they mature (Dorn *et al.* 1999). Lastly, hake size distribution off the west coast of North America appears to follow a size gradient from smaller in the south to larger individuals in the north, due partly to the tendency of adults to move north in the summer (Dorn *et al.* 1999). However the degree of these tendencies can also vary. The portion of the hake stock inhabiting BCS waters in the summer (from about 30% to 40%) increased in the 1990s and by the end of the 1990s many remained off the west coast of Vancouver Island year-round

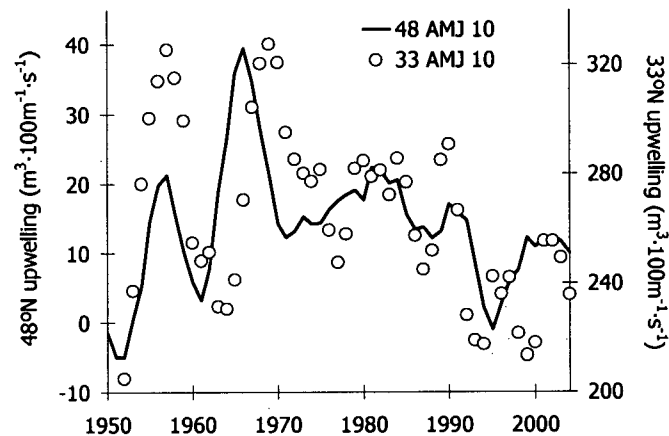


Figure 4.11: Comparison of changes in upwelling measured at 48°N and 33°N during April, May, and June. Note that the upwelling data was smoothed with a LOWESS filter using a second degree polynomial and 10-year smoothing window.

(McFarlane *et al.* 2000). This change appears to have been driven by upwelling variation off the west coast of North America. Benson *et al.* (2002) hypothesised that decreased summer upwelling after 1989 suppressed euphausiid production off the coast of California, but increased it off the coast of Vancouver Island, specifically the southwest. These processes also do not consider the effect of small resident hake populations along the west coast.

Note that in Figure 4.11 there is an overlap in declining upwelling in both time series from 1989 to 1995. The 48°N and 33°N upwelling time series appear to change at the same time and to move in the same direction through most of the period from 1950 to 2004. One exception to this trend was the period from the mid 1960s to the mid 1970s when the 48°N time series appears to have been lagged by two years to the changes in the 33°N time series. This lag was not an artefact of the LOWESS smoothing routine as it also was seen in the raw data. The trend in upwelling at the two stations suggests that the only time in the 54 years from 1950 to 2004 when there was a coincidence of historic low upwelling in both the north and central portions of the California current was in the 1990s lending credence to the hypothesized euphausiid-as-prey mechanism. However, Benson *et al.* (2002) found that the single best predictor of hake movement to BCS waters was the extent of upwelling at the 33°N station. Thus, it was likely not the conditions here that were drawing hake north but the poor conditions in the south forcing them to the BCS in search of food. For these reasons it may be difficult to find the BCS model capable of reproducing the full extent of observed changes in hake populations that were expected to have occurred. Indeed the BCS model suggested that throughout the simulation the vast majority (about 80%) of hake diet was euphausiids. Without any reason for a prey shift to occur from dynamics originating within the BCS model it is not surprising that the model failed to replicate any diet shift that may have occurred. A way of dealing with this issue might be modelling hake purely as an adult group with recruitment tied to the upwelling index at 33°N. However, the fact that after 1990s hake began to spawn in the BCS ecosystem implies that a large shift has occurred in this species, and thus will affect trophic dynamics of the BCS ecosystem in ways that are not related to the past. This type of change in both the behaviour and distribution of hake seems more related to the wide

ranging shifts expected from global climate change than to the decadal changes in trophic relations that have been observed for other BCS species.

4.2.2.4. British Columbia Shelf marine mammals

The only marine mammal for which a reference time series of biomass was available for comparison to the BCS model was harbour seals. Figure 3.18 suggests that harbour seal in the BCS ecosystem experienced a similar increase in biomass as that which occurred in the SoG ecosystem after a moratorium was placed upon killing seals. One notable difference between the impact of the increased

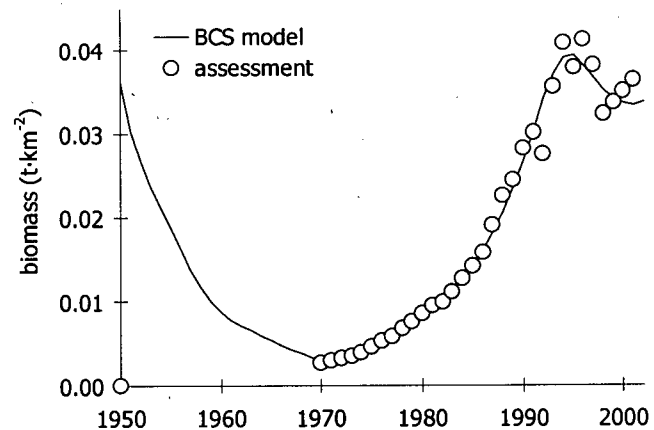


Figure 4.12: Comparison of changes in simulated and stock assessment biomasses for seals when predation by toothed whales was included in the 'best fit BCS model'.

seal biomass in the BCS versus the SoG was that seals did not exert as great predation mortality upon salmon, especially chinook and coho in the larger scale model. The BCS simulation also did not originally include any toothed whale predation upon seals. When toothed whale predation upon seals was included (as 1% of total odontocetæ diet composition in Ecopath) AND vulnerability of seal prey was set to 4, the fit of the simulated seal biomass to the reference biomass time series was even closer, than in the 'best fit' BCS model (Figure 4.12). The similarity of the biomass trajectories for harbour seals in the SoG and BCS models suggests that harbour seals were also well below carrying capacity at the scale of the whole BCS ecosystem. Like the SoG model seal prey in the BCS model were all estimated to have a high vulnerability setting implying the seal population was below carrying capacity (Christensen and Walters 2004). The last few years of the simulation suggested that any further expansion of harbour seal biomass in the BCS was being checked by the effect of decreased food availability from the collapse of primary production at the end of the BCS simulation. The relative scarcity of seal prey

after 1998 also resulted in expanded predation mortality arising from toothed whales due to the need for seals to spend more time foraging thus making them more likely to be eaten. Whether or not this may have occurred in the BCS ecosystem is impossible to say in the absence of any reliable diet composition changes in orcas. Given the increased seal biomass, their suitability as a food source for orcas seem a likely mechanism controlling the unlimited expansion of seal biomass.

4.2.3. The Northeast Pacific

Two changes appear in many of the species modelled in the Northeast Pacific (NEPac) simulation. The first was a general increase in biomass beginning around 1977, *e.g.*, for arrowtooth flounder, Pacific cod, sablefish, halibut, pollock, pink salmon, chum salmon, sockeye salmon, coho salmon, northern rockfish, Atka mackerel, and rock sole. The second was the tendency of most of these species to exhibit declining biomasses after 1989, *e.g.*, Pacific cod, sablefish, halibut, pollock, pink salmon, chum salmon, sockeye salmon, coho salmon, northern rockfish, Atka mackerel, and rock sole. The remainder of the species in the NEPac simulation, especially the flatfishes, had biomass changes in the same directions but some years before the ones mentioned above, *e.g.*, plaice, yellowfin sole, and chinook salmon. The timings of these two changes (1977 and 1989) coincide with regime shifts described in the introduction and, in greater detail, the relevant physical and biological effects in Hare and Mantua (2000). While the general effect upon biomasses of the two regime shifts was opposite, the increases associated with the 1977-shift were so large that, for most species in the simulation, the declines following the 1989-shift were still higher than historic averages. An important issue for planning and management, therefore, is whether the 1989-shift will continue to push biomasses down or whether a smaller, short-term cycle was manifested upon a larger, longer-scaled one which may reassert itself in the near future.

4.2.3.1. Northeast Pacific multi-stanza groups

Perhaps the most dramatic change in the NEPac ecosystem in the last 50 years has been the steady increase of arrowtooth flounder (ATF) biomass since the mid 1970s, see Figure 3.27. In the Bering Sea / Aleutian Islands (BSAI), from 1976 to 2003, the spawning stock biomass (SSB) of female ATF increased from about

212,000 t to 530,000 t, *i.e.*, a 2.5 fold increase (Wilderbuer and Sample 2003).

During the same time the SSB of female

ATF in the Gulf of Alaska (GoA) increased from approximately 213,000 t to 1,267,000 t, *i.e.*, an almost 6 fold increase (Turnock *et al.* 2003). The increases, therefore, were

asymmetric with the biomass gain in the GoA being larger in both relative and absolute terms. Figure 4.13 shows how the relative sizes of the female ATF SSBs changed from

1976 (the earliest year with overlapping assessments for both ATF stocks) to 2003. It appears that in 1976 the two stocks had roughly equal size female SSB. After 1976 the GoA SSB appears to have expanded more rapidly than the BSAI stock. There is even a suggestion that a reversal in relative sizes of the two SSBs may have occurred in the mid 1970s, if one follows the trend in Figure 4.13 back from the first known data point. This

logic (though unsupported by empirical data) implies that the relative biomass shift of ATF in the GoA may be even larger than what is known to have occurred. Another

interesting trend in the relative sizes of the female SSBs was the decline in the ratio of GoA female SSB over BSAI female SSB from 1985 to 1995. This effect was due to several years of good recruitment to the age 1+ stock in the BSAI in the mid 1980s and in 1986 particularly. In the GoA, while recruitment to the age 3+ population was higher than the long-term average from 1985 onwards, the years following 1993 were often witness to recruitment about two times the long-term average. These recruitment trends explain

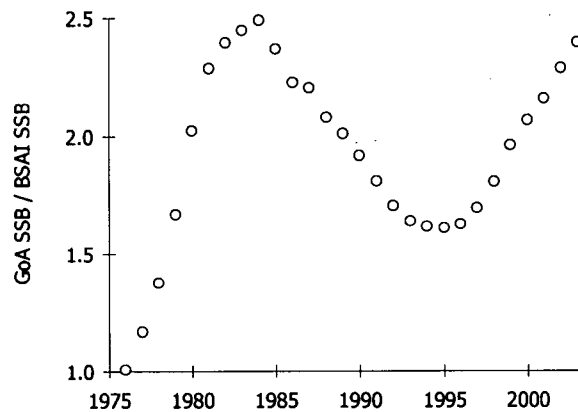


Figure 4.13: Changes in the ratio of female arrowtooth flounder spawning stock biomass (SSB) in the Gulf of Alaska (GoA) to the Bering Sea Aleutian Islands (BSAI) from 1976 to 2003.

why the relative increase in the GoA slowed in the mid 1980s and accelerated again in the 1990s.

In the NEPac model this biomass increase suggested that ATF was well below carrying capacity at the start of the simulation because the optimised vulnerabilities of prey to ATF adults were very high (Christensen and Walters 2004). Further, the bottom-up forcing emulated by the model as the mid 1970s shift to increased phytoplankton production, allowed adult ATF to spend less time feeding, thus decreasing predation mortality while increasing the average weight of each fish. While the simulation suggested that NEPac ATF biomass peaked in the late 1990s, then declined somewhat, stock assessment data shows that the biomass increased in every year after 1976 (Turnock *et al.* 2003 and Wilderbuer and Sample 2003). The slight decline in simulated ATF biomass after the *late* 1990s appears to have been caused by predators consuming more juvenile ATF in the *early* 1990s as they became much more common. There is no empirical evidence, however, to suggest whether or not ATF juveniles have become more common in the diets of other predatory species. Regardless of whether there may be increased predation upon ATF, the regime shift hypothesis, that the NEPac has changed to make ATF more productive *is* supported by other research. Wilderbuer *et al.* (2002) showed that variability in Eastern Bering Sea ATF productivity was linked to decadal patterns in the ocean environment. Thus at the scale of the NEPac there was a significant change in the ocean environment favourable to both recruitment and survival that allowed ATF biomass to increase rapidly after about 1976. The increase in average phytoplankton biomass acting as a bottom-up mechanism to increase production likely governed the changes observed in NEPac ATF biomass. As will be seen in subsequent sections on the NEPac model, this pattern persists across not only other demersal species but also in species of the pelagic environment.

Walleye pollock in the NEPac ecosystem are regarded as at least two separate populations; one stock in the GoA and the other in the EBS (Dorn *et al.* 2003). In the NEPac model, however the walleye pollock group is a mixture of the two. One consequence of this mixing is the dynamics of the NEPac model will tend to reflect

changes happening to the EBS stock as it tended to be many times larger than the GoA stock for much of the simulated time period, see Figure 4.14. This dichotomy in pollock stock structure could effect the overall meaning of how changes in NEPac pollock were simulated. In the NEPac model pollock biomass began to increase in the late 1970s much like other fishes in the ecosystem (Francis *et al.* 1998, Hare and

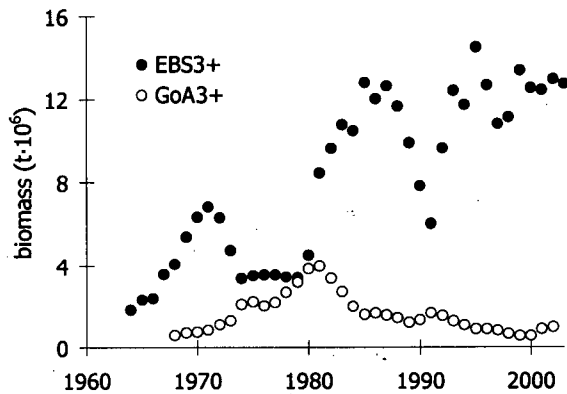


Figure 4.14: Changes in biomasses of age 3+ walleye pollock in the Gulf of Alaska (GoA) and eastern Bering Sea (EBS) from 1964 to 2003.

Mantua 2000). As shown in Figure 4.14, however, this increase actually began earlier in the 1970s in the GoA while the EBS stock biomass started to climb in the late 1970s. The GoA stock also began a decline in the early 1980s, but in the NEPac model the dynamics were masked by the overwhelming effect on the combined biomasses of the continued climb of the EBS stock. Interestingly, Turnock *et al.* (2003) noted that the largest item in GoA ATF diet, for individuals larger than 40 cm, was pollock. Given the rather large increase in GoA ATF biomass described above, and its known feeding habits, the decline of GoA pollock may be due to predation and fishing mortality. However, this was not observed in the NEPac model.

The NEPac model suggested that the overall increase of pollock biomass beginning in the late 1970s was largely due to decreased mortality because of less time spent feeding for both adult and juvenile pollock. Note that the decline in EBS pollock biomass in 1996 may simply be due to age-related distribution changes and not be a real phenomenon (Ianelli *et al.* 2003). It does not appear that any environmental changes in 1977 affected NEPac pollock by increasing recruitment. It was shown in Anonymous (2003) that while the regime changes of 1977 and 1989 were associated with changed recruit per spawner indices of many NEPac groundfishes, EBS pollock were not. However Palmer (2003) suggested that many fishes including pollock experienced faster growth after 1977, associated with warmer EBS conditions. This switch to faster growth in the EBS was

created by new oceanographic conditions which fostered increased production of zooplankton and forage fishes, *i.e.*, bottom-up forcing very similar to the bottom-up signal simulated in the NEPac model by increased phytoplankton production following the mid 1970s. At the scale of the NEPac model, therefore, pollock biomass changes are very similar to what we might expect from climate variation at the scale of the Pacific Decadal Oscillation with a definite regime change in 1977 (Mantua *et al.* 1997). Of further interest is the mixed evidence for a further regime shift to pre-1977 conditions, in 1989. It was noted in Hare and Mantua 2000 that while the 1977-shift appeared in many NEPac biological and physical oceanographic time series the 1989-shift was not as prevalent. The results from the NEPac model suggest that while there may have been a regime shift, as evidenced by somewhat decreased phytoplankton biomasses after 1990, *e.g.*, Figure 3.60, this decrease never fell below the long-term average phytoplankton production. Therefore, any bottom-up forcing throughout the NEPac model was always higher after 1977 than before. Pollock biomass dynamics in the NEPac appear to support the hypothesis that there was not a regime shift in 1989 by staying at higher biomasses to the end of the both the simulation and assessment data sets. Thus at the scale of the NEPac ecosystem the biomass trend exhibited by pollock responds as might be expected to regime change driven by bottom-up processes very similar to the PDO, a climate trend measured over a very similar area.

Pacific cod was similar to walleye pollock in two ways, the biomass trend and the distribution of biomass within the NEPac ecosystem with far more in the BSAI than in the GoA (Dorn *et al.* 2003 and Thompson and Dorn 2003). Unlike pollock, there is no compelling evidence to suggest there are separate GoA and BSAI stocks (Dorn *et al.* 2003). Also, the relative decline of NEPac Pacific cod was slightly greater than that of walleye pollock following the late 1980s (Figure 3.28). The NEPac model showed that as ATF and pollock adult biomasses increased in the 1980s they exerted increasingly high mortality upon Pacific cod juveniles. This was despite the fact that Pacific cod juveniles were a very small portion of pollock and ATF diets (Yang and Nelson 1999). Also contributing to a decline in Pacific cod adult biomass was an increase in the predation mortality exerted by sea lions beginning in the mid 1980s. Both Dorn *et al.* (2003) and

Thompson and Dorn (2003) state that an important ecosystem control on the biomass dynamics of Pacific cod was from its many predators. It was stressed, however, by both Dorn *et al.* (2003) and Thompson and Dorn (2003) that the primary ecosystem effect upon biomass dynamics of Pacific cod arose from regime changes like those suggested to have occurred in 1977 and 1989 described by Hare and Mantua (2000).

Another interesting aspect of changes in Pacific Cod biomass in the NEPac ecosystem was the contrast of the time scale over which it changed, compared to Pacific cod in the BCS ecosystem. Unlike ATF and pollock, independent assessments of biomass were available for Pacific cod for the smaller-scale BCS ecosystem. At the smaller area scale the Pacific cod biomass appears to have experienced about four different 'regimes' since 1977; decrease, increase, decrease, and stagnation at low levels (Figure 3.14 and Sinclair *et al.* 2001). At the larger scale of the NEPac ecosystem there appear to be only two major changes in Pacific cod biomass since 1977; expansion to the late 1980s, then a decline. There is perhaps a suggestion that a new phase of increased biomasses may ensue after the last years of simulation, given increasing recruitment after 1995 (Thompson and Dorn 2003). These different rates of population expansion and contraction at different scales mirror the different rates of bottom-up forcing in the BCS and NEPac models, which were associated with differently scaled climate phenomena: upwelling experienced over tens of thousands of square kilometres in the BCS, and the Pacific Decadal Oscillation as measured over millions of square kilometres. This further suggests that because of the fundamentally different behaviour of the BCS Pacific cod population's biomass it may be separate from, or least a subpopulation of, the NEPac Pacific cod population.

Like Pacific cod, the trend of adult halibut biomass in the NEPac model was similar to that of pollock, though halibut showed much less variability in interannual changes (Figure 3.30). The 1977-regime shift has been considered responsible for improved halibut recruitment across the NEPac ecosystem. Though growth slowed in Alaskan fish after 1970, growth of BCS halibut did not (Clark *et al.* 1999). These changes may be due to density dependent responses to variations in the halibut stock (Clark and Hare 2002).

An important aspect of halibut biology is that while halibut of the west coast of North America are managed and assessed in separate statistical 'stocks' there is so much intermingling and migration within the entire NEPac ecosystem that halibut 'stocks' are, in fact, interrelated (IPHC 1998).

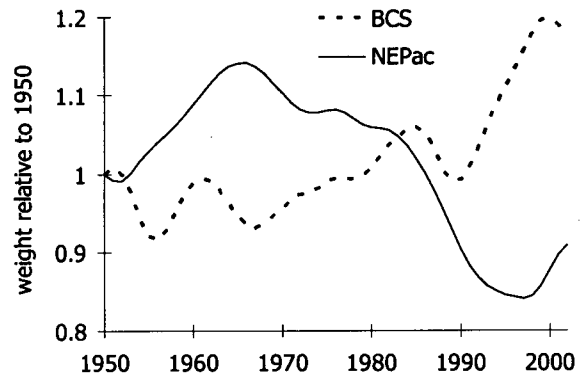


Figure 4.15: Changes of adult halibut weight, relative to 1950 in the NEPac and BCS 'best fit' models from 1950 to 2002.

The NEPac model showed that after 1977 adult halibut biomass began to expand rapidly. This expansion was fostered, in part by increased biomass from recruitment after 1977. This increased recruitment following 1977 agrees with the what Clark *et al.* (1999) concluded about post-regime shift halibut recruitment. The NEPac model also predicted decreasing weight for adult halibut. Interestingly, the BCS model suggested the opposite for adult halibut weight as suggested by Clark *et al.* (1999), see Figure 4.15. Therefore, while both the BCS and NEPac halibut biomasses began to expand in 1977, the underlying mechanics behind these expansions were very different. The fit between the NEPac adult halibut biomass and reference assessment data was much better than the fit between the BCS adult halibut biomass and reference data, Figures 3.15 and 3.30. This result shows that at the scale of the NEPac Ecosystem halibut biomass responded to the bottom-up regime change of 1977 similarly to other demersal fishes. The fact that there is much movement of halibut within the NEPac ecosystem implies therefore that halibut population at the smaller BCS-scale must also be affected by the large-scale climate change. Perhaps the complication of different scaled climate effects overlapping with population effects like density dependence helps explain why the BCS adult halibut biomass trajectory could not be completely reconciled with reference data despite a good knowledge of halibut fishing history.

Sablefish in the NEPac ecosystem was different from the other demersal species in that while its biomass increased dramatically after the 1977 regime shift there was a similar expansion of biomass in the 1960s despite the absence of a regime shift (Figure 3.29).

Sablefish are believed to exist as two stocks in the NEPac ecosystem; a northern one in the BSAI / GoA and a southern one stretching from the southern BCS to Baja California. It is believed that there is some overlap of the two stocks in BCS waters and juveniles are known to move extensively (Hart 1973). For the purposes of the NEPac model the northern population was the effective ecosystem stock, though some effects from the southern population may be in play, they were not explicitly accounted for as their effect on the whole NEPac ecosystem would have been minor.

The NEPac model was capable of emulating changes in adult sablefish biomass after the 1977 regime shift, but was not successful in recreating either the biomass expansion of the 1960s or the collapse of the 1970s. Sigler *et al.* (2003) argue that the collapse in biomass of the 1970s was due to fishing mortality. The NEPac model included a time series of F which was, indeed, higher during the 1970s, but fishing mortality changes appear to have had no significant effect

on adult biomass changes in the NEPac model. A possible cause of this problem was the NEPac models poor emulation of the recruitment anomalies that assessment models predicted to have been likely from 1960 to 2003, (Sigler *et al.* 2003) (Figure 4.15). It can be seen that the NEPac model predicted that the juvenile group dramatically increased in

biomass after the late 1970s suggesting that the regime shift of 1977 allowed for increased average recruits per spawner. The numbers of age 2 sablefish were converted by their natural logarithm before graphing in Figure 4.15 because they spanned a numerical gap of two orders of magnitude from a low of 1.7 million in 1974 to a high of 145.9 million in 1962. The mean number was more than twice as large (22 million) as the median (9 million) showing how the few high recruitment years could have a much greater effect than the many low recruitment years. These recruitment anomalies apparently respond to climate signals (Sigler *et al.* 2003) but do so at a higher frequency

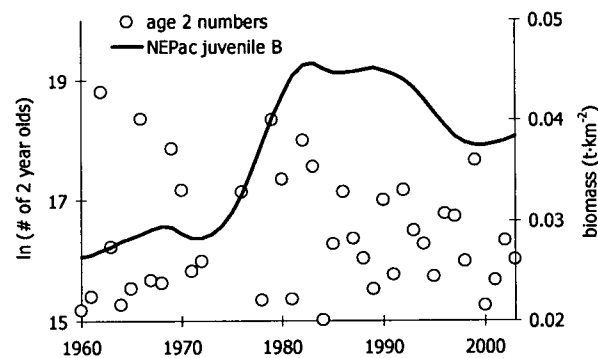


Figure 4.16: Comparison of changes in juvenile sablefish biomass in 'best fit' NEPac model versus estimated numbers of two year olds from stock assessment data; note log scale for age 2 fish.

than those which have apparently influenced many of the other groundfish in the NEPac ecosystem.

A further complication that arises from juvenile dynamics was that sablefish as larvae feed upon copepods while young-of-the-year feed primarily upon euphausiids (Sigler *et al.* 2001). Thus it might be expected that zooplankton and krill dynamics are very important to the survival of very young sablefish (McFarlane and Beamish 1992). However, the juvenile sablefish group in the NEPac model was composed of individuals up to six years old and sablefish are increasingly piscivorous after their first year (Sigler *et al.* 2003). Therefore, if a critical phase did exist in the larval or young of the year stage with a critical relationship to zooplankton and krill abundance, the juvenile group would not detect such signals as modelled.

It was also pointed out in Sigler *et al.* (2003) that coho and chinook are important predators upon young-of-the-year sablefish. The NEPac model did not include this link because even very small amounts of juvenile sablefish in coho and chinook diets, *e.g.*, 0.1%, resulted in a group ecotrophic efficiency greater than one, that is to say: more would have been used in the model than was biologically available (Christensen *et al.* 2005). Such issues may arise when trying to capture the effect of predators with large biomasses upon groups with small biomasses where those prey are a very small portion of the predator's diet. In such cases, the prey may show up irregularly, or not at all, in diet composition studies. Therefore, the effects of relaxing or increasing such predation can be difficult to gauge (Christensen and Walters 2004). Sablefish have, therefore, very complex responses to environmental cues such from food availability and predation. One way to accommodate these issues would be to further partition sablefish with groups like larvae and young-of-the-year.

4.2.3.2. Northeast Pacific salmon

Of the five salmon species in the NEPac model, four (pink, chum, sockeye, and coho) appeared to have very similar biomass dynamics, while chinook salmon biomasses

behaved quite differently. One reason for this may be that the vast majority of the chinook salmon biomass in North America is derived from regions south of Alaska, see, e.g., catch statistics in Eggers *et al.* (2003). Given that chinook salmon tend to be more coastal in their oceanic phase of life and do not often disperse more than 1,000 km from their natal stream (Healey 1991) it is likely that if any oceanic or climate effect was manifested in their populations it would have been derived from upwelling and changes to the California Current. It would be unlikely, therefore, that climate changes in the GoA, and any associated bottom-up forcing, would have much effect on so-called 'NEPac' stocks of chinook salmon. This reasoning was supported by Mantua *et al.* (1997) who demonstrated that changes in the production of chinook from the southern contiguous states was out of phase with the production of sockeye, pink and chum in the NEPac ecosystem. Thus, it was not surprising to see the NEPac model was incapable of reproducing biomass dynamics of chinook salmon as reconstructed from catch data (Figure 3.36).

Sockeye and pink salmon populations have been used in several studies linking climate change to changes in the fish populations of the NEPac ecosystem. Of the five salmon species in the NEPac model, sockeye and pink were the two that showed the most agreement between predicted and reference biomass time series, see Figures 3.32 and 3.34. Hare and Francis (1994) demonstrated that for four

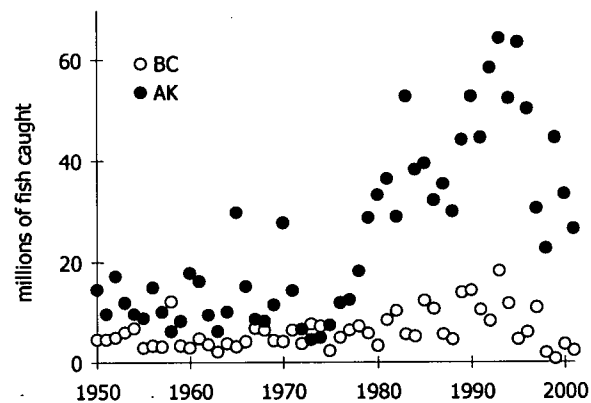


Figure 4.17: Comparison of changes in catches of sockeye salmon in British Columbia (BC) and Alaska (AK) between 1950 and 2001.

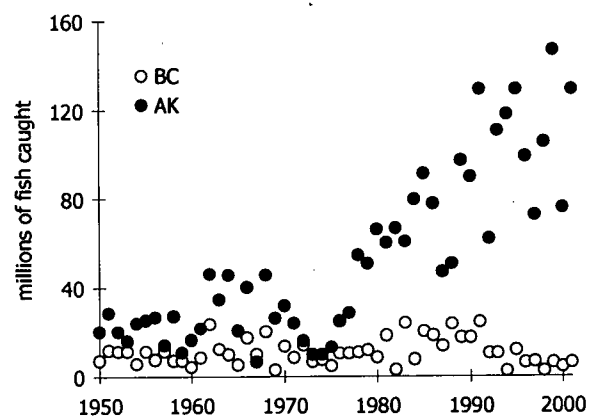


Figure 4.18: Comparison of changes in catches of pink salmon in British Columbia (BC) and Alaska (AK) between 1950 and 2001.

regional populations of these two salmon species; western Alaskan sockeye, central Alaskan sockeye, southeast Alaskan pink, and central Alaskan pink, there were synchronous changes in production in the late 1940s and late 1970s. The 1970s shift was witness to huge increases in the productivity of both species. However, while Peterman *et al.* (1998) agreed that Bristol Bay (western Alaska) sockeye stocks increased after the 1977-regime shift they also concluded that this was not the case for Fraser River (south BC) stocks. In contrast, Beamish *et al.* (2004) suggest that there were significant increases in Fraser stocks after the 1977 regime shift. The majority of both species originate from Alaskan rivers and streams (Figures 4.17 and 4.18), thus the NEPac model would likely emulate the dynamics of that larger group. Figures 4.17 and 4.18 illustrate the differing histories of the two subpopulations through representations of catch, a likely reflection of the relative abundances of the populations of the species in the two areas. In both cases it is clear that while Alaska tended to produce more of these species before 1977, after 1977 the relative abundance became heavily skewed in favour of Alaska. These divergent population trends agree with the research reported in Peterman *et al.* (1998) who found that such regional differences may be due to events occurring early after the entry of the salmon into the ocean environment.

Hare and Francis (1994) posited three mechanisms to explain why the 1977 shift was favourable for pink and sockeye production. The first was that warmer sea surface temperatures in the NEPac ecosystem implied that the salmon from Alaska did not have to migrate as far to return to their natal streams: reducing exposure time to predation and that declining populations of both Steller sea lions and northern fur seals (Hill and DeMaster 1998) would have even further reduced predation mortality. Secondly, increases in zooplankton biomass would have significantly improved the feeding environment for these two salmonids. The NEPac model would not have been able to explicitly examine the dynamics of the former hypothesis as it was not explicitly spatial. An implicit examination through changes in sea lion predation actually shows that for both sockeye and pink sea lions exerted *more* predation mortality upon the two after 1977. This contradiction was because the NEPac model was not tuned to any reference time series of sea lion population changes, and actually predicted they would increase. As

for the improved feeding hypothesis, the NEPac model did show that feeding time for both sockeye and pink salmon decreased after 1977 suggesting a better foraging environment (or fewer competitors) and, indeed, both sockeye and pink biomasses were seen to be highly correlated to carnivorous zooplankton biomass ($R^2 > 0.98$).

Chum and coho were intermediate in their biomass changes, Figures 3.33 and 3.35, and were also modelled as intermediate between chinook (highly piscivorous and concentrated in the south) and the pink / sockeye (zooplanktivorous and concentrated in the north). Figure 4.19 illustrates that prior to the 1977 regime shift the number of coho salmon caught in BC was almost always greater than the Alaska catch. However, after the regime change, Alaskan catch increased while BC catch decreased so Alaskan catch was consistently higher. Although based upon catch data it does suggest that the majority of coho biomass in the NEPac ecosystem used to reside in its southern portion, whereas it now appears to reside, or at least originate, in natal

streams from Alaska. The story for chum was much the same as for sockeye and pink biomass changes and the effects within BC and Alaskan populations. In chum, however, the response to the bottom-up forcing did not appear to be as pronounced as in pink and sockeye (Figure 4.20). This effect may be due to the different diet chum have. Kaeriyama *et al.* (2004) found that while NEPac pink and sockeye fed largely on squid and zooplankton, chum fed extensively upon gelatinous zooplankton. Therefore, chum may

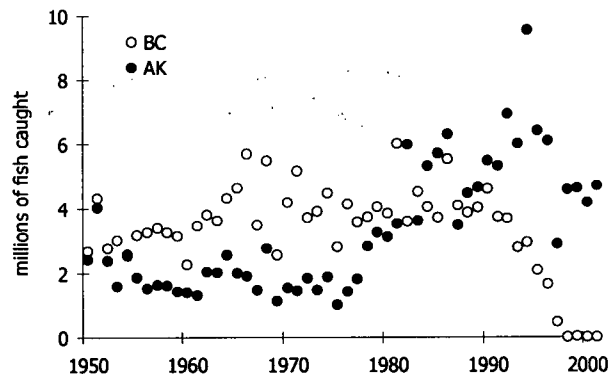


Figure 4.19: Comparison of changes in catches of coho salmon in British Columbia (BC) and Alaska (AK) between 1950 and 2001.

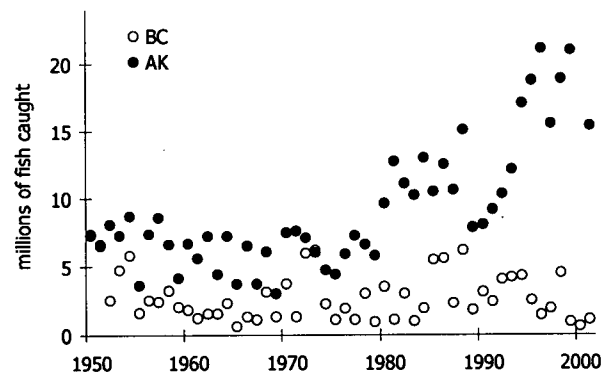


Figure 4.20: Comparison of changes in catches of chum salmon in British Columbia (BC) and Alaska (AK) between 1950 and 2001.

feed at a different trophic level than pink or sockeye further removed from the direct impact of any bottom-up forcing.

It would appear that in the NEPac ecosystem it is possible to characterise the biomasses of pink, sockeye, and to a lesser extent chum salmon, as having increased after 1977. As shown in Figures 4.17, 4.18, and 4.20 much of this increase was due to the overwhelming influence of Alaskan origin fish biomasses after 1977. This does not argue that NEPac ecosystem changes do not influence sockeye, pink, and chum salmon from BC, but rather that there are other impacts, *e.g.*, in fresh water or estuarine environments that were not explicitly dealt with in the NEPac model. As Peterman *et al.* (1998) point out there can be a variety of mechanisms affecting spawning and survival numbers as even a number of Bristol Bay sockeye stocks became less productive after 1977. Coho and chum also appear to be illustrative of the conclusions of Peterman *et al.* (1998) and Meuter *et al.* (2002a) that regional populations separated by up to 1,000 km were likely to exhibit synchronous production changes. This distance effect is probably exacerbated during the fresh water phases of any salmon's life history and likely also reflects the variety of fresh and salt water residence times of especially sockeye and chinook. What the NEPac model does suggest is that at the scale of the NEPac ecosystem there are shared effects for salmon in their marine phases, and especially for the more pelagic pink, sockeye and chum that have increased their production, *i.e.*, biomass in the NEPac model since 1977. For more coastal species, *e.g.*, chinook and coho, the dynamics controlling their biomasses over the last fifty years appear to be more related to smaller-scale upwelling effects closer to their natal rivers. This may explain why the SoG and BC shelf models provided more satisfactory fits between reference and predicted data series for coho and chinook biomasses (however, see section 4.2.2.2. for special concerns for chinook in the BC shelf model).

4.2.3.3. Northeast Pacific demersal fishes

Many of the 'round' demersal fishes in the NEPac model, *e.g.*, northern rockfish, Atka mackerel and hake had biomass trends similar to the NEPac multistanza demersal fishes:

increases in the 1970s and declines in the 1990s. The biomasses of many NEPac flatfishes, *e.g.*, Alaska plaice, yellowfin sole and rock sole followed these rises and declines but their modelled response times were different from their reference stock assessment trends. Pacific Ocean perch biomass behaved differently from other demersal species in the NEPac simulation but did appear to behave in much the same way as the Pacific Ocean perch population in the BCS model.

Northern rockfish are managed as two separate stocks, GoA and BSAI, although rather limited investigations have failed to demonstrate the existence of separate populations (Spencer and Ianelli 2003a). Indeed, the changes of the biomasses of the two northern rockfish 'stocks' in the NEPac ecosystem have been very similar and share the overall characteristics exhibited by the summed assessment data which was compared to the NEPac model biomass changes in Figure 3.38. In the NEPac model northern rockfish ate krill almost exclusively as suggested by Yang (1993) and the vulnerability setting that produced the best fit of simulated northern rockfish biomass to the reference assessment biomass was low (1.5). As a result the northern rockfish biomass was very highly correlated to changes in krill biomass ($R^2 = 0.996$). The average fishing mortality upon this species was quite low so the modelled biomass dynamics appear to be largely controlled by primary production changes. Because northern rockfish was modelled without regard to life history stages there was no way to examine the ideas expressed by Courtney *et al.* (2003) that year class abundance could be affected by availability of larval and post-larval zooplankton food resources. As for the effect of changes in the abundance of krill upon northern rockfish, Courtney *et al.* (2003) suggest that competition for krill prey from pollock may also be considerable. This theory was not supported by dynamics within the NEPac model, though, which showed that most krill predation mortality likely arose from invertebrates like jellies and squid, while fishes such as pollock and northern rockfish exerted a relatively small portion of the total mortality on krill. It would be unlikely that the rockfish compete with the invertebrates noted above as they would tend to be in pelagic areas of the NEPac ecosystem. If, however the pollock and rockfish compete for krill in limited spatial areas then competition may be of import but this was not examined in the NEPac model.

The Atka mackerel stock of the NEPac ecosystem is concentrated in and around the Aleutian Islands (Lowe *et al.* 2003). There is a limited number that exist in the GoA, often detected as small bycatch, but these populations appear to have declined after having supported a foreign fishery in the 1970s and 1980s (Lowe and Lauth 2003). Atka mackerel biomass in the NEPac model went through a cycle of waxing and waning from 1977 to 1997, similar to changes in Aleutian Islands 1+ biomass described in Lowe *et al.* (2003). One of the most obvious contributors to the post 1980s decline was increasing fishing mortality upon the stock. Figure 4.21 shows that the fully selected fishing mortality (*i.e.*, of fish large enough to be fully recruited into the fishery) began to rise after 1990. By the beginning of the 21st century, the F was usually 0.6 year⁻¹ or greater, although this was below the threshold $F_{40\%}$ of 0.847 year⁻¹ (fishing mortality that would reduce the fully selected female spawning biomass to 40% of its unfished level) estimated for the stock (Lowe *et al.* 2003). In the NEPac model Atka mackerel were seen to respond to this increased mortality with a declining biomass. It was unlikely that predation was responsible for biomass decline in Atka mackerel because predation mortality declined throughout the simulation. Atka mackerel biomass declining as a result of bottom-up mechanisms was also unlikely because the Atka mackerel biomass trajectory was optimised with a low vulnerability for its prey. In the NEPac model Atka mackerel fed mostly upon zooplankton. In the absence of changes in fishing mortality, changes in the biomass of prey items were not sufficient to cause a similar magnitude of decrease in Atka mackerel biomass after 1990. Thus, in the NEPac model, while the 1977 regime shift appears to have been largely responsible for increased Atka biomass from 1977 to 1990, fishing mortality was the most likely explanation for biomass declines after 1990.

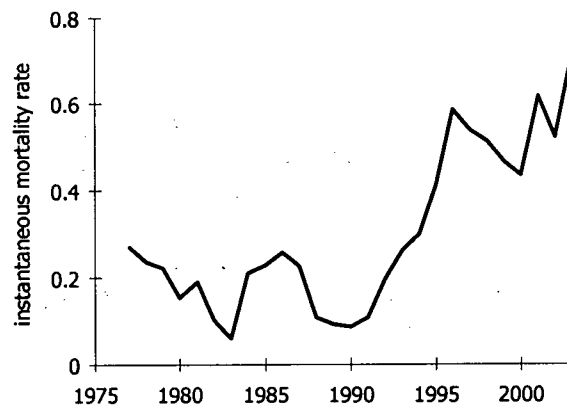


Figure 4.21: Changes in fishing mortality of fully selected Atka mackerel from 1975 to 2003 in the Aleutian Islands .

In the NEPac model, hake biomass was seen to change in a fashion very similar to what was observed in the BCS model, Figures 3.24 and 3.40. In fact, the fit of the NEPac simulated biomass to the trend derived from stock assessment data was more satisfactory in the larger-scale NEPac model. As pointed out in section 4.2.2.3, most of the biomass of the coastal hake stock has been in the California current ecosystem with adults moving into BC waters to feed during the summers. After 1990, however, an increasingly large portion of the hake stock moved into the BCS and began to stay on an annual basis, even to reproduce (McFarlane *et al.* 2000). The dynamics of hake biomass in the NEPac model appeared to be very similar to those seen in Atka mackerel. The expansion of prey biomass in the mid 1970s gave rise to larger hake biomasses which began to decline in the 1990s, after dramatic rises in fishing mortality.

That the NEPac model was able to reproduce the magnitude and timing of biomass changes of hake more satisfactorily than the BCS model could be due to at least two possible causes. In the first case the approach used to calculate hake biomass in the NEPac ecosystem was the same as for the BCS ecosystem: a simple fraction of the assessed biomass on the whole west coast. Because of the known changes in the distribution and behaviour of hake already alluded to, however the reproduction of the biomass in the model may be simply due to chance. Remember from section 4.2.2.3 that Benson *et al.* (2002) found that the best predictor of hake biomass in the BCS area, *i.e.*, the southeast corner of the NEPac ecosystem as modelled, was upwelling at 33°N. Because so much of the known dynamics of the west coast hake stock has been under the control of mechanisms that originate *outside* the NEPac ecosystem, any correlation between the assessment and simulated biomass should be viewed with suspicion. On the other hand, it may be that there have been large-scale bottom-up processes occurring across the scale of the NEPac and California current ecosystems, which are more similar to the NEPac ecosystem and have thus been captured by the NEPac model. Again, however the point should be made that the scale of the mechanism is beyond the scope of the model, though it may be linked. A more satisfactory approach would be to model the California Current ecosystem, or even the west coast of North America to see how

bottom-up forcing might have acted upon hake in the ecosystem encompassing their entire biomass.

Alaska plaice, yellowfin sole and rock sole shared many characteristics in the NEPac model from the prey they pursued (mostly small benthic invertebrates, section 2.4.5.) to their life history parameters. However, In Figures 3.41, 3.42, and 3.43 biomass trajectories for the three (from the NEPac model and reference assessment data) diverged more than one might have expected, given their biological similarities. Yellowfin sole and Alaskan plaice biomass changes were more similar to each other than either was to rock sole. Indeed, rock sole biomass changes were different from all other demersal species in the NEPac model. Whereas the yellowfin sole and Alaskan plaice biomasses began to rise dramatically in the 1970s, rock sole biomass increase was most vigorous after 1980. Wilderbuer and Walters (2003), showed that during the 1980s, age 4 recruitment for the rock sole population was low in the 1970s and 1990s and high during the 1980s. However, in the case of yellowfin sole age 5, and Alaska plaice age 3, recruitment Wilderbuer and Nichol (2003) and Spencer *et al.* (2003) showed that the periods of highest recruitment were in the 1970s.

Differences in biomass dynamics of rock sole arising from recruitment processes were not explicitly accounted for in the NEPac model. This may explain why the model failed to capture the decline in rock sole biomass in the 1990s which Wilderbuer and Walters (2003) attribute to poor recruitment. This suggests that the regime shift of 1977 affected rock sole in the NEPac ecosystem in a manner different than other demersal species. Remember, it has been shown that most other demersal species biomass trends could be explained by the NEPac model dynamics as manifested upon the 'adult' groups or the groups largely modelled as adults, *i.e.*, not as multi stanzas. Why rock sole was different may be due to some habitat requirement or advection condition for larvae or juveniles that changes with climate variation. As was argued for the rock sole population modelled in the BCS model there are likely severe limitations on the habitat for spawning in this species (Wilderbuer *et al.* 2002 and Fargo and Wilderbuer 2000). Therefore, the processes governing the dynamics of recruitment could easily be manifested at a different

scale of area and time than what was being shown for most of the species in the NEPac model.

Both yellowfin sole and Alaska plaice biomass changes in the NEPac model were optimised with low vulnerability settings for their prey. This resulted in high correlations to the biomasses of their prey. The NEPac model suggested that the biomass variation in most demersal species, especially the adult stages, was likely driven by the changes in availability of their prey, which was in turn governed by bottom-up forcing from changes in phytoplankton production.

4.3. Climate variation and modelled ecosystem changes

In general the demersal species of the NEPac model exhibited increased biomass after 1977, followed by a plateau or slightly declined biomass in the 1990s reflecting the large 1977, and less obvious 1989, regime shifts. As a general result the groundfish populations of the Northeast Pacific were better emulated by the NEPac model than the BCS model. One exception was rock sole perhaps because of smaller-scale dynamics having shaped changes in its recruitment. Bottom-up effects upon salmon biomass changes were, in some cases, better represented in the smaller-scale SoG and BCS models, *i.e.*, coho and chinook. In other salmonids, *i.e.*, pink, sockeye and chum, however, the large-scale NEPac model provided a more satisfactory explanation for bottom-up driven biomass changes. For other species, especially slow-growing, long-lived fishes, mammals and birds, changes in mortality due to fisheries or bycatch appear to have played a dominant role in shaping biomass trajectories with bottom-up mechanisms helping improve the fit of the modelled to reference data. In this section, the potential links of climate to bottom-up forcing in the three ecosystem models in this study will be explored.

4.3.1. Climate variation and the Strait of Georgia model

The most striking features of the predicted primary production anomaly (PPA) in the SoG model were the declines of the 1960s and 1990s. These changes in phytoplankton

biomass were seen to be very similar to changes in three climate change indicators, especially when their spring and summer values were examined, Figures 3.45-3.52. The effects of river flow and salinity in the SoG vary over relatively small areas ~ thousands of km². The third indicator which showed variation similar to that of modelled phytoplankton biomass was upwelling measured at 48°N. Variation in upwelling processes are manifested over larger areas ~ tens of thousands of km². However the changes in water movement off the North American west coast influence the water that is carried in to the SoG by ocean currents (Davenne and Masson 2001). Remember, too, that in the EwE model phytoplankton biomass was averaged over the year, yet the association for years of high biomass was indicated by values from only spring and summer months of climate indicator time series. This apparent contradiction may merely reflect most of the total annual phytoplankton biomass typically being produced in the bright spring and summer months (Harrison *et al.* 1983). This would be especially so for years of high biomass if the spring bloom was prolonged into the early summer months. Unfortunately seasonal dynamics like timing mismatches between spring phytoplankton production and larval feeding could not be explicitly modelled.

Nitrogen has long been regarded as an important factor of phytoplankton production in the SoG ecosystem (Harrison *et al.* 1983 and Yin *et al.* 1997). Yin *et al.* (1997) found that on a day-to-day basis, nitrogen concentration in the central SoG can be controlled by the variations in the entrainment of nutrient rich deep water during fluctuations in Fraser River runoff. Such small time scale processes would not be manifested in any dynamics accounted for in the SoG model, however, the persistent seasonal trends of flow variation would. The characteristics, *e.g.*, density, salinity, temperature, oxygenation and nutrient concentration, of the water being entrained, however, is determined by offshore upwelling (Masson 2002). The timing of the most intense upwelling events usually lag the timing of the Fraser River Spring freshet by as much as two months (Li *et al.* 2000). This shelf water is carried to the SoG in deep water renewal (DWR) events, which have a periodicity of about a month but have different characteristics, depending on the season. In the summer DWR events are characterised by warm, saline, low oxygen water that is rich in nutrients, and in the winter by cold, slightly saltier, high oxygen, low nutrient

water (Masson 2002). Thus, there are complex processes that link the delivery of nutrients to phytoplankton in the SoG ecosystem, which link physical processes that operate on overlapping area and time scales. A final factor to consider is the misconception that the water from the Fraser River is particularly helpful to primary production in and of itself. To the contrary, the fresher water of the Fraser River plume tends to be both lower in nitrogen and higher in turbidity, inhibiting the growth of phytoplankton in and below this lens of less dense water (Harrison *et al.* 1983). Notwithstanding this limitation, entrainment via estuarine circulation has been identified as the primary source of nitrogen in the photic zone (Yin *et al.* 1997).

The climate indicators which influence these physical processes in the SoG were Fraser River flow, salinity, and upwelling measured at 48°N. Of these, salinity is a measure of surface conditions and can not indicate the condition of DWR events that may have taken place during the period modelled. It would be possible in principle to use surface salinity as a delayed indicator of DWR events because the deep water would have been entrained by estuarine circulation in the SoG. However, the complexity of mixing of the various rivers and precipitation through tides and currents in the SoG, would render such a back-calculation a horrendous task. What the climate indicators suggested in this study was that high phytoplankton biomass was predicted to occur in the SoG model when: spring and summer Fraser River flow was lower than average, spring salinity was relatively high, and spring coastal winds fostered poor downwelling or even weak upwelling.

Two effects from the Fraser river would be likely when flow is low during the spring and summer; less light extinction where the plume occurs in the SoG, and a smaller salinity gradient between the surface and deep water layers. In this simple dynamic it would be likely that if there was a lower gradient between the surface (euphotic) zone and nutrient rich deep water, entrainment would be facilitated. Furthermore, a lower salinity difference between the two layers would also foster the mixing of nutrients into the euphotic zone via wind mixing. Wind mixing was identified by Martell *et al.* (2001) as a correlate of changes of simulated phytoplankton biomass in an earlier SoG Ecosim model. From this interaction it might be hypothesized that the tendency of the SoG model

to predict years of low phytoplankton biomass when spring summer runoff is low could be due to the delivery of nutrients to the photic zone without excessive shading. The highest flows for the Fraser River tend to be in May, June and July. Therefore even in 'low' spring-summer flow years the flow is much greater than at any other time of the year. This implies that enhanced entrainment of nutrients would continue with as little shading as possible in spring-summer lower-flow years.

Conversely, Li *et al.* (2000) used a biological physical box model of the SoG Juan de Fuca system to show that plankton populations, *i.e.*, zooplankton *and* phytoplankton were relatively insensitive to changes in physical drivers unless those mechanisms affected rate processes like mortality and growth. Thus, changes in zooplankton growth and mortality from environmental forcing caused changes in phytoplankton biomass, not the climate forcing itself. The SoG model suggested otherwise as the biomass of herbivorous and carnivorous zooplankton were very highly correlated to phytoplankton biomasses.

In the 'best fit' SoG model vulnerability settings for predator-prey linkages in these groups were left at the default Ecosim value: 2, *i.e.*, mixed bottom-up top-down control. Regardless, the high correlation of zooplankton to phytoplankton biomasses in the SoG model persisted even if vulnerabilities were set to very high values. Furthermore, the vulnerability settings at these lower trophic level linkages had little effect on the biomass changes further up the food web. That is, changes in the vertebrate groups, which had reference data were not affected by the vulnerability settings of the zooplankton groups in the model. This could mean that the apparent changes in phytoplankton biomass were merely what was necessary to drive zooplankton biomass changes actually responsible for changes to the vertebrates examined in detail in the SoG model. The link to climate via phytoplankton remains a more parsimonious explanation, however, and further examination of the zooplankton bottom-up mechanism would require more detailed modelling of those groups to further elucidate how environmental conditions may have fostered herbivorous versus carnivorous zooplankters while accounting for the roles of recruitment and transportation in those groups.

As an amplification of the relationships between the three environmental variables described in this section; salinity, Fraser River flow and coastal upwelling, an interesting contrast appeared between data from the two salinity stations: Chrome Island (inside the SoG) and Race Rocks (just outside the SoG in the Strait of Juan de Fuca, which connects to the Pacific coast) and the other two variables. Correlations were calculated for the two salinity station values against coastal upwelling and Fraser River flow, with all data smoothed using a LOWESS filter with a ten year window and a second degree polynomial. This was intended to see how changes were occurring in the three variables at, roughly, a decadal time scale. Though both stations' salinities tended to be negatively correlated with Fraser River flow, the salinity values at Chrome Island were more strongly correlated at all times of the year, with the spring and summer values being strongest. On the other hand, while both salinity stations showed a tendency to be positively correlated to coastal upwelling in the spring and summer, the salinity at Race Rocks tended to be stronger and also correlated to late winter and early summer upwelling. Correlations between Fraser River flow and upwelling were weak at all times, suggesting that the two are not directly linked. Geographically, this makes sense as Race Rocks is closer to the upwelled water source and Chrome Island is closer to the mouth of the Fraser River. Thus, it would appear that, at a decadal time scale, upwelling, salinity, and Fraser River flow have tended to co-vary. Further, while upwelling and Fraser flow both appear to have contributed to changes in surface salinity (the Fraser directly and upwelling indirectly as it was entrained) the influence of the former was stronger within the confines of the SoG.

In the SoG model changes predicted for phytoplankton biomass were most strongly associated with oceanographic processes that varied on time scales of a decade, especially for data from spring and summer months (Figures 3.47-3.54). In Figures 3.48, 3.50, 3.52, and 3.54 it can be seen that when the data were smoothed over longer time steps the correlations between phytoplankton biomass tended to be out of phase with flow, salinity, and upwelling. As discussed above there are even more complex interactions between the mechanisms that could have produced changes in phytoplankton biomass in the SoG. It has long been recognised that the SoG functions as an estuary with

relatively less saline water flowing out to the Pacific on the surface and relatively more saline water flowing in at depth (Thomson 1981, Harrison *et al.* 1983). However, the manner in which the tidal flow, currents and winds might alter the mixing of the surface and deep water, and how this might influence primary production has only been described in a very coarse way. Yin *et al.* (1997) showed that variations in daily Fraser River flow may cause changes in phytoplankton production, but this was on very short time scales. This SoG EwE model suggested that phytoplankton production was most correlated to spring and summer Fraser River flow, that is, when flow was highest. However, while PPA changes were associated with high flow months, phytoplankton production is actually highest in periods when Fraser flow is relatively low. So, in one sense, the SoG model supports Yin *et al.* (1997): phytoplankton production being most responsive to months when flow tends to be highest. However, in another sense the SoG model refutes Yin *et al.* (1997) in that high phytoplankton production periods was specifically coincident with times when high flow was actually abated. Such contradictions may reflect time delayed feedback loops beyond the scope of the SoG EwE model. The modelling work of Li *et al.* (2000) does little to resolve this issue. In their box model of the SoG – Juan de Fuca system they found that physical processes did not directly affect the abundance of phytoplankton.

In the absence of any long-term monitoring work which integrates changes of phytoplankton production in the SoG it will be difficult to determine which physical mechanisms are important. The most parsimonious explanation suggested by this study is that upwelling at 48°N and Fraser River flow during the spring and summer interact to produce changes in nutrients in the SoG, as evidenced by changes in surface salinity, which effect the potential production of phytoplankton. When peak Fraser flow is relatively low nutrients could still be entrained in large quantities but the shading from the large and turbid freshwater lens would be minimised. The variation in these mechanisms tends to be at a decadal scale, with the decade after 1990 being witness to very low phytoplankton production. A surprising consequence of this might be applied to Fraser River flow under future climate change scenarios. Morrison *et al.* (2002) suggest that greenhouse-associated climate change will, by 2070 to 2099, cause the peak flow of

the Fraser River to be earlier, and smaller, than historic norms of the 20th Century. If other environmental factors like upwelling, wind and sea surface temperature continue to vary as they have historically then phytoplankton production in the SoG may actually tend to be higher, assuming a simplistic estuarine circulation mechanism driving nutrients supply, and the assumption that lower peak flows would result in less shading in the euphotic zone.

4.3.2. Climate variation and the British Columbia Shelf model

A persistent feature of the BCS model was that the predicted PPA was highly correlated with coastal upwelling time series, see Figures 3.56 and 3.57. While it has proven to be difficult to explain how phenomena such as Fraser River flow and upwelling may have caused nutrient induced increases or decreases in phytoplankton production in the SoG, such mechanisms are better understood for the BCS ecosystem.

As discussed in the introduction, there is a correlation between ecosystem scale and the time scale at which processes within it are manifested. At the relatively smaller scale of the SoG ecosystem, smaller-scale physical processes such as surface waves, internal waves, tidal rise and fall and turbulence become increasingly relevant to explaining phytoplankton population changes, which are manifested over distances ranging from hundreds of metres to tens of kilometres (Daly and Smith 1993). As can be seen in Figure 1.10 the land-sea interface of the SoG is characterised by fjords, inlets and narrows which range from hundreds of meters to tens of kilometres in length and width. Therefore, it is not unreasonable to infer that larger-scale processes such as upwelling, though dominant in determining long-term annual and interannual changes may not have as great variability as the day-to-day and weekly processes that occur in the many small sub-regions of the SoG. At the scale of the BCS, the preponderance of water area, and volume, taken up by open coast environments on the west coast of Vancouver Island and Haida Gwai'i may overwhelm the variance of all the small bays and inlets. Thus, in the BCS model, a relatively simpler mechanism can be posited to directly link changes in a

physical process (upwelling) to changes in a biological one (phytoplankton production) because time scale and area scale may be well matched.

As described in section 1.1.2., wind is the mechanism that drives upwelling (or downwelling for that matter). Francis *et al.* (1998) describe how at area scales over which upwelling is manifested, $\sim 10^4$ to 10^5 km², climate change is linked to changes in ecosystems: climate variation → changes in surface pressure fields → changes in surface winds → changes in upper ocean circulation → changes in timing, and species within, phytoplankton blooms → changes in zooplankton community. The changes in the zooplankton community and, predators feeding directly upon it, should closely track changes in climate indicators. Higher trophic level organisms, however, will likely have a lagged effect as they usually have longer life spans, as demonstrated for the west coast of Vancouver Island by Tanasichuk (2002). Also, some fishes undergo ontogenies which can cause them to experience bottom-up climate effects in different ways during different phases of their life history, *e.g.*, feeding directly upon zooplankton during their larval phase but indirectly as adults. Changes in the mortality and biomass of adult predators will then feedback as different predation effects on the herbivores and planktivores (Francis *et al.* 1998).

In the BCS model some of these complex feedback and ontogenetic effects were emulated, *e.g.*, ontogenetic changes in multi-stanza groups and differential mortality (P/B) rates in the Ecopath portion of the model. However, the model can only provide a guide, not an absolute measure, of which trophic links facilitated bottom-up or top-down type changes. EwE does provide a relative measure of how different trophic mechanisms; changes in vulnerabilities for predator-prey linkages, predicted primary production anomalies (PPA), or a combination of the two, improved the fit of the estimated to reference time series of catch and biomass (Tables 3.1 to 3.5).

Table 3.3 shows that even under quite different global parameterisations of vulnerability in the BCS model, a PPA improved the fit of the modelled to reference data. Remember, too, that the timing and direction of the PPA were also similar even under different assumptions of trophic control (Figure 3.2). In the case of the 'best fit' BCS model, when the PPA was included there was a large improvement of the fit of the predicted to reference biomass data (Tables 3.1 and 3.2). Further, this improvement of fit was not just concentrated in the lower trophic level species, which would

Table 4.2: Changes in the sums of squared differences (SS) between reference and predicted time series of biomass in the 'best fit' BCS model under different assumptions; no changes to base vulnerabilities AND no PPA (none), a PPA alone (enviro), optimising vulnerabilities alone (no environment), and both effects combined (all effects). Smallest SS in **bold**.

	none	enviro	trophic	both
arrowtooth	20	3.78	0.93	1.16
Pacific cod	19.66	10.97	7.16	4.37
halibut	6.4	3.14	4.11	3.95
sablefish (tags)	0.54	0.4	0.43	0.33
sablefish C/F	2.97	2.83	2.19	1.64
pollock (GoA/2)	10.22	9.33	4.19	3.38
herring	11.67	13.4	11.89	9.25
pink	10.58	10.58	9.7	6.04
chum	9.21	9.21	9.46	8.46
sockeye	10.38	10.38	19.24	23.07
coho	103.93	104.19	50.07	29.94
chinook	16.84	18.15	19.52	14.14
P. O. perch	3.24	5.05	1.62	1.44
hake	7.3	4.91	5.25	4.08
rock sole	3.07	5.04	3.08	2.94
seal	25.72	14.88	2.44	1.86

respond more directly to changes in phytoplankton abundance. Table 4.2 shows the improvement of fit by species group, with reference biomass data in the 'best fit' BCS model. Note that many of the high trophic level species, while having a lower SS under the assumption of trophic control alone compared to a PPA, had an even lower SS when both effects were applied, *e.g.*, Pacific cod, sablefish, pollock, and seals. Indeed, halibut had the lowest SS with the modelled environmental effect alone. The reason for the relatively poor response of pink, chum, and sockeye salmon to the model treatments, are discussed in section 4.2.2.2., and likely stem from the movement by these species to the open ocean Alaska Gyre for the majority of their adult marine life. What is apparent, however, is that some of the longer-lived species in the model respond to a bottom-up type climate at a different time scale than the shorter lived ones, given the modelled ontogenies, mortalities, and feeding behaviours. Thus, the BCS model is capable of reproducing feedback effects across different time scales and trophic levels which were posited as necessary consequences of climate change and bottom-up forcing by Francis *et al.* (1998).

Robinson and Ware (1999) used a simple box model of the southwest coast of Vancouver Island (SWCVI) to show how climate forcing might have been linked to phytoplankton production changes and thence to known biomass changes in hake and herring from the late 1960s to late 1990s. In their model, upwelling, temperature and solar radiation were used to force trophodynamics of 8 species groups; hake, juvenile herring, adult herring, chinook salmon, dogfish, euphausiids, copepods, and diatoms. In the SWCVI model, run from 1967 to 1998, diatom production (analogous to the phytoplankton group in the BCS model) was predicted to have peaked in the mid 1980s then declined until the late 1990s (Robinson and Ware 1999). This result is consistent with predicted changes in the phytoplankton production in the BCS model, Figure 3.45. Also consistent between the models was a prediction that phytoplankton dynamics were less variable than those of the euphausiids that preyed upon them. Unlike the SoG model the BCS model predicted that phytoplankton vulnerability to euphausiids, as predators was high during the simulation, resulting in higher variation of euphausiid biomass during the period modelled.

Further evidence supporting these bottom-up climate change effects in the BCS was discussed by Tanasichuk (1999). His work showed that despite significant decline in euphausiid biomass, from 1991 to 1997, the contribution of euphausiids to the diet composition of hake was unchanged. His conclusion from this was that the decline in euphausiids was not due to hake predation but more likely due to external. *i.e.*, bottom up mechanisms. The biomass of hake also declined during that time, another trend mirrored in the bottom-up changes suggested to have occurred in the 1990s by the BCS model.

However, Tanasichuk (2002) rejects the idea that changes in physical phenomena can be linked to changes in populations of fishes off the west coast of Vancouver Island. He observed that during the 1990s the biomasses of the two dominant euphausiids, *Thysanoessa spinifera* and *Euphausia pacifica*, responded quite differently to climate phenomena like El Niño. Because of these differences in biomass change, populations of commercially important fishes responded differently to the new foraging situation. Tanasichuk (2002) argues that the lack of a coherent response by populations of dogfish,

coho salmon, hake and herring, in response to changes in euphausiid biomass, makes it difficult to contend there is a climate mechanism driving the ecosystem. The study, however, used euphausiid biomass in Barkley Sound as a proxy for biomass off the whole of southwest Vancouver Island which the author recognizes may be misleading. Further to this reasoning, the limited area of Southwest Vancouver Island would be subject to large portions of its key fish biomass, notably hake, herring, and coho moving outside of the ecosystem boundary. In the case of herring, the problem may be amplified because only the west coast of Vancouver Island (WCVI) stock was considered in Tanasichuk (2002). However, it is generally accepted that adults of the much larger SoG herring stock not only export biomass to the WCVI stock (Ware and Schweigert 2002) but also spend much of their lives as adults in the WCVI area (Robinson and Ware 1999 and Stocker *et al.* 2001). Further, if fish species can easily change their prey selection the importance of relative biomass of any one of those forage species could become trivial. Specifically, there is no compelling evidence to suggest that any of the fishes in the study are dependent upon any particular euphausiid, or other zooplankton, species. Therefore, fish biomasses may have more easily observed responses to the sum total of change in all the species upon which they may feed.

4.3.3. Climate variation and the Northeast Pacific model

The Northeast Pacific (NEPac) EWE model was quite different from the two smaller-scale models in that the PPA predicted to have occurred was best characterised by two regimes over the ≈ 50 years in the model. The first PPA regime was from 1950 to the mid 1970s, the second from the mid 1970s to the end of the simulation. Even when the model was run so that it estimated a PPA for every year of the simulation, rather than using a cubic spline function, the difference in average phytoplankton production between the two periods appears evident to the naked eye (Figure 4.22). In both cases all the PPA values were higher after 1977 than any before that year. This temporal separation of two production regimes across the NEPac area has been noted by several previous examinations of climate and marine production, *e.g.*, Francis *et al.* (1998), Clark *et al.* (1999), Hare and Mantua (2000) and Hollowed *et al.* (2001).

In the NEPac model all fish species for which time series were used exhibited a positive biomass response to the increased primary production predicted to have occurred after 1977. Note, however, that in some cases the timing of that biomass response was lagged, *e.g.*, arrowtooth flounder and Pacific halibut. Such lagged biomass responses were shown in section 4.2.3.1. to be

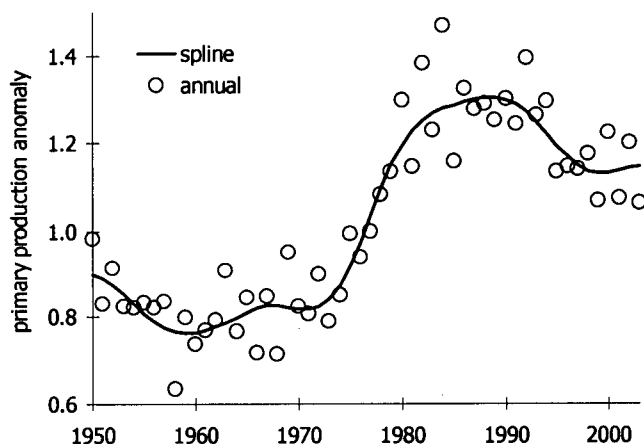


Figure 4.22: Changes in NEPac modelled PPA estimated at annual intervals versus a PPA estimated with a cubic spline function.

most likely a reflection of larger cohorts influencing total biomass as they were recruited into the adult population in subsequent years. In the NEPac model arrowtooth flounder were adults at age 3 and Pacific halibut were adults at age 4. In this manner, large recruitment events would later accumulate as biomass given the relatively low P/B rates of these two species: 0.5 year^{-1} as juveniles and $\sim 0.3 \text{ year}^{-1}$ as adults. In the case of faster-growing species like the pink, chum, and sockeye salmon groups with P/B rates between 1 and 1.4 year^{-1} , all had biomass responses timed very closely to the changes in primary production. As an example of an extremely muted response to the primary production change signal, Pacific Ocean perch did increase after 1977 but very slowly due to its slow growth rate. Further, the slight decline in annual primary production predicted by the NEPac model to have occurred in the early 1990s was manifested as declining biomass of several fish species. Note that 1977 is generally accepted as marking the time of a major regime shift (Francis *et al.* 1998), whereas there is active debate over the validity as classifying the known changes in the late 1980s / early 1990s as a *bona fide* regime shift (Hare and Mantua 2000). The NEPac model suggested that the general biomass declines were significant but not large enough to represent a shift back to biomasses more typical of the pre-1977 period. Indeed, the NEPac model suggested that by the late 1990s the decline in primary production had abated.

Polovina *et al.* (1995) devised a model to examine the mechanism that links climate change to primary production change at the area scale of the North Pacific basin and time scales of several decades. In their study, changes in the mixed layer depth (MLD) were used to drive a plankton population dynamics model. It was observed that after 1977 there was a general shallowing of the MLD in the area of the Gulf of Alaska and the Alaska Gyre. Their plankton production model suggested that this shallowing of the MLD would result in a general increase in phytoplankton production. Although their model suggested increases in phytoplankton in the GoA after 1977, the size of the increase was sensitive to assumptions of the extent that MLD changes after 1977 were associated with increased or decreased light penetration. Polovina *et al.* (1995) showed that the predicted increase in phytoplankton production in the NEPac after 1977 is corroborated by field studies and coincides with increases in the production of several fish species, as shown in section 4.2.3.

In the two smaller ecosystems in this study, many instances were seen of opposite biomass responses to changes in primary production, *e.g.*, constant increases in arrowtooth flounder and seal biomasses for both the SoG and BCS models despite significant periods of low primary production after 1970. The NEPac model, however, suggested that the change in primary production to a much higher average state after 1977 was so pervasive that all species would have experienced increased biomass. This is truly then an example of a bottom-up driven change in an ecosystem.

4.3.4. Climate variation and model scale

One way to visualise primary production variation at different area scales is by thinking of each PPA as two overlapping sine waves, one long and the other short. Such a coupling of sine waves would separate climate effects with independent phase changes over different time scales. In the case of the NEPac PPA, it is obvious that the longer-term sine wave has a much greater amplitude than any shorter-term one that might also be manifested in the system. Thus, the effect of the long-term pattern change in 1977

swamped any other climate signals at that modelled scale. In Figure 4.23. six graphs are presented to illustrate how the best fit PPAs, derived from 10 spline points, for the SoG, BCS and NEPac models, can be represented as the combined effects of two sine wave signals. For each of the three modelled PPAs the 'solver' routine in Microsoft Excel was used to fit a function consisting of two sine waves. The function assumes two sine waves, described by three parameters for each wave:

$$PPA_t = (\text{SINE}(\Sigma_{t_0} + \Lambda)) \cdot A) + ((\text{SINE}(\sigma_{t_0} + \lambda)) \cdot \alpha)$$

Where, for the longer period sine wave

Σ_{t_0} = starting point along the sine wave

$\Lambda = \Pi \cdot (\text{wave period in years} \cdot 2^{-1})^{-1}$

A = amplitude

and, for the shorter period

sine wave

σ_{t_0} = starting point along the

sine wave

$\lambda = \Pi \cdot (\text{wave period in years}$

$\cdot 2^{-1})^{-1}$

α = amplitude

As shown in Figure 4.23. the

dual sine wave function can

emulate the characteristic

changes in the PPA for all

three models. Note that the

dual sine wave function is not

meant in any way to be an

attempt to capture the fundamental structure of climate change in the models. The sine functions help to show the frequency and amplitude of change that have occurred in the PPAs of the three models. The wavelength of the two contributing waves in each model

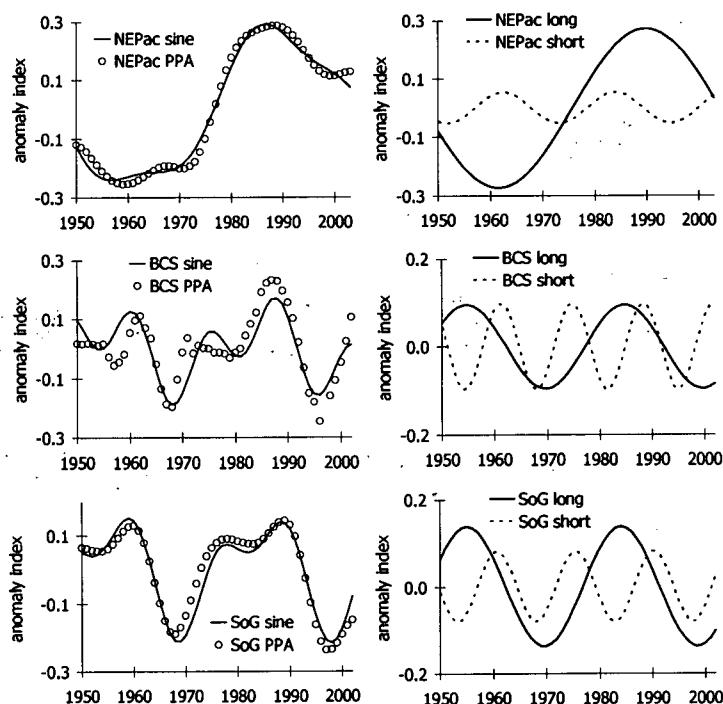


Figure 4.23: Changes in modelled PPAs reproduced by fitting two sine wave functions capturing both decadal and interdecadal variations.

was, SoG – 29 years and 15 years, BCS – 30 years and 14 years, NEPac – 57 years and 21 years.

An examination of the two sine waves approximating the NEPac PPA shows that the amplitude of the shorter frequency wave was only about 20% of that for the longer frequency wave. In the smaller scale models, however, the smaller frequency wave had an amplitude as large as (BCS), and 60% as large as (SoG), the longer frequency wave. This suggests that in the smaller area scale models, decadal scale changes in the environment are just as important as interdecadal changes in determining gross changes to primary production. The implication of changes happening on both decadal and interdecadal scales in the NEPac ecosystem is similar to results reported for production and recruitment changes, associated with climate change, in both pelagic and demersal species in the North Pacific reported in Hollowed *et al.* (2001).

The observation that changes in the NEPac PPA may occur on two time scales would also explain why there has been some uncertainty as to whether there was a generalised North Pacific regime shift in 1989. While there is a consensus in the meteorological and biological communities that there was a North Pacific regime shift in 1977 (Francis *et al.* 1998, Minobe and Mantua 1999, Beamish *et al.* 2000 and Jurado-Molina and Livingston 2002) there has been some debate over whether or not a regime shift also occurred in 1989 (Hare and Mantua 2000). Figure 4.23 shows that the small time scale component of the PPA was, indeed on a downward-trend during 1989. The overall state of the PPA, however, remained above average because the long time scale component of the PPA was at the apex of its cycle in the late 1980s. This may be an implicit manner in which the NEPac model is emulating the observations of Hare and Mantua (2000) who found that the 1989 'regime' shift was not pervasive enough to actually signal a return to pre-1977 conditions. In a more precise definition of the term regime, the PICES study group (King 2005) concluded that there was a regime shift in 1989. However, one would not expect that shifts are *cycles* so a return to pre 1977 conditions would not be expected.

In the case of the BCS PPA the magnitudes of the two component waves were effectively the same. Figure 4.23. shows that in 1989 both long and short-term waves were trending downwards, with both reaching their lowest points near the turn of the Century. Such super-positioning of the minima of both waves coincided with the collapse of herring, in the late 1960s, and the collapse of coho and chinook salmon, in the 1980s/1990s. In terms of regime changes the effect at the scale of the BCS was exhibited by ecosystem changes in 1989 as large as, if not larger than, those of 1977. Beamish *et al.* (2000) suggested that decreased ocean survival of coho salmon in the British Columbia-Washington-Oregon area was linked to a local-scale climate regime shift. Thus, coho, and perhaps chinook salmon may have responded to climate changes manifested at different scales (coastal) than pink, chum, and sockeye salmon (oceanic). This result confirms the suggestion by Levin (1992) that variability in a population reflects the scale at which the creatures experience their environment. Levin (1992) also points out that the processes driving changes in a population may therefore also reflect a larger scale than that at which data is being analysed. The longer-scale component of the BCS PPA may thus be an implicit reflection, by the BCS model, of the contribution by larger-scale climate processes to bottom-up driven changes.

The observation of apparent regime-like changes happening more often in the smaller-scale models provides a potential explanation for apparent differences in North Pacific salmon stock production. For BC salmon two major shifts appear to have occurred in biomass trends from 1985 to the present: a broad decline across all salmon species and an even more acute decline in sockeye, coho and chinook (Figures 3.19 to 3.23). At the scale of the Northeast Pacific, however, these declines are dampened (coho, chinook and sockeye) or reversed: as seen in the trends for pink and chum salmon. Indeed, at the scale of the Northeast Pacific, there has been a steadily *increasing* biomass trend for pink and chum. Thus, in general, BC salmon biomasses at present are much lower than averages since 1950, whereas for the whole Northeast Pacific salmon biomasses are similar or even higher than averages dating to 1950. BC sockeye and pink biomass responses to regimes may be confounded by inhabiting different scale ecosystems at different times in

their life histories. Beamish *et al.* 2004 reported distinct and significant shifts in the productivity of sockeye from the Fraser River that are related to regimes.

The suggestion that the BCS PPA may reflect climate indices derived from both similar and larger areas does challenge the linkage, in section 4.3.2 to upwelling processes alone. However, if the longer-scale component of the BCS PPA is reflecting larger-scale climate changes it is not from any index used here. In Figure 4.23, the long term wave component of the NEPac PPA is different in both length and phase from the BCS PPA. Thus the changes in the longer-time scale component of the BCS PPA do not appear to be derived from indices reflected in the longer-time scale component of the NEPac PPA. This may simply reflect the manner in which larger-scale and longer-term climate changes are filtered into smaller ecosystems through both physical processes, *e.g.*, upwelling, and biological processes, *e.g.*, survival and recruitment. This type of dynamic was explored by Field *et al.* (2006) who examined how bottom-up and top-down forcing in the California Current ecosystem may have responded to changes in climate indices derived from both similar and larger area scales. Field *et al.* (2006) found the most satisfactory fit of modelled California Current biomasses to reference time series resulted from trophic dynamics driven by the PDO-like changes. They also found that almost as satisfactory fits could be derived from differing combinations of effects derived from the PDO, southern transport of water, and Oregon coho survival.

Interestingly, Field *et al.* (2006) observed that the manner in which bottom-up type climate forcing impacted the model was usually manifested through a relatively small number of the trophic linkages in the model. The process of fitting predicted to reference data at all three model scales here mirrored that observation. Remember from section 2.6.1. that to help in the estimation of vulnerabilities, Ecosim has a routine to examine how the sum of squared differences (SSD) between the modelled and reference data responds to changes in the vulnerability setting for each trophic link (Christensen *et al.* (2005). Regardless of scale, changes to the SSD of all three models were impacted by the vulnerability settings in about 15 of the trophic links, usually associated with interactions of herring, miscellaneous small pelagic fishes, euphausiids, and carnivorous zooplankton

(and occasionally trophic linkages from a predator in which the biomass trajectory was markedly different from other species with reference data, e.g., seals in the SoG and BCS models).

The tendency of fishes and zooplankton near trophic level three to be crucial players in bottom-up forcing, regardless of model scale seems rather like what are also termed 'wasp-waist' ecosystems. The name is derived from the tendency of many oceanic ecosystems to have trophic dynamics dominated by a small number of clupeid species at trophic level three (Cury *et al.* 2000). The wasp-waist imagery is evoked by the number of species at each trophic level: a diversity of primary and secondary producers, relatively few species at trophic level three, and great diversity again at trophic levels above three. Thus, both bottom-up and top-down trophic dynamics may be regulated through a limited number of species at trophic level three. Bakun (2006) points out that the wasp-waist species also tend to be the lowest non-planktonic trophic level, and are thus capable of movement in response to environmental cues. In terms of the models presented here such movement could be within, across, in to, or out of, the ecosystem, especially in the herring and small pelagic groups. Bakun (2006) also demonstrates that there may be flips between which species is dominant at trophic level three. In the North Pacific he suggests that herring and juvenile pollock may be playing this role. A more well-known example can be seen in Baumgartner *et al.* (1992) who showed that populations of northern anchovy (*Engraulis mordax*) and Pacific sardine (*Sardinops sagax*) have repeatedly switched periods of biomass dominance in the California Current during the last 2000 years based upon analysis of fish remains from sediment samples. However, it has been pointed out that these conclusions may be biased because stationary sampling like sediment piston corers can not detect spatial movement. Samb and Pauly (2000) note that sardinella populations off the west coast of Africa may appear to fluctuate annually at stations off the coast but, in fact, the overall population remains relatively stable when summed over the whole coast. The apparent fluctuations may, therefore, reflect movement of the 'center-of-gravity' of the fish population to other places than the sampling location.

Because herring and miscellaneous small pelagics were often key groups in changing the manner in which modelled bottom-up forcing functioned at all three model scales, wasp-waist dynamics should also be discussed. Two principals are considered as they apply to scale. First, as model scale increases, it should be less likely that wasp-waist type species would move in to, out of, or across the ecosystem boundary simply because the larger area would more likely encompass entirely any given population. Second, large-scale distribution of fishes is more likely to be delineated by food availability, whereas at regional scales predation pressure is more likely to shape distribution patterns of fishes (Hunt and McKinnell 2006).

As explained in the introduction any ecosystem model is more likely to explain variation in described species when there is less movement of the species across the ecosystem boundary. Given this and the two considerations described in the above paragraph it should be expected that of the three ecosystem models the NEPac would be more likely to show an ecosystem response to climate derived bottom-up forcing because of the large area and because, in a wasp-waist like system, that trophic mediation is done by species that stay in the model. In section 4.2.1.1. we saw that one explanation for the poor performance of the SoG model in capturing the extremes in herring biomass changes may have arisen from the fact that the SoG herring population does not spend all year in the SoG, that amount of time can vary and much of the herring biomass is exported to other BC herring populations. Thus, if herring were regulating the transfer of energy derived from bottom-up forcing to higher trophic level species in the SoG this would have to also partly be explained by energy they captured outside the SoG ecosystem, *e.g.*, off the Southwest coast of Vancouver Island.

Another possibility is a top-down interaction with a herring predator of the type described by Bakun (2006). If a prey species eats the juveniles of a predator species it may thus suppress the biomass of that predator simulating a regime shift in the populations of both those two species and those with which they interact. Another dynamic that would produce a similar outcome are cultivation-dependensation effects described by Walters and Kitchell (2001). An extremely abundant predator eating forage fishes, thus keeps in check

populations of potential competitors for juveniles of that predator species. If that predator is significantly reduced by fishing, the reduction of predation mortality upon the forage species could allow their population to expand, resulting in compensatory decreases in the survival of juveniles of the predator. Such situations could arise if the predator is fished sufficiently that it can no longer suppress the prey species biomass thus creating a feedback loop that results in increased mortality of the predator's juveniles. Candidates for such an interaction include coho and chinook salmon, though hake would seem a more likely juvenile salmon predator. Assuming that top-down dynamics are more likely to be manifested in a smaller-scale ecosystem like the SoG, and the potential wasp-waist nature of this ecosystem, it may be that the SoG PPA is not solely derived from changes in climate. It has been noted in section 4.2.1.1. that the SoG herring population is higher than ever, while the coho and chinook populations are at all time lows. Thus even small amounts of herring predation upon juvenile coho and chinook would keep their populations suppressed. Unfortunately testing for this hypothesis would be difficult given the paradox of detecting rare prey in diet composition analyses. Such dynamics would complicate the manner in which the PPA of the SoG, or any smaller-scale ecosystem model is derived and confound comparison with climate indices. Field *et al.* (2006) attempt to address this issue by accounting for both bottom-up and top-down effects in the application of climate-derived trophic dynamics.

As a final word on the manner in which bottom-up forcing is translated into biomass at higher trophic levels across different model scales may relate to the use of 'trophic spectra'. Trophic spectra are a way of representing how biomass is distributed across trophic levels and may thus serve as indicators of ecosystem function (Gascuel *et al.* 2005). Moloney *et al.* (2005) used trophic spectra to compare structural differences by trophic level (TL) of biomass, catch, and catch·biomass⁻¹ in models of the Humboldt and Benguela currents. However, whereas they were only able to compare two present-day models here we can compare three models in two states (the beginning of the model run, 1950 and the end of the simulation, 2002).

The similarity of the parameterisation of lower trophic levels (TL 2 - TL 3.0) in all three models can be seen in the similarity of biomass, catch and catch·biomass⁻¹ plots, Figures 4.24-4.26. The largest difference in the trophic spectra at lower TLs is seen in the contrast of biomasses for all three models between 1950 and 2002. In the case of the NEPac model the low TL biomasses are larger in 2002, reflecting the higher-than-average state of the PPA at the end of simulation. In the case of the BCS and SoG models the lower TL biomasses have decreased, reflecting the lower-than-average phase of the PPA.

In the SoG biomass spectra, Figure 4.24, a wasp-waist ecosystem dynamic is suggested by the high biomasses at TL 3.4, composed mostly of herring and miscellaneous small pelagics. In the two larger-scale models the biomass near TL 3.4 is more spread out suggesting that the two larger-scale systems were less likely to have trophic dynamics mediated by a wasp-waist type mechanism. Large catches of herring (Figure 4.25) dominate both SoG spectra of catch at trophic level 3.4 (4.6 t·km⁻² in 1950 and 2.1 t·km⁻² in 2002). However, in the SoG the herring catch·biomass⁻¹ decreased between 1950 and 2002 (Figure 4.26) while at TL 4.2 the catch·biomass⁻¹

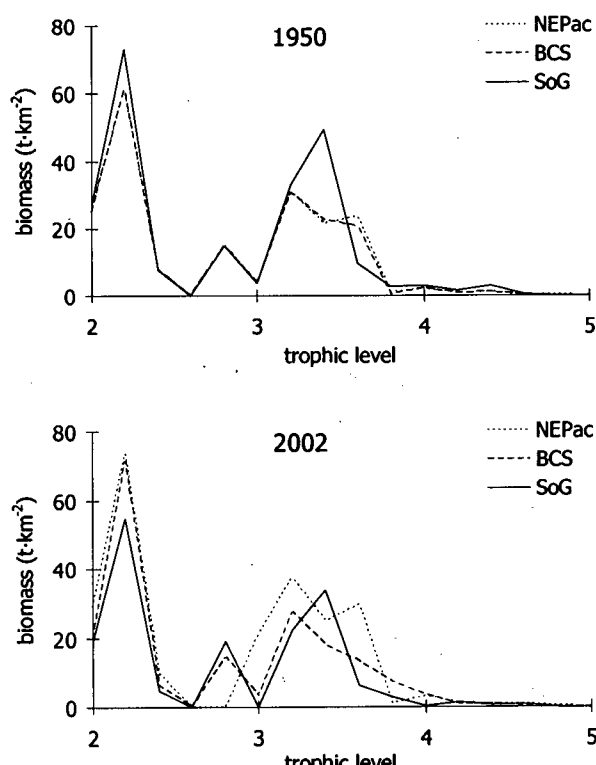


Figure 4.24: Biomass spectra of the Northeast Pacific (NEPac), BC shelf (BCS), and Strait of Georgia (SoG) models from 1950 (top graph) and 2002 (bottom graph).

increased between the two periods. Not surprisingly most of the catch at TL 4 and 4.2 is adult coho and chinook salmon. This adds further evidence to the case that a wasp-waist type prey feedback suppression of a predator could have been at first caused by too high catches of chinook and coho salmon along with other high trophic level species like lingcod, dogfish and large rockfish in the SoG.

Between 1950 and 2002 the BCS trophic spectra of biomass changes most obviously in TL 3.4 (herring) and 3.6 (miscellaneous small demersals), Figure 4.23. While BCS catches appear to be somewhat more stable across trophic levels between the two times, Figure 4.25, the catch·biomass⁻¹ tells a more interesting story. In 1950 the catch·biomass⁻¹ in the SoG was highest between TL 4.0 and 4.4 driven by large catches of the five major salmonids, lingcod and Pacific Halibut, Figure 4.26. The gap which appears in the BCS catch·biomass⁻¹ spectrum at TL 4.2 in 2002 is due almost entirely to decreases in sockeye salmon biomass and proportionally larger decreases in sockeye catch.

In comparing the 1950 and 2002 NEPac trophic spectra there are large changes in biomass (especially from TL 2.8 to 3.6, Figure 4.24) and catch (from TL 3.4 to 3.6, Figure 4.25). The biomass changes arise chiefly from the bottom-up forcing via the sustained higher than average PPA after 1977. The catch increases reflect the fisheries of the Bering Sea and Gulf of Alaska, responding to the 1977 changes. Thus, the NEPac catch·biomass⁻¹ spectrum does not change appreciably between 1950 and 2002, Figure 4.26.

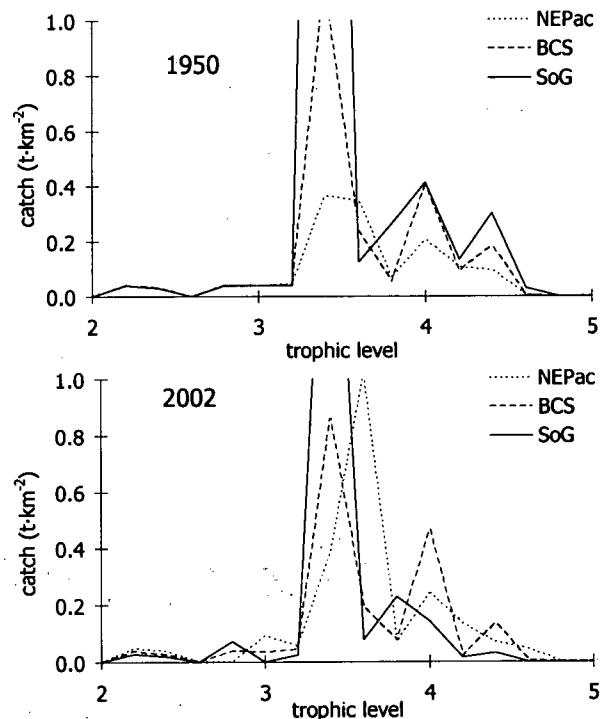


Figure 4.25: Catch spectra of the Northeast Pacific, (NEPac), BC shelf (BCS), and Strait of Georgia (SoG) models from 1950 (top graph) and 2002 (bottom graph).

The trophic spectra, thus illustrate that the SoG was more likely to be influenced by wasp-waist type dynamics, owing to the predominance of biomass in just a few species at TL 3.4. On the other hand the BCS and NEPac models were less typical of a wasp-waist configuration and, instead showed pervasive top-down influences of fisheries (declines in sockeye in the BCS model) or bottom-up forcing from climate associated increases in primary production (broad increases in biomasses for many species in the NEPac model). These observations are

consistent with the theory that top-down influences are more likely to be manifested in regional-scale ecosystems, whereas bottom-up influences will more likely be exhibited in large-scale ecosystems (Hunt and McKinnell 2006). In their comparison of the Benguela and Humboldt current ecosystems (Moloney *et al.* 2005) suggest the use of trophic spectra as an indicator for the assessment of ecosystem changes over the long-term, despite not being able to do so themselves. The usefulness of trophic spectra analysis for interpreting changes in the dynamics of the three Northeast Pacific models, over 50 years validates the advocacy of this approach by Moloney *et al.* (2005)

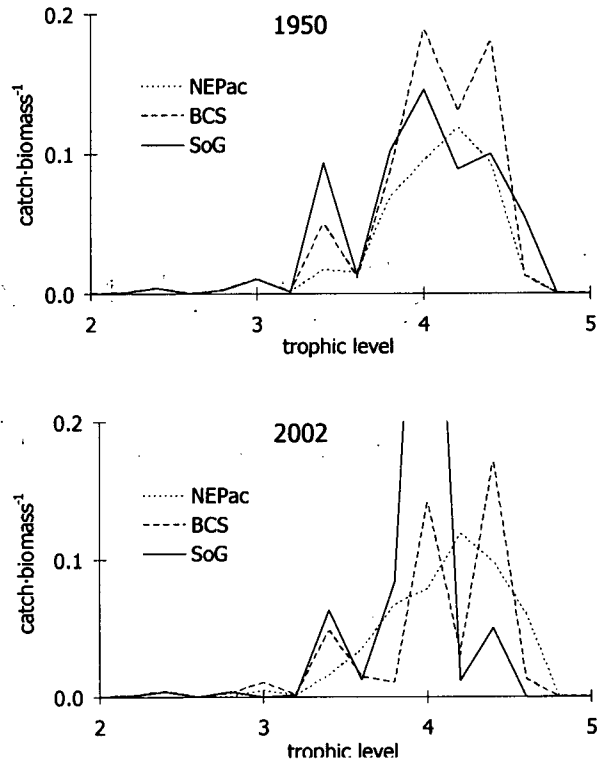


Figure 4.26: Catch-biomass⁻¹ spectra of the Northeast Pacific, (NEPac), BC shelf (BCS), and Strait of Georgia (SoG) models from 1950 (top graph) and 2002 (bottom graph).

A general axiom resulting from the primary production anomaly (PPA) time series generated by these Ecosim models is their match with climate time series of similar geographic scale, discussed in sections 4.3.1., 4.3.2. and 4.3.3. The NEPac model PPA is highly correlated with the Pacific decadal oscillation (PDO), the BCS PPA with the upwelling index at 51°N and the SoG PPA with salinity and Fraser River flows. Interestingly the highest correlation between seasonally-derived indices and PPAs tended to be those generated using data from the spring, regardless of model scale.

The similarity of climate change indices to PPAs generated by similarly scaled models reflects the internal logic defining these ecosystems. Because the NEPac ecosystem covers the GoA and BSAI region it is not surprising that the PDO, a measure of sea surface temperatures north of 20°N in the Pacific Ocean, relates well to it. Previous

research has linked the PDO to the production of salmonids (Mantua *et al.* 1997) and several species of groundfishes (Hollowed *et al.* 2001). Remember that the NEPac ecosystem was defined by the manner in which the ocean-atmospheric dynamics of the North Pacific area manifested itself as currents and upwelling / downwelling in the Northeast Pacific. Such upwelling and downwelling will have a significant effect on North Pacific sea surface temperature and is, therefore, linked to physical and chemical ecosystem changes described in the introduction.

Changes in biomasses of phytoplankton and species with time series data in the BC shelf, however, were similar to a smaller-scale climate change indicator; the upwelling index at 51°N. This finding reflects the definition of the BCS ecosystem; the coastal zone of western North America where the divergence of the upwelling California and downwelling Alaskan currents move north and south with seasonal, annual and interannual variation. The BCS model populations, even though part of larger scale NEPac metapopulations, displayed internal dynamics responding to local environmental cues which were related either to the physical mechanisms which driving upwelling, *e.g.*, wind, or those which result from it, *e.g.*, transportation or larvae and nutrients. Similar to the BCS model, changes in biomasses in the SoG model had a higher frequency than those seen in the NEPac model, reflecting the positive relationship between spatial and temporal scale (Holling 1992).

However, even in cases when bottom-up forcing was likely to be a prevalent driver in the dynamics for a model, differing rates, intensities, and directions of various species' biomasses were observed. For example, the BCS biomass trajectories of herring and Pacific cod inflected at the same times but had very different absolute changes. Whereas the biomass trajectories of halibut and orcas appear to have longer periods of inflection than other species in both models. Lastly, when the response to environmental change was tempered by known changes in fishing mortality our knowledge of trophic linkages appears to provide a realistic history of changes in the biomass of many of the fish species in the NEPac model. For instance, the biomass trajectories of NEPac Pacific Ocean perch and yellowfin sole, are opposite because of the difference in the way the

model predicts biomass of each responding to both bottom-up production and top-down mortality (fishing).

The ability of the three models to accommodate different biomass responses at different scales illustrates that such work can provide a framework for policy making. As discussed by Perry and Ommer (2003) management of human, economic, and social interactions with fished ecosystems also has a positive relationship between area and temporal scale. By identifying the scales at which certain outcomes are likely to be facilitated and the rates or magnitudes at which those changes will occur. This synthesis, therefore, represents an exciting prospect to resolve disagreements between the so-called 'bottom-up' and 'top-down' schools of research in describing populations changes in aquatic ecosystems. Ecosystem models like these, if used in a predictive mode of future dynamic simulations, could provide managers and user groups with a framework within which to devise realistic management policies for single species as well as at the ecosystem level.

References

- Acuna, E., P. Goddard and S. Kotwicki. 2003. 2002 Bottom trawl survey of the eastern Bering Sea continental shelf. AFSC Proc. Rept. 2003-01: 172 p.
- Ainley, D.G., D.W. Anderson and P.R. Kelly. 1981. Feeding ecology of marine cormorants in Southwestern North America. *Condor* 83: 120-131.
- Alverson, D.L., M.H. Freeberg, J.G. Pope and S.A. Murawski. 1994. A global assessment of fisheries bycatch and discards. FAO Fish. Tech. Pap. 339: 223 p.
- Angel, M.V. 1994. Long-term, large-scale patterns in marine pelagic ecosystems. pp. 403-439. *In* P.S. Giller, A.G. Hildrew and D.G. Raffaelli (Eds.) *Aquatic ecology: scale pattern and process*, Blackwell, Oxford.
- Angliss, R.P. and K.L. Lodge. 2002. Alaska marine mammal stock assessments, 2002. NOAA Tech. Mem. NMFS-AFSC-133: 224 pp.
- Anonymous. 1999b. Widow rockfish. DFO science stock status report A6-10: 3 pp.
- Anonymous (Ed.). 2000. Appendix A: Pacific halibut stock assessment and fishery evaluation. International Pacific Halibut Commission, Seattle. 37 pp.
- Anonymous. 2003. Groundfish biomass and recruits per spawner trends. pp. 125-131. *In* J. Boldt (Ed.) *Ecosystem Considerations for 2004, North Pacific Fisheries Management Council*, Anchorage.
- Anonymous. 2004a. Male Northern Fur Seal Counts, 1911 - 2002. NOAA National Marine Mammal Laboratory
<http://nmml.afsc.noaa.gov/AlaskaEcosystems/nfshome/pribbullnew.htm>.
- Anonymous. 2004b. Seabirds: an indicator of marine ecosystem status for coastal British Columbia, Environment Canada
http://www.ecoinfo.ec.gc.ca/env_ind/region/seabird/seabird_e.cfm.
- Arai, M. 1996. Carnivorous jellies. pp. 39-40. *In* N. Haggan (Ed.) *Mass-Balance Models of North-eastern Pacific Ecosystems*, Fisheries Centre, University of British Columbia, Vancouver, Fish. Ctr. Res. Rept. 4(1).
- Aydin, K., G.A. McFarlane, J. King and B.A. Megrey. 2003. The BASS/MODEL report on trophic models of the subarctic Pacific basin ecosystems. PICES Sci. Rept. 25: 93 p.
- Bakun, A. 2006. Wasp-waist populations and marine ecosystem dynamics: navigating the 'predator pit' topographies. *Prog. Oceanogr.* 68: 271-288.

- Bakun, A. 1973. Coastal upwelling indices, west coast of North America, 1946-71. Spec. Sci. Rep. Fish. U.S. Dep. Commer. 671: 103 pp.
- Barbeaux, S., J. Ianelli, and E. Brown. 2003. Aleutian Islands walleye pollock SAFE. Pp. 711-776. In Anonymous (Ed.) Appendix B: stock assessment and fishery evaluation report for the groundfish resources of the Gulf of Alaska, North Pacific Fishery Management Council, Anchorage.
- Baumgartner, T.R., A. Soutar, and V. Ferreira-Bartrina. 1992. Reconstruction of the history of Pacific sardine and northern anchovy populations over the past two millennia from sediments of the Santa Barbara Basin, California. Calif. Coop. Oceanic Fish. Invest. Rep. 33: 24-40.
- Beamish, R.J. Personal communication. Pacific Biological Station, 3190 Hammond Bay Road, Nanaimo, BC, Canada V9T 6N7. beamishr@pac.dfo-mpo.gc.ca.
- Beamish, R.J., M. Smith, R. Scarsbrook and C. Wood. 1976. Hake and pollock study, Strait of Georgia cruise G.B. Reed, June 16-27, 1975. Fish. Mar. Sci. Data Rec. 1: 174.
- Beamish, R.J. and D.R. Bouillon. 1993. Pacific salmon production trends in relation to climate. Can. J. Fish. Aquat. Sci. 50: 1002-1016.
- Beamish, R.J. 1995. Climate change and northern fish populations. National Research Council, Ottawa. 739 pp.
- Beamish, R.J., J.T. Schnute, A.J. Cass, C.M. Neville, and R.M. Sweeting. 2004. The influence of climate on the stock and recruitment of pink and sockeye salmon from the Fraser River, British Columbia, Canada. Trans. Am. Fish. Soc. 133: 1396-1412.
- Beamish, R.J., G.A. McFarlane, C.M. Neville and I. Pearsall. 2001. Changes in the Strait of Georgia ECOPATH model needed to balance the abrupt increases in productivity that occurred in 2000. PICES Sci. Rept. 17: 5-9.
- Beamish, R.J., C.M. Neville and A.J. Cass. 1997. Production of Fraser River sockeye salmon (*Oncorhynchus nerka*) in relation to decadal-scale changes in the climate and the ocean. Can. J. Fish. Aquat. Sci. 54: 543-554.
- Beamish, R.J., D.J. Noakes, G.A. McFarlane, W. Pinnix, R.M. Sweeting and J. King. 2000. Trends in coho marine survival in relation to the regime concept. Fish. Oceanogr. 9: 114-119.
- Beamish, R.J., B. Riddell, C.M. Neville, B.L. Thomson and Z. Zhang. 1995. Declines in chinook salmon catches in the Strait of Georgia in relation to shifts in the marine environment. Fish. Oceanogr. 4: 243-256.

- Bearman, G. (Ed.). 1989. Ocean circulation. The Open University and Pergamon Press, Milton and Oxford. 238 pp.
- Beisinger, S.R. 1995. Population trends of the marbled murrelet projected from demographic analyses. USDA Forest Service Gen. Tech. Rep. PSW-152: 385-393.
- Beattie, A. 2001. A new model for evaluating the optimal size, placement, and configuration of marine protected areas. M.Sc., University of British Columbia, Vancouver. 159 pp.
- Benson, A.J., G.A. McFarlane, S.E. Allen and J.F. Dower. 2002. Changes in Pacific hake (*Merluccius productus*) migration patterns and juvenile growth related to the 1989 regime shift. Can. J. Fish. Aquat. Sci. 59: 1969-1979.
- Benson, A. and A.W. Trites. 2002. Ecological effects of regime shifts in the Bering Sea and eastern North Pacific. Fish and Fisheries 3: 95-113.
- Bertram, D.F., D.L. Mackas and S.M. McKinnell. 2001. The seasonal cycle revisited: interannual variation and ecosystem consequences. Prog. Oceanogr. 49: 283-307.
- Bonfil, R. 1997. B.C. Groundfish Research Project, 4th and 5th quarterly reports (Jun.-Dec., 1997) October, 1997. University of British Columbia Fisheries Centre, Vancouver. 23 pp.
- Botsford, L.W. and C.A. Lawrence. 2002. Patterns of co-variability among California Current chinook salmon, coho salmon, Dungeness crab, and physical oceanographic conditions. Prog. Oceanogr. 53: 283-305.
- Boutillier, J.A., T.H. Butler, H. Bond, I. Winther and A. Phillips. 1998. Assessment of the area A crab (*Cancer magister*) fishery in British Columbia. CSAS Res. Doc. 98/86: 39 p.
- Brett, J.R. and J.M. Blackburn. 1978. Metabolic rate and energy expenditure of the spiny dogfish, *Squalus acanthias*. J. Fish. Res. Bd. Can. 35:816-821.
- Brodeur, R.D. and P. Livingston. 1988. Food habits and diet overlap of various eastern Bering Sea fishes. NOAA Tech. Mem. NWC 127: 78 p.
- Bundy, A., G.R. Lilly and P.A. Shelton. 2000. A mass balance model of the Newfoundland-Labrador shelf. Can. Tech. Rep. Fish. Aquat. Sci. 2310: 157 p.
- Burd, B.J. and R.O. Brinkhurst. 1987. Macrobenthic infauna from Hecate Strait, British Columbia. Can. Tech. Rep. Hydrogr. Ocean Sci. 88: 125 p.

- Burger, A.E. 2001. Marbled murrelets in the new millennium: a review of the biology, habitat associations, and management of this threatened species in British Columbia. Alan Burger Consulting, Victoria. 192 pp.
- Burger, A.E. 1995. Marine distribution, abundance, and habitats of marbled murrelets in British Columbia. USDA Forest Service Gen. Tech. Rep. PSW-152: 295-312.
- Burgner, R.L. 1991. Life history of sockeye salmon (*Oncorhynchus nerka*). pp. 1-118. In C. Groot and L. Margolis (Ed.) Pacific salmon life histories, University of British Columbia Press, Vancouver.
- Burkett, E.E. 1995. Marbled murrelet food habits and prey ecology. pp. 223-246. In J.F. Piatt (Ed.) Ecology and conservation of the marbled murrelet, USDA Forest Service Gen. Tech. Rep. PSW-152.
- Carter, H.R., M.L.C. McAllister and M.E. Isleib. 1995. Mortality of marbled murrelets in gill nets in North America. pp. 271-283. In C.J. Ralph, G.L.J. Hunt, M.G. Raphael and J.F. Piatt (Ed.) Ecology and conservation of the marbled murrelet, USDA Forest Service Gen. Tech. Rep. PSW-152.
- Casillas, E., L. Crockett, Y. deReynier, J. Glock, M. Helvey, B. Meyer, C. Schmitt, M. Yoklavich, A. Bailey, B. Chao, B. Johnson and Y. Pepperell. 1998. Essential fish habitat west coast groundfish appendix, National Marine Fisheries Service.
- Cass, A.J., J.R. Selsby and L.J. Richards. 1986. Lingcod maturity cruise off southwest Vancouver Island and Queen Charlotte Sound, R/V G.B. Reed, August 20 - September 5, 1985. Can. Data Rept. Fish. Aquat. Sci. 594: 58 p.
- Chavez, F.P., J. Ryan, S.E. Lluch-Cota and M. Niquen C. 2003. From anchovies to sardines and back: multidecadal change in the Pacific Ocean. Science 299: 217-221.
- Chen, D., M.A. Cane, A. Kaplan, S.E. Zebiak and D. Huang. 2004. Predictability of El Niño over the past 148 years. Nature 428: 733-736.
- Christensen, V. Personal communication. University of British Columbia Fisheries Centre, 2202 Main Mall, Vancouver, B.C., Canada, V6T 1Z4.
- Christensen, V. and C.J. Walters. 2004. Ecopath with Ecosim: methods, capabilities and limitations. Ecol. Model 172: 109-139.
- Christensen, V., C.J. Walters and D. Pauly. 2005. Ecopath with ecosim: a user's guide. University of British Columbia, Fisheries Centre, Vancouver. 154 pp.
- Christensen, V., C.J. Walters, and D. Pauly. 2002. Ecopath with Ecosim Version 5, Help system. Univ. of British Columbia, Fisheries Centre, Vancouver, Canada.

- Clark, W.G. and S.R. Hare. 2002. Effects of climate and stock size on recruitment and growth of Pacific halibut. *N. Am. J. Fish. Mang.* 22: 852-862.
- Clark, W.G. and S.R. Hare. 2001a. Assessment of the Pacific halibut stock at the end of 2001. pp. 121-196 *International Pacific Halibut Commission Report of Assessment and Research Activities, 2001.*
- Clark, W.G. and S.R. Hare. 2001b. Effects of climate and stock size on recruitment and Growth of Pacific halibut. *N. Amer. J. Fish. Manage.* 22: 852-862.
- Clark, W.G., S.R. Hare, A.M. Parma, P.J. Sullivan and R.J. Trumble. 1999. Decadal changes in growth and recruitment of Pacific halibut (*Hippoglossus stenolepis*). *Can. J. Fish. Aquat. Sci.* 56: 242-252.
- Clemens, W.A. and G.V. Wilby. 1961. Fishes of the Pacific Coast of Canada. *Bull. Fish. Res. Board. Can.* 68: 443 p.
- Cleveland, W.S. 1979. Robust locally weighted regression and smoothing scatterplots. *J. Amer. Stat. Assn.* 74: 829-836.
- Cortes, E. 1999. Standardized diet compositions and trophic levels of sharks. *ICES J. Mar. Sci.* 56: 707-717.
- Cosgrove, J.A. 2005. The first specimens of Humboldt squid in British Columbia. *PICES Press* 13: 30-31.
- Courtney, D., D.M. Clausen, J. Heifetz, D. Hanselman and J.T. Fujioka. 2003. Gulf of Alaska northern rockfish. pp. 481-530. *In* Anonymous (*Ed.*) Appendix B: stock assessment and fishery evaluation report for the groundfish resources of the Gulf of Alaska, North Pacific Fishery Management Council, Anchorage.
- Cox, S.P., T.E. Essington, J.F. Kitchell, S.J.D. Martell, C. Walters, C. Boggs and I. Kaplan. 2002a. Reconstructing ecosystem dynamics in the central Pacific Ocean, 1952-1998. II. A preliminary assessment of the trophic impacts of fishing and effects on tuna dynamics. *Can. J. Fish. Aquat. Sci.* 59: 1736-1747.
- Cox, S.P., S.J.D. Martell, C.J. Walters, T.E. Essington, J.F. Kitchell, C. Boggs and I. Kaplan. 2002b. Reconstructing ecosystem dynamics in the central Pacific Ocean, 1952-1998. I. Estimating population biomass and recruitment of tunas and billfishes. *Can. J. Fish. Aquat. Sci.* 59: 1724-1735.
- Cury, P., A. Bakun, R.J.M. Crawford, A. Jarre, R.A. Quiñones, L.J. Shannon, and H.M. Verheye. 2000. Small pelagics in upwelling systems: patterns of interaction and structural changes in "wasp-waist" ecosystems. *ICES J. Mar. Sci.* 57: 603-618.

- Denman, K.L. 1994. Scale determining biological-physical interactions in oceanic food webs. pp. 377-402. In P.S. Giller, A.G. Hildrew and D.G. Raffaelli (*Ed.*) Aquatic ecology: scale patterns and process, Blackwell, Oxford.
- Davenne, E. and D. Masson. 2001. Water properties in the Straits of Georgia and Juan de Fuca. Available from the Department of Fisheries and Oceans Institute of Ocean Sciences website at: www-sci.pac.dfo-mpo.gc.ca/osap/projects/straitofgeorgia/JdFG_e.pdf
- DFO. 1999a. Rock sole Queen Charlotte Sound (areas 5A/B) and Hecate Strait (areas 5C/D). DFO Science Stock Status Report A6-03(1999): 3 pp.
- DFO. 1999b. Lower Strait of Georgia chinook salmon. DFO Science Stock Status Report D6-12: 7 p.
- DFO. 2000. 1999 Pacific region state of the Ocean. DFO Science Ocean Status Report 1999: 38 p.
- DFO. 2001. Lingcod. DFO Science Stock Status Report A6-18: 5 p.
- DFO. 2002a. Central coast herring: DFO Science Stock Status Report B6-02. Department of Fisheries and Oceans. 3 pp.
- DFO. 2002b. Prince Rupert Herring: DFO Science Stock Status Report B6-01. Department of Fisheries and Oceans. 3 pp.
- DFO. 2002c. Queen Charlotte Islands herring: DFO Science Stock Status Report B6-03. Department of Fisheries and Oceans. 4 pp.
- DFO. 2002d. Strait of Georgia herring: DFO Science Stock Status Report B6-05. Department of Fisheries and Oceans. 4 pp.
- DFO. 2002e. West Coast Vancouver Island herring: DFO Science Stock Status Report B6-04. Department of Fisheries and Oceans. 4 pp.
- DFO. 2002f. Coho Salmon in Georgia Basin. DFO Science Stock Status Report D6-07: 6p.
- DFO. 2003. Data from the Department of Fisheries and Oceans Pacific Region BC Lighthouses Web Page:
www-sci.pac.dfo-mpo.gc.ca/osap/data/SearchTools/Searchlighthouse_e.htm.
- DFO. 2005a. 2004 Pacific region state of the Ocean. DFO Science Ocean Status Report 2004: 58 p.

- DFO. 2005b. Strait of Georgia lingcod (*Ophiodon elongatus*) assessment and advice for fishery management. DFO Can. Sci. Advis. Sec. Sci. Advis. Rep. 2005/042: 6 p.
- DFO. 2006. Commercial Catch Statistics, Summary Commercial Statistics (1996-2005). Data available on the internet at http://www-sci.pac.dfo-mpo.gc.ca/sa/Commercial/default_e.htm.
- Dorn, M., M.W. Saunders, C.D. Wilson, M. Guttormsen, K. Cooke, R. Kieser and M. Wilkins. 1999. Status of the coastal Pacific hake / whiting stock in U.S. and Canada in 1998. CSAS Res. Doc. 99/90: 101 p.
- Dorn, M., S. Barbeaux, M. Guttormsen, B. Megrey, A. Hollowed, M. Wilkins and K. Spalinger. 2003. Assessment of walleye pollock in the Gulf of Alaska. pp. 33-148. In Anonymous (Ed.) Appendix B: stock assessment and fishery evaluation report for the groundfish resources of the Gulf of Alaska, North Pacific Fisheries Management Council, Anchorage.
- Dragoo, D.E., G.V. Byrd and D.B. Irons (Ed.). 2001. Breeding status, population trends and diets of seabirds in Alaska, 2000. U.S. Fish and Wildl. Serv. Report AMNWR 01/07. 77 pp.
- Dunning, J.B. 1993. CRC handbook of avian body masses. CRC Press Inc., Boca Raton. 371 pp.
- Ebbesmeyer, C.C., D.R. Cayan, D.R. McLain, F.H. Nichols, D.H. Peterson and K.T. Redmond. 1991. 1976 step in the Pacific climate: forty environmental changes between 1968-1975 and 1977-1984. pp. 115-126. In J.L. Betancourt and V.L. Tharp (Ed.) Proceedings of the seventh annual PACLIM workshop, April 1970, California Department of Water Resources. Interagency Ecological Studies Program Tech. Rep. 26.
- Eggers, D.M., J. Irvine, M. Fukuwaka and V. Karpenko. 2003. Catch trends and status of north Pacific salmon. NPAFC Doc. 723: 34 p.
- Environment Canada. 2005. Archived Hydrometric Data. www.wsc.ec.gc.ca/hydat/H2O/.
- Fargo, J. and P.J. Starr. 2001. Turbot stock assessment for 2001 and recommendations for management in 2002. CSAS Res. Doc. 2001/150: 70 p.
- Field, J.C., R.C. Francis and K. Aydin. 2006. Top-down modeling and bottom-up dynamics: Linking a fisheries-based ecosystem model with climate hypotheses in the Northern California Current. Prog. Oceanogr. 68: 238-270.

- Fitzgerald, S., K.J. Kuletz, M. Perez, K. Rivera, D.E. Dragoo and R. Suryan. 2003. Seabirds. pp. 206-239. *In* J. Boldt (Ed.) Ecosystem Considerations for 2004, North Pacific Fishery Management Council, Anchorage.
- Fleischer, G.W., K.D. Cooke, P.H. Ressler, R.E. Thomas, S.K. de Blois, L.C. Hufnagle, A.R. Kronlund, J.A. Holmes and C.D. Wilson. 2005. The 2003 integrated acoustic and trawl survey of Pacific hake, *Merluccius productus*, in U.S. and Canadian waters off the Pacific coast. NOAA Tech. Mem. NMFS-NWFSC-65: 45.
- Ford, J.K.B., G.M. Ellis and K.C. Balcomb. 1994. Killer Whales: The Natural History and Genealogy of *Orcinus orca* in British Columbia and Washington State. 2nd edition. University of British Columbia Press, University of Washington Press, Vancouver BC, Seattle WA. 104 pp.
- Forney, K., J. Barlow, M.M. Muto, M. Lowry, J. Baker, G. Cameron, J. Mobley, C. Stinchcomb and J.V. Carretta. 2000. U.S. Pacific Marine Mammal Stock Assessments: 2000. NOAA Tech. Mem. 300: 281 p.
- Francis, R.C., S.R. Hare, A.B. Hollowed and W.S. Wooster. 1998. Effects of interdecadal climate variability on the oceanic ecosystems of the NE Pacific. *Fish. Oceanogr.* 7: 1-21.
- Froese, R. and D. Pauly. 2004. FishBase. World Wide Web electronic publication, www.fishbase.org, version (05/2004).
- Fulton, J.M., N. Arai and J.C. Mason. 1982. Euphausiids, coelenterates, ctenophores and other zooplankton from the Canadian Pacific coast ichthyoplankton survey, 1980. *Can. Tech. Rep. Fish. Aquat. Sci.* 1125: 75 p.
- Gaichas, S. and J. Boldt. 2003. Time trends in bycatch of prohibited species. pp. 251. *In* J. Boldt (Ed.) Ecosystem Considerations for 2004, North Pacific Fisheries Management Council, Anchorage.
- Gascuel, D., Y-M. Bozec, E. Chassot, A. Colomb, and M. Laurans. 2005. The trophic spectrum: theory and application as an ecosystem indicator. *ICES J. Mar. Sci.* 62: 443-452.
- Gjosaeter, J. and K. Kawaguchi. 1980. A review of the World resources of mesopelagic fish. *FAO Fish. Tech. Pap.* 151 pp.
- Goodwin, B.J. and L. Fahrig. 1998. Spatial scaling and animal population dynamics. pp. 193-206. *In* D.L. Peterson and V.T. Parker (Ed.) *Ecological scale: theory and applications*, Columbia University Press, New York.

- Gregg, E.J., L. Nichol, J.K.B. Ford, G.M. Ellis and A.W. Trites. 2000. Migration and population structure of northeastern Pacific whales off coastal British Columbia: an analysis of commercial whaling records from 1908-1967.
- Groot, C. and L. Margolis. 1991. Pacific salmon life histories. University of British Columbia Press, Vancouver. 564 pp.
- Gu  nette, S. 1996. Macrobenthos. pp. 65-67. *In* N. Haggan (Ed.) Mass balance models of northeast Pacific ecosystems, Fisheries Centre, University of British Columbia, Vancouver, Fish. Ctr. Res. Rept. 4(1).
- Haist, V., R. Hilborn and M. Wyeth. 2001. Sablefish stock assessment for 2001 and advice to managers for 2002. CSAS Res. Doc. 2001/135: 39 p.
- Hall, A. Personal Communication. Fisheries Centre, Aquatic Ecosystems Research Laboratory (AERL), 2202 Main Mall, The University of British Columbia, Vancouver, BC, Canada V6T 1Z4.
- Hanselman, D., J. Heifetz, J.T. Fujioka and J.N. Ianelli. 2003. Gulf of Alaska Pacific Ocean perch. pp. 429-480. *In* Anonymous (Ed.) Appendix B: stock assessment and fishery evaluation report for the groundfish resources of the Gulf of Alaska, North Pacific Fisheries Management Council, Anchorage.
- Hansson, L.J. 1997. Effect of temperature on growth rate of *Aurelia aurita* (Cnidaria, Scyphozoa) from Gullmarsfjorden, Sweden. Mar. Ecol. Prog. Ser. 161: 145-153.
- Hare, S.R. and N.J. Mantua. 2000. Empirical evidence for North Pacific regime shifts in 1977 and 1989. Prog. Oceanogr. 47: 103-145.
- Hare, S.R. and R.C. Francis. 1994. Climate change and salmon production in the Northeast Pacific Ocean. pp. 357-372. *In* R.J. Beamish (Ed.) Climate Change and Northern Fish Populations, Can. Spec. Publ. Fish. Aquat. Sci. 121.
- Harrison, P.J., J.D. Fulton, F.J.R. Taylor and T.R. Parsons. 1983. Review of the biological oceanography of the Strait of Georgia: pelagic environment. Can. J. Fish. Aquat. Sci. 40.
- Hart, J.I. 1973. Pacific fishes of Canada. Bull. Fis. Res. Board Can. 180: 740.
- Harvey, C.J., S.P. Cox, T.E. Essington, S. Hansson and J.F. Kitchell. 2003. An ecosystem model of food web and fisheries interactions in the Baltic Sea. ICES J. Mar. Sci. 60: 939-950.
- Hay, D., B. McCarter, K. Daniel and T. Therriault. 2005. Identifying and separating impacts of climate change and seal predation on the distribution and abundance of

herring in the Strait of Georgia. Proceedings of the 2005 Puget Sound Georgia Basin Research Conference, Puget Sound Action Team, Seattle WA.

- Healey, M.C. 1991. Life history of chinook salmon (*Oncorhynchus tshawytscha*). pp. 311-393. In C. Groot and L. Margolis (Ed.) Pacific salmon life histories, University of British Columbia Press, Vancouver.
- Heard, W.R. 1991. Life history of pink salmon (*Oncorhynchus gorbuscha*). pp. 119-230. In C. Groot and L. Margolis (Ed.) Pacific salmon life histories, University of British Columbia Press, Vancouver.
- Helser, T.E., R.D. Methot and G.W. Fleischer. 2004. Stock assessment of Pacific hake (whiting) in U.S. and Canadian waters in 2003. Pacific Fishery Management Council, Portland: 95 p.
- Heymans, J.J. 2001. The Gulf of Maine, 1977-1986. pp. 128-150. In D. Pauly (Ed.) Fisheries impacts on North Atlantic ecosystems: models and analysis, Fish. Ctr. Res. Rept. 9(4).
- Hiatt, T. and J. Terry. 2003. Time trends in groundfish discards. pp. 250. In J. Boldt (Ed.) Ecosystem Considerations for 2004, North Pacific Fisheries Management Council, Anchorage.
- Hilborn, R., A.M. Parma and M. Maunder. 2002. Exploitation rate reference points for West Coast rockfish: are they robust and are there better alternatives? N. Am. J. Fish. Mang. 22: 365-375.
- Hilborn, R. and M. Mangel. 1997. The Ecological Detective. Princeton University Press, Princeton NJ. 315 pp.
- Hill, P.S. and D.P. DeMaster. 1998. Alaska marine mammal stock assessments 1998. National Marine Mammal Laboratory Alaska Fisheries Science Center, Seattle. 165 pp.
- Hobday, A.J. and G.W. Boehlert. 2001. The role of coastal ocean variation in spatial and temporal patterns in survival and size of coho salmon (*Oncorhynchus kisutch*). Can. J. Fish. Aquat. Sci. 58: 2021-2036.
- Holladay, B.A. and B.L. Norcross. 1995. Diet diversity as a mechanism for partitioning nursery grounds of pleuronectids. Proceedings of the International Symposium on North Pacific Flatfish. Alaska Sea Grant College Program Report 95-04, University of Fairbanks: 177-204.
- Holling, C.S. 1992. Cross-scale morphology, geometry, and dynamics of ecosystems. Ecol. Monogr. 62: 447-502.

- Hollowed, A.B. and W.S. Wooster. 1992. Variability of winter ocean conditions and strong year classes of Northeast Pacific groundfish. ICES Mar. Sci. Symp. 195: 433-444.
- Hollowed, A.B., S.R. Hare and W.S. Wooster. 2001. Pacific basin climate variability and patterns of Northeast Pacific marine fish production. Prog. Oceanogr. 49: 257-282.
- Hunt, G.L.Jr., and S.McKinnell. 2006. Interplay between top-down, bottom-up, and wasp-waist control in marine ecosystems. Prog. Oceanogr. 68: 115-124.
- Hunt, G.L.Jr., H. Kato and S.M. McKinnell. 2000. Predation by marine birds and mammals in the subarctic north Pacific Ocean. PICES Sci. Rept. 14: 165.
- Hunt, S.L., T.J. Mulligan and K. Komori. 1999. Oceanic feeding habits of chinook salmon, *Oncorhynchus tshawytscha*, off northern California. Fish. Bull. 97: 717-721.
- Ianelli, J.N., S. Barbeaux, G. Walters and N. Williamson. 2003. Eastern Bering Sea walleye pollock stock assessment. pp. 39-126. In Anonymous (Ed.) Appendix A: Stock assessment and fishery evaluation report for the groundfish resources of the Bering Sea / Aleutian Islands regions, North Pacific Fisheries Management Council, Anchorage.
- Iguchi, N. and T. Ikeda. 1999. Production, metabolism and P:B ratio of *Euphausia pacifica* (Crustacea: Euphausiacea) in Toyama Bay, southern Japan Sea. Plankton Biol. Ecol. 46: 68-74.
- Innes, S., D.M. Lavigne, W.M. Earle and K.M. Kovacs. 1987. Feeding rates of seals and whales. J. Animal Ecol. 56: 115-130.
- IPHC. 1998. The Pacific halibut: biology, fishery, and management. Int. Pac. Hal. Comm. Tech. Rep. 40: 64 p.
- Jagiello, T. and A. Sinclair. 2002. Proceedings of the joint Canada - USA review group on the stock assessment of coastal Pacific hake / whiting stock off the west coast of North America February 20 - 22, 2002. CSAS Proc. Ser. 2002/002: 16 p.
- Jones, B.C. and G.H. Geen. 1977. Food and Feeding of Spiny Dogfish (*Squalus acanthias*) in British Columbia waters. J. Fish. Res. Board Can. 34: 2067-2078.
- Jones, I.L. and F.M. Hunter. 2002. Annual adult survival of least auklets (Aves, Alcidae) varies with large-scale climatic conditions of the north Pacific Ocean. Oecologia 133: 38-44.
- Jørgensen, L.A., S.E. Jørgensen and S.N. Nielsen. 2000. Ecotox, CD-ROM. Elsevier Science B.V., Amsterdam.

- Jurado-Molina, J. and P. Livingston. 2002. Climate-forcing effects on trophically linked groundfish populations: implications for fisheries management. *Can. J. Fish. Aquat. Sci.* 59: 1941–1951.
- Jurk, H. and A. Trites. 2000. Experimental attempts to reduce predation by harbor seals on out-migrating juvenile salmonids. *Trans. Am. Fish. Soc.* 129: 1360–1366.
- Kaeriyama, M., M. Nakamura, M. Yamaguchi, H. Ueda, G. Anma, S. Tagaki, K. Aydin, R.V. Walker and K.W. Myers. 2000. Feeding ecology of sockeye and pink salmon in the Gulf of Alaska. *N. Pac. Anadr. Fish. Comm. Bull.* 2: 55–63.
- Kieser, R. 1983. Hydroacoustic biomass estimates of bathypelagic groundfish in Georgia Strait, January, February, and April, 1981. *Can. Manuscr. Rep. Fish. Aquat. Sci.* 1715: 88 p.
- King, J.R. 2005. Report of the Study Group on Fisheries and Ecosystem Responses to Recent Regime Shifts. North Pacific Marine Science Organization (PICES) Scientific Report No. 28: 162p.
- King, J.R., V.V. Ivanov, V. Kurashov, R.J. Beamish and G.A. McFarlane. 1998. General circulation of the atmosphere over the North Pacific and its relationship to the Aleutian Low. *NPAFC Doc* 318: 18 p.
- King, J.R., G.A. McFarlane and R.J. Beamish. 2000. Decadal-scale patterns in the relative year class success of sablefish (*Anoplopoma fimbria*). *Fish. Oceanogr.* 9: 62–70.
- Kronlund, A.R., M. Wyeth and R. Hilborn. 2002. Review of survey, commercial fishery and tagging data for sablefish (*Anoplopoma fimbria*) in British Columbia (supplement to the November 2001 sablefish stock assessment). *CSAS Res. Doc.* 2002/074: 109 p.
- Larson, R.L. 1986. Seasonal changes in the standing stocks, growth rates and production rates of gelatinous predators in Saanich Inlet, British Columbia. *Mar. Ecol. Prog. Ser.* 33: 89–98.
- LeBrasseur, R.J. 1966. Stomach contents of salmon and steelhead trout in the Northeast Pacific Ocean. *J. Fish. Res. Board Can.* 22: 85–100.
- Levin, S.A. 1992. The Problem of pattern and scale in ecology. *Ecol.* 73:1943–1967.
- Li, M., A. Gargett and K.L. Denman. 2000. What determines seasonal and interannual variability of phytoplankton and zooplankton in strongly estuarine systems? Application to the semi-enclosed estuary of Strait of Georgia and Juan de Fuca Strait. *Estuarine, Coastal and Shelf Science* 50: 467–488.

- Longhurst, A. 1995. Seasonal cycles of pelagic production and consumption. *Prog. Oceanogr.* 36: 77-167.
- Love, M. 1996. Probably more than you want to know about the fishes of the Pacific coast. Really Big Press, Santa Barbara. 381 pp.
- Lowe, S.A. and R. Lauth. 2003. Assessment of Gulf of Alaska Atka mackerel. pp. 699-718. *In* Anonymous (Ed.) Appendix B: stock assessment and fishery evaluation report for the groundfish resources of the Gulf of Alaska, North Pacific Fishery Management Council, Anchorage.
- Lowe, S.A., J.N. Ianelli, H.H. Zenger and R. Lauth. 2003. Stock assessment of Aleutian Islands Atka mackerel. pp. 711-776. *In* Anonymous (Ed.) Appendix A: stock assessment and fishery evaluation report for the groundfish resources of the Bering Sea / Aleutian Islands regions, North Pacific Fishery Management Council, Anchorage.
- Mackas, D.L., R.E. Thomson and M. Galbraith. 2001. Changes in the zooplankton community of the British Columbia continental margin, 1985-1999, and their covariation with oceanographic conditions. *Can. J. Fish. Aquat. Sci.* 58: 685-702.
- Mackas, D.L. 1991. Seasonal cycle of zooplankton off Southwestern British Columbia, 1979-1980. *Can. J. Fish. Aquat. Sci.* 49: 903-921.
- Mantua, N.J. 1999. The Pacific Decadal Oscillation. A brief overview for non-specialists. Available via the internet at <http://tao.atmos.washington.edu/pdo/>.
- Mantua, N.J., S.R. Hare, Y. Zhang, J.M. Wallace and R.C. Francis. 1997. A Pacific interdecadal climate oscillation with impacts on salmon production. *Bull. Am. Meteorol. Soc.* 78: 1069-1079.
- Martell, S.J.D. 1999. Reconstructing lingcod biomass in Georgia Strait and the effect of marine reserves on lingcod populations in Howe Sound. M.Sc., University of British Columbia, Vancouver. 89 pp.
- Martell, S., J. Boutillier, H. Nguyen and C. Walters. 2000. Reconstructing the offshore *Pandalus jordani* trawl fishery off the west coast of Vancouver Island and simulating alternative management policies. CSAS Res. Doc. 2000(149): 38 pp.
- Martell, S., C. Walters, A. Beattie, T. Nayar and R. Briese. 2001. Simulating historical changes in the Strait of Georgia ecosystem using ECOPATH and ECOSIM. *PICES Sci. Rept.* 17: 9-16.
- Martell, S.J.D., A.I. Beattie, C.J. Walters, T. Nayar and R. Briese. 2002. Simulating fisheries management strategies in the Strait of Georgia ecosystem using Ecopath with Ecosim. pp. 16-23. *In* K. Cochran (Ed.) The use of ecosystem models to

- investigate multispecies management strategies for capture fisheries, Fish. Ctr. Res. Rept. 10(2).
- Martin, G. 2005. Sea life in peril - plankton vanishing. San Francisco Chronicle July 12: A-1.
- Mason, J.C., A.C. Phillips and O.D. Kennedy. 1984. Estimating the spawning stocks of Pacific hake (*Merluccius productus*) and walleye pollock (*Theragra chalcogramma*) in the Strait of Georgia, B.C. from their released egg production. Can. Tech. Rep. Fish. Aquat. Sci. 1289: 51.
- Masson, D. 2002. Deep water renewal in the Strait of Georgia. Estuar. Coast. Shelf S. 54: 115-126.
- Matishov, G.G. and V.V. Denisov. 1999. Ecosystems and biological resources of Russian European seas at the turn of the 21st century. Murmansk Marine Biological Institute, Murmansk. 118 pp.
- McFarlane, G.A., J.P. King and R.J. Beamish. 2000. Have there been recent changes in climate? Ask the fish. Prog. Oceanogr. 47: 147-169.
- McFarlane, G.A. and R.J. Beamish. 1992. Climatic influence linking copepod production with strong year-classes in sablefish, *Anoplopoma fimbria*. Can. J. Fish. Aquat. Sci. 49: 743-753.
- Meuter, F.J., D.M. Ware and R.M. Peterman. 2002a. Spatial correlation patterns in coastal environmental variables and survival rates of salmon in the north-east Pacific Ocean. Fish. Oceanogr. 11: 205-218.
- Meuter, F.J., R.M. Peterman and B.J. Pyper. 2002b. Opposite effects of ocean temperature on survival rates of 120 stocks of Pacific salmon (*Oncorhynchus spp.*) in northern and southern areas. Can. J. Fish. Aquat. Sci. 59: 456-463.
- Minobe, S. and N.J. Mantua. 1999. Interdecadal modulation of interannual atmospheric and oceanic variability over the North Pacific. Prog. Oceanogr. 43: 163-192.
- Minobe, S. 2000. Spatio-temporal structure of the pentadecadal variability over the North Pacific. Prog. Oceanogr. 47: 381-408.
- Moku, M., K. Kawaguchi, H. Watanabe and A. Ohno. 2000. Feeding habits of three dominant myctophid fishes, *Diaphus theta*, *Stenobrachius leucopsarus* and *S. nannochir*, in the subarctic and transitional waters of the western North Pacific. Mar. Ecol. Prog. Ser. 207: 129-140.
- Moloney, C.L., A. Jarre, H. Arancibia, Y-M. Bozec, S. Neira, J.-P. Roux, and L.J. Shannon. 2005. Comparing the Benguela and Humboldt marine upwelling

- ecosystems with indicators derived from inter-calibrated models. ICES J. Mar. Sci. 62: 493-502.
- Moore, R.D. and I.G. McKendry. 1996. Spring snowpack anomaly patterns and winter climatic variability, British Columbia, Canada. Water Resour. Res. 32: 623-632.
- Morrison, J., M.C. Quick and M.G.G. Foreman. 2002. Climate change in the Fraser River watershed: flow and temperature projections. J. Hydrol. 263: 230-244.
- Murie, D.J., D.C. Parkin, B.G. Clapp and G.G. Krause. 1994. Observations on the distribution and activities of rockfish, *Sebastes* spp., in Saanich Inlet, British Columbia from the Pisces IV submersible. Fish. Bull. 92: 313-323.
- Nagasawa, K. 1998. Predation by salmon sharks (*Lamna ditropis*) on Pacific salmon (*Oncorhynchus* spp.) in the north Pacific Ocean. N. Pac. Anadr. Fish. Comm. Bull. 1: 419-433.
- National Audubon Society (2002). The Christmas Bird Count Historical Results [Online]. Available <http://www.audubon.org/bird/cbc> [accessed in 2004]
- Nevins, H., J.T. Harvey, M. Miller, D. Jessup, S. Lyday and J. Roletto. 2005. Report on California Seabird Mortality Event, January - May 2005. Monterey Bay National Marine Sanctuary Data Summary, June 20, 2005: 4 p.
- Nyblade, C.F. 1979. The Strait of Juan de Fuca intertidal and subtidal benthos, 2nd annual report: Spring 1977 - Winter 1978. U.S. Environmental Protection Agency, Washington. 129 pp.
- Okey, T. and D. Pauly. 1999. A trophic mass-balance model of Alaska's Prince William Sound ecosystem for the post-spill period 1994-1996, 2nd ed. Fish. Ctr. Res. Rept. 7(4): 137 pp.
- Olesiuk, P.F. 1999. An assessment of the status of harbour seals (*Phoca vitulina*) in British Columbia. CSAS Res. Doc. 99/33: 71 p.
- O'Neill, R.V.O. and A.W. King. 1998. Homage to St. Michael; or, why are there so many books on scale? pp. 3-16. In D.L. Peterson and V.T. Parker (Eds.) Ecological scale: theory and applications, Columbia University Press, New York.
- Pahl-Wostl, C. 1998. Ecosystem organization across a continuum of scales: a comparative analysis of lakes and rivers. pp. 141-170. In D.L. Peterson and V.T. Parker (Eds.) Ecological scale: theory and applications, Columbia University Press, New York.

- Palmer, M.C. 2003. Environmental controls of fish growth in the southeastern Bering Sea. pp. 133-137. *In* J. Boldt (Ed.) Ecosystem Considerations for 2004, North Pacific Fisheries Management Council, Anchorage.
- Palomares, M.L.D. and D. Pauly. 1998. Predicting the food consumption of fish populations as functions of mortality, food type, morphometrics, temperature and salinity. *Mar. Freshwat. Res.* 49: 447-453.
- Parrish, R.H., F.B. Schwing and R. Mendelssohn. 2000. Mid-latitude wind stress: the energy source for climatic shifts in the North Pacific Ocean. *Fish. Oceanogr.* 9: 224-238.
- Paul, A.J., K.O. Coyle and L. Haldorson. 1995. Mesoscale variation in spring abundance of copepod nauplii prey of larval flatfish in a southeast Alaskan bay. *Proceedings of the International Symposium on North Pacific Flatfish*. Alaska Sea Grant College Program Report 95-04, University of Fairbanks: 117-132.
- Pauly, D., A. Trites, E. Capuli and V. Christensen. 1998. Diet composition and trophic levels of marine mammals. *ICES J. Mar. Sci.* 55: 467-481.
- Pauly, D., V. Christensen and N. Haggan. 1996. Mass-balance models of north-eastern Pacific ecosystems. *Fish. Ctr. Res. Rept.* 4: 131 p.
- Pauly, D., V. Christensen, R. Froese, A. Longhurst, T. Platt, S. Sathyendranath, K. Sherman and R. Watson. 2000. Mapping fisheries onto marine ecosystems: a consensus approach for regional, oceanic and global integrations. *CM 2000/T ICES 2000 Annual Science Conference* 16 pp.
- Perry, R.I. and R.E. Ommer. 2003. Scale issues in marine ecosystems and human interactions. *Fish. Oceanogr.* 12: 513-522.
- Piatt, J.F. and J.L. Naslund. 1995. Abundance, distribution, and population status of marbled murrelets in Alaska. pp. 285-294. *In* J.F. Piatt (Ed.) *Ecology and conservation of the marbled murrelet*, USDA Forest Service Gen. Tech. Rep. PSW-152.
- Polovina, J.J. 2002. Application of Ecosim to investigate the impact of the lobster fishery on endangered monk seals in. pp. 24-25. *In* V. Christensen, G. Reck and J.L. Maclean (Eds.) *Proceedings of the INCO-DC Conference Placing Fisheries in Their Ecosystem Context*, ACP-EU Fish. Res. Rep. 12.
- Polovina, J.J., G.T. Mitchum and G.T. Evans. 1995. Decadal and basin-scale variation in mixed layer depth and the impact on biological production in the Central and North Pacific, 1960-88. *Deep-Sea Res.* 42: 1701-1716.

- Preikshot, D. 2005. Data sources and derivation of parameters for generalised northeast Pacific Ocean Ecopath with Ecosim models. In S. Gu  nette and V. Christensen (*Eds.*) Food web models and data for studying fisheries and environmental impacts on eastern Pacific ecosystems. UBC Fisheries Centre Research Report 13(1): 179-206.
- Preikshot, D. and A. Beattie. 2001. Fishing for answers: analysis of ecosystem dynamics, trophic shifts and salmonid population changes in Puget Sound, WA, 1970-1999, Fish. Ctr. Res. Rept. 9(6): 33 pp.
- Rand, P.S. and D.J. Stewart. 1997. Prey fish exploitation, salmonine production, and pelagic food web efficiency in Lake Ontario. Can. J. Fish. Aquat. Sci. 57: 318-327.
- Reynolds, J.D., N.K. Dulvy and C.M. Roberts. 2002. Exploitation and other threats to fish conservation. pp. 319-341. In P.J.B. Hart and J.D. Reynolds (*Eds.*) Handbook of fish biology and fisheries, Vol. 2, Blackwell Science Ltd.
- Rexstad, E.A. and E.K. Pikitch. 1986. Stomach contents and food consumption estimates of Pacific hake, *Merluccius productus*. Fish. Bull. 84: 947 - 956.
- Robinson, C.L.K. and D.M. Ware. 1994. Modelling pelagic fish and plankton trophodynamics off southwestern Vancouver Island, British Columbia. Can. J. Fish. Aquat. Sci. 51: 1737-1751.
- Robinson, C.L.K. and D.M. Ware. 1999. Simulated and observed response of the southwest Vancouver Island pelagic ecosystem to oceanic conditions in the 1990s. Can. J. Fish. Aquat. Sci. 56: 2433-2443.
- Rogers, D.E. 1999. Estimates of annual salmon runs from the North Pacific, 1951-1998. Fisheries Research Institute, University of Washington, Seattle: 10 pp.
- Rugh, D.J., M.M. Muto, S.E. Moore and D.P. DeMaster. 1999. Status review of the eastern north Pacific stock of gray whales. NOAA Tech. Mem. NMFS-AFSC-103: 96.
- Ryding, K.E. and J.R. Skalski. 1999. Multivariate regression relationships between ocean conditions and early marine survival of coho salmon (*Oncorhynchus kisutch*). Can. J. Fish. Aquat. Sci. 56: 2374-2384.
- Saether, B.-E. and O. Bakke. 2000. Life history variation and contribution of different demographic traits to the population growth rate in birds: a comparative approach. Ecology 81: 642-653.
- Salo, E.O. 1991. Life History of chum salmon (*Oncorhynchus keta*). pp. 231-310. In C. Groot and L. Margolis (*Eds.*) Pacific salmon life histories, University of British Columbia Press, Vancouver.

- Samb, B. and D. Pauly. 2000. On 'variability' as a sampling artefact: the case of *Sardinella* in north-western Africa. *Fish Fish.* 1:206-210.
- Sandercock, F.K. 1991. Life history of coho salmon (*Oncorhynchus kisutch*). pp. 397-445. In C. Groot and L. Margolis (Eds.) *Pacific salmon life histories*, University of British Columbia Press, Vancouver.
- Saunders, M.W. and G.A. McFarlane. 1998. Pacific hake - Strait of Georgia stock assessment for 1997 and recommended yield options for 1998. PSARC Working Paper G97.
- Schirripa, M.J. and J.J. Colbert. 2006. Interannual changes in sablefish (*Anoplopoma fimbria*) recruitment in relation to oceanographic conditions within the California Current System. *Fish. Oceanogr.* 15: 25-36.
- Schnute, J.T., R. Haigh, B.A. Krishka and P. Starr. 2001. Pacific Ocean perch assessment for the west coast of Canada in 2001. CSAS Res. Doc. 2001/138: 90 pp.
- Schweigert, J. and C. Fort. 1999. Stock assessment of British Columbia herring in 1999 and forecast of potential harvest in 2000. CSAS Res. Doc. 99/178: 99 p.
- Schweigert, J. 2003. Stock assessment of British Columbia herring in 2003 and forecast of potential harvest in 2004. CSAS Res. Doc. 2004/005: 102 p.
- Schwing, F.B., O'Farrell, J.M. Steger and K. Baltz. 1996. Coastal upwelling indices: west coast of North America 1946-1995. NOAA-TM-NMFS-SWFSC 231: 50 p.
- Schwing, F.B., T. Murphee and P.M. Green. 2002. The northern oscillation index (NOI): a new climate index for the northeast Pacific. *Prog. Oceanogr.* 53: 115-139.
- Schwing, F.B., T. Murphee and P.M. Green. 2002. The northern oscillation index (NOI): a new climate index for the northeast Pacific. *Prog. Oceanogr.* 53: 115-139.
- Schwing, F.B., O'Farrell, J.M. Steger and K. Baltz. 1996. Coastal upwelling indices: west coast of North America 1946-1995. NOAA-TM-NMFS-SWFSC 231: 50 p.
- Sea Around Us. 2006. A global database on marine fisheries and ecosystems. World Wide Web site www.seaaroundus.org. Fisheries Centre, University British Columbia, Vancouver (British Columbia, Canada). [Visited 2 Feb 2006]
- Shaw, W., G.A. McFarlane and R. Kieser. 1990. Distribution and abundance of the Pacific hake (*Merluccius productus*) spawning stocks in the Strait of Georgia, British Columbia, based on trawl and acoustic surveys in 1981 and 1988. *I.N.P.F.C. Bull.* 50: 121-134.

- Sherman, K., L.M. Alexander and B.D. Gold (Eds.). 1990. Large marine ecosystems: patterns, processes and yields. American Association for the Advancement of Science, Washington. 242 pp.
- Sigler, M.F., C.R. Lunsford, J.T. Fujioka and S.A. Lowe. 2003. Alaska sablefish assessment for 2004. pp. 223-292. *In* Anonymous (Ed.) Appendix A: stock assessment and fishery evaluation report for the groundfish resources of the Bering Sea / Aleutian Islands regions, North Pacific Fisheries Management Council, Anchorage.
- Sigler, M.F., T.L. Rutecki, D.L. Courtney, J.F. Karinen and M.-S. Yang. 2001. Young of the year sablefish abundance, growth, and diet in the Gulf of Alaska. *Alaska Fish. Res. Bull.* 8: 57-70.
- Sinclair, A., S. Martell and J. Boutillier. 2001. Assessment of Pacific cod off the west coast of Vancouver Island and in Hecate Strait, November 2001. CSAS Res. Doc. 2001/159: 60 p.
- Smith, B.D. and G.S. Jamieson. 1989. Exploitation and mortality of male Dungeness crabs (*Cancer magister*) near Tofino, British Columbia. *Can. J. Fish. Aquat. Sci.* 46: 1609-1614.
- Spencer, P.D. and J.N. Ianelli. 2003a. Northern rockfish. pp. 611-652. *In* Anonymous (Ed.) Appendix A: Stock assessment and fishery evaluation report for the groundfish resources of the Bering Sea / Aleutian Islands regions, North Pacific Fishery Management Council, Anchorage.
- Spencer, P.D. and J.N. Ianelli. 2003b. Pacific Ocean perch. pp. 563-610. *In* Anonymous (Ed.) Appendix A: Stock assessment and fishery evaluation report for the groundfish resources of the Bering Sea / Aleutian Islands regions, North Pacific Fisheries Management Council, Anchorage.
- Spencer, P.D., G. Walters and T.K. Wilderbauer. 2003. Alaska plaice. pp. 511-552. *In* Anonymous (Ed.) Appendix A: Stock assessment and fishery evaluation report for the groundfish resources of the Bering Sea / Aleutian Islands regions, North Pacific Fisheries Management Council, Anchorage.
- St.-Pierre, G. and R.J. Trumble. 2000. Diet of juvenile Pacific halibut, 1957-1961. *International Pacific Halibut Commission Tech. Rep.* 43: 16 p.
- Stocker, M., A. Mentzelopoulos, G. Bartosh, J. Hrynishyn, J. Burns and N. Fowler (Eds.). 2001. Fish Stocks of the Pacific Coast. Fisheries and Oceans Canada, Vancouver. 152 pp.

- Sturdevant, M.V. 1999. Forage fish diet overlap, 1994-1996, Restoration project 98163C final report. National Marine Fisheries Service Alaska Fisheries Science Center Auke Bay Laboratory, Juneau, AK. 107 pp.
- Sullivan, P.J., A.M. Parma and W.G. Clark. 1997. The Pacific halibut stock assessment of 1997. International Pacific Halibut Commission Sci. Rept. 79: 84 pp.
- Sydeman, W.J., M.M. Hester, J.A. Thayer, F. Gress, P. Martin and J. Buffa. 2001. Climate change, reproductive performance and diet composition of marine birds in the southern California Current system, 1969-1997. *Prog. Oceanogr.* 49: 309-329.
- Tanasichuk, R.W., D.M. Ware, W.A. Shaw and G.A. McFarlane. 1991. Variations in the diet, daily ration and feeding periodicity of Pacific hake (*Merluccius productus*) and spiny dogfish (*Squalus acanthias*) off the lower west coast of Vancouver Island. *Can. J. Fish. Aquat. Sci.* 48: 2112-2128.
- Tanasichuk, R.W. 2002. Implications of interannual variability in euphausiid population biology for fish production along the south-west coast of Vancouver Island: a synthesis. *Fish. Oceanogr.* 11: 18-30.
- Tanasichuk, R.W. 1999. Interannual variation in the availability and utilization of euphausiids as prey for Pacific hake (*Merluccius productus*) along the south west coast of Vancouver Island. *Fish. Oceanogr.* 8: 150-156.
- Tasker, M.L., C.J. Camphuysen, J. Cooper, S. Garthe, W.A. Montevecchi and S.J.M. Blaber. 2000. The impacts of fishing on marine birds. *ICES J. Mar. Sci.* 57: 531-547.
- Taylor, F.H.C. and L.W. Barner. 1976. The distribution and abundance of hake, pollock and dogfish in the Strait of Georgia in 1975 determined by digital echo-integration. *Manuscr. Rep. Ser. Fish. Res. Board Can.* 1411: 51 p.
- Thompson, G.G. and M.W. Dorn. 2003. Assessment of the Pacific Cod stock in the Eastern Bering Sea and Aleutian Islands area. pp. 127-222. *In* Anonymous (*Ed.*) Appendix A: stock assessment and fishery evaluation report for the groundfish resources of the Bering Sea / Aleutian Islands regions, North Pacific Fisheries Management Council, Anchorage.
- Thompson, G.G., H.H. Zenger and M.W. Dorn. 2003. Assessment of the Pacific cod stock in the Gulf of Alaska. pp. 149-242. *In* Anonymous (*Ed.*) Appendix B: stock assessment and fishery evaluation report for the groundfish resources of the Gulf of Alaska, North Pacific Fisheries Management Council, Anchorage.
- Thomson, B.L. 1994. Spiny dogfish. pp. 204-217. *In* M. Stocker (*Ed.*) Groundfish stock assessment for the west coast of Canada in 1993 and Recommended yield options for 1994, *Can. Tech. Rep. Fish. Aquat. Sci.* 1975.

- Thomson, R.E. 1981. Oceanography of the British Columbia Coast. Can. Spec. Publ. Fish. Aquat. Sci. 56: 291 p.
- Trenberth, K.E. and J.W. Hurrell. 1994. Decadal atmosphere-ocean variations in the Pacific. *Climate Dynamics* 9: 303-319.
- Trites, A. and D. Pauly. 1998. Estimating mean body masses of marine mammals from maximum body lengths. *Can. J. Zool.* 76: 886-896.
- Trites, A. and K. Heise. 1996. Marine mammals. pp. 51-55. *In* V. Christensen (Ed.) Mass-balance models of Northeastern Pacific ecosystems, Fish. Ctr. Res. Rpt. 4 (1).
- Trites, A. and P.A. Larkin. 1996. Changes in the abundance of Steller sea lions (*Eumetopias jubatus*) in Alaska from 1956 to 1992: how many were there? *Aquat. Mamm.* 22: 153-166.
- Trites, A., P.A. Livingstone, S. Mackinson, M. Vasconcellos, A.M. Springer and D. Pauly. 1999. Ecosystem change and the decline of marine mammals in the Bering sea: testing the ecosystem shift and commercial whaling hypothesis, Fish. Ctr. Res. Rept. 7(1). 106 pp.
- Turnock, B.J., T.K. Wilderbauer and E.S. Brown. 2003a. Gulf of Alaska flatfish. pp. 313-340. *In* Anonymous (Ed.) Appendix B: stock assessment and fishery evaluation report for the groundfish resources of the Gulf of Alaska, North Pacific Fisheries Management Council, Anchorage.
- Turnock, B.J., T.K. Wilderbuer and E.S. Brown. 2003b. Arrowtooth flounder. pp. 369-406. *In* Anonymous (Ed.) Appendix B: stock assessment and fishery evaluation report for the groundfish resources of the Gulf of Alaska, North Pacific Fishery Management Council, Anchorage.
- Urban, D.L. 2003. Spatial analysis in ecology (ENV 352): trend surface analysis and interpolation. Duke University Nicholas School of the Environment and Earth Science Landscape Ecology Laboratory. Available online at <http://www.nicholas.duke.edu/landscape/classes/env352/env352.html>.
- Vermeer, K. and S.G. Sealy. 1984. Status of the nesting seabirds of British Columbia. pp. 29-40. *In* R.W. Schrieber (Ed.) Status and conservation of the World's seabirds, International Council for Bird Preservation Tech. Publ. 2.
- Wakabayashi, K. 1986. Interspecific feeding relationships on the continental shelf of the eastern Bering Sea, with special reference to Yellowfin sole. *Int. N. Pac. Fish. Comm. Bull.* 47: 3-30.

- Walters, C., and J.F. Kitchell. 2001. Cultivation/depensation effects on juvenile survival and recruitment: implications for the theory of fishing. *Can. J. Fish. Aquat. Sci.* 58: 39-50.
- Walters, C. and J. Korman. 1999. *Salmon Stocks*. Pacific Fisheries Resource Conservation Council, Vancouver, BC. 38 pp.
- Walters, C. and F. Juanes. 1993. Recruitment limitations as a consequence of natural selection for use of restricted feeding habitats and predation risk taking by juvenile fishes. *Can. J. Fish. Aquat. Sci.* 50: 2058-2070.
- Walters, C. and S. Martell. 2004. *Fisheries ecology and management*. Princeton University Press, Princeton, NJ. 399 pp.
- Walters, C.J., S.J.D. Martell, and J. Korman. 2006. A stochastic approach to stock reduction analysis. *Can. J. Fish. Aquat. Sci.* 63: 212-223.
- Walters, C., D. Pauly, V. Christensen and J.F. Kitchell. 2000. Representing density dependent consequences of life history strategies in aquatic ecosystems: EcoSim II. *Ecosystems* 3: 70-83.
- Walters, C., D. Pauly and V. Christensen 1998. Ecospace: prediction of mesoscale spatial patterns in trophic relationships of exploited ecosystems, with emphasis on the impacts of marine protected areas. *Ecosystems* 2: 539-554.
- Ware, D.M. and G.A. McFarlane. 1989. Fisheries production domains in the Northeast Pacific Ocean. *Can. Spec. Publ. Fish. Aquat. Sci.* 108: 359-379.
- Ware, D.M. and G.A. McFarlane. 1995. Climate-induced changes in Pacific hake (*Merluccius productus*) abundance and pelagic community interactions in the Vancouver Island upwelling system. pp. 509-521. *In* R.J. Beamish (Ed.) *Climate Change and Northern Fish Populations*, *Can. Spec. Publ. Fish. Aquat. Sci.* 121.
- Ware, D.M. and J. Schweigert. 2002. Metapopulation dynamics of British Columbia herring during cool and warm climate regimes. *CSAS Res. Doc.* 2002/107. 36 pp.
- Wehle, D.H.S. 1983. The food, feeding and development of young tufted and horned puffins in Alaska. *Condor* 85: 427-442.
- Wilderbuer, T.K., A.B. Hollowed, W.J. Ingraham, P.D. Spencer, M.E. Conners, N.A. Bond and G.E. Walters. 2002. Flatfish recruitment response to decadal climatic variability and ocean conditions in the eastern Bering Sea. *Prog. Oceanogr.* 55: 235-247.
- Wilderbuer, T.K. and D. Nichol. 2003. Yellowfin sole. pp. 293-338. *In* Anonymous (Ed.) *Appendix A: Stock assessment and fishery evaluation report for the groundfish*

resources of the Bering Sea / Aleutian Islands regions, North Pacific Fisheries Management Council, Anchorage.

Wilderbuer, T.K. and G. Walters. 2003. Rock sole. pp. 409-462. *In* Anonymous (Ed.) Appendix A: stock assessment and fishery evaluation report for the groundfish resources of the Bering Sea / Aleutian Islands regions, North Pacific Fisheries Management Council, Anchorage.

Wilderbuer, T.K. and T.M. Sample. 2003. Arrowtooth flounder. pp. 367-408. *In* Anonymous (Ed.) Appendix A: stock assessment and fishery evaluation report for the groundfish resources of the Bering Sea / Aleutian Islands regions, North Pacific Fishery Management Council, Anchorage.

Willams, E.H. and T.J. Quinn. 2000a. Pacific herring, *Clupea pallasii*, recruitment in the Bering Sea and north-east Pacific Ocean, I: relationships among different populations. *Fish. Oceanogr.* 9: 285-299.

Willams, E.H. and T.J. Quinn. 2000b. Pacific herring, *Clupea pallasii*, recruitment in the Bering Sea and north-east Pacific Ocean, II: relationships to environmental variables and implications for forecasting. *Fish. Oceanogr.* 9: 300-315.

Wong, C.S., F.A. Whitney, R.J. Matear and K. Iseki. 1998. Enhancement of new production in the northeast subarctic Pacific Ocean during negative North Pacific index events. *Limnol. Oceanogr.* 43: 1418-1426.

Yang, M.S. and M.W. Nelson. 1999. Food habits of the commercially important groundfishes in the Gulf of Alaska in 1990, 1993, and 1996. NOAA Tech. Memo. AFSC 112: 187 p.

Yang, M.-S. 1993. Food habits of the important groundfishes in the Aleutian Islands in the Gulf of Alaska. NOAA Tech. Memo., NMFS-AFSC 22: 150 p.

Yin, K., P.J. Harrison and R.J. Beamish. 1997. Effects of a fluctuation in Fraser River discharge on primary production in the central Strait of Georgia, British Columbia, Canada. *Can. J. Fish. Aquat. Sci.* 54: 1015-1024.

Appendix 1

Table A.1.1: Pedigree chart of EwE basic input parameters used for groups in the SoG model. Definitions of colour codes for each parameter are given below. A quantitative description of these colour codes can be found in Christensen *et al.* (2005).

Biomass

- Estimated by Ecopath
- From other model
- Guesstimate
- Approximate or indirect method
- Sampling based, low precision
- Sampling based, high precision

P/B and Q/B

- Estimated by Ecopath
- Guesstimate
- From other model
- Empirical relationship
- Similar group/similar system
- Similar group/same system
- Same group/similar system
- Same group/same system

Diet Composition

- General knowledge of related group
- From other model
- General knowledge of group
- Qualitative diet study
- Quantitative, limited, diet study
- Quantitative, detailed, diet study

Catch

- Guesstimate
- From other model
- FAO statistics
- National statistics
- Local study, low precision/incomplete
- Local study, high precision/complete

Group	B	P/B	Q/B	Diet	Catch
arrowtooth juv.					
arrowtooth ad.					
P. cod juv.					
P. cod ad.					
P. halibut juv.					
P. halibut ad.					
sablefish juv.					
sablefish ad.					
pollock juv.					
pollock ad.					
herring juv.					
herring ad.					
birds pelag pisciv					—
birds demer pisciv					—
birds zooplanktiv					—
odontocetae					—
mysticetae					—
sea lions					—
seals					—
salmon shark					—
pelagic sharks					—
dogfish					—
rajidae / ratfish					—
pink					—
chum					—
sockeye					—
coho juv.	—	—	—	—	—
coho ad.	—	—	—	—	—
chinook juv.	—	—	—	—	—
chinook ad.	—	—	—	—	—
Pac. Ocean perch	—	—	—	—	—
northern rockfish	—	—	—	—	—
rockfish other	—	—	—	—	—
Pac. hake	—	—	—	—	—
Atka mackerel	—	—	—	—	—
lingcod	—	—	—	—	—
yellowfin sole	—	—	—	—	—
rock sole	—	—	—	—	—
plaice	—	—	—	—	—
flatfish other	—	—	—	—	—
myctophids	—	—	—	—	—
misc. small demersals	—	—	—	—	—
misc. pred. pelagics	—	—	—	—	—
misc. small pelagics	—	—	—	—	—
krill	—	—	—	—	—
carc. zooplankton	—	—	—	—	—
herb. zooplankton	—	—	—	—	—
jellies	—	—	—	—	—
large squids	—	—	—	—	—
small squids	—	—	—	—	—
shrimps	—	—	—	—	—
crabs	—	—	—	—	—
bivalves	—	—	—	—	—
echinoderms	—	—	—	—	—
other benthos	—	—	—	—	—
phytoplankton	—	—	—	—	—
macrophytes	—	—	—	—	—

Table A.1.2: Pedigree chart of EwE basic input parameters used for groups in the BCS model. Definitions of colour codes for each parameter are given below. A quantitative description of these colour codes can be found in Christensen *et al.* (2005).

Biomass

- Estimated by Ecopath
- From other model
- Guesstimate
- Approximate or indirect method
- Sampling based, low precision
- Sampling based, high precision

P/B and Q/B

- Estimated by Ecopath
- Guesstimate
- From other model
- Empirical relationship
- Similar group/similar system
- Similar group/same system
- Same group/similar system
- Same group/same system

Diet Composition

- General knowledge of related group
- From other model
- General knowledge of group
- Qualitative diet study
- Quantitative, limited, diet study
- Quantitative, detailed, diet study

Catch

- Guesstimate
- From other model
- FAO statistics
- National statistics
- Local study, low precision/incomplete
- Local study, high precision/complete

Group	B	P/B	Q/B	Diet	Catch
arrowtooth juv.					
arrowtooth ad.					
P. cod juv.					
P. cod ad.					
P. halibut juv.					
P. halibut ad.					
sablefish juv.					
sablefish ad.					
pollock juv.					
pollock ad.					
herring juv.					
herring ad.					
birds pelag pisciv					—
birds demer pisciv					—
birds zooplanktiv					—
odontocetæ					—
mysticetæ					—
sea lions					—
seals					—
salmon shark					—
pelagic sharks					—
dogfish					—
rajidae / ratfish					—
pink					—
chum					—
sockeye					—
coho juv.	—	—	—	—	—
coho ad.	—	—	—	—	—
chinook juv.	—	—	—	—	—
chinook ad.	—	—	—	—	—
Pac. Ocean perch	—	—	—	—	—
northern rockfish	—	—	—	—	—
rockfish other	—	—	—	—	—
Pac. hake	—	—	—	—	—
Atka mackerel	—	—	—	—	—
lingcod	—	—	—	—	—
yellowfin sole	—	—	—	—	—
rock sole	—	—	—	—	—
plaice	—	—	—	—	—
flatfish other	—	—	—	—	—
myctophids	—	—	—	—	—
misc. small demersals	—	—	—	—	—
misc. pred. pelagics	—	—	—	—	—
misc. small pelagics	—	—	—	—	—
krill	—	—	—	—	—
carn. zooplankton	—	—	—	—	—
herb. zooplankton	—	—	—	—	—
jellies	—	—	—	—	—
large squids	—	—	—	—	—
small squids	—	—	—	—	—
shrimps	—	—	—	—	—
crabs	—	—	—	—	—
bivalves	—	—	—	—	—
echinoderms	—	—	—	—	—
other benthos	—	—	—	—	—
phytoplankton	—	—	—	—	—
macrophytes	—	—	—	—	—

Table A.1.3: Pedigree chart of EwE basic input parameters used for groups in the NEPac model. Definitions of colour codes for each parameter are given below. A quantitative description of these colour codes can be found in Christensen *et al.* (2005).

Biomass

- Estimated by Ecopath
- From other model
- Guesstimate
- Approximate or indirect method
- Sampling based, low precision
- Sampling based, high precision

P/B and Q/B

- Estimated by Ecopath
- Guesstimate
- From other model
- Empirical relationship
- Similar group/similar system
- Similar group/same system
- Same group/similar system
- Same group/same system

Diet Composition

- General knowledge of related group
- From other model
- General knowledge of group
- Qualitative diet study
- Quantitative, limited, diet study
- Quantitative, detailed, diet study

Catch

- Guesstimate
- From other model
- FAO statistics
- National statistics
- Local study, low precision/incomplete
- Local study, high precision/complete

Group	B	P/B	Q/B	Diet	Catch
arrowtooth juv.					
arrowtooth ad.					
P. cod juv.					
P. cod ad.					
P. halibut juv.					
P. halibut ad.					
sablefish juv.					
sablefish ad.					
pollock juv.					
pollock ad.					
herring juv.					—
herring ad.					—
birds pelag pisciv					—
birds demer pisciv					—
birds zooplanktiv					—
odontocetæ					—
mysticetæ					—
sea lions					—
seals					—
salmon shark					—
pelagic sharks					—
dogfish					—
rajidae / ratfish					—
pink					—
chum					—
sockeye					—
coho juv.	—	—	—	—	—
coho ad.	—	—	—	—	—
chinook juv.	—	—	—	—	—
chinook ad.	—	—	—	—	—
Pac. Ocean perch					—
northern rockfish					—
rockfish other					—
Pac. hake					—
Atka mackerel					—
lingcod					—
yellowfin sole					—
rock sole					—
plaice					—
flatfish other					—
myctophids					—
misc. small demersals					—
misc. pred. pelagics					—
misc. small pelagics					—
krill					—
carn. zooplankton					—
herb. zooplankton					—
jellies					—
large squids					—
small squids					—
shrimps					—
crabs					—
bivalves					—
echinoderms					—
other benthos					—
phytoplankton			—	—	—
macrophytes			—	—	—

Table A.1.4: EwE basic input parameters used for multi-stanza groups in the final, mass balanced SoG, BCS, and NEPac models.

SoG	B (t·km ⁻²)	P/B (year ⁻¹)	Q/B (year ⁻¹)
Arrowtooth juv.	0.003	0.500	4.422
arrowtooth ad.	0.030	0.300	2.000
P. cod juv.	0.176	0.800	3.421
P. cod ad.	0.300	0.660	1.800
P. halibut juv.	0.001	0.500	2.550
P. halibut ad.	0.005	0.300	1.000
sablefish juv.	0.017	0.300	4.412
sablefish ad.	0.100	0.200	2.200
pollock juv.	0.087	0.800	6.715
pollock ad.	2.500	0.400	2.000
herring juv.	4.256	1.100	8.064
herring ad.	10.000	0.700	4.400
BCS			
arrowtooth juv.	0.008	0.500	4.414
arrowtooth ad.	0.070	0.300	2.000
P. cod juv.	0.176	0.800	3.421
P. cod ad.	0.300	0.660	1.800
P. halibut juv.	0.023	0.500	2.550
P. halibut ad.	0.175	0.300	1.000
sablefish juv.	0.067	0.300	4.400
sablefish ad.	0.400	0.200	2.200
pollock juv.	0.024	0.800	6.715
pollock ad.	0.700	0.400	2.000
herring juv.	1.233	0.800	7.272
herring ad.	2.000	0.650	4.400
NEPac			
arrowtooth juv.	0.024	0.500	4.560
arrowtooth ad.	0.280	0.250	2.000
P. cod juv.	0.282	0.800	3.421
P. cod ad.	0.480	0.660	1.800
P. halibut juv.	0.022	0.500	2.550
P. halibut ad.	0.170	0.300	1.000
sablefish juv.	0.034	0.300	4.400
sablefish ad.	0.203	0.200	2.200
pollock juv.	0.113	0.800	6.715
pollock ad.	3.268	0.400	2.000
herring juv.	0.277	0.800	7.272
herring ad.	0.450	0.650	4.400

Table A.1.5: EwE basic input parameters for bird and mammal groups in the mass balanced SoG, BCS, and NEPac models.

SoG	B (t·km⁻²)	P/B (year⁻¹)	Q/B (year⁻¹)
birds pelag pisciv	0.012	0.223	120.248
birds demer pisciv	0.008	0.114	119.479
birds zooplanktiv	0.001	0.186	228.125
odontocetae	0.060	0.030	13.100
mysticetae	0.010	0.020	13.370
sea lions	0.140	0.060	12.700
seals	0.340	0.140	15.950
BCS			
birds pelag pisciv	0.001	0.159	278.205
birds demer pisciv	0.003	0.176	164.945
birds zooplanktiv	0.003	0.186	247.942
odontocetae	0.036	0.030	13.100
mysticetae	0.155	0.020	13.370
sea lions	0.019	0.060	12.700
seals	0.040	0.160	15.950
NEPac			
birds pelag pisciv	0.002	0.129	202.630
birds demer pisciv	0.016	0.061	148.904
birds zooplanktiv	0.001	0.175	253.793
odontocetae	0.036	0.030	13.100
mysticetae	0.155	0.020	13.370
sea lions	0.174	0.060	12.700
seals	0.001	0.160	15.950

Table A.1.6: EwE basic input parameters for pelagic fishes groups in the mass balanced SoG, BCS, and NEPac models.

SoG	B (t·km ⁻²)	P/B (year ⁻¹)	Q/B (year ⁻¹)	EE	P/Q
salmon shark	0.020	0.200	1.200		
pelagic sharks	0.015	0.140	1.00		
pink	0.020	1.400	8.900		
chum	1.000	1.000	7.000		
sockeye	0.020	1.270	8.400		
coho juv.	0.958	2.400	7.871		
coho ad.	0.200	1.300	3.240		
chinook juv.	1.244	2.400	11.864		
chinook ad.	0.330	1.400	5.00		
myctophids	4.500	0.500	6.800		
pred. pelagics	0.001	0.450	6.600		
small pelagics	15.000	2.300			0.300
BCS					
salmon shark	0.020	0.200	1.200		
pelagic sharks	0.030	0.140	1.000		
pink	0.200	1.400	8.900		
chum	0.400	1.000	7.000		
sockeye	0.200	1.270	8.400		
Coho	0.250	1.100	7.700		
chinook	0.390	0.740	5.000		
myctophids	4.500	0.500	6.800		
pred. pelagics	0.210	0.450	6.600		
small pelagics		2.300		0.950	0.300
NEPac					
salmon shark	0.020	0.200	1.200		
pelagic sharks	0.030	0.140	1.000		
pink	0.200	1.400	8.900		
chum	0.400	1.000	7.000		
sockeye	0.200	1.270	8.400		
coho	0.250	1.100	7.700		
chinook	0.390	0.740	5.000		
myctophids	4.500	0.500	6.800		
pred. pelagics	0.210	0.450	6.600		
small pelagics		2.300		0.950	0.300

Table A.1.7: EwE basic input parameters for demersal fishes groups in the mass balanced SoG, BCS and NEPac models.

SoG	B (t·km ⁻²)	P/B (year ⁻¹)	Q/B (year ⁻¹)	P/Q
dogfish	2.500	0.190	2.700	
rajidae / ratfish	1.200	0.300	1.320	
Pacific Ocean				
perch	0.000	0.100	2.400	
rockfish other	0.800	0.180	2.600	
Pacific hake	10.000	0.800	2.400	
lingcod	3.000	0.350	2.400	
yellowfin sole	0.001	0.190	2.400	
rock sole	0.460	0.220	2.300	
flatfish other	4.000		3.000	0.200
small demersals	5.500		5.256	0.300
BCS				
dogfish	1.300	0.100	2.700	
rajidae / ratfish	0.835	0.300	1.320	
Pacific Ocean				
perch	0.500	0.100	2.400	
rockfish other	1.000	0.180	2.600	
Pacific hake	0.930	0.500	2.400	
lingcod	0.363		2.400	0.100
yellowfin sole	0.001	0.190	2.400	
rock sole	0.144	0.220	2.300	
flatfish other	1.300		3.000	0.200
small demersals	7.000		5.256	0.300
NEPac				
dogfish	1.300	0.100	2.700	
rajidae / ratfish	0.835	0.300	1.320	
Pac. Ocean perch	1.300	0.100	2.400	
northern rockfish	0.158	0.900	2.600	
rockfish other	1.000	0.180	2.600	
Pac. hake	0.093	0.500	2.400	
atka mackerel	0.269	0.600	3.000	
lingcod	0.363		2.400	0.100
yellowfin sole	0.505	0.190	2.400	
rock sole	0.572	0.220	2.300	
Alaska plaice	0.461	0.250	2.000	
flatfish other	1.300		3.000	0.200
small demersals	7.000		5.256	0.300

Table A.1.8: EWE basic input parameters for invertebrate groups in the mass balanced SoG, BCS and NEPac models.

SoG	B (t·km ⁻²)	P/B (year ⁻¹)	Q/B (year ⁻¹)	EE	P/Q
krill	30.000	6.000	24.800		
carn. zooplankton	20.000	7.000	20.000		
herb. zooplankton	27.000	22.000	80.000		
jellies	12.500	9.600	13.000		
large squids	0.050	2.600	6.400		
small squids		3.000	15.000	0.900	
shrimps	0.500	1.200	9.667		
crabs	3.800	1.500	3.500		
bivalves	7.700	0.900			0.200
echinoderms	15.000	0.300			0.250
other benthos	43.000	4.500			0.300
phytoplankton	40.000	130.000			
macrophytes	8.000	9.000			
Detritus	10.000				
BCS					
krill	18.000	6.000	24.800		
carn. zooplankton	25.000	7.000	20.000		
herb. zooplankton	25.000	27.000	80.000		
jellies	12.500	9.600	13.000		
large squids	0.500	2.600	6.400		
small squids		3.000	15.000	0.900	
shrimps	5.650	1.200	9.670		
crabs	3.800	1.500	3.500		
bivalves	7.700	0.900			0.200
echinoderms	14.800	0.300			0.250
other benthos	43.000	4.500			0.300
phytoplankton	22.000	130.000			
macrophytes	9.000	9.000			
Detritus	10.000				
NEPac					
krill	18.000	6.000	24.800		
carn. zooplankton	25.000	7.000	20.000		
herb. zooplankton	25.000	27.000	80.000		
jellies	12.500	9.600	13.000		
large squids	0.500	2.600	6.400		
small squids		3.000	15.000	0.900	
shrimps	5.650	1.200	9.670		
crabs	3.800	1.500	3.500		
bivalves	7.700	0.900			0.200
echinoderms	14.800	0.300			0.250
other benthos	43.000	4.500			0.300
phytoplankton	22.000	130.000			
macrophytes	9.000	9.000			
Detritus	10.000				

Table A.1.9: Diet compositions for adult (normal type) and juvenile (**bold type**) multi-stanza groups.

	arrowtooth	P. cod	halibut	sablefish	pollock	herring
atf. j.	0.004		0.002	0.004		
atf. a.			0.020	0.006		
P. cod j.	0.016	0.010	0.010	0.010 0.010	0.010	
P. cod a.			0.006			
P. halibut j.	0.010					
sablefish j.	0.001					
pollock j.	0.002	0.001	0.002	0.002 0.002	0.002	
pollock a.	0.030	0.030	0.100	0.030		
herring j.	0.010		0.005 0.001	0.003		
herring a.	0.020	0.010	0.005 0.005	0.007		
raj. / ratf.	0.020		0.02			
pink	0.010		0.001			
chum	0.010		0.001			
sockeye	0.010					
rockfish ot.	0.010		0.010			
atka mack		0.010	0.010			
rock sole			0.020			
flatfish ot.	0.020		0.060 0.030			
mycto.	0.010		0.010	0.010	0.001	
sm. dem.	0.100 0.150	0.150 0.030	0.150 0.100	0.138 0.150	0.070 0.079	
sm. pel.	0.130 0.230	0.050 0.030	0.042	0.020 0.200	0.020 0.079	
krill	0.150 0.220	0.050 0.115		0.080 0.200	0.442 0.183	0.370 0.132
c. zoopl.		0.419		0.020 0.190	0.100 0.307	0.230 0.304
h. zoopl.		0.109			0.020 0.286	0.400 0.434
Jellies				0.130	0.007	
l. squids			0.010	0.050		
sm. squids	0.028	0.01	0.010	0.010	0.01	
shrimps	0.110 0.150	0.050 0.056	0.300	0.080	0.150 0.017	0.010
crabs		0.220 0.056	0.330 0.190	0.040	0.020 0.017	
bivalves		0.010				
echino		0.020			0.020	
o. benthos	0.299 0.250	0.389 0.175	0.198	0.150 0.250	0.145 0.015	0.120
detritus				0.220		

Table A.1.10: Diet compositions for marine bird groups .

	pelag. pisciv.	demer. pisciv.	zoo. planktiv.
pollock juv.	0.020	0.002	
herring juv.	0.050	0.005	
herring ad.	0.020	0.010	
myctophids	0.602	0.020	
misc. sm.			
dem.	0.060	0.667	
sm. pelag.	0.160	0.100	
krill	0.010	0.036	0.570
carn. zoop.		0.010	0.430
large squids	0.010	0.010	
small squids	0.040	0.047	
shrimps		0.015	
oth. benthos	0.028	0.078	

Table A.1.11: Diet compositions for marine mammal groups.

	odontocetae	mysticetae	sea lions	seals
P. cod juv.			0.001	0.001
P. cod ad.			0.039	
sablefish juv.	0.001		0.001	
sablefish ad.	0.005		0.003	
pollock juv.	0.020		0.005	0.009
pollock ad.	0.080		0.200	0.100
herring juv.	0.010	0.005	0.005	0.010
herring ad.	0.020	0.003	0.005	0.010
mysticetae	0.0001			
sea lions	0.020			
seals	0.0001			
dogfish	0.050			
rajidae / ratfish			0.020	
pink	0.010		0.050	0.100
chum	0.020		0.050	0.150
sockeye	0.040		0.032	0.100
coho	0.005		0.050	0.100
chinook	0.005		0.050	0.100
Pac. Ocean				
perch	0.010		0.001	0.001
northern				
rockfish	0.005		0.001	0.001
rockfish other	0.010		0.001	0.001
Pac. hake			0.001	0.010
atka mackerel	0.020		0.020	
yellowfin sole	0.010			
rock sole	0.010		0.025	
plaice	0.020		0.030	
flatfish other			0.040	
myctophids	0.100			
misc. small				
demersals	0.050		0.050	0.020
misc. pred.				
pelagics	0.040		0.010	0.010
misc. small				
pelagics	0.119	0.140	0.232	0.230
krill		0.160		
carn.				
zooplankton		0.013		
large squids	0.210		0.020	0.010
small squids	0.110	0.030	0.020	0.010
shrimps		0.001		
crabs		0.012		
bivalves		0.090		
echinoderms		0.050		
other benthos		0.496	0.038	0.027

Table A.1.12: Diet compositions for pelagic fish groups. Note; ssk = salmon shark, psk = pelagic sharks, sock = sockeye, chin = chinook, myct = myctophids, ppel = predatory pelagics, and spel = miscellaneous small pelagics.

	ssk	psk	pink	chum	sock	coho	chin	myct	ppel	spel
pollock ad.	0.033									
herring juv.				0.005		0.010	0.010			
herring ad.						0.005	0.005			
dogfish	0.033									
pink	0.100	0.020								
chum	0.167	0.030								
sockeye	0.300	0.050								
coho	0.087	0.005								
chinook	0.013	0.005								
Pac. Ocean perch							0.005			
rockfish other							0.005			
myctophids	0.033	0.030	0.030	0.005	0.030	0.255	0.200		0.100	
small demersals		0.100	0.064	0.075	0.026	0.005	0.001			0.050
pred. pelagics	0.020	0.020								
small pelagics	0.047	0.030	0.103	0.125	0.030	0.236	0.335		0.250	0.050
krill		0.050	0.090	0.055	0.044	0.124	0.170	0.230	0.020	0.200
carn. zooplankton			0.391	0.299	0.368	0.020		0.220	0.010	0.320
herb. zoopl.			0.100	0.140	0.083			0.220		0.180
jellies			0.006	0.109	0.003					
large squids	0.100	0.550								
small squids	0.067	0.050	0.102	0.020	0.400	0.345	0.225		0.600	
shrimps		0.030	0.014	0.012	0.001			0.010	0.020	0.030
crabs		0.030	0.014	0.012			0.044			0.010
bivalves			0.001	0.005						
other benthos			0.088	0.138	0.015			0.320		0.160

Table A.1.13: Diet compositions for some demersal fish groups. Note; dogf = dogfish, raj ra = rajidae / ratfish, POP = Pacific Ocean perch, NRF = northern rockfish, ORF = rockfish other, AM = Atka mackerel, ling = lingcod.

	dogf	raj ra	POP	NRF	ORF	hake	AM	ling
arrowt juv.								0.003
arrowt ad.								0.005
P. cod juv.	0.002							0.015
P. cod ad.								0.005
pollock juv.	0.004		0.002			0.005	0.002	0.003
pollock ad.	0.069					0.010		0.012
herring juv.	0.020					0.050		0.010
herring ad.	0.005					0.003		0.010
raj ra	0.017							
coho	0.001							
chinook	0.001							
POP								0.005
rockfish other	0.001							0.010
Pac. hake	0.002					0.002		0.002
yellowfin sole								0.030
rock sole	0.003							0.020
plaice								0.010
flatfish other	0.016		0.040			0.006		0.005
sdem	0.098	0.010	0.020		0.100	0.017	0.040	0.205
pred. pel.								
small pel.	0.206					0.007		0.550
krill	0.139		0.670	0.930	0.200	0.701	0.150	
car. zoopl	0.099			0.050		0.101	0.220	
herb. zoopl						0.050	0.220	
jellies	0.037						0.190	
small squids					0.100			
shrimps	0.008	0.010	0.190		0.130	0.001		
crabs	0.073	0.130			0.050			
bivalves	0.004	0.170					0.020	
echinoderms		0.180						
other benthos	0.195	0.500	0.078	0.020	0.420	0.047	0.158	0.100

Table A.1.14: Diet compositions for flatfish groups. Note; YFS = yellowfin sole, r sole = rpck sole, OFF = other flatfish, and sdem = small demersals.

	YFS	r sole	plaice	OFF	sdem
pollock juv.				0.001	
flatfish other					0.010
myctophids					
sdem	0.037	0.164		0.040	0.020
pred. pel.					
small pel.	0.003	0.004			0.250
krill	0.007				0.010
carn. zoopl	0.093	0.060	0.100		0.010
small squids	0.005				0.010
shrimps	0.022	0.001		0.100	0.030
crabs	0.052	0.015		0.050	0.040
bivalves	0.157	0.020	0.350		0.010
echinoderms	0.081	0.003		0.200	0.040
other benthos	0.543	0.733	0.550	0.609	0.570

Table A.1.15: Diet compositions used for the invertebrate groups. Note; cz = carnivorous zooplankton, hz = herbivorous zooplankton, lsq = large squids, ssq = small squids, biv = bivalves, echino is echinoderms, and betho is other benthos, mycto = myctophids, and msp = miscellaneous small pelagics.

	krill	cz	hz	jelly	lsq	ssq	shrimp	crabs	biv	echino	benthos
mycto					0.050						
msp					0.100						
krill		0.050		0.120	0.100	0.250	0.250				
cz	0.025	0.050		0.330	0.150	0.450	0.250		0.100		0.005
hz	0.075	0.850		0.300	0.100	0.250	0.250		0.050		0.010
jelly				0.050							
ssq					0.500	0.050					
crabs								0.050			
biv								0.100			
echino								0.010			
benthos								0.550		0.700	0.050
phyto	0.900	0.050	1.000	0.200					0.550		0.400
macro								0.100		0.250	0.100
detritus							0.250	0.190	0.300	0.050	0.435

Table A.1.16: Time series available as reference data for the NEPac BCS, and SoG models. Note that mortality refers to available time series of either fishing (F), or total (Z) mortality, or both.

Species Group	B ($t\text{-km}^{-2}$)	Mortality (year^{-1})	Catch ($t\text{-km}^{-2}$)
odontocetae	SoG		
sea lions	NEPac		
harbour seal	SoG, BCS		
pelagic pisciv. birds	SoG		
demer pisciv. birds	SoG		
atka mackerel	NEPac	NEPac	NEPac
arrowtooth floun	BCS, NEPac		BCS, NEPac
Pacific cod	BCS, NEPac	BCS, NEPac	BCS, NEPac
Pacific halibut	BCS, NEPac	BCS, NEPac	BCS, NEPac
sablefish	BCS, NEPac		BCS, NEPac
walleye pollock	BCS, NEPac	BCS, NEPac	BCS, NEPac
Pacific hake	BCS, NEPac		BCS, NEPac
Pacific Ocean perch	BCS, NEPac	BCS, NEPac	BCS, NEPac
Northern rockfish	NEPac	NEPac	NEPac
yellowfin sole	NEPac	NEPac	NEPac
rock sole	BCS, NEPac	NEPac	BCS, NEPac
Alaska plaice	NEPac	NEPac	NEPac
Pacific herring	BCS	BCS	BCS, NEPac
chinook salmon	SoG, BCS, NEPac		
chum salmon	BCS, NEPac		
coho salmon	SoG, BCS, NEPac		
pink salmon	BCS, NEPac		
sockeye salmon	BCS, NEPac		
lingcod	SoG		

Appendix 2

Table A.2.1. Vulnerability settings, by predator group, for models in this study.

	SoG	BCS	NEPac
arrowtooth juv.	2	∞	3.5
arrowtooth ad.	2	∞	424
P. cod juv.	2	2.02	1
P. cod ad.	2	∞	∞
P. halibut juv.	2	50	∞
P. halibut ad.	2	50	1.79
sablefish juv.	2	1	1
sablefish ad.	2	∞	1
pollock juv.	2	1	∞
pollock ad.	2	3.57	1.2
herring juv.	10	5.46	2
herring ad.	1	1.09	2
birds pelag pisciv	5.31	2	2
birds demer pisciv	2.25	2	2
birds zooplanktiv	2	2	2
odontocetae	1	1.21	2
mysticetae	2	2	2
sea lions	2	2	2
seals	9.27	2.24	2
salmon shark	2	2	2
pelagic sharks	2	2	2
dogfish	2	2	2
rajidae / ratfish	2	2	2
pink	2	1.82	1.33
chum	2	1	1.25
sockeye	2	5	2.26
coho juv.	1.36	NA	NA
coho ad.	1.45	∞	1
chinook juv.	1	NA	NA
chinook ad.	2.58	30.2	1
Pac. Ocean perch	2	2	2.1
northern rockfish	NA	NA	1.5
rockfish other	2	2	2
Pac. hake	2	1	1.37
atka mackerel	NA	NA	1.01
lingcod	4.89	2	2
yellowfin sole	2	2	1
rock sole	2	2.17	1.8
plaice	NA	NA	1.33
flatfish other	2	2	2
myctophids	2	43	2
misc. small demersals	2	2	2

Table A.2.1. (continued)

	SoG	BCS	NEPac
misc. pred. pelagics	2	2	2
misc. small pelagics	2	2	2
krill	2	18.7	2
carn. zooplankton	2	1	2
herb. zooplankton	2	6.01	2
jellies	2	2	2
large squids	2	2	2
small squids	2	2	2
shrimps	2	2	2
crabs	2	2	2
bivalves	2	2	2
echinoderms	2	2	2
other benthos	2	2	2

Appendix 3

Table A.3.1: Correlation coefficients of the best fit Strait of Georgia PPA and Fraser River flow at Hope, BC, averaged over seasonal periods (as groups of months indicated by abbreviations based upon the first letters of the months used). Smoothing windows for each correlation, i.e., 10, 20, 30, or 40 years, are shown in the PPA columns. All correlations significant at an $\alpha = 0.05$ are in bold. The largest correlation for each smoothing window is outlined.

	PPA 10	PPA 20	PPA 30	PPA 40
NDJ	0.018	-0.148	-0.214	-0.229
DJF	0.112	-0.039	-0.099	-0.116
JFM	0.195	0.123	0.105	0.140
FMA	-0.004	-0.131	-0.125	-0.092
MAM	-0.189	-0.217	-0.240	-0.164
AMJ	-0.305	-0.184	-0.292	-0.340
MJJ	-0.299	-0.189	-0.303	-0.203
JJA	-0.277	-0.358	-0.470	-0.420
JAS	-0.268	-0.282	-0.320	-0.395
ASO	-0.242	-0.244	-0.388	-0.315
SON	-0.066	-0.066	-0.136	-0.178
OND	-0.041	-0.006	-0.142	-0.161
OCT to APR	-0.005	-0.178	-0.229	-0.225
AMJJAS	-0.291	-0.377	-0.316	-0.314
MJJAS	-0.295	-0.285	-0.161	-0.283
AMJJ	-0.319	-0.324	-0.259	-0.336
AMJJA	-0.296	-0.407	-0.261	-0.332

Table A.3.2: Correlations coefficients of the best fit Strait of Georgia PPA and ocean salinity at Chrome Island, BC, averaged over seasonal periods (as groups of months indicated by abbreviations based upon the first letters of the months used). Smoothing windows for each correlation, i.e., 10, 20, 30, or 40 years, are shown in the PPA columns. All correlations significant at an $\alpha = 0.05$ are in bold. The largest correlation for each smoothing window is outlined.

	PPA 10	PPA 20	PPA 30	PPA 40
DJF	0.341	0.519	0.400	0.411
JFM	0.383	0.521	0.469	0.500
FM	0.353	0.437	0.378	0.453
FMA	0.439	0.593	0.636	0.602
FMAM	0.467	0.568	0.617	0.566
MA	0.476	0.646	0.736	0.682
MAM	0.487	0.591	0.631	0.564
AMJ	0.358	0.341	0.236	0.217
AMJJ	0.400	0.304	0.156	0.141
MJJ	0.376	0.208	0.046	0.041
JJA	0.343	0.130	-0.026	-0.033
MJJAS	0.351	0.084	0.015	0.049
OCT to APR	0.387	0.518	0.397	0.419
YEAR	0.372	0.419	0.263	0.232

Table A.3.3: Correlations coefficients of the best fit Strait of Georgia PPA and ocean salinity at Race Rocks, BC, averaged over seasonal periods (as groups of months indicated by abbreviations based upon the first letters of the months used). Smoothing windows for each correlation, i.e., 10, 20, 30, or 40 years, are shown in the PPA columns. All correlations significant at an $\alpha = 0.05$ are in bold. The largest correlation for each smoothing window is outlined.

	PPA 10	PPA 20	PPA 30	PPA 40
DJF	0.459	0.653	0.674	0.703
JFM	0.587	0.753	0.814	0.831
FM	0.564	0.795	0.840	0.866
FMA	0.568	0.800	0.837	0.861
FMAM	0.617	0.777	0.820	0.851
MA	0.495	0.770	0.782	0.805
MAM	0.564	0.770	0.795	0.837
AMJ	0.575	0.704	0.762	0.788
AMJJ	0.557	0.670	0.732	0.747
MJJ	0.566	0.641	0.707	0.711
JJA	0.522	0.607	0.700	0.688
MJJAS	0.537	0.635	0.725	0.733
OCT to APR	0.472	0.648	0.699	0.744
Annual	0.504	0.647	0.705	0.731

Table A.3.4.: Correlations coefficients of the best fit Strait of Georgia PPA and upwelling at 48°N averaged over seasonal periods (as groups of months indicated by abbreviations based upon the first letters of the months used). Smoothing windows for each correlation, i.e., 10, 20, 30, or 40 years, are shown in the PPA columns. All correlations significant at an $\alpha = 0.05$ are in bold. The largest correlation for each smoothing window is outlined.

	PPA 10	PPA 20	PPA 30	PPA 40
DJF	0.261	0.253	0.092	0.330
JFM	0.246	0.183	-0.012	0.143
FMA	0.308	0.295	0.132	0.071
FMAM	0.259	0.143	-0.043	0.015
MA	0.366	0.461	0.371	0.410
MAM	0.184	0.217	0.263	0.325
AMJ	-0.061	-0.100	0.025	0.068
AMJJ	-0.145	-0.114	0.049	0.096
MJJ	-0.194	-0.183	0.091	0.129
MJJAS	-0.171	0.041	0.202	0.202
JJA	-0.070	0.109	0.260	0.233
SON	0.179	0.169	-0.139	-0.206
OCT to APR	0.311	0.263	0.075	0.354
Annual	0.202	0.220	0.095	0.345

Table A.3.5.: Correlations coefficients of the best fit BC shelf PPA and upwelling at 48°N averaged over seasonal periods (as groups months indicated by abbreviations based upon the first letters of the months used). Smoothing windows for each correlation, i.e., 10, 20, 30, or 40 years, are shown in the PPA columns. All correlations significant at an $\alpha = 0.05$ are in bold. The largest correlation for each smoothing window is outlined.

	PPA 10	PPA 20	PPA 30	PPA 40
DJF	0.053	-0.177	-0.256	-0.043
MA	0.172	0.130	-0.070	0.048
MAM	0.016	0.031	-0.056	-0.016
AMJ	-0.044	0.053	-0.051	-0.148
AMJJ	-0.076	0.095	0.095	0.046
MJJ	-0.127	0.056	0.206	0.188
MJJAS	0.027	0.391	0.467	0.358
JJA	0.131	0.449	0.454	0.340
SON	0.212	0.288	0.206	0.094
OCT to APR	0.090	-0.083	-0.234	-0.019
Annual	-0.003	0.063	-0.063	0.034

Table A.3.6.: Correlations coefficients of the best fit BC shelf PPA and upwelling at 51°N averaged over seasonal periods (as groups of months indicated by abbreviations based upon the first letters of the months used). Smoothing windows for each correlation, i.e., 10, 20, 30, or 40 years, are shown in the PPA columns. All correlations significant at an $\alpha = 0.05$ are in bold. The largest correlation for each smoothing window is outlined.

	PPA 10	PPA 20	PPA 30	PPA 40
DJF	0.022	-0.208	-0.175	-0.042
MA	-0.167	-0.390	-0.606	-0.513
MAM	-0.237	-0.469	-0.620	-0.547
AMJ	-0.022	-0.179	-0.496	-0.533
AMJJ	-0.307	-0.369	-0.605	-0.642
MJJ	-0.507	-0.639	-0.583	-0.663
MJJAS	-0.192	-0.276	-0.083	0.133
JJA	-0.247	-0.382	-0.023	0.254
SON	0.199	0.260	0.243	0.104
OCT to APR	-0.071	-0.240	-0.325	-0.218
Annual	-0.037	-0.266	-0.394	-0.232

Table A.3.7.: Correlations coefficients of the best fit BC shelf PPA and upwelling at 54°N averaged over seasonal periods (as groups of months indicated by abbreviations based upon the first letters of the months used). Smoothing windows for each correlation, i.e., 10, 20, 30, or 40 years, are shown in the PPA columns. All correlations significant at an $\alpha = 0.05$ are in bold. The largest correlation for each smoothing window is outlined.

	PPA 10	PPA 20	PPA 30	PPA 40
DJF	-0.310	-0.512	-0.435	-0.342
MA	-0.291	-0.517	-0.656	-0.549
MAM	-0.295	-0.510	-0.593	-0.548
AMJ	-0.116	-0.016	-0.254	-0.434
AMJJ	-0.253	-0.140	-0.214	-0.380
MJJ	-0.435	-0.430	-0.273	-0.299
MJJAS	-0.122	-0.235	0.093	0.084
JJA	-0.227	-0.436	-0.096	0.259
SON	0.085	0.153	0.158	-0.003
OCT to APR	-0.391	-0.509	-0.593	-0.617
Annual	-0.327	-0.489	-0.573	-0.609

Table A.3.8: Correlations coefficients of the best fit Northeast Pacific PPA and the Aleutian low pressure index averaged annually. Smoothing windows for each correlation, i.e., 10, 20, 30, or 40 years, are shown in the PPA columns. All correlations significant at an $\alpha = 0.05$ are in bold. The largest correlation for each smoothing window is outlined.

	PPA 10	PPA 20	PPA 30	PPA 40
Annual ALPI	0.647	0.715	0.775	0.865

Table A.3.9: Correlations coefficients of the best fit Northeast Pacific PPA and the Pacific decadal oscillation averaged over seasonal periods (as groups of months indicated by abbreviations based upon the first letters of the months used). Smoothing windows for each correlation, i.e., 10, 20, 30, or 40 years, are shown in the PPA columns. All correlations significant at an $\alpha = 0.05$ are in bold. The largest correlation for each smoothing window is outlined.

	PPA 10	PPA 20	PPA 30	PPA 40
FEB to JUL	0.774	0.893	0.950	0.980
AMJJ	0.755	0.910	0.953	0.975
AUG to JAN	0.671	0.768	0.929	0.968
SON	0.651	0.841	0.883	0.926
Annual	0.754	0.895	0.943	0.979

Table A.3.10: Correlations coefficients of the best fit Northeast Pacific PPA and the northern oscillation index averaged over seasonal periods (as groups of months indicated by abbreviations based upon the first letters of the months used). Smoothing windows for each correlation, i.e., 10, 20, 30, or 40 years, are shown in the PPA columns. All correlations significant at an $\alpha = 0.05$ are in bold. The largest correlation for each smoothing window is outlined.

	PPA 10	PPA 20	PPA 30	PPA 40
NOV to MAR	-0.477	-0.670	-0.815	-0.867
JFM	-0.503	-0.714	-0.890	-0.921
APR to OCT	-0.598	-0.832	-0.901	-0.906
Annual	-0.553	-0.771	-0.947	-0.975

Table A.3.11: Correlations coefficients of the best fit Northeast Pacific PPA and the north Pacific index averaged over seasonal periods (as groups of months indicated by abbreviations based upon the first letters of the months used). Smoothing windows for each correlation, i.e., 10, 20, 30, or 40 years, are shown in the PPA columns. All correlations significant at an $\alpha = 0.05$ are in bold. The largest correlation for each smoothing window is outlined.

	PPA 10	PPA 20	PPA 30	PPA 40
NOV to MAR	-0.602	-0.691	-0.782	-0.909
AMJ	-0.275	-0.379	-0.470	-0.506
APR to OCT	-0.127	-0.314	-0.412	-0.501
MJJ	-0.17	-0.299	-0.512	-0.611
JJA	-0.052	-0.149	-0.241	-0.238
Annual	-0.661	-0.838	-0.918	-0.987